

Metals and Polycyclic Aromatic Hydrocarbons in Environmental Matrices of the Fleet Lagoon, UK and Toxicological Investigations using the Marine Polychaete Hediste diversicolor

Sarah Bagwell

July 2019

A thesis submitted in partial fulfilment of the requirements of Bournemouth University
for the degree of Doctor of Philosophy

Bournemouth University, Faculty of Science and Technology, Talbot Campus, Fern
Barrow, Poole, Dorset, BH12 5BB, United Kingdom

This page left intentionally blank

This copy of the thesis has been supplied on condition that anyone who consults it is understood to recognise that its copyright rests with its author and due acknowledgement must always be made of the use of any material contained in, or derived from, this thesis.

This page left intentionally blank

Abstract

Contamination within the marine environment is ubiquitous and may contain both metals and polycyclic aromatic hydrocarbons (PAH's) individually or within complex mixtures. Contamination may bind directly to organic particles within sediment and may remain undisturbed or re-released during periods of hydrodynamic activity. Sediment may therefore act as both source and sink for complex mixtures of contamination and bio-accumulate in sediment dwelling organisms including the marine polychaete *Hediste diversicolor*.

Following exposure, an organism may deploy a variety of biochemical, cellular, molecular and behavioural alterations to maintain homeostasis and reduce the effects of the insult.

Biomarkers are used within environmental monitoring to forecast adverse outcome pathways via the assessment of endpoints including those of cellular, molecular, behavioural, tissue, systemic and organism responses and alterations. However, research is primarily conducted upon bioaccumulation and adverse outcome pathways of exposure to individual contaminants although environmentally, mixtures of contaminants including metals and PAH's are omnipresent.

Concentrations of metals and PAH's in the environmental matrices of the Fleet Lagoon, Dorset, UK were analysed in order to obtain environmentally relevant concentrations of contaminants. Specific metals and PAH's were found to exceed the Threshold and Potential effects limits of the Canadian sediment quality guidelines.

Granulometric composition showed spatial variance throughout the lagoon where all sites were identified as extremely poorly to moderately poorly sorted. Relationships between sediment fractions, Cu, Zn and Pb were identified. Additionally, both metals and PAH's were found to bioaccumulate in *H diversicolor*. Total metal sediment analysis and worm tissue concentration were not relational excluding As, where a positive correlation was identified. Sediment digestion using BCR sequential extraction revealed a positive relationship

between worm tissue concentrations for Cu. However, proteinase K sediment digestion identified positive correlation between Cu, Pb and worm tissue concentration. Furthermore, BCR sequential extraction was found to overestimate the bioavailable fraction. Isomer source analysis identified that PAH's found at all sites excluding site 2, were from pyrolytic origins. PAH's at site 2 were identified as being from petrogenic sources.

Exposure investigations using the environmentally relevant concentrations of Pb and pyrene found in sediment of the Fleet lagoon identified that both contaminants, alone and in combination negatively affect burrowing rates of *H diversicolor*. Although, burrowing rates of the combined Pb and pyrene exposure groups were faster than those exposed to Pb alone. Acetylcholinesterase was inhibited by both Pb and pyrene (alone and in combination) although more notably by pyrene. However, burrowing rates do not correlate to AChE activity.

The presence of pyrene in combination with Pb was found to reduce Pb assimilation by *H diversicolor*. Furthermore, both Pb and pyrene were found to produce reactive oxygen species which may not be suitably controlled by glutathione-s-transferase, cytochrome P450, superoxide dismutase as 8-OHdG adducts post exposure were identified. Additionally, potential inhibition of both GST and CYP450 were observed during the assimilation phases for all exposure groups.

Energetic alterations following exposure were identified in all exposure groups suggesting that exposure to these contaminants induces high energetic demands in *H diversicolor*. Results from this study demonstrate for the first time that the bioaccumulation of Pb and pyrene by *H diversicolor* elicit behavioural, biochemical and energetic changes which may have negative effects on populations which reside in marine environments where Pb and pyrene are present.

This page left intentionally blank

Table of Contents

Abstract	v
Table of Contents	viii
List of Tables	xiii
List of Figures	xv
List of Appendices	xviii
Abbreviations	xix
1. Introduction	1
1.1 Overview	1
1.2 Literature Review	3
1.2.1 Threats to the marine environment	3
1.3 Marine Metal Pollution.....	7
1.3.1 Heavy Metals?	7
1.3.2. Bioavailability of Metals within the Marine Environment	7
1.3.3 Marine Metal Contamination Inputs	8
1.3.4 Toxicity of Metal Pollution	9
1.4 Polycyclic Aromatic Hydrocarbon Environmental pollution	12
1.4.1 Polycyclic Aromatic Hydrocarbon Environmental Inputs.....	12
1.4.2 PAH's Characteristics and Toxicity	13
1.4.3 PAH Toxicity Pathways.....	16
1.4.4 Metal –PAH Co -Toxicity.....	16
1.5 Marine Organisms as Sentinels of Metal Pollution	18
1.5.1 Marine quality guidelines.....	19
1.5.2 Marine Polychaete species in Biomarker Research	19
1.5.3 The Polychaete <i>Hediste diversicolor</i> , <i>Hediste</i> or <i>Nereis</i> ?	20
1.5.4 <i>Hediste diversicolor</i> Physiology	20
1.5.5 Lifecycle.....	21
1.5.6 Role in Lagoon ecosystems	21
1.6 Biomarkers	22
1.6.1 Detoxification Enzymes, molecules and Cellular Effects.....	24
1.6.2 Energy Homeostasis.....	26
1.6.3 Genotoxicity	27
1.6.4 Metallothionein.....	28
1.6.5 Acetylcholinesterase.....	30

1.6.6 Behaviour Alterations	31
1.7 Research aim and objectives.....	32
Chapter 2. Materials and Methods	34
2.1 Introduction	34
2.1.1 Collection of samples and pre-processing	34
2.2 Sediment Characteristics	36
2.2.1 Loss on Ignition.....	36
2.2.2 Sediment characterisation	37
2.3 Chemical analysis	38
2.3.1 Preparation of Equipment.....	38
2.3.2 Chemical Determination of Total Metals in Sediment.....	38
2.3.3 Metal Content in Worm tissue	39
2.3.4 Sequential Sediment Processing.....	40
2.3.5 Proteinase K Extraction	41
2.3.6 Determination of PAH's in sediment and water.....	41
2.3.7 Extraction of Pore Water from sediment.....	41
2.3.8 Pore water analysis.....	42
2.3.9 Preparation of worm tissue for PAH analysis using HPLC.....	42
2.3.10 HPLC Pyrene and 1-Hydroxypyrene Analysis.....	42
2.4.1 HPLC individual PAH determination	44
2.4.2 Pyrene Sediment Determination	44
2.5 Tank set up.....	45
2.5.1 General set up	45
2.5.2 <i>Hediste diversicolor</i>	45
2.5.3 <i>Hediste diversicolor</i> feeding regime	46
2.6 Spiking of sediment with metals and pyrene.....	46
2.6.1 Sediment spiking for exposure experiments.....	46
2.6.2 Acetone tank	47
2.7 Quality Control	48
2.7.1 Total metal sediment analysis.....	48
2.7.2 Sequential sediment extraction	48
2.7.3 Total metal worm tissue analysis	48
2.7.4 HPLC Pyrene and 1-OHP analysis.....	49
2.7.5 HPLC PAH determination	50
2.7.6 Varian Vista - PRO ICP - OES	51
2.8 Data analysis	52

3. Metal concentrations in environmental matrices of the Fleet Lagoon, UK, and bioavailability to the marine polychaete <i>H diversicolor</i>	53
3.1 Introduction	53
3.2. Study Site	57
3.2.1 Study Site Information	57
3.3 Fleet Lagoon Sample Sites	61
3.4 Materials and Methods	62
3.4.1 Sampling.....	62
3.5 Results.....	66
3.5.1Sedimet Characterisation.....	66
3.6 Discussion.....	87
3.6.1 Sediment characteristics.....	87
3.6.2 Metals bioavailability.....	91
3.7 Conclusion.....	97
4. Polycyclic aromatic hydrocarbons in Lagoon sediments and bioaccumulation by the marine polychaete <i>H diversicolor</i>	100
4.1 Introduction	100
4.2 Materials and Methods	103
4.2.1Site description.....	103
4.3 Results.....	105
4.3.1 PAH concentrations of environmental matrices	105
4.3.2 Isomer source identification	109
4.4 Discussion	112
4.4.1 Comparisons of historic and current PAH concentrations.....	112
4.4.2 PAH concentrations from present study.....	113
4.5 Conclusion.....	119
5. Behavioural and neurotoxicity assessment of <i>H diversicolor</i> following exposure to environmentally relevant concentrations of Cu, Pb and pyrene.....	121
5.1 Introduction	121
5.2 Materials and methods.....	124
5.2.1Chemicals	124
5.2.2 <i>H diversicolor</i>	124
5.2.3 Sediment spiking and tank set up.....	124
5.2.4 Burrowing Behaviour Assessment.....	125
5.2.5 Acetylcholinesterase Activity	126
5.2.6 Total Metal sediment and Worm Tissue Determination	126

5.2.7 Pyrene Sediment and Worm Tissue Determination	127
5.3 Statistical analysis.....	127
5.4 Results.....	127
5.6 Discussion	143
5.6.1 Cu test series	143
5.7 Conclusion.....	150
6. Bioaccumulation and biochemical responses of <i>H diversicolor</i> following exposure to Pb and pyrene.	151
6.1 Introduction	151
6.2 Materials and Methods	153
6.2.1 Chemicals	154
6.2.2 Super Oxide Dismutase Activity.....	155
6.2.3 Cytochrome p450 Activity.....	155
6.2.4 Glutathione-S-Transferases Activity	156
6.2.5 8 – hydroxy - 2' - deoxyguanosine	157
6.2.6 Metallothionein activity.....	157
6.3 Statistical analysis.....	158
6.4 Results.....	158
6.4.1 Sediment Pb concentration.....	159
6.4.2 Pyrene sediment results	159
6.4.3 Worm Tissue Pb concentration Results	160
6.4.4 Worm Tissue Pyrene and 1-Hydroxypyrene metabolite concentrations	163
6.4.5 Biochemical responses.....	167
6.4.6 Relationships of worm tissue concentrations and biochemical responses	180
6.5 Discussion	180
6.5.1 Pb assimilation and excretion	180
6.5.2 Metallothionein's	184
6.5.3 Regulation of reactive oxygen species.....	185
6.5.4 Induction of oxidative damage in DNA by Pb and Pyrene	189
6.6 Conclusion.....	190
7. Energy alterations of <i>H diversicolor</i> following exposure to pyrene and Pb.....	192
7.1 Introduction	192
7.2 Materials and methods.....	195
7.2.1 Reagents.....	195

7.2.2 Tank Set up and sediment spiking	195
7.2.3 Worm tissue energy determination	195
7.2.4 Statistical analysis	197
7.3 Results.....	198
7.3.1 Worm tissue Pb concentrations	198
7.3.2 Protein determination	199
7.3.3 Lipid determination	202
7.3.4 Total carbohydrate determination	204
7.3.5 Statistical relationships	207
7.4 Discussion	208
7.5 Conclusion.....	211
8 General Discussion	213
8.1 Thesis summary and contribution to original knowledge	213
8.2 Metal bioavailability from environmental matrices of the Fleet lagoon, Dorset UK.....	213
8.3 Polycyclic aromatic hydrocarbons within the environmental matrices of the Fleet lagoon and bioaccumulation by <i>H diversicolor</i>	216
8.4 Behavioural alterations of <i>H diversicolor</i> following exposure to Cu, Pb and pyrene individually and in combination.	218
8.5 Biochemical responses following exposure to Pb and pyrene by <i>H diversicolor</i>	220
8.6 Energetic costs of Pb and pyrene exposure.	224
8.7 Limitations	226
8.7.1.....	226
8.7.2 Cu exposure to <i>H diversicolor</i>	227
8.7.3 Pyrene assimilation.....	227
8.8 Further research	228
8.9 Conclusion.....	229
9. References	233
Appendix 1.....	268
Appendix 2.....	269

List of Tables

Table 1 Molecular and cellular effects of metals on marine invertebrate species.....	11
Table 2 Polycyclic aromatic Hydrocarbons found within the Marine environment.....	14
Table 3 Research regarding PAH toxicity and marine organisms.....	15
Table 4 Sediment spiking concentrations.....	47
Table 5 Results for certified reference material.....	48
Table 6 Results for analysis (mg kg ⁻¹) of certified reference material TORT-2.....	49
Table 7 Retention times, linearity (r^2 and RSD (%)) of calibration curves for 16 individual PAH from PAH calibration mix traceable certified reference material.....	51
Table 8 DL and MDL for Varian ICP - OES	52
Table 9 GPS coordinates of all 10 sample sites of the Eastern Shoreline of the Fleet Lagoon	61
Table 10 Particle size analysis (mean +/- 1SE) of sediment samples ($n = 3$) taken from sample locations of the Fleet lagoon as detailed in Chapter 2 (2.1.1.1).....	66
Table 11 Particle descriptors of sediment samples taken from sample locations in the Fleet Lagoon	67
Table 12 Concentrations (dry weight mg kg ⁻¹) of As, Ni, Pb and Zn from 10 sample locations (sample: $n = 3$) of the Eastern shoreline of the Fleet Lagoon, Dorset	70
Table 13 Metal concentrations ($\mu\text{g l}^{-1}$) in water samples ($n = 1$) from all 10 sample locations of the Fleet Lagoon, Dorset	71
Table 14 Concentrations of metals (mean +/- 1SE) (dry weight mg kg ⁻¹) in worm tissue.....	72
Table 15 As concentrations (mean +/- 1SE) (mg kg ⁻¹ dry weight) each step of the BCR sequential analysis	74
Table 16 Cu concentrations (mean +/- 1SE) (mg kg ⁻¹ dry weight) each step of the BCR sequential analysis	75
Table 17 Ni concentrations (mean +/- 1SE) (mg kg ⁻¹ dry weight) each step of the BCR sequential analysis	76
Table 18 Pb concentrations (mean +/- 1SE) (mg kg ⁻¹ dry weight) each step of the BCR sequential analysis	77
Table 19 Zn concentrations (mean +/- 1SE) (mg kg ⁻¹ dry weight) each step of the BCR sequential analysis	78
Table 20 Concentrations of metals ($\mu\text{l l}^{-1}$) found in pore water analysis.....	79
Table 21 Proteinase K sediment digestion.....	80

Table 22 Pearson's correlation results of total metal concentrations and the individual steps of the BCR sequential sediment digestion	81
Table 23 Correlations between metal concentrations found in sediment (mg kg^{-1}) and worm weight.....	82
Table 24 PAH concentrations for sediment samples ($n = 3$) taken from 10 sample sites of the Fleet Lagoon	106
Table 25 PAH Concentrations of worm tissue $\mu\text{g ml}^{-1}$	108
Table 26 PAH analysis of Fleet lagoon sediment conducted by Nunney and Smith (1995) ($\mu\text{g kg}^{-1}$ dry weight).....	113
Table 27 Initial analysis of sediment following addition of manufactured sea water prior to the addition of worms.....	125
Table 28 Initial analysis of sediment following addition of manufactured sea water prior to the addition of worms.....	154
Table 29 Pb concentrations found in sediment from all Pb test conditions for the duration of the experiment.....	159
Table 30 Pyrene concentrations in sediment from all test conditions throughout the duration of the experiment.....	160
Table 31 Pb concentrations (mg kg^{-1}) in worm tissue ($n = 3$) from Pb exposed conditions taken on sample days over the duration of the test experiment.....	198
Table 32 Pyrene concentrations ($\mu\text{g kg}^{-1}$) in worm tissue ($n=3$) taken from individuals from all pyrene exposed conditions.....	199

List of Figures

Figure 1 Metal inputs into the marine environment.....	5
Figure 2 Organism response following metal exposure.....	9
Figure 3 Sources of environmental PAH inputs.....	13
Figure 4 <i>H. diversicolor</i> morphological features.....	21
Figure 5 Sources to Adverse outcome pathway.....	22
Figure 6 Toxicity of metals and PAH's.....	23
Figure 7 detoxification of Reactive oxygen (ROS).....	24
Figure 8 Chromatograph depicting pyrene detection using a Perkin Elmer 200 series HPLC pump and 275 auto injector.....	43
Figure 9 Chromatograph illustrating 1-hydroxypyrene detection using a Perkin Elmer 200 series HPLC pump and 275 auto injector.....	43
Figure 10 Calibration chart for 1-hydroxypyrene.....	50
Figure 11 Calibration chart for pyrene.....	50
Figure 12 Map depicting the Fleet Lagoon highlighting freshwater inlets.....	58
Figure 13 Geology of the Fleet Lagoon.....	60
Figure 14 Fleet lagoon tidal flow.....	60
Figure 15 Fleet lagoon sample locations.....	61
Figure 16 Fleet lagoon digital images.....	62
Figure 17 Loss on ignition results.....	68
Figure 18 BCR step 1 and proteinase k comparisons.....	84,85
Figure 19 Fla /(Fla+Pyr) Vs Ant (Ant+Phe) graph.....	110
Figure 20 HMW/LMW Vs Fla/Pyr graph.....	111
Figure 21 Acetone and control tanks Burrowing behaviour results($n=10$).....	127
Figure 22 Cu 15 mg kg ⁻¹ spiked sediment test series results showing burrowing behaviour time (s) and concentrations of Cu in whole worm tissue and sediment.....	129
Figure 23 Burrowing time (s) for ($n=10$ individual worms) Cu 15.8 mg kg ⁻¹ +Pyrene 480 µg kg ⁻¹ test condition over a period of 20 min.....	130
Figure 24 Burrowing time (s) for ($n=10$ individual worms) Pb9.2 mg kg ⁻¹ test condition over a period of 20 min.....	132
Figure 25 Burrowing time (s) for ($n=10$ individual worms) Pb9.2 mg kg ⁻¹ +Pyrene 970 µg kg ⁻¹ test condition over a period of 20 min.....	133

Figure 26 Burrowing time (s) for ($n=10$ individual worms) Pb4.5 mg kg ⁻¹ test condition over a period of 20 min.....	135
Figure 27 Burrowing time (s) for ($n=10$ individual worms) Pb4.5 mg kg ⁻¹ + Pyrene 480 µg kg ⁻¹ test condition over a period of 20 min.....	136
Figure 28 Burrowing time (s) for ($n=10$ individual worms) Pyrene 970 µg kg ⁻¹ test condition over a period of 20 min.....	138
Figure 29 Burrowing time (Secs) for ($n=10$ individual worms) Pyrene 480 µg/Kg test condition over a period of 20 min.....	139
Figure 30 AChE activity for worms exposed to test conditions Pb4.5 mg kg ⁻¹ , Pyrene 480µg kg ⁻¹ , Pb4.5 mg kg ⁻¹ + Pyrene 480 µg kg ⁻¹ and control for a period of 7 days.....	140
Figure 31 AChE activity for worms exposed to the test conditions Pb9.2 mg kg ⁻¹ , Pb9.2 mg kg ⁻¹ + Pyrene 970 µg kg ⁻¹ , Pyrene 970 µg kg ⁻¹ and control (µg mg ⁻¹) for a period of 7 days.....	141
Figure 32 show mean worm tissue Pb concentrations; Pb9.2 mg kg ⁻¹ and Pb9.2 mg kg ⁻¹ +Pyrene 970 µg kg ⁻¹	161
Figure 33 show mean worm tissue Pb concentrations; Pb4.5 mg kg ⁻¹ and Pb4.5 mg kg ⁻¹ +Pyrene 480 µg kg ⁻¹	162
Figure 34 Pyrene and 1-OHP(ug kg ⁻¹) concentrations found in worm tissue ($n=3$) from test conditions Pb4.5 mg kg ⁻¹ + Pyrene 480µg kg ⁻¹	163
Figure 35 Pyrene and 1-OHP concentrations found in worm tissue ($n=3$) from test conditions Pb9.2 mg kg ⁻¹ + Pyrene 970µg kg ⁻¹	164
Figure 36 Pyrene and 1-OHP concentrations found in worm tissue ($n=3$) from test condition Pyrene 480µg kg ⁻¹	165
Figure 37 Pyrene and 1-OHP concentrations found in worm tissue ($n=3$) from test condition Pyrene 970µg kg ⁻¹	166
Figure 38 SOD activity expressed as 50% inhibition of SOD for the test conditions Pb9.2 mg kg ⁻¹ , Pyrene970µg kg ⁻¹ , and Pb9.2 mg kg ⁻¹ +Pyrene970 µg kg ⁻¹	167
Figure 39 SOD activity expressed as 50% inhibition of SOD for the test conditions Pb4.5mg kg ⁻¹ , Pyrene480µg kg ⁻¹ , and Pb4.5 mg kg ⁻¹ +Pyrene480µg kg ⁻¹	169
Figure 40 GST Activity(U mol min ⁻¹) of worms ($n=3$) from test conditions Pb9.2 mg kg ⁻¹ , Pyrene 970µg kg ⁻¹ , Pb9.2 mg kg ⁻¹ + Pyrene 970 µg kg ⁻¹ and control.....	171
Figure 41 GST(U mol min ⁻¹) activity for worms ($n=3$) from test conditions Pb4.5 mg kg ⁻¹ , Pyrene480µg kg ⁻¹ and the mixture Pb4.5 mg kg ⁻¹ +Pyrene480 µg kg ⁻¹	173
Figure 42 Cytochrome P450 concentrations (nmol/ml) for individuals ($n=3$) exposed to the test conditions Pb9.2 mg kg ⁻¹ , Pyrene970 µg kg ⁻¹ and the mixture Pb9.2 mg kg ⁻¹ + Pyrene 970 µg kg ⁻¹	175
Figure 43 Cytochrome P450 concentrations (nmol/ml) for individuals ($n=3$) exposed to the test conditions Pb4.5mg kg ⁻¹ , Pyrene480 µg kg ⁻¹ and the mixture Pb4.5 mg kg ⁻¹ + Pyrene 480 µg kg ⁻¹	177
Figure 44 8-OHdg concentrations (pg/ml) for individuals ($n=3$) exposed to test conditions Pb9.2 mg kg ⁻¹ , Pyrene970 µg kg ⁻¹ , Pb9.2 mg kg ⁻¹ +Pyrene970 µg kg ⁻¹ and the control group.....	179

Figure 45 8-OHdg concentrations ($\mu\text{g ml}^{-1}$) for individuals ($n=3$) exposed to the test conditions Pb4.5 mg kg^{-1} , Pyrene480 $\mu\text{g kg}^{-1}$, Pb4.5 mg kg^{-1} +Pyrene480 $\mu\text{g kg}^{-1}$ and the control group.....	180
Figure 46 Protein concentrations ($\mu\text{g/ml}$) for worms ($n=3$) from test conditions Pb9.2 mg kg^{-1} , Pyrene970 $\mu\text{g kg}^{-1}$ and Pb9.2 mg kg^{-1} +Pyrene970 $\mu\text{g kg}^{-1}$	200
Figure 47 Protein concentrations ($\mu\text{g/ml}$) for worms($n=3$) from test conditions Pb4.5 mg kg^{-1} , Pyrene480 $\mu\text{g kg}^{-1}$ and Pb4.5 mg kg^{-1} +Pyrene480 $\mu\text{g kg}^{-1}$	201
Figure 48 Lipid concentration for test conditions Pb9.2 mg kg^{-1} , Pyrene $\mu\text{g kg}^{-1}$, Pb9.2 mg kg^{-1} +Pyrene970 $\mu\text{g kg}^{-1}$ and control group (sample size $n=3$).....	202
Figure 49 Lipid determination for test conditions Pb4.5 mg kg^{-1} , Pyrene480 $\mu\text{g kg}^{-1}$, Pb4.5 mg kg^{-1} +pyrene480 $\mu\text{g kg}^{-1}$ and the control group (sample size $n=3$).....	204
Figure 50 Total carbohydrate results for worms ($n=3$) exposed to test conditions Pb9.2 mg kg^{-1} , Pyrene970 $\mu\text{g kg}^{-1}$, Pb49.2 mg kg^{-1} +pyrene970 $\mu\text{g kg}^{-1}$	205
Figure 51 Total carbohydrate results for worms ($n=3$) exposed to test conditions Pb4.5 mg kg^{-1} , Pyrene480 $\mu\text{g kg}^{-1}$, Pb4.5 mg kg^{-1} +pyrene480 $\mu\text{g kg}^{-1}$	206

List of Appendices

Appendix 1. PAH analysis of water and sediment conducted by the external laboratory, I2 analytical Ltd, UK.....	270
Appendix 2 Glutathione Calibration graph.....	271

Abbreviations

AChE- Acetylcholinesterase

Ag-Silver

Ant-Anthracene

As-As

ATP-Adenosine triphosphate

AVS-Acid Volatile sulphides

Au-Gold

Bi-Bismuth

Ca-Calcium

Cd-Cadmium

CdS-Cadmium Sulfate

Co-Cobalt

Cr-Chromium

Cu-Cu

CuO-Cu oxide

CYP450- Cytochrome P450

DL-Detection limits

DNA-Deoxyribonucleic acid

EA-Environment agency

EPA- European Protection Agency

Fe-Iron

FeS-Iron sulfide

Flu- Fluoranthene

Ga-Gallium

GCMS-Gas chromatography mass spectrometry

GST- Glutathione-S-Transferase

H₂O₂-Hydrogen peroxide

HCl-Hydrochloric acid

Hg-Mercury
HgCl₂-Mercuric chloride
HPLC-High pressure liquid chromatography
HMW-High molecular weight
HNO₃-Nitric acid
In-Indium
Ir- Iridium
K-Potassium
K_a-Kurtosis
K_{oc}-Organic carbon partition coefficient
K_{ow}- Octanol water partition
LMW-Low molecular weight
MDL-Method detection limits
Mn-Manganese
Mo-Molybdenum
MT-Metallothionein
MTLP-Metallothionein like proteins
Ni-Ni
PAH-Polycyclic aromatic hydrocarbons
PEL-Potential effects limits
Pb-Pb
Pd-Palladium
PHE-Phenanthrene
Pt-Plutonium
Pyr-Pyrene
Rh-Rhodium
ROS-Reactive oxygen species
Sb-Antimony
Se-Selenium
SEM-Simultaneously extracted metal
Sk_a-Skewness
Sn-Tin

SOD-Super oxide dismutase

TEL- Threshold effects limits

Ti-Titanium

V-Vanadium

X_a-Average grain size

Zn-Zn

ZnO-Zn Oxide

1-OHP-1-hydroxypyrene

8-OHdG-8-hydroxy-2`-deoxyguanosine

σ_a-Sediment sorting

ACKNOWLEDGEMENT

I would like to offer my deepest thanks to my supervisors Dr Iain Green and Associate Professor Roger Herbert. They have both guided me through this process and without their expertise, endless patience and kindness this thesis would never have been written. I would like to offer my thanks to Nikky Jones who trained me to use the HPLC and was always there to help when things undoubtedly went wrong. As always, my husband Mark Bagwell has offered unwavering support. Without his encouragement, I would have never applied for a PhD and without his understanding, never have completed it. To my children Bernie and Amelia, you have always supported me and cheer me along. Lastly, I am very grateful to Bournemouth University for allowing me to complete this research and providing me with funding to do so.

Declaration

I declare that the work in this thesis was made in accordance with the requirements of the University's code of Practice for Research Degrees and that it has not been submitted for any other academic award. The work is the candidate's own. Work is done with the assistance of others as indicated.

1. Introduction

1.1 Overview

Oceans provide a sink for many manufactured and naturally occurring chemicals of which, 16 polycyclic aromatic hydrocarbons (PAH's) and certain metals are considered priority pollutants (EPA, 2018). As a consequence, marine organisms may be exposed to mixtures of these contaminants where bioaccumulation (Brown and Takada, 2017) may result in unpredictable co-toxic effects, subsequently altering the ecological risk (Gauthier et al., 2014). Yet, the majority of marine organism toxicity research is conducted on single contaminants (Banni et al., 2009), even though co-toxicities of contaminant exposures are frequently hypothesised (Fleeger et al., 2007, Gauthier et al., 2014). For example, Chen et al. (2018), demonstrated the depression of antioxidant response following exposure to mixtures of either Cu, Cd or Pb and benzo [a] pyrene in the mussel *Mytilus coruscus* than found in single exposures. Consequently, there is a requirement to investigate the interactions of contaminant mixtures to determine the risk posed to marine organisms (Wang et al., 2011a).

PAH's are released into the environment through natural pyrolytic events (volcanic eruptions and forest fires), combustion of fossil fuels and biomass, direct and in direct oil spills and natural seepage from oil shale (Boitsov et al., 2009; Jiao et al., 2009; Luo et al., 2008; Page et al., 1999). PAH's assimilate within marine organisms through epidermal uptake and ingestion (Gauthier et al., 2014). Once assimilated, metabolism of PAH's alters the chemical structure, allowing excretion (Geissing et al., 2003). However, some intermediate metabolic products of PAH's are observed to be highly carcinogenic and / or mutagenic (Barhoumi et al., 2011).

Metals in the environment naturally derive from the Earth's crust through erosion and abrasion of rocks and sediment (Garrett, 2000).

However, metal concentrations within the marine environment have increased due to industrialisation, direct and indirect dumping of waste, and leachate from land (Frignani and Bellucci, 2004; González-Fernández et al., 2011; Ibrahim and Mutawie, 2013). Certain metals are essential for biological function and therefore mechanisms exist for regulation, accumulation and excretion (Luoma and Rainbow, 2005; Rainbow et al., 1990). However, high environmental concentrations of essential metals and uptake of non-essential metals via ion mimicry may elicit toxicity (Berthet et al., 2003; Wang and Fisher, 1999a).

A limited number of investigations regarding the toxicities of metals and PAH exposure have been conducted, where results demonstrate more than additive effects on mortality rates (Gauthier et al., 2016), biochemical markers of oxidative stress (Chen et al., 2018; Díaz-Jaramillo et al., 2017; Gauthier et al., 2016; Gopalakrishnan et al., 2011; Wang et al., 2011a), neurotoxicity (Banni et al., 2009), and altered assimilation of metals / PAH's (Diaz-Jaramillo et al., 2017; Gauthier et al., 2016; Wang et al., 2011a; Banni et al., 2009).

Importantly, the hydrophobic nature of PAH's and the affinity of metal ion sorption to sediment and organic particulates results in sedimentary settlement potentially leading to concentrations higher than those found in the water column (Gauthier et al., 2014).

Consequently, it is necessary to conduct investigations into the risk following exposure to mixtures of contaminants using sediment dwelling marine organisms such as the common ragworm *Hediste diversicolor* (O.F.Muller, 1776) to elucidate the toxicological responses (Wang et al., 2011a). This PhD research will investigate the toxicological responses of *H. diversicolor* following exposure to metals and PAH's (alone and in combination) to determine additive toxicities.

1.2 Literature Review

1.2.1 Threats to the marine environment

1.2.1.1 Marine pollution

Anthropogenic industrial activities and increased human population progressively contribute to the rise of marine pollution via direct inputs such as burning of fossil fuels, oil spills (Yunker et al., 2002), dumping of waste (Jambeck et al., 2015) and sewage overflows (Au et al., 2000). Indirect inputs from agricultural and industrial land runoff contribute pesticides, fertilizer and petrochemicals, whilst leachate from landfill sites may contain metals and petrochemicals (Polidoro et al., 2016). Aside from the concentrations of pollutants, the transboundary nature of the marine environment allows long distance transport of pollutants within the water column, which accumulates in regions governed by tidal flows including coastal habitats such as lagoons and estuaries (Echeveste et al., 2016).

Climate change, associated sea water temperature rise, reduction of oxygen and the alteration of seawater chemistry, such as increased acidity related to increased carbon dioxide levels, may further influence the toxicity of marine pollution (Deutsch et al., 2015). Temperature and pH modification are recognised factors in the alteration of some chemical pollutants (Xue et al., 2016) and have been evidenced to increase toxicity following exposure (Cao et al., 2018; Lewis et al., 2016; Marangoni et al., 2019; Nardi et al., 2018; Rodríguez-Romero et al., 2014b). Additionally, sea temperature rise may increase the metabolic rate and ventilation of many marine organisms, influencing contaminant assimilation and potential toxicity (Schiedek et al., 2007). Co - toxic effects of temperature and pH alterations were demonstrated by Nardi et al. (2015) who detailed disturbances to oxidative stress and immune system function. Increased bioaccumulation of trace metals from sediment in the polychaete *H diversicolor* were reported at lowered pH levels (Rodríguez-Romero et al., 2014a). However, reduced pH (7.5) increased cellular defence responses in *H diversicolor* (Freitas et al.,

2017), highlighting the need for further research regarding pollution and climate change driven sea water alterations.

Coastal lagoons are shallow water ecosystems that are partly or fully enclosed via depositional barriers from the sea and which are heavily influenced by tidal flushing, freshwater inputs, depth and evaporation (Bird, 1994). Within these environments, high levels of ecosystem system services are provided including watershed protection, leisure activities, protective nurseries for important biota and carbon sequestration (Gedan et al., 2011). Moreover, high productivity and shelter provides a habitat for many protected species including seagrass, fishery species and wading birds (Newton et al., 2014). Yet, lagoons are subjected to terrestrial, atmospheric and aquatic pollution inputs including metals, pesticides, pharmaceuticals, plastics and PAH's, which may be present either individually or within complex mixtures (De Wit et al., 2017). Such contaminants may be persistent and accumulate within the environment due to low tidal flushing and water exchange, degrade to more toxic states and elicit deleterious effects upon marine organisms (Rossi et al., 2016).

Upon entry to the marine environment, sediments remain the sink for such pollutants as shown in Figure 1 (Remaili et al., 2016a).

Adsorption of pollutants to organic matter within the water column, which subsequently settle upon bottom sediment results in acute and chronic capture of contamination (Peng et al., 2009). However, sediment may further act as a source for contamination during periods of hydrodynamic action, bioturbation by invertebrates, marine vessels and anthropogenic disturbance, which serves to re - release contamination back into both the pore water fraction surrounding sediment and the water column (Bryan and Langston, 1992; Eggleton and Thomas, 2004; Remaili et al., 2016b).

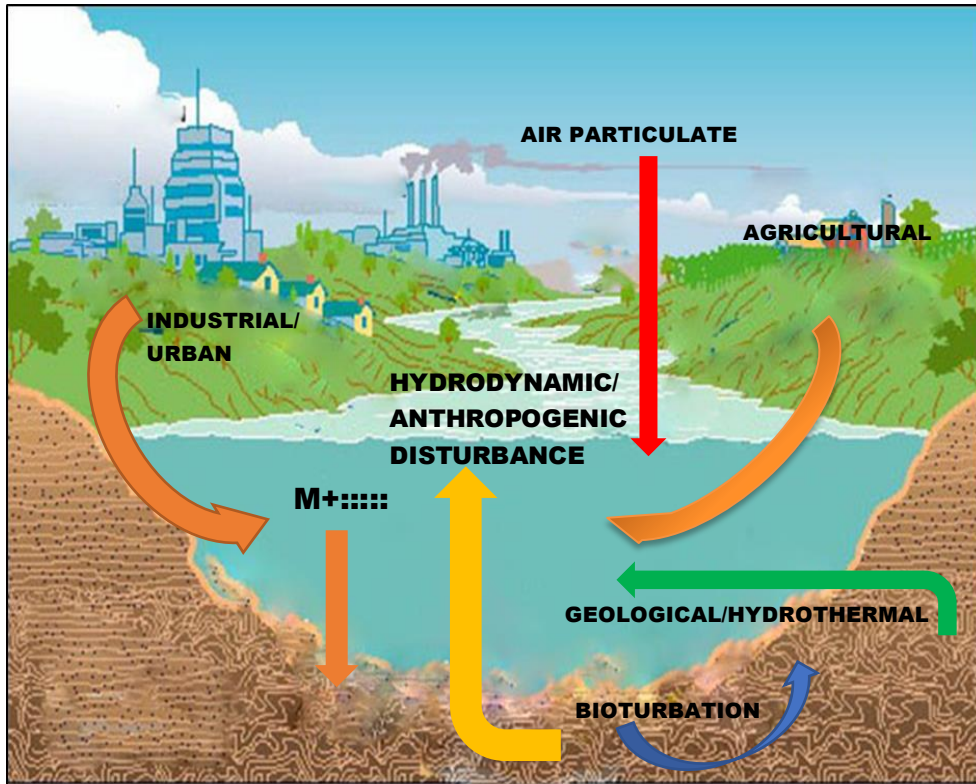


Figure 1. Metal inputs into the marine environment. Air particulate matter derives from anthropogenic sources including industrial / urban burning of fossil fuels and natural sources such as volcanic eruptions. Agricultural inputs include use of pesticides and wastewater. Industrial and urban inputs include wastewater leachate, leachate from land fill and direct dumping of contaminated waste. Bioturbation of sediment by benthic invertebrates allows the re - release of sediment bound metals. Geological processes and hydrothermal venting provide direct natural inputs. M+::::: denotes metals from sources binding to organic particulate matter within the water column which then settles on to the sediment bed.

1.3 Marine Metal Pollution

1.3.1 Heavy Metals?

Within this review, the term heavy metals will not be used as there appears to be inconsistencies throughout scientific literature regarding which metals belong to this group. Duffus (2002) detailed how confusions regarding metals labelled 'heavy' appear to arise from a lack of definition, with some authors using either mass, density, specific gravity or atomic number as means of classification. Furthermore, the term 'heavy metal' has not yet been defined by any authoritative body such as the International Union of Pure and Applied Chemistry (Hübner et al., 2010). Therefore, each metal within this study will be treated separately in accordance with individual toxicological properties.

1.3.2. Bioavailability of Metals within the Marine Environment

Bioavailability of metals may be defined as the fraction of total metal readily available for uptake by organisms via water, sediment and food which in turn, elicit effects upon the organism (Rainbow et al., 2009a). Metal speciation / fractionation (i.e. the chemical form) is the primary factor that governs bioavailability, which is further influenced by environmental conditions such as temperature and aqueous chemistry including pH (Park et al., 2014), salinity (Li et al., 2008) and dissolved oxygen (Maruya et al., 2012). Metals are commonly bound to sediment via ion exchange, precipitation or adsorption (Gaillard et al., 1986). The bioavailability of the different fractions are frequently analysed using sequential chemical extraction methods such as the three stage extraction scheme (SM&T) which supersedes the BCR (commission of the European Communities, Community Bureau of Reference 1992) (Pini, 2014). This three-step sequential chemical extraction procedure targets the soluble and exchangeable fraction (F1), reducible fraction (F2), and the

oxidizable fraction (F3), leaving the residual fraction (F4) (Pueyo et al., 2008; Yoo et al., 2013).

Within seawater, metal elements are present as ions, organic or inorganic complexes, and as insoluble compounds adsorbed to suspended particulates (Du Laing et al., 2009). Ionic forms are considered to have high bioavailability due to penetration of the mucous membranes in marine organisms (Bajger et al., 2011). However, ingestion of contaminated sediment particles provides an additional contamination exposure pathway for depositional feeders (Buffet et al., 2011). Yet, sequential extraction analysis does not address bio-accessible fractions solubilized during the gastrointestinal processes following ingestion of contaminated sediment particles (Bignasca et al., 2011). Therefore, the applicability of using sequential extraction alone when determining bioavailability of metals using deposit feeding fauna as chosen species may be questioned. The use of biomimetic approaches, including that of the digestive enzyme proteinase K, are evidenced to mimic the complexation and exchange with ligands of metals within the gastric environment of sediment dwelling marine invertebrates (Bignasca et al., 2011; Ianni et al., 2010; Rosado et al., 2016; Turner, 2006), increasing the accuracy of bioavailability assessment. However, the superiority of biomimetic digestion over sequential extraction techniques to determine metals bioavailability are yet to be fully established.

1.3.3 Marine Metal Contamination Inputs

Metals are naturally present within the environment, emitted into the atmosphere from aerosol particulate matter from volcanic eruptions or the water column via hydrothermal venting (Resing et al., 2015), and released from rocks and sediment through natural erosion processes (Hechun et al., 1988; Vriens et al., 2019). Metals are then subject to transport in solid or dissolved form via tides, currents, rivers and streams (Young and Ishiga, 2014). Yet, anthropogenic industrial activity including electroplating, mining operations,

manufacture and disposal of batteries, smelting, burning of fossil fuels and contaminated materials (Ibrahim et al., 2016) progressively contributes to the accumulation of metals, in particular As, Cd, Cu, Fe, Pb, Ni, and Zn into the marine environment through aerosol particulate matter, land run off, leachate and dumping of toxic wastes at sea (Chiarelli et al., 2014).

1.3.4 Toxicity of Metal Pollution

Metals which have eco toxicological relevance (Ag, As, Au, Bi, Cd, Co, Cr, Cu, Fe, Ga, Hg, In, Ir, Mn, Mo, Ni, Pb, Pd, Pt, Rh, Sb, Se, Sn, Ti, V, and Zn) do not biodegrade, resulting in their toxicity and behaviour being influenced by chemical and physio - chemical processes of the marine environment (Álvarez-Muñoz et al., 2016). Some metals, such as Mn, Fe, Cu and Zn are crucial trace nutrients for biological reactions although sufficiently high exposure elicits toxic effects (Aboul-Ela et al., 2011). Cellular response following metal exposure is therefore related to the concentration level, exposure time (long or short term) and individual metal (Figure 2).

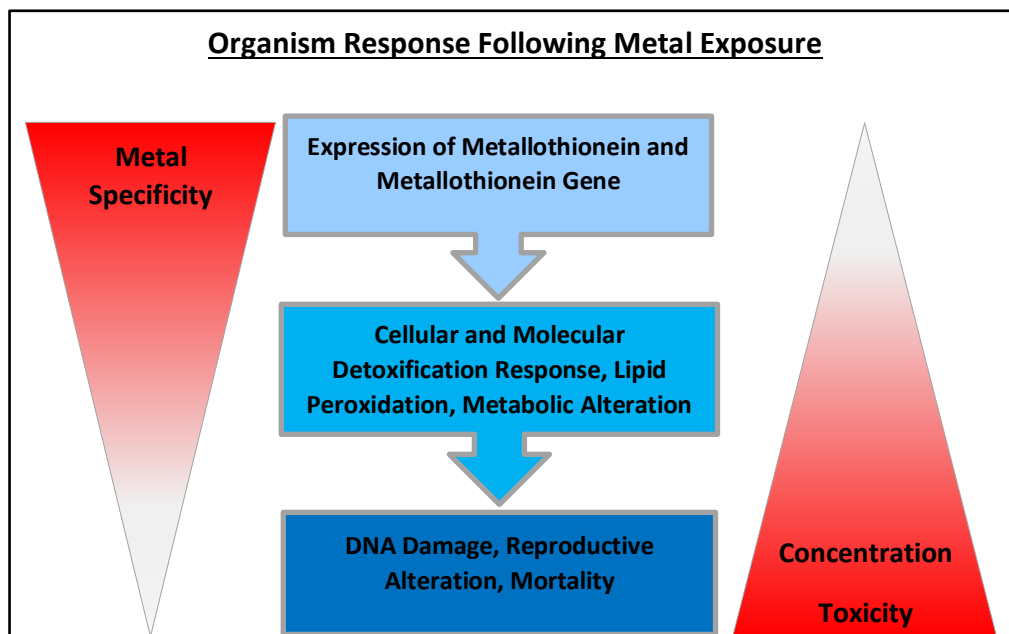


Figure 2. Organism response following metal exposure. Schematic illustration depicting traditional biomonitoring analysis whereby metal specificity, concentration levels and individual toxicities may result in a cascade of cellular and molecular expression.

The current literature regarding the toxicity of metals to marine invertebrates (Table 1), demonstrates multiple negative observations across a range of species, from laboratory experiments including oxidative stress and cellular damage. Furthermore, studies regarding fecundity and gamete health status highlight negative influences that may be evidenced at population levels and have far reaching negative effects upon the ecosystem health.

Table 1. Molecular and cellular effects of metals on marine invertebrate species.

Species	Metal	Methodology	Results	Author (s)
<i>Hediste diversicolor</i> (Common ragworm) and <i>Scrobularia plana</i> (Peppery furrow shell)	Ag	10 µg l ⁻¹	Oxidative stress, apoptosis and DNA strand damage using microscopy techniques	(Mouneyrac et al., 2014)
	CdS	10 µg l ⁻¹		
	Au	100 µg l ⁻¹		
	ZnO	10 µg l ⁻¹		
	CuO	10 µg l ⁻¹ in dosed sea water		
<i>Mizuhopectin yessoensis</i> (Japanese scallop)	Cd	0.3 mg l ⁻¹ Cd dosed sea water	DNA strand breaks in gill cells using comet assay	(Slobodskova et al., 2012)
<i>Hydroides elegans</i> (serpulid worm)	Ag nano-particles	1, 10, 100, 1000 µg L ⁻¹	Growth and development retardation of larval stages and reduced settlement	(Chan and Chiu, 2015)
<i>Crepidula onyx</i> (slipper snail)				
<i>Balanus amphitrite</i> (striped barnacle)				
<i>Nereis virens</i> (King ragworm)	Cu	250 mg kg ⁻¹ spiked sediment	Reduced settlement of larvae calculated using observation and statistical analysis	(Watson et al., 2008)
	Cu	500 µg l ⁻¹	Reduced Embryonic survival using observation	
<i>Mytilus galloprovincialis</i> (Mussel)	As (III) and As (v)	50 µg l ⁻¹ in dosed sea water	Increased oxidative Stress and apoptosis, and cell development using microscopy techniques. Osmotic regulation disruption and energy metabolism interference using assay techniques	(Yu et al., 2016a)
<i>Ciona intestinalis</i> (sea squirt)	Ni nano-particles	<100nm dosed in seawater	Lipid peroxidation and DNA fragmentation of sperm plasma membrane and cells, decreased fertilization and mitochondrial membrane hyperpolarization.	(Gallo et al., 2016)
<i>Magallana gigas</i> (Pacific oyster)	Pb	5 µg l ⁻¹ in dosed sea water	Altered Ca ²⁺ homeostasis and fatty acid oxidation.	(Meng et al., 2018)
<i>Gibbula umbilicalis</i> (Flat top shell)	HgCl ₂	20 mg l ⁻¹ in dosed seawater	Acetylcholinesterase inhibition	(Cabecinhas et al., 2015)
<i>Mytilus galloprovincialis</i> (Mussel)	Cr(VI)	1-50 ng l ⁻¹ in dosed seawater	Reduced lysosomal membrane stability (digestive gland).	(Franzellitti et al., 2012)

Exposure to the metals As, Cd, Cu, Cr, Au, Ni and Ag were reported to initiate oxidative stress responses detected as biomarkers of antioxidant defence and lipid peroxidation (Franzellitti et al, 2012; Slobodskova et al., 2012; Mouneyrac et al., 2014; Gallo et al., 2016; Yu et al., 2016). However, where these antioxidant defences were not sufficient to regulate reactive oxygen species, further toxic responses were observed: reduction of lysosomal membrane stability (Franzellitti et al., 2012); fragmentation of sperm plasma membrane and cells (Gallo et al., 2016); apoptosis in coelomocyte cells (Mouneyrac et al., 2014); and DNA strand breaks (Mouneyrac et al., 2014; Slobodskova et al., 2012, Gallo et al., 2016). In addition, Meng et al., (2018) and Yu et al., (2016) demonstrated the energetic costs of Pb and As pollution exposure respectively, indicating a reduction in health status. Importantly, exposure of *Hydroides elegans* and *Nereis virens* larval stages to Cu and Ag demonstrated mortality and settlement (Chin and Chui et al., 2015; Watson et al., 2008), which may impact populations, biodiversity and biomass in environments where these contaminants are present at the concentrations investigated.

1.4 Polycyclic Aromatic Hydrocarbon Environmental pollution

1.4.1 Polycyclic Aromatic Hydrocarbon Environmental Inputs

PAH's are a group of several hundred organic chemical compounds comprising hydrogen and carbon atoms with two or more fused aromatic rings (Kuppusamy et al., 2016). They originate from a variety of natural and anthropogenic sources (Figure 3). However, global industrialization, increased requirement for energy, reliance on fossil fuels, subsequent processing and combustion of petroleum products containing PAH's results in a worldwide distribution of contamination within the terrestrial and aquatic environments (Gauthier et al., 2014; Luna-Acosta et al., 2015).

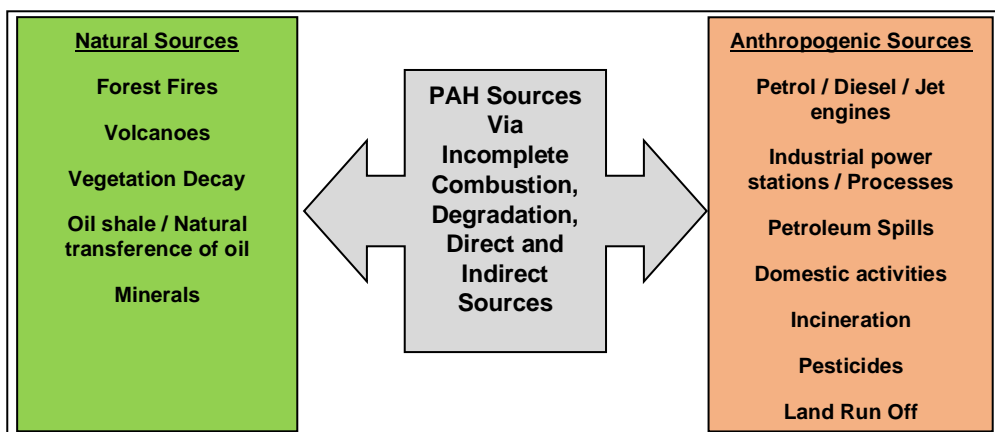


Figure 3. Sources of environmental PAH inputs. Anthropogenic and Natural processes which include incomplete combustion of petroleum products, fossil fuels and biomass. Further inputs include indirect geophysical release and direct anthropogenic inputs.

Pyrolytic PAH's derive from incomplete combustion of organic matter after which, the products condense to low molecular weight organic molecules, whereas petrogenic PAHs originate from the incomplete combustion of fossil fuels (Xue et al., 2016).

1.4.2 PAH's Characteristics and Toxicity

Individual PAH's illustrate an inverse relationship between Octanol-Water coefficient (K_{ow}) and water solubility whereby individual compounds with low water solubility show high K_{ow} , high molecular weight and high lipophilicity (Hylland, 2006). However, both pyrolytic and petrogenic PAH's as detailed in Table 2, can be found in complex mixtures within the marine environment (Hylland, 2006).

Table 2. Polycyclic aromatic Hydrocarbons found within the marine environment (Lee et al., 2013).

PAHs	Ring	Molecular Weight	Aqueous Solubility ($\mu\text{g l}^{-1}$)	Henry's Law Constant	Log K_{ow}
Acenaphthylene	2	152.2	3,930	$1.0^{10^{-1}}$ Pa/m³/mol	3.7
Acenaphthene	2	154.2	insoluble	$2.6^{10^{-1}}$ Pa/m³/mol	3.9
Fluorene	2	166.2	1,900	$6.5^{10^{-1}}$ Pa/m³/mol	4.18
Phenanthrene	3	178.2	1,050	$2.3^{10^{-1}}$ Pa/m³/mol	4.57
Anthracene	3	178.2		$2.0^{10^{-1}}$ Pa/m³/mol	4.45
Fluoranthene	3	202.3	201	$1.1^{10^{-1}}$ Pa/m³/mol	5.23
Pyrene	4	202.3	132	$4.1^{10^{-1}}$ Pa/m³/mol	5.18
Chrysene	4	228.3	1.9	2.1 Pa/m³/mol	5.81
Benzo[<i>b,k,j</i>] fluoranthene	4	252.3	0.8	$1.0^{10^{-1}}$ Pa/m³/mol	6.11
Benzo[<i>e</i>]pyrene	5	252.3	0.006	$3.3^{10^{-1}}$ Pa/m³/mol	6.44
Benzo[<i>a</i>]pyrene	5	252.3	1.6	6.2 Pa/m³/mol	6.13
Perylene	5	252.3	0.4	2.3 Pa/m³/mol	6.25
Indeno[1,2,3- <i>cd</i>] pyrene	5	276.3	2.6	$2.9^{10^{-1}}$ Pa/m³/mol	7.00
Benzo[<i>g,h,i</i>] perylene	6	276.3	0.7	$27^{10^{-1}}$ Pa/m³/mol	6.22

Temperature and salinity of seawater effects the solubility of PAH's where reduced solubility is observed with increasing salinity, and increased solubility observed with increasing temperature, thus allowing partitioning effects between dissolved and sorbed phases (Wang et al., 2001). Moreover, PAH's with relatively high Henry's law constants will evaporate from the surface of the water whereas high molecular weight PAH's will bind to organic colloidal particles such as marine bacteria and fulvic acids present in the water column prior to sediment deposition (Fleeger et al., 2007). As a result, sediment dwelling marine organisms may be exposed to chronic levels of PAH's directly via tissue contact or indirectly from contaminated particle and food ingestion. The toxic responses to PAH exposure are detailed in Table 3.

Table 3. PAH toxicity to marine invertebrate organisms.

Species	PAH	Test Methodology	Results	Author(s)
<i>Hediste diversicolor</i> (Common ragworm)	Benzo(a) pyrene	0.1, 0.5 mg ⁻¹ dosed sea water	Inhibition of antioxidant enzymes after 10-day exposure from intestinal tissue and coelomocytes. Destabilisation of lysosome membranes. DNA strand breaks.	(Catalano et al., 2012)
<i>Chlamys farreri</i> (Chinese Scallop)	Benzo (a) pyrene	0.1 µg ⁻¹ dosed sea water	Oxidative damage DNA strand breaks	(Guo et al., 2017)
<i>Chlamys farreri</i> (Chinese Scallop)	Chrysene	0.2, 0.8, 3.2 µg ⁻¹ dosed sea water	DNA strand breaks, lipid peroxidation at all exposure levels	(Xiu et al., 2016)
<i>Pecten maximus</i> (King scallop)	Phenanthrene	200 µg ⁻¹ dosed sea water	Oxidative stress and lipid peroxidation in haemolymph	(Hannam et al., 2010)
<i>Ruditapes philippinarum</i> (Manilla clam)	Phenanthrene Benzo (b) pyrene	86.7, 88.8, 544 and 763 ng g ⁻¹ spiked sediments in tanks with filter sea water	Lipid peroxidation and increased glutathione-s-transferases following exposure to all treatments. DNA strand breaks decreased over time in all exposures	(Martins et al., 2013)

Biomarkers of oxidative stress were reported for all exposures (Guo et al., 2017; Xiu et al., 2016; Martins et al., 2013; Catalano et al., 2012; Hannam et al., 2010). Importantly, lipid peroxidation and / or DNA strand breaks were reported in all cases and may result from insufficient regulation of reactive oxygen species (Chen et al., 2018).

1.4.3 PAH Toxicity Pathways

The non - polar behaviour of PAH's allow passive diffusion across cellular membranes, resulting in their ready uptake and subsequent detection within the tissues of marine organisms including the crested oyster *Ostrea equestris* (Pie et al., 2015), the Pacific oyster *Magallana gigas* (Zacchi et al., 2018) and marine polychaete *Perinereis rullieri* (Nesto et al., 2010). Biological responses to PAH exposure involve the action of the cytochrome P450 oxidase enzyme superfamily. These enzymes utilise a variety of compounds as substrates including contaminants, which are oxidised to produce polar compounds with enhanced water solubility, enabling the enhanced excretion and reduction of toxicity (Parente et al., 2014). Paradoxically, PAH's toxicity may be attributed to metabolism of the parent compound via cytochrome P450's resulting in carcinogenic, genotoxic and reactive oxygen metabolites (Nebert and Dalton, 2006).

Incorporation of PAH's into cellular membranes may expand membranes thereby altering fluidity (Wang et al., 2011a), with subsequent change in ion regulation further reducing the activity of the cell (Sikkema et al., 1995). Additionally, toxicity may be induced via light activation whereby excitation of PAH's to upper energy states leads to the formation of reactive oxygen species (ROS) or reaction with oxygen to form intermediate endoperoxides and quinones as stable end products, which are acknowledged to invoke lipid peroxidation and DNA damage (Gauthier et al., 2014).

1.4.4 Metal –PAH Co -Toxicity

Within the marine environment, exposure to chronic and diverse mixtures of contaminants, including metals and PAH's may exert antagonistic, additive, more than additive or non - additive co- toxicity to organisms (Gauthier et al., 2014). Despite this, the joint toxicity of

these pollutants are rarely examined (Fleeger et al., 2007).

Moreover, the behaviour and characteristics of each contaminant within a mixture may influence the uptake rate of each individual compound thereby increasing the assimilation, body concentration, subsequent toxicity and potential for bioaccumulation by trophic transfer (Gauthier et al., 2014).

Effects of co - toxicity have been observed. For example, Xiaolei et al, (2007) demonstrated that exposure to Cu^{2+} increased the cellular membrane sorption of PAH's during cellular ion transport.

Furthermore, Wang et al. (2011a) describe exposure to mixtures of Benzo [a] pyrene and cadmium increasing the rate of cadmium uptake in the clam *Ruditapes philippinarum*.

Although the capability of metal - PAH mixtures to elicit toxicity may be dependent upon the individual characteristics of each contaminant and their influences on each other, toxicity may arise from accumulative and influential action of each substance. Actions include mucus secretion (a favourable binding agent for PAH's) following surface contact and subsequent ingestion (Gauthier et al., 2014); metal exposure inhibiting cytochrome P450 enzymes responsible for the phase 1 metabolism of PAH (Wang et al., 2011a); PAH's eliciting an inhibitory effect upon metallothionein detoxification of metals following exposure to both contaminants (Costa et al., 2009) and mutual induction of ROS by both PAH's and metals resulting in cellular damage from lipid peroxidation and DNA damage via formation of 8-hydroxyguanine adducts (Peter et al., 2006; Yoo-Na and Mi-Young, 2011; Yu et al., 2006). However, understanding of mixed exposure remains limited. To address the current gaps in knowledge, altered metal / PAH uptake, inhibition of biochemical detoxification enzymes / proteins, alterations of behaviour and energy expenditure following exposure will be investigated in the present study.

1.5 Marine Organisms as Sentinels of Metal Pollution

Commonly, biomonitoring includes the use of marine invertebrate species, in particular bivalves as environmental biomarkers due to factors including ubiquitous distribution, low mobility, population abundance, and accessibility (Duarte et al., 2017; Viarengo and Nott, 1993). As invertebrate species occupy intermediate consumer positions in pelagic and benthic food webs, information gained from such investigations may be used to determine bioaccumulation through trophic transfer and ecosystem structural shifts which may result in the relocation or decline of resources and reduced biodiversity (Viarengo et al., 2007).

The use of *Mytilus edulis* within the international “Mussel Watch” program initiated during the 1970’s (Schöne and Krause Jr, 2016), evidenced accumulation and related toxicity to contamination (Luna-Acosta et al., 2015) both, globally along coastlines and in areas of environmental concern (Laitano and Fernández-Gimenez, 2016). However, marine invertebrate species which occupy different trophic levels may also exhibit varying toxicity to contamination. Therefore, to assess the health of an ecosystem, it is vital to examine effects upon species with differing physiologies that reside in contaminated environments (Viarengo et al., 2007). For example, marine sediment dwelling organisms including *H diversicolor* may be exposed to mixtures of contaminants which differ from those found in the water column. Furthermore, differing modes of feeding and the sedentary or active use of the environment may result in additional uptake pathways for contamination (Viarengo et al., 2007). Consequently, the sole use of an intermediate species from a contaminated environment to determine bioavailability and toxicity may provide an inaccurate assessment of risk.

1.5.1 Marine quality guidelines

To identify risks associated with contamination within marine matrices, quality guidelines have been developed. Hence, both water and sediment guidelines exist, developed from both empirical approaches identifying the relationship between contaminant concentration and toxic response in biota (Li et al., 2014) and theoretical approaches based on the prediction of bioavailability through equilibrium partitioning between matrices (Peña-Icart et al., 2017).

Empirical guidelines utilise threshold and probable effects levels (TEL / PEL) demonstrating risk associated to marine biota from specific concentrations. Commonly used empirical data based guidelines include the Floridian, Canadian, ANZECC and NOAA sediment quality guidelines, which were formulated from numerable toxicological investigations (CCME, 2001; McCauley et al., 2000). However, it is important to note that these quality guidelines are based upon single contaminant exposure. To date, there are no validated quality guidelines for mixed contaminant exposure for marine organisms.

1.5.2 Marine Polychaete species in Biomarker Research

The ragworm *H diversicolor* (O.F.Muller 1776), (phylum Annelida, class Polychaeta, order Aciculate, family Nereididae) is considered a key ecological species due its role in sediment bioturbation (Gillet et al., 2012; Sizmur et al., 2013) and as an important food source for wading birds and fish (Dierschke et al., 1999; Rosa et al., 2008; Santos et al., 2009). Additionally, this species is considered a suitable candidate for biological monitoring due to its broad distribution (Virgilio et al., 2009), limited dispersal ability and presence within polluted environments (Scaps, 2002). *H diversicolor*

has further been successfully used as a biomarker of contamination exposure within laboratory studies (Buffet et al., 2011; Cong et al., 2014; Freitas et al., 2017; Maranhão et al., 2015; Mouneyrac et al., 2003; Pires et al., 2016) and in the field (Aberson et al., 2011, 2016; Burlinson and Lawrence, 2007).

1.5.3 The Polychaete *Hediste diversicolor*, *Hediste* or *Nereis*?

Taxonomic status of the genus *Nereis* continues to be unclear as species of *Nereis virens* and *Nereis diversicolor* are generally denoted as *Neanthes virens* and *Hediste diversicolor*. Scaps (2002) conducted a comprehensive biological and ecological study upon the species *Hediste diversicolor* and further noted that molecular biologists use *Hediste* whereas ecologists prefer *Nereis*. For the purposes of consistency throughout this study, this species will be referred to as *H diversicolor*.

1.5.4 *Hediste diversicolor* Physiology

H diversicolor are found in brackish waters throughout the North Temperate Zone from Europe to the North American coast inhabiting Y or U - shaped burrows (Scaps, 2002). A temperate estuary inhabitant, this species can tolerate large variations in salinity and temperature with populations found in large densities that commonly feature gender ratios skewed towards the female (Kristensen, 1984). They are omnivorous with feeding methods including active predation, suspension and deposit feeding (Duport et al., 2006). Morphological features (Figure 4), include a flattened appearance with prominent dorsal blood vessel, reversible proboscis, four eyes, four pairs of tentacular cirri and two frontal antennae (Scaps, 2002).

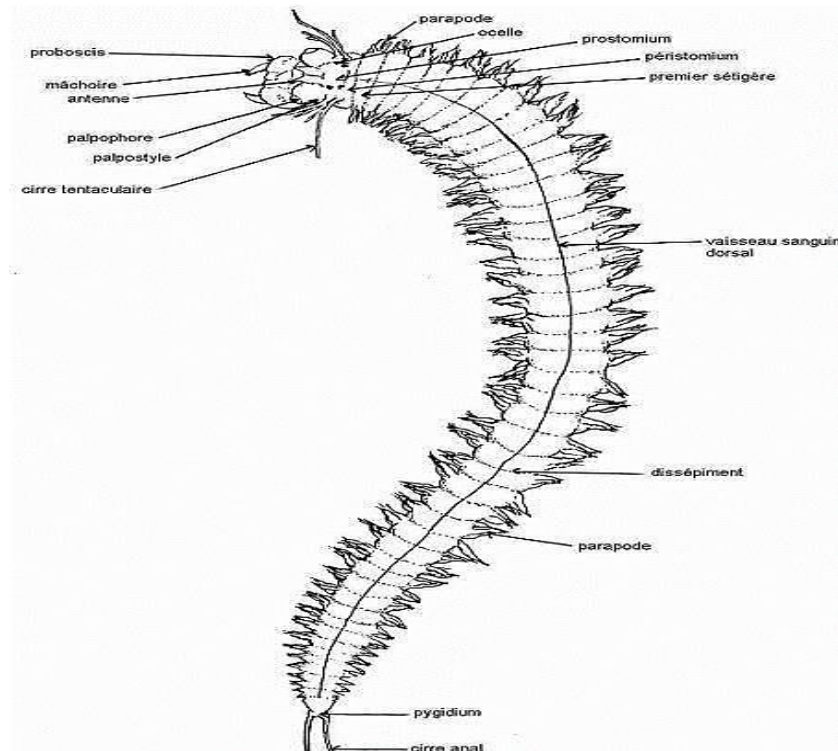


Figure 4. *Hediste diversicolor* morphological features (Scaps 2002).

1.5.5 Lifecycle

H diversicolor are gonochoristic, with adults reaching full maturity between 1 - 3 years with length ranging between 6 - 12cm consisting of 90 - 120 chaetigers (Scaps, 2002). Mature individuals are observed as brown / red in colour due to carotenoid pigments however, colouration changes to green during spawning caused by the presence of biliverdin and breakdown of haemoglobin in the gut, coelomic cavity and epidermis cellular walls (Scaps, 2002). Spawning occurs during the summer and autumn in accordance with environmental triggers and pheromone population coordination however, these events are terminal for both sexes (Hiddink et al., 2002).

1.5.6 Role in Lagoon ecosystems

H diversicolor is considered a keystone species due to high population densities found within sediment (Scaps, 2002) and as the

primary food source for wading birds (Baird et al., 1985; Moreira, 1999). The efficiency of suspension feeding of this species is considered high with Riisgard et al. (1996) suggesting that the extraction of phytoplankton and suspended particles from water exerts control of phytoplankton blooms. Furthermore, Moreira et al. (2006) detailed how reduced feeding by this species correlated to contaminant exposure, had deleterious effects upon the levels of detritus within sediment. Importantly, burrowing behaviour of this species provides a regulatory influence on the oxygenation of anoxic sediment (Kalman et al., 2009), which may affect the bioavailability of contaminants.

1.6 Biomarkers

Biomarkers are used within environmental monitoring to forecast toxic effects following exposure to contaminants (Buffet et al., 2011), via the assessment of a variety of endpoints and markers. Viarengo et al. (2007), developed the concept of adverse outcome pathways linking cellular, molecular and tissue alterations following exposure to adverse individual and population effects, thereby providing a method to calculate environmental risk (Connon et al., 2012) as illustrated Figure 5.

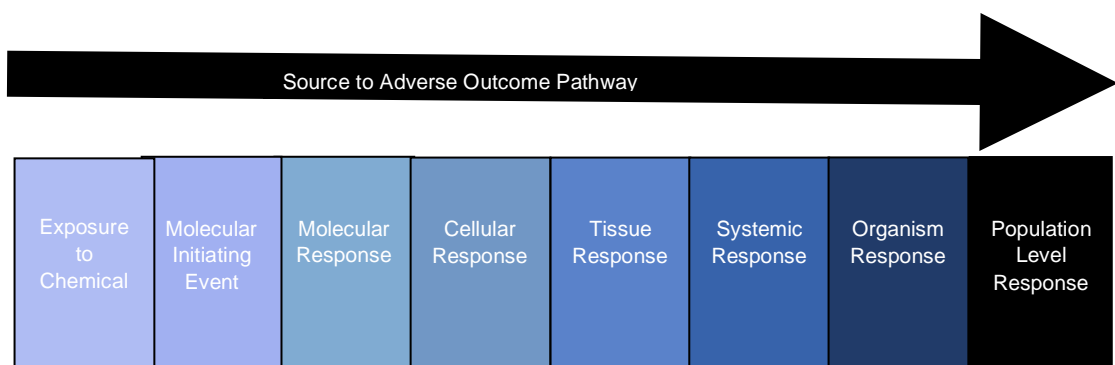


Figure 5. Sources to Adverse outcome pathway. Adverse Outcome Pathway illustrating the progressive effects whereby exposure to the chemical initiates a molecular response which may eventually Pb to deleterious effects at population level.

Analysis of multiple level interactions using adverse outcome pathways following exposure may categorise specific contaminants to ecosystem level effects and alterations to ecosystem services (Connon et al., 2012). However, to quantify the illustrated outcome pathways directly relating to health and survival of an organism using environmental levels of metals and PAH's, the mechanisms of individual and co-toxicity must first be identified as illustrated in Figure 6.

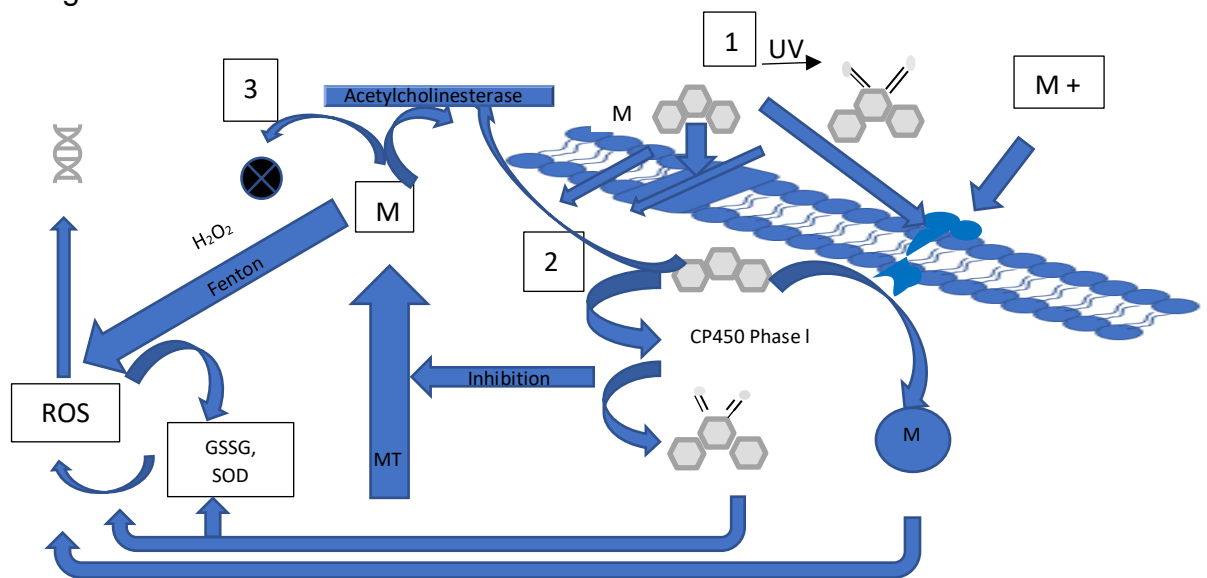


Figure 6. Toxicity of metals and PAH's. Schematic illustration which highlights the cellular and molecular toxicity of metals and PAH's. 1., PAH's bind readily to cell membrane increasing concentration, metals (M) may diffuse through membrane dependant on specificity, or via ion channels. UV radiation may alter PAH's to quinones. PAH's may damage cellular membrane and ion channels therefore increasing PAH and metal diffusion. PAH may form cation π bonds with metals at cellular interface which may increase diffusion. Metal exposure may increase mucus secretion allowing increased binding of PAH. 2. PAH initiate cytochrome P450 may metabolise compounds during phase 1 to form quinones which may exert carcinogenic, mutagenic effects and further increase reactive oxygen species (ROS). PAH may affect the formation and functioning of detoxification granules and inhibit metallothionein (MT). This in turn may increase ROS. 3. Metals may bind to enzymes, inhibit acetylcholinesterase, and undergo fenton reactions increasing ROS. PAH's and quinones may overwhelm the detoxification system (GSSG, SOD), increasing ROS resulting in lipid peroxidation. Increased ROS may elicit DNA damage in the form of 8-hydroxy-2-deoxyguanosine lesions (Gauthier et al., 2014).

1.6.1 Detoxification Enzymes, molecules and Cellular Effects

Reactive oxygen species (ROS; Figure 7), are ubiquitous to all aerobic organisms, where their generation is related to the metabolism of oxygen reduction in which reduction of oxygen to water, ATP production, microsomal transport chains and activities of detoxification enzymes produce (ROS) as intermediates (Canesi and Corsi, 2016). However, metals (e.g. Cd, Ni, Hg, Pb) and PAH's taken up by organisms can further stimulate the production of (ROS) through redox cycling or depletion of protein bound sulfhydryl groups (Lister et al., 2015). Photo activation, formation of PAH - dihydrodiols and inhibition of the cytochrome P450 detoxification enzymes following PAH exposure further contribute to ROS production (Gauthier et al., 2014).

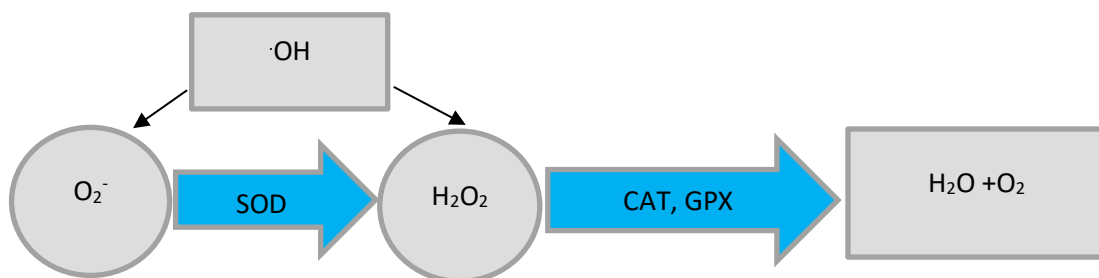


Figure 7. Detoxification of Reactive oxygen (ROS): O_2^- , superoxide anion; H_2O_2 , hydrogen peroxide; $\cdot OH$, hydroxyl radical; SOD, superoxide dismutase; CAT, catalase; GPX, glutathione peroxidase (Canesi., 2015).

The processes which produce and those which scavenge ROS are balanced in equilibrium (Wan et al., 2015): the presence of ROS stimulating the production of antioxidant detoxification enzymes including glutathione – S – transferases (GSTs), catalase (CAT), glutathione reductase (GR), glutathione peroxidase (GPx), and superoxide dismutase (SOD). When ROS production exceeds the detoxification capacity, oxidative stress such as lipid peroxidation and lysosomal membrane damage may occur (Lister et al., 2015; Viarengo et al., 1989; Wan et al., 2015).

Loss of membrane integrity can lead to cellular death or interference with cell signalling pathways causing tissue abnormalities and ultimately reduces an organism's health status (Moore, 2004). To counter this insult, ROS defence mechanisms are utilised including the antioxidant enzyme superoxide dismutase (SOD) (Kim et al. 2011). SOD's are ubiquitous in eukaryotes and observed as three forms: Cu / Zn (Cu / Zn - SOD), iron SOD (Fe - SOD) and manganese SOD (Mn - SOD) (Kim et al., 2011). This enzyme catalyses the reaction dismutation of superoxide: $2O_2 + 2H^+ \rightarrow H_2O_2$ (Canesi, 2015; Manduzio et al., 2003), whereby induced oxidative stress from superoxide will be eliminated by the increase in SOD activity (Wang et al., 2016).

The assessment of further detoxification enzymes in particular, the glutathione transferase family of enzymes in relation to metal and PAH exposure are commonly used biomarkers (Martín-Díaz et al., 2008). Glutathione is an exploited substrate in phase II detoxification reactions where these enzymes catalyse the reactions with metals and metabolism of lipophilic organic contaminants (Solé et al., 2009). The analysis of these enzymes shows effects of contaminant exposure (Buffet et al., 2011; Jing et al., 2006; Martín-Díaz et al., 2008). However, a lack of glutathione following exposure to these pollutants has also been observed leading to cellular oxidative damage (Chelomin et al., 2005; Regoli et al., 2011).

Additionally, enzyme responses may be influenced by environmental factors such as seasonal temperature variations and alterations of pH and salinity. This theory was evidenced by Bocchettit et al. (2008), who described seasonal variations in enzymatic activity in bivalve species and concluded that the use of these biomarkers as indicators of effects must be considered in relation to environmental alterations. Furthermore, Freitas et al. (2016) described alterations in oxidative biomarkers of the polychaete *Diopatra neapolitana* when exposed to differing salinities. They concluded that salinity effects

upon enzyme responses must be incorporated into laboratory studies to avoid confounding results.

Cytochrome P450 are a superfamily of heme thiolate proteins which are key to the detoxification of contaminants and considered a reliable biomarker to evaluate the exposure effects of PAH's (Yim et al., 2017). These enzymes perform reactions designated as hydrolysis, reduction and oxidation (Rougée et al., 2014) to render the xenobiotic more soluble, facilitating excretion. However, these reactions may produce carcinogenic and mutagenic products therefore increasing harmful effects of exposure (Gauthier et al., 2014). Although, carcinogenic and mutagenic effects may accrue over chronic time scales, increased ROS formation from PAH quinones may also result in DNA damage via 8 – hydroxy – 2 - deoxyguanosine adducts (8 - OHdG) (Chen et al., 2018; Gauthier et al., 2014).

1.6.2 Energy Homeostasis

Energy metabolism, regulation of energy expenditure and allocation to biological functions are fundamental parts of an organism's health status (Sokolova et al., 2012). However, survival in contaminated environments may alter energy homeostasis as requirements of detoxification and avoidance of contamination increases energy expenditure (Nilin et al., 2012). This may Pb to an overall decline in population fitness and subsequent reduced food quality for higher organisms (Walker et al., 2007; Yeung et al., 2017).

Fitness costs were demonstrated by Pook et al. (2009) who observed a decrease in lipid and carbohydrate levels in *H. diversicolor* associated with chronic metal pollution indicting the energy cost of the detoxification system. Pook et al. (2009) further demonstrate how the increase in detoxification enzymes and associated protein synthesis is recognised as resource intensive Leading to the restriction of energy or reproduction, growth and repair.

Energetic alterations of lipids, carbohydrates, proteins and metabolism following metals exposure have been observed: the presence of urea in the mussel *Mytilus galloprovincialis* was related to a direct energy homeostasis imbalance resultant from Cu exposure (Nechev et al., 2007); the reduction in metabolic rate of the marine clam *Mesodesma mactroides* on exposure to Cu (Giacomin et al., 2014) and depletion of cellular protein following cadmium exposure resultant from increased detoxification protein synthesis in the mollusc *Crassostrea virginica* (Cherkasov et al., 2006). It is interesting to note that although individuals in a chronically polluted environment may maintain an albeit stressed energy homeostasis, allowing the fulfilment of certain functions including maturation and growth, negative effects of energy alteration may not be observed if only a narrow range of energy budgets are assessed. For instance, energy alterations of reproductive processes have been observed, including the reduction of mitochondrial activity of invertebrate sperm (Au et al., 2000; Caldwell et al., 2011). However, such observations may not generally be included in energy budget testing due to time/species breeding constraints.

1.6.3 Genotoxicity

Chronic and acute exposure to metal (s) and PAH (s) may result in the production of ROS exceeding the capacity of the antioxidant system of the individual, resulting in oxidative stress and cellular damage (Lister et al., 2015; Viarengo et al., 1989; Wang et al., 2016). Nucleotide exposure in particular the base guanine (Topal et al., 2017) can initiate alteration of DNA bases via oxidation, leading to the formation of the DNA lesion 8-hydroxy-2'-deoxyguanosine (8-OHdG) (Oliveira et al., 2010b). The consequence of which can lead to DNA strand breakage and misreading, altered gene expression, microsatellite and chromosomal instability, cytostasis and neoplastic growth (Oliveira et al., 2010b).

The use of 8 - OHdG as a biomarker of environmental contaminants have been studied by the researchers Topal et al. (2017) Oliveira et al. (2010) and Sui et al. (2008) who all found increased 8 - OHdG levels following contaminant exposures. Additionally, the detection of a micronucleus following evaluation of elevated 8 - OHdG levels is an established cytogenetic assay which may indicate accumulated genetic damage (Oliveira et al., 2010b).

1.6.4 Metallothionein

Metallothionein's (MTs) have a widely established role in the context of metal detoxification as these thiol rich molecules have three primary detoxification functions:

- 1) Homeostatic regulation of metals. MT induction is directly linked to exposure to essential metals (especially Cu and Zn) which may be used as a store for synthesis of metalloenzymes (Amiard et al., 2007).
- 2) Non - essential metal regulation. Cadmium, mercury cations or those which share stoichiometric characteristics with Cu and Zn (Ryvolova et al., 2012).
- 3) Neuroprotective mechanisms and oxidative stress defence mechanisms (Mao et al., 2012).

MT concentrations detected in either whole soft or digestive tissues (Le et al., 2016) are widely established as a biomarker for monitoring metallic aquatic pollution (Oaten et al., 2017), due to the presence of these proteins in many animals including marine invertebrates (Serafim and Bebianno, 2007). However, following exposure to metals and PAH, inhibition of MT was observed in the Manilla clam *Ruditapes philippinarum* (Wang et al., 2011a), and the sole *Solea senegalensis*, increasing stress upon the detoxification system (Costa et al., 2008). The expression of these proteins following metal exposure is not the only detoxification function as metals are also found in mineral rich granules (Wang et al., 2011a, Rainbow et al.,

2006). For example, Mouneyrac et al. (2003), observed metal containing extracellular granules present in the epicuticle, spherocrystals and mineralized lysosomes in the gut wall and epidermal cells in which were found a variety of metals including Zn, Fe, Pb, As, Ca, and K in the polychaete *H diversicolor*. Moreover, the ultimate fate of excessive concentrations of metals bound to MTs are believed to involve the incorporation of the metal into these intracellular metal rich granules, although this process is not fully understood (Barka, 2007; Hopkin, 1990).

Mouneyrac et al. (2003) further described how the analysis of metallothionein like proteins did not increase upon exposure to individual metals, which infers non specificity. However, this may be due to the fast rate of turnover of these proteins in invertebrates upon exposure (Langston et al., 1989), a consideration which must be recognised when using MTs as biomarker of metal exposure. Further inconsistencies of MT induction have been evidenced by Oaten et al., (2017) who detail seasonal variations of MT induction in the clam *Ruditapes philippinarum*.

Nonetheless, the induction of MTs by metal exposure has been demonstrated for marine invertebrates (Bebianno et al., 1993; Brown et al., 2004; Olafson et al., 1979; Viarengo et al., 1987) leading to the adoption of this test as a biomarker of metal exposure (Amiard et al., 2007). Although, growing evidence of inconsistencies include that MT expression may also be dose - dependent whereby, when exposure exceeds specific thresholds, the MT expression is not positively correlated (Mao et al., 2012), which may relate to toxicity reducing detoxification processes (Amiard et al., 2007). Furthermore, stress has been shown to induce the expression of MT including events such as anoxia, starvation (Lee and Nam, 2016), thermal stress (Cooper et al., 2013; Serafim and Bebianno, 2001), and fitness and handling (Cooper et al., 2013).

MT expression may therefore be indicative of an organisms physiological response following exposure to specific metal pollution and not an indication of stress (Piña and Barata, 2011) or exposure to mixed metal pollution. However, MT expression remains an intrinsic part of any metal exposure study although current literature acknowledges that MTs are not solely involved in detoxification and transport of metals (Abebe et al., 2007; Chen et al., 2018; Liebeke et al., 2013; Rainbow P. S et al., 2007; Wang et al., 2011a).

1.6.5 Acetylcholinesterase

Cholinesterase's are responsible for the removal of acetylcholine from synaptic clefts in eukaryotes and are found in two isoforms: acetylcholinesterase and butyrylcholinesterase (Viarengo et al., 2007). The enzyme acetylcholinesterase (AChE) is responsible in terminating the neurotransmission by clearing acetylcholine from synaptic clefts by way of hydrolysis resulting in the products choline and acetate (Liu et al., 2014b). AChE inhibition results in the increase of acetylcholine in the synaptic cleft and subsequent overstimulation of the postsynaptic membrane (Liu et al., 2014b).

Acute toxicity of chemical pollutants such as organophosphates and carbamate insecticides results in the inhibition of AChE (Day and Scott, 1990; Rajkumar and Samuel, 2013). Therefore, assessing the AChE activity of an organism following contaminant exposure has led to its use as a diagnostic tool within ecotoxicology.

Numerous studies have effectively identified the inhibition of cholinesterase activity following marine invertebrate exposure to sub lethal levels of organophosphates, metals and PAH's (Benitez-Trinidad et al., 2014; Brown et al., 2004; Cabecinhas et al., 2015; Canty et al., 2007; Dailianis et al., 2003; Gauthier et al., 2016). Conversely, there are studies which showed no cholinesterase inhibition. For example, Vidal-Liñán et al., (2016) studied the effects of PCB – 153 on *Mytilus galloprovincialis* and found no affect to AChE activity.

1.6.6 Behaviour Alterations

Behavioural alterations of organisms following contaminant exposure may provide an unobtrusive, early warning biomarker in ecotoxicology when such changes are possible to quantify (Macedo-Sousa et al., 2008). Alterations may occur due to the exposure concentration overwhelming detoxification processes eliciting toxicity that in turn, leads to deterioration of health which may then have deleterious effects upon contaminated ecosystems (Lee and Johnston, 2007). Observed behavioural alterations following metal (s) and PAH (s) exposure include contamination avoidance behaviour in the earthworm *Lumbricus rubellus* (Zn) (Ma and Bonten, 2011), reduced feeding of the copepod *Schizopera knabeni* (phenanthrene and Cu) (Silva et al., 2009), reduced burrowing activity of the ragworm *H. diversicolor* (silver and silver nanoparticles) (Cong et al., 2014), and reduced burrowing success of *H. diversicolor* (Cu) (Burlinson and Lawrence, 2007). Conversely, behavioural alterations including reduced burrowing and feeding have been observed following low concentration Zn nanoparticle exposure when cellular biomarkers showed little alterations in both the clam *Scobicularia plana* and ragworm *H. diversicolor* (Buffet et al., 2011). However, altered behaviours may have far reaching negative effects for populations of invertebrate species that function as key species within ecosystems related to increased predation and reduced fitness (Sokolova et al., 2012).

1.7 Research aim and objectives

PAH and metal pollution within the marine environment exist within complex mixtures (Fleeger et al., 2007; Gauthier et al., 2014). However, toxicological investigations using mixtures of these contaminants are scant. Additionally, there is limited research regarding the adverse outcome pathways from cellular to organism response following exposure, which is necessary to understand ecosystem level effects (Cannon et al., 2012). Therefore, there are important gaps in the understanding of the consequences of marine pollution. This present study will contribute to addressing this situation. The aim of this study is to investigate the effects of environmentally relevant levels of Cu, Pb and pyrene exposure (individually and in combination) in the marine ragworm *H. diversicolor*. The Fleet lagoon, Dorset, UK was used as a study location to obtain environmentally relevant concentrations of described contaminants following a site survey and to identify bioaccumulation within resident populations of *H. diversicolor*. Additionally, sediment characteristics of the study site were investigated and the bioavailability of metals from sediment was conducted to determine the relationship between sediment properties and metal bioavailability. PAH isomer analysis was determined to identify potential sources of this contamination in the Fleet Lagoon. Controlled exposure experiments were conducted to investigate the assimilation, excretion, biochemical, behavioural and energetic effects of contaminant exposure (individually and in combination) on *H. diversicolor*.

The objectives of the present study were:

1. To identify and quantify concentrations of metals within the water and sediment of the Fleet lagoon. Bioavailability of metals from the environmental matrices were assessed by

identification and quantification of metals within the tissue of resident *H diversicolor*. Bioavailable fractions of metals from the sediment were determined using sequential extraction and proteinase K sediment digestion. The accuracy of these techniques regarding bioaccumulation of metals by *H diversicolor* was investigated (Chapter 3).

2. To determine and quantify concentrations of PAH's in water and sediment of the Fleet Lagoon, isomer source analysis and bioaccumulation to resident *H diversicolor* (Chapter 4).
3. To investigate behavioural change and neurotoxic alterations in *H diversicolor* following exposure to Cu, Pb and pyrene (individually and in combination) (Chapter 5).
4. To assess the assimilation, excretion and biochemical responses of Pb and pyrene exposure (individually and in combination) in *H diversicolor* (Chapter 6).
5. To examine the energetic demands of Pb and pyrene (individually and in combination) exposure in *H diversicolor* (Chapter 7).

Chapter 2. Materials and Methods

2.1 Introduction

Research conducted in this study includes the identification and quantification of metals and polycyclic aromatic hydrocarbons (PAH's) found in sediment and water of the Fleet Lagoon, Dorset, UK. Results found from this field work were then used to select 2 metals and one PAH for use at environmentally relevant concentrations in a series of *H diversicolor* exposure experiments using spiked sediment. General methods of field work, metal and PAH sediment and worm tissue extraction and analysis, sediment spiking and tanks trials used in this study are described in this chapter. Further methods relating to specific research are included in detail in relevant chapters.

2.1.1 Collection of samples and pre-processing

2.1.1.1 Site selection

10 sites along the Eastern shoreline of the Fleet lagoon, Dorset, UK were identified as sample locations. The rationale included covering the full length of the lagoon, including natural embayment's where contamination may accrete. Additionally, care was taken when identifying locations to ensure safe access to the shoreline from adjoining public and private land as some areas of the shoreline are inaccessible by foot.

2.1.1.2 Sediment collection

H diversicolor burrow into sediment to depths of ~18cm (Scaps, 2002). Therefore, to account for the potential exposure of contamination from the surrounding environment, a sediment depth of 20 cm was used. Samples ($n = 3$) were taken from each site using a depth marked stainless steel sediment corer from the Eastern shoreline. Areas where samples were taken were identified using a

Garmin 64s - d GPS and locations chosen within ~ 2m² in areas free from large rocks and pebbles. Upon extraction of sediment, samples for metals analysis were placed into labelled plastic bags. Guidelines of environmental PAH analysis states that sample collection and storage must not be conducted using plastic equipment due to the potential of adhesion (Kelly et al., 2000). Therefore, samples for PAH analysis were placed into amber glass bottles. Care was taken to ensure that the sediment filled the bottles to the top to prevent loss of contaminant via volatility. Tin foil was placed onto the top of the bottle prior to sealing with the plastic lid and then placed into labelled plastic bags. All samples were stored in isothermal bags whilst in the field and returned to the laboratory at Bournemouth University within 6 h where samples were frozen at - 20°C until analysis.

2.1.1.3 Water collection

300 ml amber glass bottles were used to collect water samples from each sample location for PAH analysis. Bottles were fully submerged to completely fill the bottle and lids replaced. This procedure was conducted to ensure that there was not any headspace or air bubbles in the sample bottle which may affect PAH analysis due to their volatility (Kelly et al., 2000).

Water samples for metal analysis were conducted in conjunction using 100 ml polypropylene bottles. All PAH and metal sample bottles were fully labelled and placed into cool boxes during the sampling processes.

*2.1.1.4 Collection of *Hediste diversicolor**

Holes created by sediment extraction were initially used to recover *H diversicolor*. Sediment was turned over carefully using a hand fork at depths of ~ 20 cm. If worms were not present, further digging was done around the sample location. Worms ($n = 10$ per site) were carefully removed from the sediment and placed into labelled plastic containers which contained water from the sample location. All

samples were kept at the site in cool boxes and the worms were returned to the Laboratory at Bournemouth University within 6 h.

Once at the laboratory, worms were identified using a magnifying glass. Positive identification was made using the key described by Barnes (1994). Worms were then placed in aerated containers for 48 h which contained manufactured sea water (15 ppt salinity, 17°C) to depurate their guts (Zhou et al., 2003). Worms were then placed individually into labelled containers and frozen at - 20°C until analysis.

2.1.1.5 Preparation of sediment samples for metal analysis

Sediment samples from each sample location ($n = 3$) were thoroughly mixed to form a single bulk sample. Homogenised sediment (~ 20 g) from each sample was then removed randomly and placed onto a large watch glass. This process was repeated until each watch glass contained ~ 60 g of sediment (~ 20 g from each sample) to represent each sample location. Samples were then left for a period of 48 h to dry at room temperature.

Dried sediment was passes through a 200 µm mesh sieve and 0.3 g of sieved sediment was then placed into labelled polypropylene tube prior to chemical digestion.

2.2 Sediment Characteristics

2.2.1 Loss on Ignition

Loss on ignition was determined using the method developed by (Wang et al., 2011b), where 30 g of wet sediment was placed in heat proof crucibles and heated at 105°C until a constant weight achieved. The samples were re-weighed then placed in a Carbolite muffle furnace for 12 h at 550°C. Samples were cooled, then re-weighed. LOI was formulated using Eq. (1).

$$\frac{(W_s) - Wa}{W_s - (W_c)} * 100 \quad (1)$$

Where:

W_s = Weight of sediment which has been dried at 105°C until a constant weight achieved.

Wa = Weight of ash produced following heating to 550°C for 12 h

W_c = Weight of cooled crucible dried at 105°C for 1 h.

2.2.2 Sediment characterisation

Grain size distribution of the sediment samples ($n = 3$) were measured using a Malvern Mastersizer 3000 laser diffraction particle size analyser. The following fractions and related particle size (μm) were determined; clay (0.06), Very Fine Silt (3.9), Fine Silt (7.8), Medium Silt (15.6), Coarse Silt (31), Very Fine Sand (63), Fine Sand (125), Coarse Sand (500), Very Coarse Sand (1000), Granule (2000).

Geometric grain size distribution was determined using the method described by Folk and Ward (1957). Initially, grain size values are logarithmically transformed to a phi scale (Eq (2)):

$$\Phi = -\log_2 d \quad (2)$$

Where:

d = grain diameter in millimetres.

The mean size of sediment particles are determined using corresponding phi scale units (Blott and Pye, 2001) (Eq (3)):

$$M_z = \frac{\Phi_{16} + \Phi_{50} + \Phi_{84}}{3} \quad (3)$$

Spread of sizes around the average (sorting) are determined using Eq. (4), skewness Eq.(5) and kurtosis Eq (6):

$$\sigma = \frac{\Phi_{84} - \Phi_{16}}{4} + \frac{\Phi_{95} - \Phi_5}{6.6} \quad (4)$$

$$S_k = \frac{\Phi_{16} + \Phi_{84} - 2\Phi_{50} + \Phi_5 + \Phi_{95} - 2\Phi_{50}}{2(\Phi_{84} - \Phi_{16}) + 2(\Phi_{95} - \Phi_5)} \quad (5)$$

$$K_G = \frac{\Phi_{95} - \Phi_5}{2.44(\Phi_{75} - \Phi_{25})} \quad (6)$$

2.3 Chemical analysis

2.3.1 Preparation of Equipment

All glassware and plastic equipment used in this series of experiments were acid washed using 10% HNO₃ for a minimum of 12 h. Equipment was then rinsed in distilled water and finally in deionised water (Millipore 18 M Ω) prior to use.

2.3.2 Chemical Determination of Total Metals in Sediment

Total concentrations of metals within the sediment samples were determined in accordance with the method developed by McGrath and Cunliffe (1985) using *aqua regia* digestions as follows; 0.3 g of sediment were placed in polypropylene digestion tubes to which 3 ml of 70% HNO₃ (PrimaPlus trace analysis grade, Fischer Scientific, UK) and 9 ml of 37% HCl (PrimaPlus trace analysis grade, Fischer Scientific, UK) added. Samples were pre-digested for 2 h prior to heating at 60°C overnight. The temperature was then increased to 105°C until approximately 2 ml of fluid remained. The temperature was then decreased to 50°C and samples left to cool until all moisture was removed, and then samples were cooled to room temperature. 20 ml of 5% HNO₃ was then added to the samples which were then shaken to re-suspend the digests. Samples were

centrifuged at 2000 rpm for 2 min and the supernatant removed for analysis by ICP-OES (Varian vista Pro, Varian inc. California, USA).

2.3.3 Metal Content in Worm tissue

All worms ($n = 10$, per site) were depurated for a period of 48 h in clean manufactured sea water (15 ppt salinity, 17°C) prior to freezing. Individual worms were defrosted and washed using 18 M Ω ultrapure water to remove sediment particles. Worms were then dried at 70°C for 24 h until a constant weight was achieved. The weight of dry worms was then recorded, and length measured using a calibrated Vernier. Individual worms were dried at 70° for 24 h or until a constant weighed was achieved. A minimum of 0.025 g of tissue, typically 1 small size worm, was placed into a digestion tube to which 5 ml of 70% HNO₃ (PrimarPlus trace analysis grade, Fischer Scientific, UK) was added. The tubes were placed into digestion block at 60°C for 1 h. Digestion tubes were agitated and temperature increased to 90°C for a further 2 h until tissue was no longer visible and samples were clear. Tubes were left to cool and if fat deposits were visible, samples were further treated by the addition of 2.5 ml of 100 vol H₂O₂ (PrimarPlus trace analysis grade, Fischer Scientific, UK) followed by heating at 90°C for a further 2 h. The digestion block temperature was then increased to 100°C until tube contents were almost completely evaporated. The digestion block temperature was then decreased to 50°C until tube contents nearly dry. Tubes were removed and left to cool when contents were dry and weighed. The contents were then re-suspended by adding 8 ml of 5% HNO₃. Tubes were agitated and left for a further 30 min to ensure dissolution of metal salts. Tubes were then re-weighed to determine the sample volume gravimetrically. Metal analysis for Ag, As, Cu, Cr, Ni, Pb and Zn was conducted using ICP - OES (Varian Vista Pro).

2.3.4 Sequential Sediment Processing

The bioavailability of metals from sediment was determined using analytical grade reagents using the method described by Pueyo et al., (2008) as detailed:-

1) Step 1: The acid extractable and carbonate fractions were obtained, whereby 0.5 g of each sediment sample in triplicate was digested using 20 ml of 0.11 mol l⁻¹ acetic acid for 16 h using a shaker at a speed of 30 ± 10 rpm and temperature of 22 ± 5°C. The suspension was then centrifuged for 20 min at 3000 rpm, supernatant removed and refrigerated at 6°C until analysis. The sediment residue was then washed in 20 ml distilled water, shaking for 15 min at 30 ± 10 rpm at 22 ± 5°C, and centrifuged for 20 min at 4200 rpm.

2) Step 2: The reducible fractions: Fe / Mn (hydr-) oxides; were obtained using 20 ml 0.5 mol l⁻¹ hydroxylammonium chloride (hydroxylamine hydrochloride) added to the sediment sample residue obtained from step 1. The samples were shaken for 16 h at a speed of 30 ± 10 rpm and temperature of 22 ± 5°C. The suspension was then centrifuged for 20 min at 4200 rpm, supernatant removed and refrigerated at 6°C until analysis. The sediment residue was then washed in 20 ml distilled water, shaking for 15 min at 30 ± 10 rpm at 22 ± 5°C, and centrifuged for 20 min at 4200 rpm.

3) Step 3: 5 ml of 8.8 mol l⁻¹ hydrogen peroxide was added to the sediment samples in triplicate. The samples were digested at room temperature for 1 h with occasional manual shaking. The samples were then heated in a water bath to 85°C and digested for a further 1 h until approximately 3 ml of solution remained. A further 5 ml of 8.8 mol l⁻¹ hydrogen peroxide was then added and the sample heated again to 85°C for 1 h. Sample volume was then reduced until approximately 1 ml of solution remained. 25 ml of 1.0 mol l⁻¹ ammonium acetate was then added to the samples which were then

agitated for 16 h using an orbital shaker at a speed of 30 ± 10 rpm and temperature of $22 \pm 5^\circ\text{C}$. The suspension was then centrifuged for 20 min at 3000 rpm, the supernatant removed and refrigerated at 6°C until analysis. The sediment residue was then washed in 20 ml distilled water, shaking for 15 min at 30 ± 10 rpm at $22 \pm 5^\circ\text{C}$, and centrifuged for 20 min at 4200 rpm.

2.3.5 Proteinase K Extraction

The bioavailable fraction was determined using proteinase K following a procedure described by Turner (2006). Proteinase K solution (0.4 mg ml^{-1}) was dissolved in 1.179 g of potassium dihydrogen phosphate (KH_2PO_4) and 4.300 g of disodium hydrogen phosphate (Na_2HPO_4) in 1l of distilled water (pH 7.4). 0.5 g of each sediment sample in triplicate was weighed and placed in a centrifuge tube to which 25 ml of proteinase K solution was added. The samples were then shaken at 250 rpm for 3 h at room temperature on an orbital shaker. The samples were then centrifuged for 20 min at 4200 rpm and the supernatant removed. Metal concentrations for As, Cu, Ni, Pb, and Zn were determined by ICP - OES (Varian Vista Pro).

2.3.6 Determination of PAH's in sediment and water

Samples of sediment and water were sent to a commercial laboratory (I2 analytical Laboratory, Watford, UK) for determination of PAH concentrations by GCMS.

2.3.7 Extraction of Pore Water from sediment

Samples of pore water obtained from sediment from each study site were collected in the laboratory as per the method described by Tang et al. (2016) where samples were centrifuged at 2600 g for 20 min to extract pore water. Samples were filtered using Millex $0.45 \mu\text{m}$

disposable syringe filter units attached to a 5 ml syringe and refrigerated until analysis.

2.3.8 Pore water analysis

Samples were analysed at the I2 UKAS accredited analytical Laboratory in Hertfordshire, UK. Determination of metals in water was conducted by acidification and filtration followed by analysis using ICP-MS.

2.3.9 Preparation of worm tissue for PAH analysis using HPLC

All worms were depurated in clean manufactured sea water (15 ppt salinity, 17°C) for 48 h prior to freezing (Malmquist et al., 2015). All tissue was then extracted as described in Carrasco Navarro et al., (2011). Organisms were defrosted and homogenized using an IKA T10 ULTRA-TURRAX homogenizer in 2 ml methanol at full speed for 1 min. Samples are centrifuged at 500 g for 10 min. The supernatant was then drawn through a Millex disposable 0.22 µm syringe filter unit attached to a 5 ml syringe and transferred to brown HPLC vials and stored at – 20 °C until analysis.

2.3.10 HPLC Pyrene and 1-Hydroxypyrene Analysis

Quantification of pyrene and 1 - hydroxypyrene (1-OHP) in sediment and whole worm tissue from *H diversicolor* was conducted using a Perkin Elmer HPLC / UV using analytical grade reagents as described by Giessing et al. (2003). The method comprised of acetonitrile / water gradient using a reverse phase C18 (octadecyl) column. The acetonitrile / water (v / v) gradient profile was 50 : 50 for 5 min, 100 : 0 for 10 min at a flow rate of 1 ml min⁻¹. The system consisted of a Perkin Elmer series 200 pump, and Perkin Elmer 275 auto sampler. The injection volume was 1 µl using a 15 µl injection loop and using ethanol as the wash solvent. Detection was performed at 339 nm with specific retention times of ~12 min for pyrene and ~9 min for 1 - hydroxypyrene. Quantification was

performed by measurement of peak area as illustrated in Figures 8 and 9, using calibration curves obtained from dissolving 0.202 g of pyrene in 10 ml of acetone (100 mM) and 0.002 g of 1-hydroxypyrene (1 mM) in 10 ml methanol.

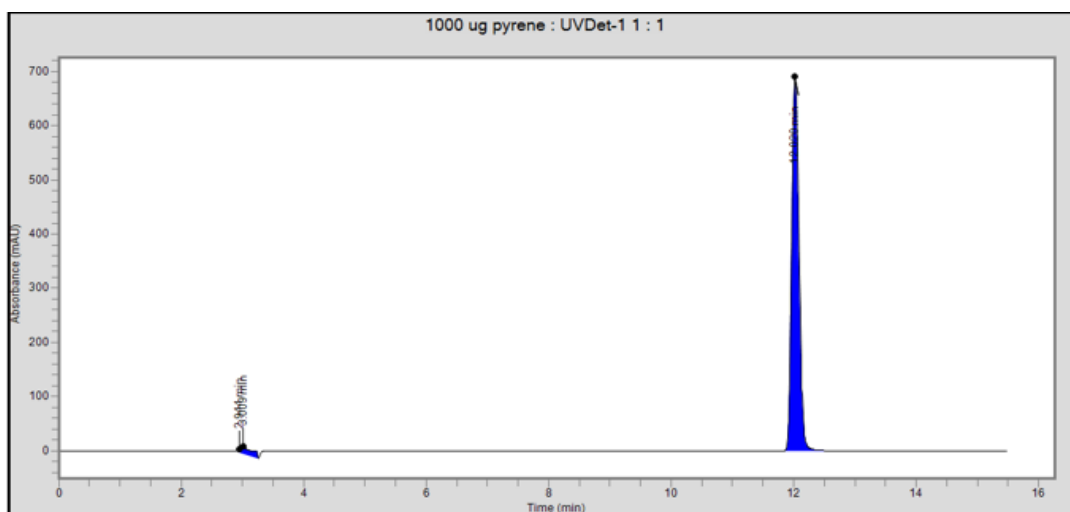


Figure 8. Chromatograph depicting pyrene detection using a Perkin Elmer 200 series HPLC pump and 275 auto injector. Retention time for pyrene was ~12 min.

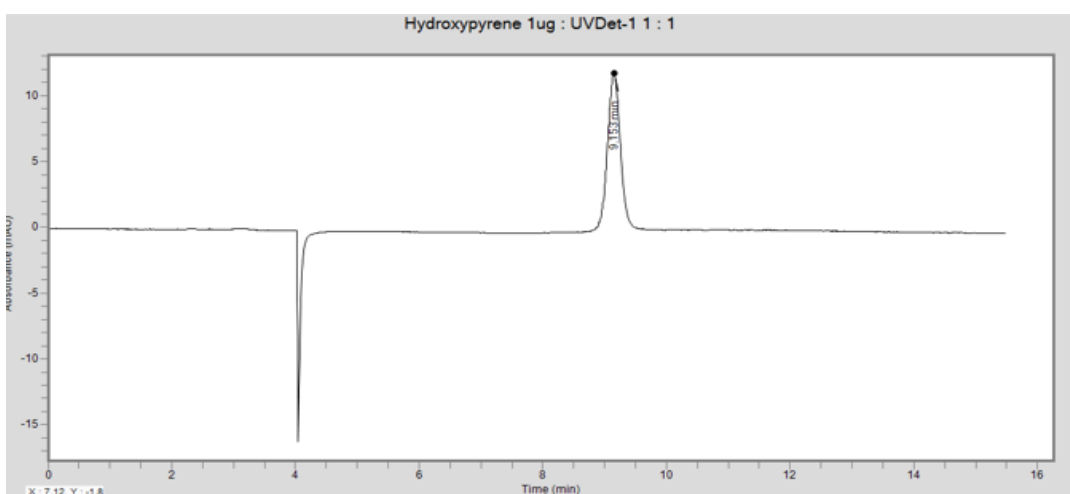


Figure 9. Chromatograph illustrating 1-hydroxypyrene detection using a Perkin Elmer 200 series HPLC pump and 275 auto injector. Retention time for 1 - hydroxypyrene was ~ 9 min.

2.4.1 HPLC individual PAH determination

Quantification of individual PAH's in worm tissue was conducted as described by Serpe et al. (2010), using a Perkin Elmer HPLC / UV. All reagents used were analytical grade. The method comprised of acetonitrile / water gradient using a reverse phase C18 (octadecyl) column. The gradient elution acetonitrile / water (v / v) profile started with an initial mobile phase at 60 : 40 (v / v), changing linearly to 100% acetonitrile in 14 min followed by a decrease to 60 : 40 after 5 min. Flow rate increased from 1.8 ml min⁻¹ to 3.5 ml min⁻¹ at 18 min followed by decrease to 2.5 ml min⁻¹. The total run time was 35 min. The system consisted of a Perkin Elmer series 200 pump, and Perkin Elmer 275 auto sampler. The injection volume was 1 µl using a 15 µl injection loop and using ethanol as the wash solvent. Detection was performed at 294 nm with specific retention for each PAH detailed in Table 6. Quantification was performed by measurement of peak area using calibration curves obtained from original 10 µg ml⁻¹ PAH calibration mix traceable certified reference material (Sigma Aldrich, UK).

2.4.2 Pyrene Sediment Determination

Pyrene sediment concentrations were determined following the method developed by Zheng et al. (2015). All reagents used were analytical grade. 0.2 g of sediment was added to centrifuge tube. 2 ml of acetonitrile was added to the sample, lid replaced and shaken vigorously using vortex mixer for 2 min.

The sample was then centrifuged for 5 min at 3000 rpm. The upper solution transferred to a glass vial. 5 ml of ultrapure water was added to a separate glass test tube. 80 µl of dichloromethane was added to 1 ml of the upper solution and then injected into the ultrapure water using a glass Pasteur pipette. The solution was then centrifuged for a

further 5 min at 3000 rpm. The dichloromethane extract was then removed from the bottom of the tube using a glass Pasteur pipette and evaporated under a continuous stream of nitrogen. The sample was then re-suspended using 1ml of methanol and transferred to a glass HPLC vial. The samples were analysed immediately using HPLC.

2.5 Tank set up

2.5.1 General set up

Plastic tanks of 24 l (40 x 25 x 25 cm) capacity were used to conduct exposure experiments in a series of tests. Tanks were contained in a secure controlled environment with a set mean temperature of 17°C and photoperiod of 12 h.

For each experiment, control systems consisting of tanks containing 6 kg of commercially available clean sediment ~20 cm deep and artificial sea water (tropic marin salt Ltd) (15 ppt salinity). The tanks were aerated using commercially available aquatic pumps and maintained at 17°C.

For all treatments using spiked sediment tanks – spiked sediments were placed into one 24 l tank per test condition. Manufactured sea water was then poured on top of the sediment and aerated using an aquatic pump. Tanks were left for a period of 4 h to settle prior to addition of live worms.

2.5.2 *Hediste diversicolor*

H diversicolor used in laboratory trials were obtained from a commercial source (Sustainable Feeds Ltd, UK). Worms were identified as *H diversicolor* as previously described in section 2.1.1.4. The wet paper containing live worms was floated on top of a plastic sheet attached to the tank and in contact with the manufactured sea water (15 ppt salinity, 17°C) for 1 h to allow acclimatisation to temperature (Craig, 2018, Sustainable Feeds Ltd, personal

communication). Worms were then carefully removed and placed into allocated tanks.

2.5.3 *Hediste diversicolor* feeding regime

Worms were fed a diet of commercially available fish food (Love Fish Ltd) twice per week as advised by Craig (2018) (Sustainable Feeds Ltd, UK, personal communication). To ensure that sufficient food was provided, food weight equivalent to 1 - 2% of the biomass of worms per tank was added. Metal analysis of fish food showed: Cu ($0.153 \pm 0.04 \mu\text{g kg}^{-1}$); Pb (below detectable limits); Ni ($0.017 \mu\text{g kg}^{-1}$); Zn ($109.1 \pm 0.09 \mu\text{g kg}^{-1}$). Energy determinants of the fish food revealed: carbohydrate content, $0.98 \pm 0.01 \text{ mg g}^{-1}$; Protein content, $0.49 \pm 0.17 \mu\text{g mg}^{-1}$; Lipid content, $0.63 \pm 1.02 \text{ mg g}^{-1}$.

2.6 Spiking of sediment with metals and pyrene

2.6.1 Sediment spiking for exposure experiments

Cu levels found in Chapter 3 were used to obtain the median concentration of all sample locations. For Cu, the median (31.80 mg kg^{-1}) and $\frac{1}{2}$ the median (15.95 mg kg^{-1}) were used initially. High or total mortality of worms occurred at these levels. Consequently, the Cu levels were reduced to 7.5 mg kg^{-1} and 3.7 mg kg^{-1} and the experiments repeated.

Pb concentrations found in Chapter 3 were used to obtain median values of 9.2 mg kg^{-1} and $\frac{1}{2}$ the median 4.5 mg kg^{-1} for Pb.

Pyrene concentrations found in Chapter 3 were considered too high to use in this series of experiments. Concentrations from the obtained results below the Threshold Effects Limits of the Canadian Sediment Quality Guidelines (TEL) were then used to formulate the median for these lower concentrations of $970 \mu\text{g kg}^{-1}$ and $480 \mu\text{g kg}^{-1}$.

Spiking of sediment was conducted by formulation of a stock solution for each chemical which was then added to 6 kg of dry sediment for

each test exposure (Table 4) to obtain the individual or mixed contaminant concentrations required.

Table 4. Sediment spiking concentrations.

Test Exposure	Stock solution chemical	Stock solution addition (g)	Solvent	Stock solution concentration (mg l ⁻¹)	Addition to 6kg dry sediment (ml)
Cu 31.80 mg kg ⁻¹	Cu Chloride	2.115	Analytical Water	10,000	19.5
Cu 15.95 mg kg ⁻¹	Cu Chloride	2.115	Analytical Water	10,000	9.6
Cu 7.5 mg kg ⁻¹	Cu Chloride	2.115	Analytical Water	10,000	4.7
Cu 3.7 mg kg ⁻¹	Cu Chloride	2.115	Analytical Water	10,000	2.4
Pb 9.2 mg kg ⁻¹	Pb Chloride	0.1342	Analytical Water	1,000	55.2
Pb 4.5 mg kg ⁻¹	Pb Chloride	0.1342	Analytical Water	1,000	27.6
Pyrene 970 µg kg ⁻¹	Pyrene	0.2	Analytical Grade Acetone	2000	0.291
Pyrene 480 µg kg ⁻¹	Pyrene	0.2	Analytical Grade Acetone	2000	0.146

The solution (s) were mixed into the sediment using a glass stirring rod. 6kg of dry sediment was weighed and placed into large plastic (tin foil bags were used for individual and mixed exposures using pyrene) sample bags. The bags were then sealed, and the sediment rolled by hand to ensure thorough mixing. Bags were placed into a dark cupboard and left for 6 d to allow interactions between the contaminant (s) and the solid phase to develop.

2.6.2 Acetone tank

In addition to the control tanks and to ensure that the acetone used to dissolve pyrene did not adversely affect worms, 38.6 ml g⁻¹ of acetone were added to 6 kg of dry sediment, stirred with a glass rod and rolled by hand to ensure thorough mixing. Bags were left in a dark cupboard for 6 days to acclimate.

2.7 Quality Control

2.7.1 Total metal sediment analysis

Toronto Harbour certified reference material (TH - 2, National water Research Institute, Ontario, Canada) and solvent blanks were analysed alongside samples when conducting total metal sediment analysis as per section 2.3.2. Blanks were used to identify contamination. All analysis was accepted when results for the reference material were within the quoted certified minimum and maximum concentrations as shown in Table 5.

Table 5. Results for certified reference material. Analysis conducted alongside total metal sediment determination for this test series. Results shown are mean values ($n=2$)

Metal	Certified		Chapter 3	Chapter 5	Chapter 6	Chapter 7
	values $\mu\text{g kg}^{-1}$		Values	Values	Values	Values
	Min	Max	$\mu\text{g kg}^{-1}$	$\mu\text{g kg}^{-1}$	$\mu\text{g kg}^{-1}$	$\mu\text{g kg}^{-1}$
Cadmium	4.76	5.68	5.60+/-0.12	5.62+/-0.08	5.01+/-0.27	5.18+/-0.31
Chromium	112	134	124+/-8	113+/-6	130+/-7	128+/-6
Cu	117	131	122+/-5	119+/-4	117+/-4	120+/-5
Pb	180	208	180+/-11	182+/-9	184+/-8	180+/-2
Ni	38.7	47.3	47.0+/-0.27	47.2+/-0.10	47.1+/-0.11	47.1+/-0.08
Zn	852	964	866+/-26	960+/-12	954+/-11	936+/-11

2.7.2 Sequential sediment extraction

To determine the accuracy of results, the certified standard BCR 701 and blanks were analysed as per the detailed steps with recovery levels: Cadmium (95 - 109%), Chromium (72 - 118%), Cu (76 - 127%), Ni (85 - 123), Pb (79 - 137%), Zn (90 - 127%). All results obtained were within the certified minimum/maximum values.

2.7.3 Total metal worm tissue analysis

Analysis of the certified reference material lobster hepatopancreas (TORT - 2, National Research Council Canada, Ontario, Canada)

and blanks were conducted alongside determination of total metals in worm tissue. Results gained were within the certified minimum / maximum values detailed in Table 6.

Table 6. Results for analysis (mg kg^{-1}) of certified reference material TORT - 2. Results were obtained alongside determination of total metal in worm tissue for this study. Results shown are mean values ($n = 2$)

Metal	Certified Values		Chapter 3	Chapter 5	Chapter 6	Chapter 7
	mg kg^{-1}		Values	Values	Values	Values
	Min	Max	mg kg^{-1}	mg kg^{-1}	mg kg^{-1}	mg kg^{-1}
Cd	26.1	27.3	26.2 \pm 0.5	27.1 \pm 0.1	26.6 \pm 0.4	27.3 \pm 0.1
Cr	0.62	0.92	0.79 \pm 0.02	0.86 \pm 0.05	0.90 \pm 0.02	0.89 \pm 0.02
Cu	96	116	98.5 \pm 1.6	97.1 \pm 0.17	97.3 \pm 1.2	96.2 \pm 0.09
Pb	0.22	0.48	0.47 \pm 0.02	0.48 \pm 0.05	0.47 \pm 0.03	0.46 \pm 0.01
Ni	2.31	2.69	2.65 \pm 0.05	2.69 \pm 0.06	2.68 \pm 0.02	2.61 \pm 0.05
Zn	174	190	179 \pm 2	175 \pm 3	180 \pm 3	189 \pm 3

2.7.4 HPLC Pyrene and 1-OHP analysis

Six sequential dilutions (1000, 700, 500, 300, 100 and 1 $\mu\text{g kg}^{-1}$) were conducted to obtain calibration curves for 1-hydroxypyrene and pyrene (Figures 10 and 11 respectively), with regression coefficients of $r^2 > 0.99$ for pyrene and > 0.97 for 1 - OHP. The limit of quantification for both pyrene and 1 - OHP was determined where the signal to noise ratio did not fall below 10 : 1. The minimum quantification for pyrene was 500 ng and 1 μg for 1 - OHP. Blank samples were run following each concentration analysis in order to assess contamination carry over. No carry over was detected using this method.

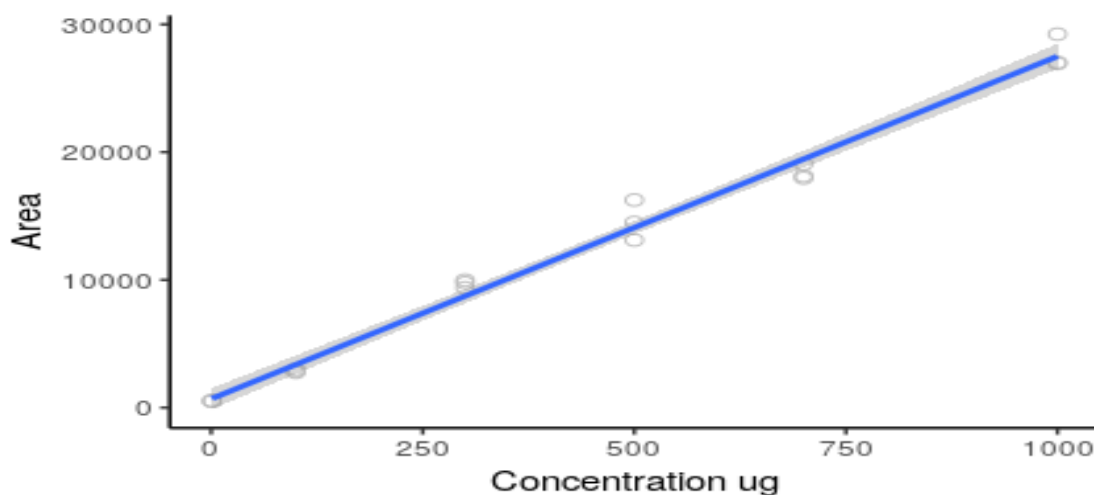


Figure 10. Calibration chart for 1-hydroxypyrene. Sequential dilutions were performed ($n = 3$) at 1000, 700, 500, 300, 100 and 1 $\mu\text{g kg}^{-1}$. The shaded area depicts the 95% confidence interval.

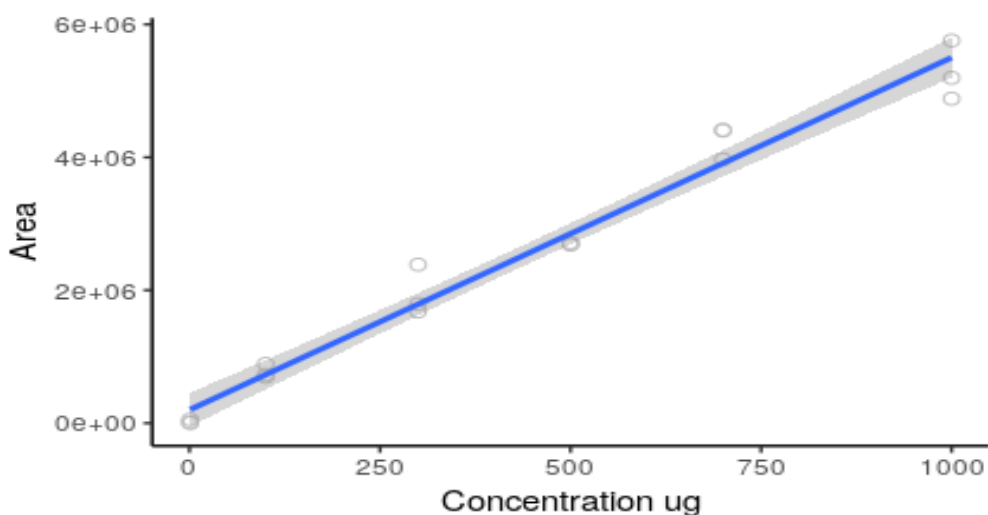


Figure 11. Calibration chart for pyrene. Sequential dilutions were performed ($n = 3$) at 1000, 700, 500, 300, 100, 1 $\mu\text{g kg}^{-1}$. The shaded area depicts the 95% confidence interval.

2.7.5 HPLC PAH determination

Five sequential dilutions (1, 3, 5, 7 and 10 $\mu\text{g ml}^{-1}$) were performed using a PAH calibration mix traceable certified reference material (Sigma Aldrich, UK) containing 16 individual PAH's, each with a

concentration of 10 µg ml⁻¹. The limits of quantification for all individual PAH's was determined where the signal to noise ratio did not fall below 10 : 1. The minimum quantification for all individual PAH's was 1 µg. Blanks were run following each analysis to identify carry over however, no carry over was identified. Individual retention times and regression coefficients are detailed in Table 7.

Table 7. Retention times, linearity (r^2 and RSD (%) of calibration curves for 16 individual PAH from PAH calibration mix traceable certified reference material.

PAH	Retention Time (min)	Linearity (r^2)	RSD %
Naphthalene	4.5	0.9721	6.19
Acenaphthylene	8.8	0.9788	7.22
Acenaphthene	9.2	0.9850	10.95
Fluorene	9.4	0.9781	8.69
Phenanthrene	9.6	0.9757	9.14
Anthracene	9.8	0.9701	2.78
Fluoranthene	10.0	0.9762	4.68
Pyrene	10.2	0.9716	12.95
Benz (a) anthracene	10.5	0.9680	11.73
Chrysene	11.0	0.9634	5.99
Benzo (b) fluoranthene	11.1	0.9786	7.65
Benzo (k) fluoranthene	11.3	0.9621	6.74
Benzo (a) pyrene	11.5	0.9665	8.61
Dibenz (a, h) anthracene	12.0	0.9783	8.07
Benzo (g h i) perylene	12.2	0.9755	10.67
Indeno (1, 2, 3 – C, D) pyrene	16.8	0.9923	11.14

2.7.6 Varian Vista - PRO ICP - OES

Metal analysis was conducted using a Varian Vista - PRO ICP - OES (Inductively Coupled Plasma, Optical Emission Spectrometry) instrument with detection limits (DL) and method detection limits (MDL) as shown in Table 8. MDL is defined as the minimum concentration of a substance which can be measured and reported with 99% confidence (Ketkar and Bzik, 1998). The ICP - OES was calibrated using Fisher Scientific ME / 1001 / 08 multi-element standards.

Table 8. DL and MDL for Varian ICP - OES.

Metal	DL mg l ⁻¹	MDL mg l ⁻¹
Cadmium	0.00041	0.00138
Chromium	0.00048	0.00159
Cu	0.00075	0.00251
Pb	0.00294	0.00979
Ni	0.00146	0.00487
Zn	0.00430	0.01435

2.8 Data analysis

All data obtained from experiments within the present study were analysed using R i386 version 3.4.2 statistical software (R core team, 2017). Results from sampled environmental matrices, worm tissue and biochemical tests are reported using the mean result \pm 1 standard error unless otherwise specified. All data were tested to meet assumptions for parametric tests, namely normality and homogeneity of error variances using the Shapiro- Wilk and Levene's test respectively. Data which did not meet assumptions were transformed using \log^{10} , arcsine or square root transformation. Two - way ANOVA's were performed to identify differences between one dependant and two independent variables. Differences between test groups and those of the control were assessed for differences using a one-way ANOVA. If assumptions were not met, Welch's robust ANOVA used as appropriate. Welch two way t – tests were performed to determine differences between means of two unmatched samples. Following ANOVA analysis, a *post hoc* comparison test of means with equal number of samples (*n*) was conducted using Tukey HSD test (ANOVA). Pearson's product moment correlation was applied to raw or transformed data to identify correlations between variables. If data assumptions were not met, Spearman's rank order correlation was used.

3. Metal concentrations in environmental matrices of the Fleet Lagoon, UK, and bioavailability to the marine polychaete *H diversicolor*

3.1 Introduction

Saline lagoons are listed as priority habitats in Annex 1 of the Habitats Directive (EU, 1992), defined as “Areas of shallow coastal water, wholly or partially separated from the sea by sand banks, shingle or less frequently, rocks” (Brown et al., 1997). These sites constitute 5.3% of European coastlines (Razinkovas et al., 2008). Separation from the surrounding environment results in a sublittoral habitat which acts as a sink for particulates including organics and fine sediment (Bamber et al., 1992; Barnes et al., 2008). Shallow water depths, freshwater inputs and evaporation result in variable salinity, water temperature and stratification of pH (Kjerfve, 1994). These unique environments provide highly productive ecosystems and vital habitat for species of fauna and flora (Razinkovas et al., 2008). Furthermore, shallow water depths, fluctuating environmental parameters and reduced tidal flushing associated with these environments further increase the likelihood of eutrophication, via leachate from land containing nitrogen compounds (Nixon et al., 2001). Indeed, the Fleet Lagoon, Dorset, UK received eutrophication status in 2001 ascribed to substantial blooms of planktonic algae including the dinoflaellate *Prorocentrum micans* (EA, 2016a). Subsequently, the lagoon was designated as Nitrogen Vulnerable Zone (NVZ) in 2002 resulting in steps to reduce nitrate - nitrogen concentrations of all freshwater inputs to the lagoon (EA, 2016).

However, anthropogenic pollution containing metals can also enter this habitat from sources including leachate from land, air particulates, and water exchange. Upon entry to the marine environment, metals may sorb to particulates within the water column which settle on the sea bed, allowing sediment to act as both sink and source for metal pollution during periods of natural modification

(Eggleton and Thomas, 2004; Fan et al., 2002; Frémion et al., 2016; Remaili et al., 2016a) and anthropogenic disturbance (Atkinson et al., 2007; Bryan and Langston, 1992). Thus, acute and chronic concentrations of metals may be available to benthic species with bioavailable fractions assimilated via ion mimicry, cellular active transport, passive diffusion across the cellular membranes and uptake of contaminated matrices (Chun-Mei et al., 2016; Luoma and Rainbow, 2005; Wang and Fisher, 1999b).

Sediment dwelling marine organisms are further exposed during feeding (Bignasca et al., 2011; Luoma and Rainbow, 2005; Mayer et al., 1997; Rainbow P. S et al., 2009a, b; Rosado et al., 2016; Turner, 2006; Williams et al., 2010; Zhen and Lawrence, 1999) where large quantities of sediment are ingested to satisfy dietary requirements due to low levels of intra - sediment food particles (Granberg and Forbes, 2006). Upon ingestion, metals may undergo biological regulation including partitioning into proteins and granules, transportation via proteins and enzymes to support physiological function (Depledge and Rainbow, 1990; Jorge et al., 2016; Serafim and Bebianno, 2007; Viarengo and Nott, 1993), deposition in tissue and excretion (Berthet et al., 2003). However, toxicity may arise when bioaccumulation of metals exceed the capability of regulatory systems (Rainbow et al., 1990).

Metal bioavailability is defined as the fraction of the total metal concentration directly obtainable via uptake pathways, which is related to the speciation of the contaminant and its ability to release from its bound particulate (Luoma, 1983; Meyer, 2002; Rainbow, 1995; Rosado et al., 2016). Therefore, toxicity determination of metals is a complex issue, where reliance on total concentrations of metals within sediment as a predictive criterion for sediment quality assessment fails to identify the role of metal speciation, uptake, and how environmental alterations effect metal speciation (Yin et al., 2014). Metals exist within marine sediment in differing species associated with discrete sedimentary solid phases including

carbonates, organic matter, sulphides and the crystalline lattice of minerals (Alvarez et al., 2014; Pueyo et al., 2008; Tang et al., 2016; Zhang et al., 2014).

Changes in the physiochemical environmental conditions including pH, salinity, dissolved oxygen and redox potential, may elicit desorption from bound fractions resulting in the remobilisation of metals into pore and overlying water, altering chemical speciation (Atkinson et al., 2007; Birch, 2017; Chun-Mei et al., 2016). Moreover, altered metals bioavailability following physiochemical changes have been observed: increased Fe (III) uptake in phytoplankton following exposure to reduced pH (7.7) (Breitbarth et al., 2010); exposure to pH (7.85) increased Ag bioaccumulation in the cuttlefish *Sepia officinalis* (Bustamante et al., 2009); higher salinity levels (25 ppt) increased Cd uptake in the killifish *Fundulus heteroclitus* (Dutton and Fisher, 2011).

Consequently, fractionation analysis of sediment to assess bioavailability, such as the Community Bureau of Reference (BCR) (Pueyo et al., 2008) and Tessier's procedure (Tessier et al., 1979) are commonly employed (Ma et al., 2016). These methods utilise chemicals and reagents as extractants, which act as oxidising, reducing and complexing agents to partition metals into separate fractions (Pueyo et al., 2008).

However, limitations regarding the accuracy of metal bioavailability determination through use of extracted metals in solution are subject to debate (Yin et al., 2014) as ingestion of metal contaminated sediment and associated alteration of metal specificity via gastrointestinal products are not addressed (Ianni et al., 2010). Additionally, within aerobic sediments, sulphate reduction to acid volatile sulphides (AVS) attributed to anoxic bacteria decreases the concentration of free metal ions therefore reducing bioavailability (De Jonge et al., 2009). Analysis of simultaneously extracted metal concentrations (SEM) associated with AVS is conventionally

considered a relevant method to determine important metals which have solubility products lower than FeS and MnS (DiToro and DeRosa, 2001). The formation of the sediment toxicology model, is based upon the prediction $AVS / SEM > 1$, where metals may be released into the pore water in toxic concentrations (DiToro and DeRosa, 2001; Ribeiro et al., 2013). However, debate surrounding the applicability of this method to quantify bioavailability is centred upon how metal specificity and bioaccumulation are not directly related to AVS - SEM in sediment (Arfaeina et al., 2016). Moreover, AVS - SEM does not detect changes of metal speciation via sediment bioturbation (Remaili et al., 2018) or abiotic influences (Celia et al., 2016; Correia and Costa, 2000; De Jonge et al., 2009; Yin et al., 2014; Zhuang and Gao, 2014) allowing highly contaminated sediment to be identified as low risk (Remaili et al., 2018).

To determine bioaccumulation of metals following ingestion of contamination by marine sediment dwelling organisms, levels found within the tissue and digestive fluids have been extracted and quantified (Turner and Olsen, 2000). Although this approach may demonstrate accuracy, practically this proves largely unworkable due to the small amounts of fluids extracted per organism, length of procedure time, impracticality of quantifying large sample numbers (Turner and Olsen, 2000) and quantifiable levels of pre adsorbed analytes (Bignasca et al., 2011). To overcome this difficulty, the digestive environment of sediment dwelling marine organisms may be simulated through use of pepsin, trypsin and protease K digestive enzymes to mimic the extraction of bioavailable metals via ingestion of sediment (Mayer et al., 1997; Turner, 2006; Turner and Olsen, 2000). Development of methods and accepted research by Bignasca et al (2010), Ianni et al. (2010), Maruya et al. (2012), Mayer et al. (1997), Peña-Icart et al. (2014), Rosado et al. (2016), Turner and Olsen (2000), have led to the use of the digestive enzyme proteinase

K to assess the effects of gastrointestinal processes of polychaetes and bioavailability of metals.

As no universally accepted approach to determine the bioavailability of metals to benthic invertebrates exists, it is necessary to apply a broad approach. Individually, each method may provide valuable information regarding the uptake and behaviour of metals in the marine environment. However, an integration of several methods may be required to further understand bioavailability and bioaccumulation.

For the first time, this study aims to identify metal bioavailability to the marine polychaete *H diversicolor* from sediment and water from the Eastern shoreline of the Fleet Lagoon, Dorset. Ten sites along the Eastern shoreline of the lagoon were selected to address the following objectives:

- (1) To determine metal concentrations in environmental matrices of the Fleet lagoon
- (2) Investigate the bioavailability of metals from sediment to *H diversicolor* using several techniques
- (3) Assess the relationship between sediment characteristics and metal bioavailability

3.2. Study Site

3.2.1 Study Site Information

The Fleet Lagoon, Dorset, UK, illustrated in Figure 12, is located along the south Dorset coast (50°37'N, 02°30'E). It is formed from the impoundment of marine water (Dyrynda and Cleator, 1995) behind the natural coastal shingle barrier of Chesil Beach, which extends 13.1 km from Portland to Abbotsbury (Weber et al., 2006). Physical characteristics include those of an inlet lagoon, with strong tidal currents and coarse sediments extending from Smallmouth to the entrance of the Narrows (Robinson, 1983). The lagoon basin exhibits reduced tidal currents and flushing, variable salinity and fine

sediments (Dyrynda and Cleator, 1995) with the main body of water entering at Smallmouth from Portland Harbour situated at the Southeast end of the lagoon (Robinson, 1983).

Seawater percolates into the Fleet via Chesil beach, with small influxes occurring during periods of storm surges (Robinson, 1983). Freshwater inputs (Figure 12), derive from 7 streams, shore runoff, and groundwater seepage from greensand aquifers and chalk which underlie the area (Johnston and Gilliland, 2000).

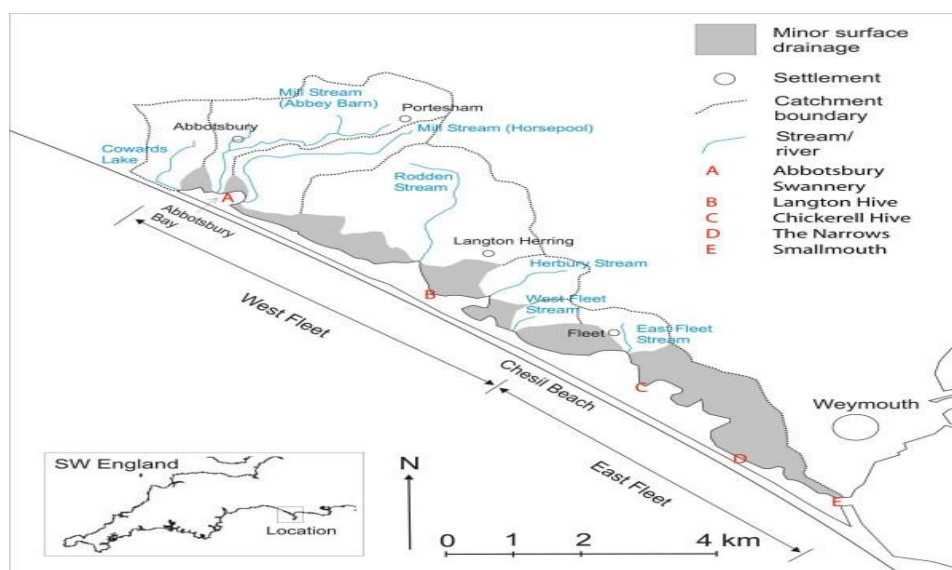


Figure 12. Map depicting the Fleet Lagoon highlighting freshwater inlets (Weber et al. 2006).

Width varies from 900 m at Littlesea to 65 m at the Narrows, with depths ranging from 3 – 5 m in the inlet channel to 2 m in the lagoon basin (Langston et al., 2006). The micro tidal range exhibited in Portland in addition to double low cycles result in low water stands of 3 - 4 hours (Dyrynda and Cleator 1995). However, tidal flow structure is primarily governed by currents extending through the Smallmouth inlet, allowing this area to be predominantly marine in character with average salinities in this region of 35 ppt (Ebrahimi et al., 2007). Widening of the lagoon at Littlesea and attenuation of tidal currents due to lagoon bed friction and shallow water depths allows weak penetration into the Eastern Fleet area with weak flushing and

circulation characteristics resulting in varied salinities (Langston et al., 2006). Dissipated wave energy and short-wave attenuation at the Abbotsbury embayment allows chemical and sediment mixing resulting in brackish water salinity (16 ppt) (Robinson, 1983).

These unique physical characteristics provides habitats for a range of species including the protected seagrass *Zostera marina*, the lagoon polychaete worm *Armandia cirrhosa* (Dyrynda and Cleator 1995), and waterfowl species (Langston et al., 2006). One aquaculture oyster farm is present near Ferrybridge in which *Magallana gigas* are grown and harvested (Weber et al., 2006). Physical characteristics and presence of protected species have led to designations: Grade 1. site of special scientific interest (SSSI) due to its physical characteristics and biodiversity; Ramsar wetland of world importance, a Priority Habitat (EU Habitats Directive); Special Protection Area (SPA) (EC Directive on Conservation of Wild Birds); Special Area of Conservation (Johnston and Gilliland, 2000).

However, agricultural, industrial and domestic contamination may enter the lagoon via migration of ground leachate downwards from the Southern limb of the Weymouth anticline due to the impermeable surface of Oxford Clay found in regions of the lagoon shore shown in Figure 13 (West, 2010).

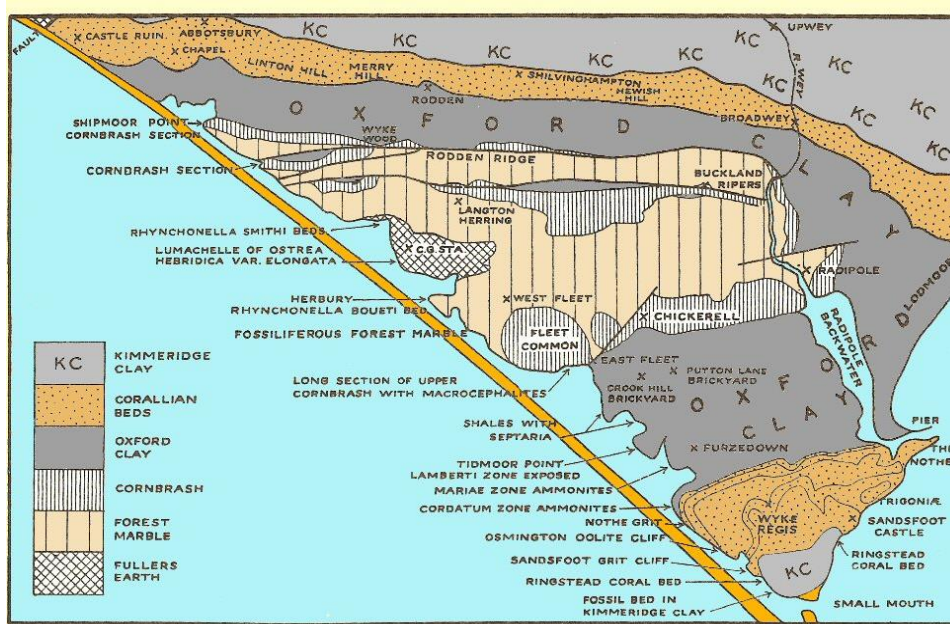


Figure 13. Geology of the Fleet Lagoon (West 2010).

Additionally, large discontinuous macropores found within chalk and greensand aquifers of the Lagoon further operate as preferential flow pathways allowing rapid movement of chemicals through unsaturated zones (West, 2010). Further transference of contaminants into the lagoon may occur from Portland Harbour governed by tidal exchange (Figure 14), by radioactive dye tidal flow tracing studies performed by Kershaw (2008).

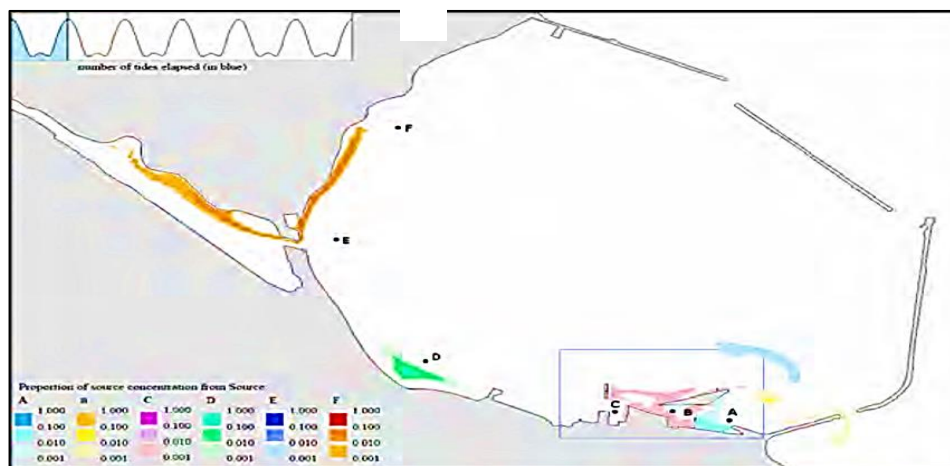


Figure 14. Fleet lagoon tidal flow. The tidal flow from Portland harbour, Dorset (UK) was investigated using radioactive tracer following one tide (Kershaw, 2008)

3.3 Fleet Lagoon Sample Sites

During the period May - August 2017, sediment, water and *H diversicolor* were obtained during environmental sampling of the Eastern shoreline of the Fleet Lagoon, Dorset (UK). Coordinates for all sample locations were obtained using a handheld Garmin 64s - d unit, and sample locations shown in Table 9 and Figures 15 and 16.

Table 9. GPS coordinates of all 10 sample sites of the Eastern Shoreline of the Fleet Lagoon.

Site Number	GPS Co-ordinates
1	50.653812, -2.603280
2	50.641185, -2.578046
3	50.637375, -2.560536
4	50.631441, -2.558219
5	50.623220, -2.543284
6	50.615214, -2.515561
7	50.614642, -2.514546
8	50.602059, -2.495491
9	50.593778, -2.493517
10	50.586531, -2.478239

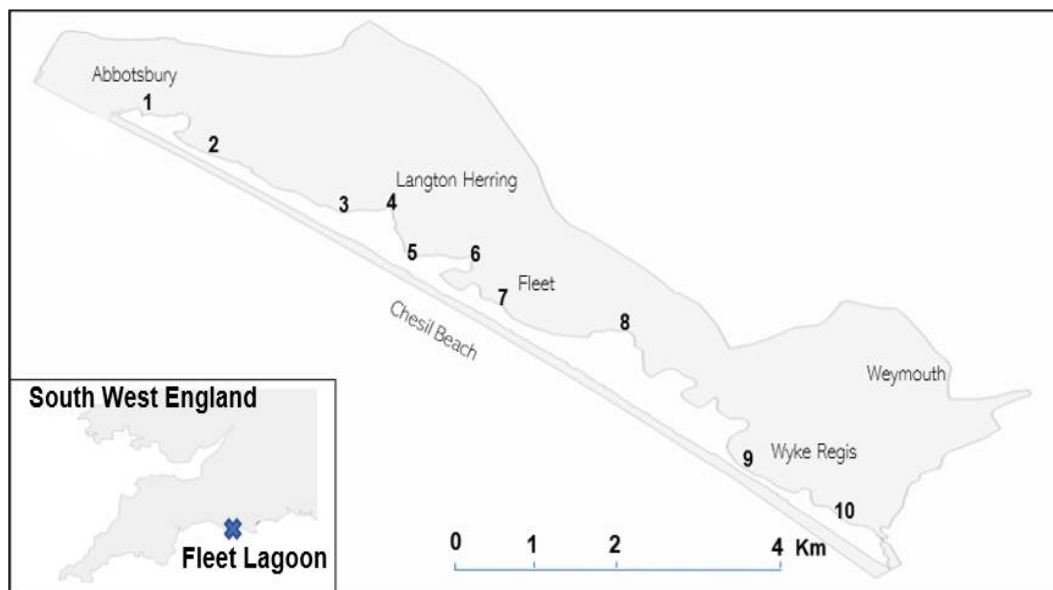


Figure 15. Fleet lagoon sample locations. 10 sample locations on the Eastern shoreline of the Fleet Lagoon, Dorset (UK).



Figure 16. Fleet lagoon digital images. 10 sample sites along the Eastern shoreline of the Fleet Lagoon.

3.4 Materials and Methods

3.4.1 Sampling

3.4.1.1 Collection of sediment and water for metal and PAH analysis

Sediment ($n = 3$, per site) and water samples ($n = 1$, per site) were obtained from the Fleet Lagoon Dorset between the periods 17th May and 28th August 2017. Sediment extraction was conducted as detailed in Chapter 2 (2.1.1.2). All samples were returned to the Laboratory at Bournemouth University within 6 h and refrigerated at 4°C until analysis.

3.4.1.2 Collection of *H. diversicolor*

H diversicolor were sampled from the Fleet Lagoon as detailed in Chapter 2 (2.1.1.4). However, worms were not located at sites 8 or 9 which may be due to the sediment characteristics at the shoreline. It was not practical to venture further into the middle of the lagoon due to the presence of deep mud which would render this activity

extremely hazardous. Furthermore, sediment concentrations of metals and PAH may differ than found near the shoreline. All worms were returned to the Laboratory at Bournemouth University within 6 h and placed in clean manufactured sea water (15 ppt salinity, 17°C) for a period of 48 h to depurate guts. Worms were then frozen at -20°C until analysis.

3.4.1.3 Collection of Water samples for metal analysis.

Water samples for metal analysis were conducted as described in Chapter 2 (2.1.1.3). All metal sample bottles were fully labelled and placed into isothermal boxes during the sampling processes. All samples were returned to the Laboratory at Bournemouth University within 6 h and refrigerated at 4°C until analysis.

3.4.1.4 Sediment Characterisation

Grain size distribution and loss on ignition analysis of the sediment samples were measured as detailed in Chapter 2 (2.2.2, and 2.2.1 respectively).

3.4.1.5 Reagents and Solutions

All chemicals purchased were analytical grade from Sigma Aldrich (UK). All reagents were produced using Millipure Ultra-pure water. All glassware was washed in 20% HNO₃ and then rinsed in 10% HNO₃. Finally, glassware was rinsed in distilled water. Digestion / centrifuge tubes used in these procedures were purchased from Sigma Aldrich.

3.4.1.6 Chemical Determination of Total metals and sequential sediment extraction

Total concentrations of metals and sequential extraction from the sediment samples were conducted as detailed in Chapter 2 (2.3.2 and 2.3.4 respectively). Quality control of sediment digestions was determined through use of the analysis of Certified References

materials with results detailed in Chapter 2 (2.7.1) and (2.7.2) respectively.

3.4.1.7 Total metal in water

Water samples for metal analysis were sent to a commercial laboratory (I2 analytical Laboratory, Watford, UK) for determination of metal concentrations by ICP - MS.

3.4.1.8 Worm tissue metal analysis

Individual worms were analysed as described in Chapter 2 (2.3.3). Quality control of samples was determined through digestion of certified reference materials the results of which, are fully detailed in Chapter 2 (2.7.3).

3.4.1.9 Proteinase K Extraction

The bioavailable fraction was determined using proteinase K following a procedure proposed by Turner (2006). A 0.4 mg ml⁻¹ Proteinase K solution was prepared using phosphate buffer (pH 7.4, 1.179 g of potassium dihydrogen phosphate (KH₂PO₄) and 4.300 g of disodium hydrogen phosphate (Na₂HPO₄) in 1 l of distilled water). 0.5 g of each sediment sample in triplicate was weighed and placed in a centrifuge tube to which 25 ml of the proteinase K solution was added. The samples were then shaken at 250 rpm for 3 h at room temperature. The samples were then centrifuged for 20 min at 4200 rpm and the supernatant removed. Metal concentrations for Ag, As, Cu, Ni, Pb, and Zn was determined by ICP - OES (Varian Vista Pro).

2.4.2.0 Statistical analysis

All data were analysed using Ri386 statistics version 3.4.2 and significance determined by $p = < 0.05$ in all instances. All analysis was tested to meet the assumptions for parametric tests. When

assumptions were not met, data was transformed using square root, arcsine or log¹⁰ transformation. Shapiro - Wilk tests were then performed to assess normality of transformed data. Levene's tests were then performed to determine equality of variance. One - way ANOVA's were performed to determine differences of mean values across sites for particle descriptors and LOI followed by Tukey *post hoc* test to identify specific site differences. One - way ANOVA's were also performed to determine site differences for sediment Cu, Ni and Pb concentrations, proteinase K digestion and BCR digestion. Welch's robust ANOVA's were performed to determine differences of median values across sites when raw or transformed data failed to meet assumptions for parametric tests specifically, skewness and kurtosis, As total metal concentration and worm weights. Pairwise comparisons were performed following Welch's robust ANOVA's to identify site differences for skewness and kurtosis results.

Pearson's correlation coefficient was conducted on raw or transformed data to identify linear correlations: sediment characteristics and total metal concentrations; total metal sediment and pore water metal concentrations; total metal concentrations and BCR steps; porewater metal and worm tissue metal concentrations; LOI and total metal concentrations; LOI and sediment characteristics. When transformed data did not meet the assumptions for Pearson's correlations, Spearman's correlations were performed specifically: porewater metal and BCR metal concentrations; worm tissue metal concentrations and worm weight; proteinase K metal digestion and worm tissue metal concentrations; total metal and worm tissue concentrations; water and worm tissue metal concentrations; worm tissue metal concentrations and BCR steps; water and pore water metal concentrations; water metal and BCR steps.

Partial correlation's using worm weight as the controlling factor were used to identify the influence of worm weight on whole worm tissue concentrations.

3.5 Results

3.5.1 Sediment Characterisation

3.5.1.1 Particle size analysis

Results of the particle size analysis of the 10 sampled sites are shown in Table 10.

Table 10. Particle size analysis (mean +/- 1SE) of sediment samples ($n = 3$) taken from sample locations of the Fleet lagoon as detailed in Chapter 2 (2.1.1.1).

Site	Clay (0.06µm)	Very Fine Silt (3.9 µm)	Fine Silt (7.8 µm)	Medium Silt (15.6 µm)	Coarse Silt (31 µm)	Very Fine Sand (63 µm)	Fine Sand (125 µm)	Medium Sand (250 µm)	Coarse Sand (500 µm)	Very Coarse Sand (1000 µm)
1	27.54+/- 0.3	17.46+/- 0.22	17.25+/- 0.22+/- 0.15	17.36+/- 0.59	15.41+/- 0.20	4.95+/- 0.11	<0.01	0	0	0
2	13.79+/- 0.5	11.24+/- 0.47	12.59+/- 0.74	16.19+/- 0.47	19.09+/- 0.31	24.78+/- 0.20	2.29+/- 0.81	0	0	0
3	25.58+/- 0.7	18.64+/- 0.91	15.86+/- 0.65	15.28+/- 0.32	12.53+/- 0.33	7.34+/- 0.19	4.44+/- 0.16	0.31+/- 0.02	0	0
4	20.55+/- 0.11	16.93+/- 0.29	16.99+/- 0.59	16.78+/- 0.88	14.89+/- 0.19	8.94+/- 0.16	3.65+/- 0.29	1.25+/- 0.04	0.04+/- 0.01	0
5	6.84+/- 0.23	5.99+/- 0.3	7.59+/- 0.83	11.27+/- 0.47	14.29+/- 0.30	19.78+/- 0.51	26.89+/- 0.41	7.32+/- 0.16	0.02+/- 0.001	0
6	9.07+/- 0.31	7.65+/- 0.61	10.29+/- 0.81	14.97+/- 0.08	16.53+/- 0.55	19.39+/- 0.48	19.73+/- 0.37	2.34+/- 0.09	0	0
7	6.19+/- 0.41	5.96+/- 0.55	6.53+/- 0.49	9.55+/- 0.11	14.80+/- 0.29	19.51+/- 0.33	22.88+/- 0.28	14.46+/- 0.14	0.90+/- 0.01	0
8	4.079+/- 0.67	3.74+/- 0.81	5.07+/- 0.19	10.70+/- 0.20	12.20+/- 0.36	21.87+/- 0.71	29.97+/- 0.26	12.33+/- 0.61	2.49+/- 0.3	0.01+/- 0.001
9	4.76+/- 0.97	4.29+/- 0.25	6.17+/- 0.37	9.72+/- 0.16	19.39+/- 0.16	18.70+/- 0.33	19.62+/- 0.31	17.59+/- 0.29	15.41+/- 0.48	0.32+/- 0.01
10	4.14+/- 0.2	2.73+/- 0.28	3.59+/- 0.53	5.27+/- 0.13	8.99+/- 0.08	15.81+/- 0.26	28.73+/- 0.29	30.48+/- 0.33	9.65+/- 0.33	0.98+/- 0.02

Analysis revealed that the proportions of measured fractions between the size ranges 0.06 - 2000 µm were variable ranging from; 4 - 27% clay (0.06 µm), 3 - 18% Very Fine Silt (3.9 µm), Fine Silt (7.8 µm) 4 - 17%, Medium Silt (15.6 µm) 5 - 17%, Coarse Silt (31µm) 9 - 17%, Very Fine Sand (63 µm) 5 - 21%, Fine Sand (125 µm) < 1 - 30%,

Medium Sand (250 μm) < 1 - 25%, Coarse Sand (500 μm) < 1 - 11%,
Very Coarse Sand (1000 μm) 0 - < 1%.

All sites were characterised as extremely poorly to moderately poorly sorted detailed in Table 11. All sites were predominately composed of very fine to medium sand and silt. However, there was a general characteristic of reduced silt concentrations from site 1 - 10 and an increase in sand concentrations from site 1 - 10.

Table 11. Particle descriptors of sediment samples taken from sample locations in the Fleet Lagoon: x_a denotes the mean grain size (+/- 1SE) per location ($n = 3$); σ_a sediment sorting, Sk_a , skewness of sample (mean +/- 1SE) , K_a , Kurtosis of sample (mean +/- 1SE) (Pini, 2014). Sample descriptors were calculated as per the method described by Folk and Ward (1957).

Site	x_a	σ_a	Sk_a	K_a	Description
1	14.28	1.71	-.406	0.07	Poorly sorted
	+/- 0.027	+/- 0.05	+/- 0.02	+/- 0.01	
2	12.50	1.28	-.329	1.14	Poorly sorted
	+/- 0.031	+/- 0.04	+/- 0.01	+/- 0.02	
3	12.5	5.25	0.18	-0.03	Extremely
	+/- 0.17	+/-0.05	+/- 0.04	+/- 0.04	Poorly Sorted
4	11.12	1.14	-1.133	0.619	Poorly sorted
	+/- 0.22	+/- 0.02	+/- 0.02	+/- 0.03	
5	11.11	0.636	1.00	0.064	Moderately sorted
	+/-0.8	+/- 0.04	+/- 0.04	+/- 0.04	
6	11.11	0.808	1.00	0.063	Moderately Sorted
	+/- 0.6	+/-0.03	+/- 0.02	+/- 0.02	
7	11.11	5.025	-.079	-2.035	Extremely
	+/- 0.08	+/- 0.09	+/-0.04	+/- 0.01	Poorly Sorted
8	11.38	1.301	1.03	-0.042	Poorly sorted
	+/- 0.07	+/- 0.04	+/- 0.02	+/- 0.03	
9	11.59	0.894	-.242	-1.799	Poorly Sorted
	+/- 0.05	+/- 0.03	+/- 0.03	+/- 0.02	
10	11.04	0.98	1.19	0.07	Poorly Sorted
	+/- 0.2	+/- 0.02	+/- 0.03	+/- 0.03	

Results from one - way ANOVA's reveal significant differences between sites for X_a ($F_{(9, 20)} = 15.32, p = < 0.01$). Tukey *Post hoc* test showed significant differences of means were found for sites 2 - 10 and site 1, sites 4 - 8 and site 3, sites 3 - 8 and site 10. One - way

ANOVA identified significant differences for σ_a between sites ($F_{(9, 20)} = 474.8$, $p = < 0.01$) for all means excluding those between sites 4 & 2, 8 & 2, 7 & 3 and 10 & 9 identified as significantly different by Tukey *post hoc* tests.

Sk_a and Ka results for all site locations did not meet the assumptions for parametric tests on raw or transformed data. Therefore, Welch's robust ANOVA's were performed which showed differences between median values for all site locations ($F_{(9)} = 2431.2$, $p = < 0.01$) and ($F_{(9)} = 8249.3$, $p = < 0.01$) respectively.

3.5.1.2 Loss on Ignition Content

Percentage loss on ignition results showed variation between all sample sites (Figure 17).

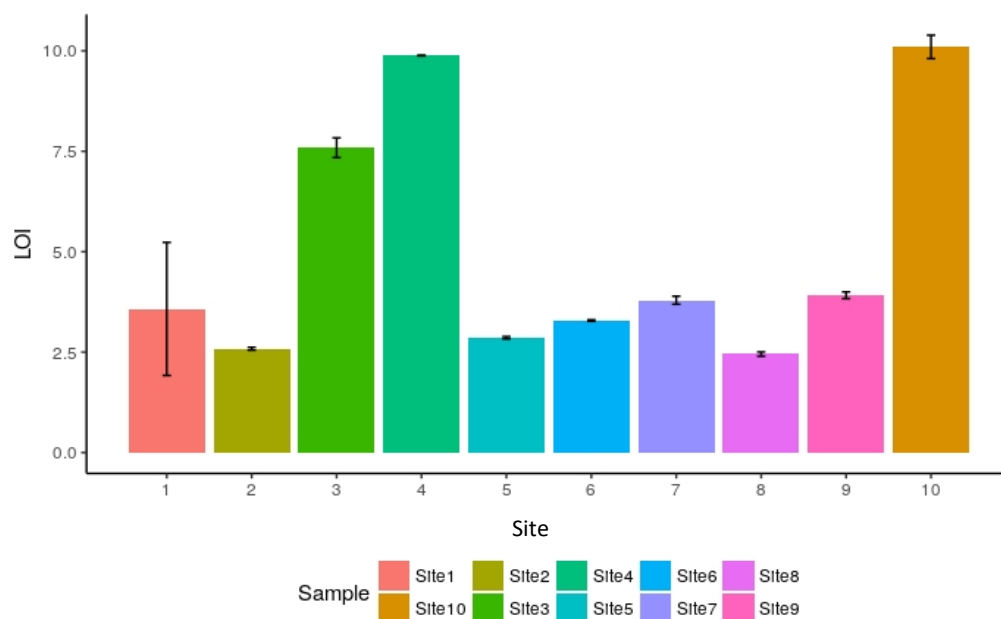


Figure 17. Percent loss on ignition results for 10 sample sites from the Fleet Lagoon. Error bars indicate the +/- 1 SE.

Lowest mean loss on ignition values ranged across the sample sites: 2.45% (site 8); 2.59% (Site 2); 2.86% (Site 5); 3.29% (Site 6); 3.58% (Site 1); 3.79% (Site 7); and 3.91% (site 9). Highest mean values for loss on ignition were found at site 10 (10.1%), site 3 (7.59%) and site 4 (9.89%).

One - way ANOVA's showed significant differences between sites ($F_{(9, 20)} = 92.88, p = < 0.01$). Tukey *post hoc test* revealed significant differences between sites 1 - 9 with site 10, sites 4 - 9 with site 3 and sites 1, 2 and 9 with site 4. All other sites were not found to be significantly different from each other.

3.5.1.3 Total Metal Content of Sediment

Total metal concentrations ($n = 3$) for the element's As, Cu, Ni, Pb and Zn from each of the 10 sample sites are detailed in Table 12. All results are reported in dry weight mg kg^{-1} . Concentrations for As and Ni range from the lowest values of 2.9 mg kg^{-1} and 3.19 mg kg^{-1} respectively at site 6 to the highest of 57.9 mg kg^{-1} at site 8 for As and site 3 at 68.2 mg kg^{-1} for Ni. Cu values ranged from the lowest of 4.5 mg kg^{-1} at site 1 to 51.29 mg kg^{-1} at site 10. Pb show variation between the lowest of 8.8 mg kg^{-1} at site 2 and highest of 84.8 mg kg^{-1} at site 10. Zn values ranged from the lowest of 23.7 mg kg^{-1} at site 2 to the highest of 242.4 mg kg^{-1} at site 10.

Table 12. Concentrations (dry weight mg kg⁻¹) of As, Ni, Pb and Zn from 10 sample locations (sample: *n* = 3) of the Eastern shoreline of the Fleet Lagoon, Dorset. Canadian sediment quality guidelines which detail the threshold effects level (TEL) (values over TEL highlighted in blue) and probable effects levels (PEL) (values over PEL highlighted in red) Mean values are reported +/- 1SE.

Site Number	As	Cu	Ni	Pb	Zn
1	47.55 +/- 3.96	4.55 +/- 0.59	23.19 +/- 1.67	60.79 +/- 8.09	132.37 +/- 13.54
2	4.84 +/- 0.93	8.81 +/- 3.95	4.85 +/- 0.54	8.88 +/- 0.46	23.74 +/- 1.65
3	49.06 +/- 5.13	24.25 +/- 4.68	68.23 +/- 7.37	38.55 +/- 5.07	205.49 +/- 1.97
4	7.75 +/- 0.20	11.22 +/- 5.32	7.54 +/- 0.50	20.19 +/- 2.00	49.30 +/- 12.09
5	6.58 +/- 0.64	5.16 +/- 1.90	5.58 +/- 0.22	16.84 +/- 2.07	30.20 +/- 4.30
6	2.98 +/- 0.17	6.89 +/- 1.65	3.20 +/- 0.28	14.72 +/- 1.44	26.76 +/- 2.90
7	9.75 +/- 0.70	23.32 +/- 1.13	34.10 +/- 1.94	21.15 +/- 1.33	83.99 +/- 5.22
8	57.95 +/- 7.87	26.16 +/- 4.09	57.19 +/- 5.90	37.93 +/- 1.88	129.37 +/- 11.95
9	17.12 +/- 1.06	10.58 +/- 0.61	19.03 +/- 1.04	13.15 +/- 0.92	78.05 +/- 3.81
10	29.58 +/- 2.77	51.29 +/- 13.68	20.15 +/- 4.17	94.03 +/- 0.22	242.44 +/- 18.67
TEL	7.24	18.7	-	30.2	124
PEL	41.6	108	-	112	271

Results show that As levels in sediment from sites 1, 3 and 8 exceeded the PEL with the maximum concentration of 57.95 mg kg⁻¹ found at site 8. TELs were exceeded for As (sites 4 and 7); Cu (sites 3, 7, 8 and 10); Pb (sites 1 3 8 and 10); Zn (1, 3, 8 and 10). Welch's robust ANOVA revealed significant differences between sites for As concentrations ($F_{(7)} = 436.39$, $p = < 0.01$). Whereas, one - way

ANOVA's detailed significant differences across all sites: Cu ($F_{(9, 20)} = 21.98, p = < 0.01$); Ni ($F_{(9, 20)} = 325.7, p = < 0.01$); Pb ($F_{(9, 20)} = 193.4, p = < 0.01$).

3.5.1.5 Water metal concentrations

Metal concentrations of water samples ($\mu\text{g l}^{-1}$) taken from all 10 sample locations of the Fleet Lagoon show variability (Table 13).

Table 13. Metal concentrations ($\mu\text{g l}^{-1}$) in water samples ($n = 1$) from all 10 sample locations of the Fleet Lagoon, Dorset.

Site	As	Cu	Ni	Pb	Zn
1	2.51	1.9	0.6	0.3	6.7
2	1.96	1.8	0.7	0.2	8.3
3	2.08	4.6	0.7	0.3	17
4	1.16	2.8	<0.5	0.2	5.3
5	1.79	3.4	<0.5	<0.2	4.7
6	1.45	2.1	<0.5	<0.2	4.0
7	0.85	4.8	<0.5	0.3	3.1
8	1.21	1.5	<0.5	<0.2	2.9
9	0.41	2.4	<0.5	<0.2	2.5
10	0.70	3.4	0.6	0.2	6.4

As concentrations ranged from the highest values at site 1 ($2.51 \mu\text{g l}^{-1}$) to the lowest ($0.41 \mu\text{g l}^{-1}$) at site 9. All other sample locations had values $< 0.05 \mu\text{g l}^{-1}$. Highest values for Cu were found at site 7 ($4.8 \mu\text{g l}^{-1}$), and lowest at site 8 ($1.5 \mu\text{g l}^{-1}$). Sites 2 and 3 showed the highest values for Ni ($0.7 \mu\text{g l}^{-1}$) with all other sample locations $< 0.6 \mu\text{g l}^{-1}$. The highest values of $0.3 \mu\text{g l}^{-1}$ for Pb were found in samples from sites 1, 3 and 7. Pb values at all other sample locations were $\leq 0.2 \mu\text{g l}^{-1}$. Zn values ranged from $17.0 \mu\text{g l}^{-1}$ at site 3 to $2.5 \mu\text{g l}^{-1}$ at site 9.

3.5.1.6 Total metal content in *H diversicolor* tissue

Mean total metal content of worm tissue ($n = 3$) and worm weight sampled individuals obtained from each location are detailed in Table 14.

Table 14. Concentrations of metals (mean \pm 1SE) (dry weight mg kg^{-1}) in worm tissue. Worms ($n = 3$) were obtained during sediment sampling for each site using a hand fork to turn over sediment at depths of 20 cm. *H diversicolor* were not found at sites 8 and 9.

Site Number	As (mg kg^{-1})	Cu (mg kg^{-1})	Ni (mg kg^{-1})	Pb (mg kg^{-1})	Zn (mg kg^{-1})	Mean Weight (g)
1	8.85 \pm 0.28	9.25 \pm 3.44	2.26 \pm 0.61	1.22 \pm 0.78	104.55 \pm 13.86	0.04 \pm 0.01
2	6.87 \pm 1.00	14.56 \pm 2.14	2.65 \pm 0	2.65 \pm 0	127.33 \pm 20.59	0.03 \pm 0.01
3	17.30 \pm 1.72	21.12 \pm 3.54	1.83 \pm 0.76	1.20 \pm 0.61	154.49 \pm 26.19	0.03 \pm 0.01
4	13.04 \pm 3.41	17.43 \pm 4.22	5.72 \pm 2.89	1.83 \pm 0.50	121.07 \pm 8.91	0.03 \pm 0.02
5	11.12 \pm 1.62	20.23 \pm 4.59	4.58 \pm 1.58	1.44 \pm 0.12	99.21 \pm 6.28	0.05 \pm 0.02
6	15.13 \pm 0.24	33.33 \pm 0.83	3.80 \pm 0.07	2.13 \pm 0.10	127.46 \pm 5.73	0.03 \pm 0.02
7	9.81 \pm 2.00	12.06 \pm 5.01	2.13 \pm 0.39	2.64 \pm 1.27	136.02 \pm 16.60	0.03 \pm 0.01
10	30.63 \pm 2.41	20.59 \pm 2.91	4.72 \pm 2.17	2.26 \pm 0.65	120.41 \pm 29.05	0.10 \pm 0.04

Mean worm weight varied across the sites, ranging from 0.03 to 0.10 g. The largest worms were found at site 10, which had mean values of 0.10 g whereas all other sites had significantly lighter but similar weight worms. A Welch's robust ANOVA revealed differences between individual wet worm weight (g) from each site ($F_{(7)} = 22$, $p = < 0.01$). As dry weight concentrations ranged from the lowest of 6.87 mg kg^{-1} at site 2 to 30.63 mg kg^{-1} at site 3. Dry weight tissue

concentrations for Pb had lowest values of 1.12 mg kg⁻¹ at site 3 and highest from worms taken from site 7 of 2.64 mg kg⁻¹ at site 2. Dry weight tissue concentrations for Cu ranged from 9.25 mg kg⁻¹ at site 1 to 33.33 mg kg⁻¹ for site 6. Lowest concentrations of Ni (1.83 mg kg⁻¹ dry weight) were found from worms taken from site 1, with the highest values of 4.72 mg kg⁻¹ dry weight for site 10. Zn values ranged from 99.21 mg kg⁻¹ dry weight from worms taken from site 5, with the highest values of 154.67 mg kg⁻¹ dry weight from worms taken from site 3.

3.5.1.7 BCR Sequential Analysis

BCR sequential analysis was conducted on samples ($n = 3$) taken from each sample site from the Fleet Lagoon. The total mg kg⁻¹ dry weight concentrations from steps 1 - 3 were totalled to obtain the bioavailable fraction. This revealed that the relative proportion of metal in the bioavailable fractions decreased in the order Zn > Pb > Cu > Ni > As. Results for each analysed metal are shown in Tables 15 - 19.

The bioavailable fraction of As (Table 15) ranged from the lowest value of 2.73 mg kg⁻¹ at site 6 to the highest of 5.93 mg kg⁻¹ at site 9. As was mainly present in the oxidizable fraction with an average across all sites of 64%, whereas reducible and exchangeable fractions were lower at 21% and 14% respectively.

Table 15. As concentrations (mean +/- 1SE) (mg kg⁻¹ dry weight) each step of the BCR sequential analysis. Results for each step were then totalled to obtain the overall bioavailable fraction.

As

Site Number	BCR Step 1	BCR Step 2	BCR Step 3	Bioavailable fraction (Σ Steps 1 - 3)
1	0.48 ± 0.04	0.76 ± 0.21	2.18 ± 0.08	3.416
2	0.48 ± 0.02	0.34 ± 0.06	2.51 ± 0.02	3.325
3	0.45 ± 0.21	0.73 ± 0.11	2.04 ± 0.06	3.225
4	0.64 ± 0.09	0.48 ± 0.07	2.41 ± 0.17	3.488
5	0.51 ± 0.05	0.49 ± 0.03	2.43 ± 0.08	3.431
6	0.31 ± 0.08	0.41 ± 0.13	2.02 ± 0.25	2.726
7	0.26 ± 0.15	0.93 ± 0.10	1.97 ± 0.15	3.159
8	0.53 ± 0.06	0.97 ± 0.12	2.12 ± 0.24	3.628
9	0.88 ± 0.11	2.09 ± 0.59	2.96 ± 0.09	5.930
10	0.63 ± 0.16	0.28 ± 0.05	2.41 ± 0.02	3.320

A one - way ANOVA of each step revealed significant differences between sites: Step 1; ($F_{(9, 20)} = 7.49$, $p = < 0.01$), Step 2; ($F_{(9, 20)} = 25.33$, $p = < 0.01$) and Step3; ($F_{(9, 20)} = 13.87$, $p = < 0.01$).

Cu was found as an average across all sites predominately in the oxidizable fraction (80%), with lower values for reducible (15%) and bound to carbonate fractions (8%) (Table 16).

Table 16. Cu concentrations (mean +/- 1SE) (mg·kg⁻¹ dry weight) each step of the BCR sequential analysis. Results for each step were then totalled to obtain the overall bioavailable fraction.

Cu

Site Number	BCR Step 1	BCR Step 2	BCR Step 3	Bioavailable Fraction (Σ Steps 1 - 3)
1	0.73 ± 0.13	0.33 ± 0.02	1.70 ± 0.31	2.76
2	0.75 ± 0.16	0.26 ± 0.05	5.66 ± 0.34	6.67
3	0.03 ± 0.02	1.46 ± 0.03	2.62 ± 1.12	4.12
4	0.72 ± 0.30	0.59 ± 0.03	2.94 ± 0.76	4.24
5	0.65 ± 0.24	0.35 ± 0.01	3.73 ± 3.41	4.73
6	0.62 ± 0.18	0.73 ± 0.06	8.05 ± 4.57	9.40
7	0.050 ± 0.01	4.07 ± 0.04	5.09 ± 0.31	9.21
8	0.71 ± 0.09	1.09 ± 0.10	4.90 ± 1.567	6.70
9	0 ± 0	0.97 ± 0.11	0.95 ± 0.13	1.92
10	1.14 ± 0.41	0.97 ± 0.59	20.34 ± 2.23	22.44

Significant differences between sites were revealed using one - way ANOVA's: Step 1; ($F_{(9, 20)} = 10.94$, $p = < 0.01$), Step2; ($F_{(9, 20)} = 33.58$, $p = < 0.01$) and Step3; ($F_{(9, 20)} = 6.208$, $p = < 0.01$).

The total bioavailable fraction for Ni (Table 17) ranged from, 14.23 mg kg⁻¹ at site 3 to 0.72 mg kg⁻¹ at site 6, with average percentage fractions highest for oxidizable of 60% and lower values for reducible (40%) and bound to carbonates (12%).

Table 17. Ni concentrations (mean +/- 1SE) (mg kg⁻¹ dry weight) each step of the BCR sequential analysis. Results for each step were then totalled to obtain the overall bioavailable fraction.

Ni

Site Number	BCR Step 1	BCR Step 2	BCR Step 3	Bioavailable Fraction (∑ Steps 1 - 3)
1	0.22 ± 0.03	0.39 ± 0.04	1.76 ± 0.13	2.37
2	0.29 ± 0.13	0.11 ± 0.02	0.64 ± 0.06	1.05
3	1.62 ± 0.77	4.46 ± 0.23	8.15 ± 0.45	14.23
4	0.26 ± 0.02	0.25 ± 0.01	0.52 ± 0.01	1.03
5	0.28 ± 0.05	0.26 ± 0.01	0.68 ± 0.04	1.23
6	0.13 ± 0.01	0.11 ± 0.04	0.48 ± 0.03	0.72
7	0.51 ± 0.04	3.35 ± 0.18	3.27 ± 0.05	7.13
8	0.75 ± 0.04	1.92 ± 0.24	6.45 ± 0.84	9.12
9	0.42 ± 0.02	3.68 ± 0.16	0.75 ± 0.10	4.85
10	0.26 ± 0.04	1.43 ± 0.02	1.14 ± 0.18	2.84

Significant differences were found between sites for each of analysis using one - way ANOVA's: Step1; ($F_{(9, 20)} = 23.63, p = < 0.01$), Step2; ($F_{(9, 20)} = 47.36, p = < 0.01$) and Step3; ($F_{(9, 20)} = 23.34, p = < 0.01$).

The total bioavailable Pb concentrations (Table 18) ranged from the highest values of 46.61 mg kg⁻¹ at site 10 to the lowest of 2.58 mg kg⁻¹ at site 2. Mean percentages across all sites were highest for oxidizable fraction (56%), with lower values for reducible (38%) and bound to carbonates (4%).

Table 18. Pb concentrations (mean +/- 1SE) (mg kg⁻¹ dry weight) each step of the BCR sequential analysis. Results for each step were then totalled to obtain the overall bioavailable fraction.

Pb

Site Number	BCR Step 1	BCR Step 2	BCR Step 3	Bioavailable Fraction (Σ Steps 1 - 3)
1	0.33 \pm 0.07	6.57 \pm 0.44	10.21 \pm 1.18	17.18
2	0.19 \pm 0.08	0.96 \pm 0.12	1.42 \pm 0.05	2.56
3	0.19 \pm 0.09	6.58 \pm 0.29	6.43 \pm 0.56	13.19
4	0.37 \pm 0.01	2.68 \pm 0.12	2.65 \pm 0.30	5.70
5	0.37 \pm 0.06	2.14 \pm 0.11	1.84 \pm 0.08	4.36
6	0.38 \pm 0.06	2.20 \pm 0.10	3.83 \pm 1.70	6.41
7	0 \pm 0	7.47 \pm 0.40	3.11 \pm 0.12	10.58
8	0.11 \pm 0.03	4.14 \pm 0.35	4.75 \pm 0.91	9.01
9	0 \pm 0	2.30 \pm 0.22	0.76 \pm 0.05	3.06
10	3.35 \pm 0.88	10.82 \pm 1.75	32.45 \pm 9.68	46.61

One - way ANOVA's conducted on each step revealed significant differences between each site: Step1; ($F_{(9, 20)} = 37.59, p = < 0.01$), Step2; ($F_{(9, 20)} = 79.42, p = < 0.01$), Step3; ($F_{(9, 20)} = 27, p = < 0.01$).

Percentages for oxidizable and reducible fractions of Zn (Table 19) were comparable at 40 % and 39% respectively. Zn bound to carbonates were the lowest percentage fraction of 13%.

Table 19. Zn concentrations (mean +/- 1SE) (mg·kg⁻¹ dry weight) each step of the BCR sequential analysis. Results for each step were then totalled to obtain the overall bioavailable fraction.

Zn

Site Number	BCR Step 1	BCR Step 2	BCR Step 3	Bioavailable Fraction (Σ Steps 1 - 3)
1	4.21 \pm 0.76	9.53 \pm 1.14	10.86 \pm 1.41	24.60
2	2.11 \pm 0.17	2.37 \pm 0.27	5.26 \pm 1.48	9.78
3	4.53 \pm 2.12	14.29 \pm 1.03	7.22 \pm 2.18	26.04
4	3.17 \pm 0.05	3.30 \pm 0.09	3.51 \pm 0.44	9.98
5	3.06 \pm 0.28	3.36 \pm 0.29	4.69 \pm 1.85	11.10
6	3.60 \pm 0.11	4.32 \pm 0.02	9.18 \pm 1.18	17.10
7	2.12 \pm 0.12	12.82 \pm 0.78	6.93 \pm 0.11	21.87
8	3.70 \pm 0.33	9.17 \pm 0.82	11.11 \pm 1.12	23.98
9	0.97 \pm 0.02	8.77 \pm 1.07	2.41 \pm 0.04	12.15
10	22.37 \pm 1.58	21.94 \pm 3.50	41.93 \pm 7.14	86.24

Results of one - way ANOVA's reveal significant differences between each step for every site: Step1; ($F_{(9, 20)} = 147$, $p = < 0.01$), Step2; ($F_{(9, 20)} = 65.9$, $p = < 0.01$), Step3; ($F_{(9, 20)} = 59.93$, $p = < 0.01$).

Bioavailable fractions were highest at site 10 for Zn (86.24 mg kg⁻¹), Pb (46.61 mg kg⁻¹), and Cu (22.44 mg kg⁻¹), however the lowest values were at site 2 (9.74 mg kg⁻¹, 2.58 mg kg⁻¹) for Zn and Pb respectively, and at site nine (1.19 mg kg⁻¹) for Cu.

3.5.1.8 Pore water metal analysis

Metal concentrations of pore water obtained from sediment samples for each sample location is detailed in Table 20.

Table 20. Concentrations of metals ($\mu\text{l l}^{-1}$) found in pore water analysis. Samples ($n = 1$) were extracted from sediment cores taken in conjunction with cores obtained for metal analysis.

Site Number	As ($\mu\text{l l}^{-1}$)	Cu ($\mu\text{l l}^{-1}$)	Ni ($\mu\text{l l}^{-1}$)	Pb ($\mu\text{l l}^{-1}$)	Zn ($\mu\text{l l}^{-1}$)
1	1.91	3.9	2.9	0.3	8.0
2	0.72	2.1	1.9	<0.2	3.9
3	0.97	4.5	3.9	0.4	7.2
4	1.57	2.5	2.1	0.3	8.6
5	1.67	4.2	2.7	0.7	9.1
6	0.80	4.2	4.4	0.4	5.9
7	1.33	1.9	1.8	0.2	6.6
8	2.51	4.0	2.9	4.2	40
9	0.89	5.2	2.0	0.8	11
10	0.80	6.3	10	0.8	16

Highest values for As, Pb and Zn were found at site 8 ($2.51 \mu\text{g l}^{-1}$, $4.2 \mu\text{g l}^{-1}$, and $40 \mu\text{g l}^{-1}$ respectively), with lowest values found at site 2 ($0.72 \mu\text{g l}^{-1}$). Cu and Ni had highest values at site 10 ($6.3 \mu\text{g l}^{-1}$ and $10 \mu\text{g l}^{-1}$) respectively, with lowest values of $1.9 \mu\text{g l}^{-1}$ and $1.8 \mu\text{g l}^{-1}$ respectively at site 7.

3.5.1.9 Proteinase K Metal Digestion

Proteinase K was used to digest sediment samples obtained from each sample location. Metal concentrations obtained are shown in Table 21.

Table 21. Proteinase K sediment digestion results (mean +/- 1SE) (mg kg⁻¹ dry weight) obtained from sediment samples (n = 3) extracted for use in total metal content determination.

Site Number	As (mg kg ⁻¹)	Cu (mg kg ⁻¹)	Ni (mg kg ⁻¹)	Pb (mg kg ⁻¹)	Zn (mg kg ⁻¹)
1	0.36 ± 0.01	0.39 ± 0.08	0.10 ± 0.02	0.02 ± 0.02	0.15 ± 0.06
2	0.26 ± 0.02	0.49 ± 0.13	0.12 ± 0.01	0.03 ± <0.01	0.01 ± <0.01
3	0.67 ± 0.02	0.62 ± <0.01	0.18 ± 0.03	0.02 ± 0.01	0.08 ± 0.04
4	0.32 ± 0.02	0.41 ± 0.09	0.12 ± <0.01	0.02 ± 0.01	0.03 ± <0.01
5	0.26 ± 0.02	0.35 ± 0.02	0.12 ± <0.01	0.01 ± 0.01	0.02 ± <0.01
6	0.20 ± 0.02	0.53 ± 0.17	0.08 ± <0.01	0.03 ± 0.01	0.03 ± <0.01
7	0.42 ± 0.02	0.66 ± 0.20	0.52 ± 0.19	0.10 ± 0.05	0.69 ± 0.35
8	0.63 ± 0.01	0.33 ± 0.13	0.18 ± 0.01	0.02 ± 0.01	0.01 ± <0.01
9	0.32 ± 0.02	0.51 ± <0.01	0.02 ± <0.01	0.01 ± 0.01	0.01 ± 0
10	0.33 ± 0.01	0.82 ± 0.06	0.12 ± <0.01	0.15 ± 0.01	0.53 ± 0.01

One - way ANOVA's revealed significant differences between each site for each metal: As ($F_{(9, 20)} = 12.28, p = < 0.01$); Cu ($F_{(9, 20)} = 6.00, p = 0.01$); Ni ($F_{(9, 20)} = 40.84, p = < 0.01$); Pb ($F_{(9, 20)} = 18.57, p = < 0.01$); Zn ($F_{(9, 20)} = 14.5, p = < 0.01$). Cu concentrations obtained after digestion of sediment using proteinase K are the highest totalling 4.289 mg kg⁻¹ dry weight (d.w), followed by As (3.77 mg kg⁻¹ d.w), Ni 1.57 mg kg⁻¹ d.w), Zn (1.54 mg kg⁻¹ d.w) and Pb (0.40 mg kg⁻¹ d.w). The highest concentrations following proteinase K digestion for Cu and Pb were from site 10 (0.82 mg kg⁻¹ and 0.15 mg kg⁻¹) respectively with the lowest values (0.33 mg kg⁻¹ d.w) from site 8 for Cu and site 9 (0.01 mg kg⁻¹ d.w) for Pb. Highest values for Zn and Ni were found at site 7 (0.69 mg kg⁻¹ and 1.10 mg kg⁻¹ d.w) respectively, with lowest dry weight values: 0.01 mg kg⁻¹ at site 2 for Zn, 0.05 mg kg⁻¹ for Ni at site 9. Highest values for As were 0.67 d.w mg kg⁻¹ at site 3 with lowest values of 0.20 mg kg⁻¹ d.w at site 6.

3.5.2.0 Relationships between total metal concentrations and pore water

Pearson's correlations revealed that there were no significant relationships between total metal content in sediment across all sites and that of respective concentrations of metals found in pore water: As ($r = 0.514, p = 0.682$); Cu ($r = 0.499, p = 0.157$); Ni ($r = 0.097, p = 0.314$), Pb ($r = 0.143, p = 0.221$); Zn ($r = 0.528, p = 0.096$).

3.5.2.1 Relationships between total metal sediment and BCR sequential sediment digestion concentrations

Pearson's correlations between total metal concentrations and those of each step of the BCR sequential sediment digestion showed no significant relationships as shown in Table 22.

Table 22. Pearson's correlation results of total metal concentrations and the individual steps of the BCR sequential sediment digestion

Metal	BCR Step 1	BCR Step 2	BCR Step 3
As	$r = 0.02, p = 0.07$	$r = 0.07, p = 0.08$	$r = -0.18, p = 0.51$
Cu	$r = 0.62, p = 0.09$	$r = 0.38, p = 0.44$	$r = 0.53, p = 0.23$
Ni	$r = 0.04, p = 0.52$	$r = 0.11, p = 0.06$	$r = -0.10, p = 0.42$
Pb	$r = 0.05, p = 0.72$	$r = 0.02, p = 0.32$	$r = -0.15, p = 0.23$
Zn	$r = 0.17, p = 0.22$	$r = 0.22, p = 0.09$	$r = 0.16, p = 0.45$

3.5.2.1 Relationships between porewater and sequentially extracted sediment

Spearman's correlation analysis identified a significant correlation between pore water and total BCR results for As ($r_s = 0.539, p = < 0.05$) and Zn ($r_s = 0.404, p = 0.05$).

Spearman's correlation between pore water concentration and each individual BCR step identified: BCR Step1 and Pb ($r_s = 0.66, p = < 0.01$), Zn ($r_s = 0.517, p = < 0.01$); BCR Step 2 and As ($r_s = 0.582, p = < 0.05$), BCR Step 3 and Pb ($r_s = 0.409, p = 0.050$).

3.5.2.2 Relationships between tissue metal concentration and worm weight

Spearman's correlations were performed on worm tissue metal concentrations and worm weight. Partial correlations controlling for

worm weight were also conducted between worm tissue and total metal sediment concentrations shown in Table 23.

Table 23. Correlations between metal concentrations found in sediment (mg kg⁻¹) and worm weight.

Metal	Dry worm weight (g) from sites 1 - 10 and worm tissue concentration (mg kg ⁻¹)		Partial correlations between metal sediment concentration, worm tissue metal concentration controlling for dry worm weight (g) (mg kg ⁻¹)	
	r_s	p	r_s	p
As	.42	.04	.25	.25
Cu	.32	.12	.19	.38
Ni	.32	.13	-.27	.21
Pb	.45	.03	.24	.28
Zn	.001	.60	.23	.28

Results show a significant relationship between worm tissue As ($r_s = 0.42$, $p = 0.05$) and Pb ($r_s = 0.45$, $p = 0.03$) concentrations and worm weight. However, partial correlations using worm weight as the controlling factor did not show any significant relationships.

3.5.3.3 Relationships between pore water and worm tissue metal concentration

Pearson's correlation coefficients for pore water metal concentrations and worm tissue metal concentrations show a non-significant correlation: As ($r = -0.342$, $p = 0.333$); Cu ($r = -0.096$, $p = 0.792$); Ni ($r = -0.084$, $p = 0.817$).

However, there was a negative correlation for Pb ($r = -0.631$, $p = 0.050$) and Zn ($r = -0.692$, $p = 0.027$) suggesting that as the pore water concentration for Pb and Zn increases, worm tissue concentration decreases.

3.5.3.4 Proteinase K metal digestion concentration and worm tissue concentration

Spearman's correlations revealed a strong positive correlation between proteinase K and worm tissue concentrations for Cu ($r_s = 0.642$, $p = 0.05$) and Pb ($r_s = 0.686$, $p < 0.01$) whereas, a negative

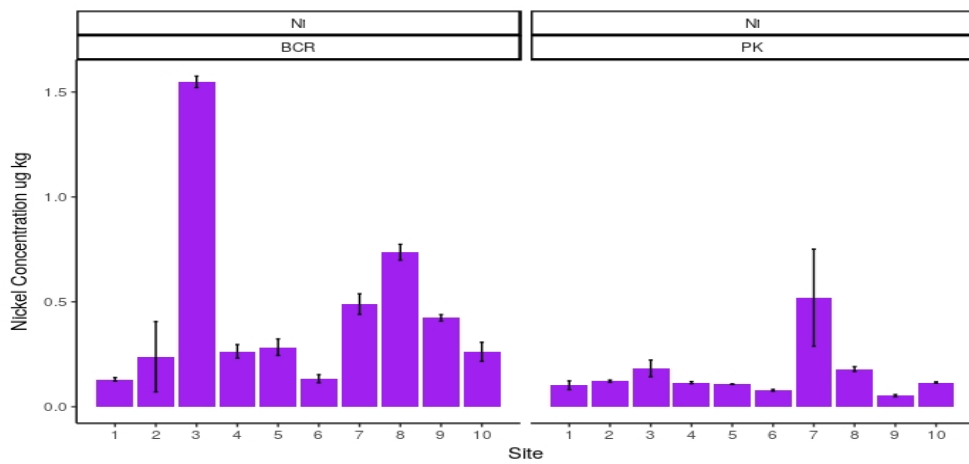
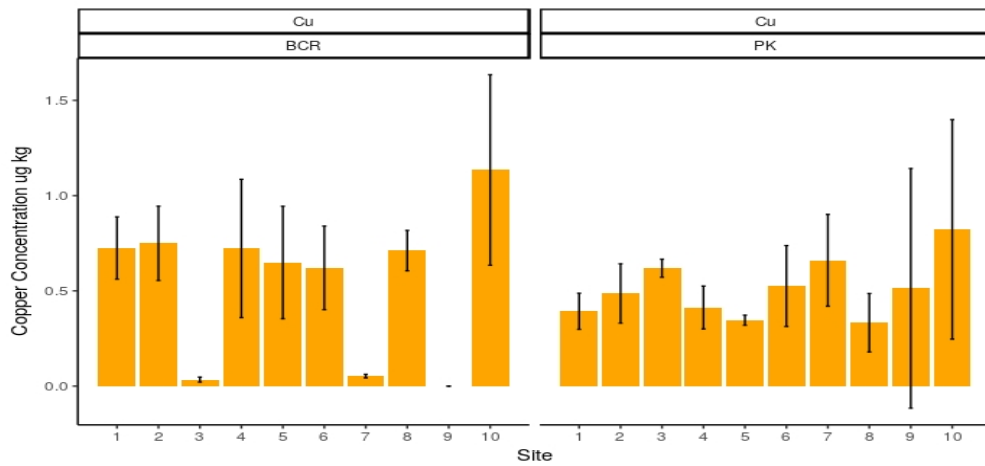
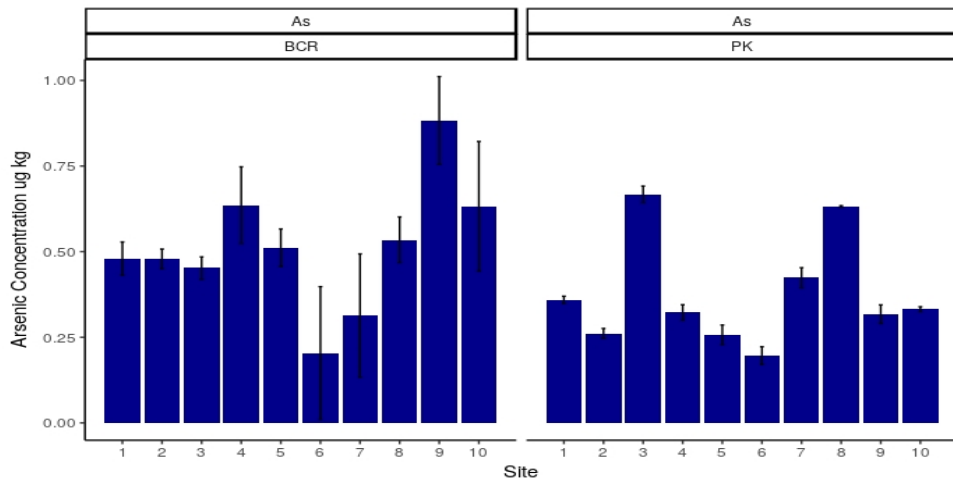
relationship was observed for Ni ($r_s = -0.40$, $p = 0.049$). There were no relationships identified for As or Zn.

3.5.3.5 Partial correlation between worm tissue metal, proteinase K and pore water metal concentrations

Partial correlations between pore water and proteinase K metal concentrations, using worm tissue metal concentrations as the controlling factor, revealed positive correlations for Cu ($p = 0.02$), Pb ($p = 0.05$) and Zn ($p = 0.01$). These results indicate that both pore water and sediment digestion influence the bioaccumulation of Cu, Pb and Zn in *H diversicolor*. However, there were no significant correlations for As ($p = 0.69$) or Ni ($p = 0.15$).

3.5.3.5 Comparison between sequential and enzymatic extraction

Enzymatic extractions for this test series were performed using a ratio of solution to solid of 50:1 (Figure 18), which is the same ratio applied to the first step of the BCR sequential extraction and therefore, comparisons between these methods are applicable. For the metals Cu, Ni, Pb, and Zn, concentrations extracted via the BCR step 1 using acetic acid are generally higher than proteinase K extraction. However, higher values for As were obtained using proteinase K than the acetic acid extraction.



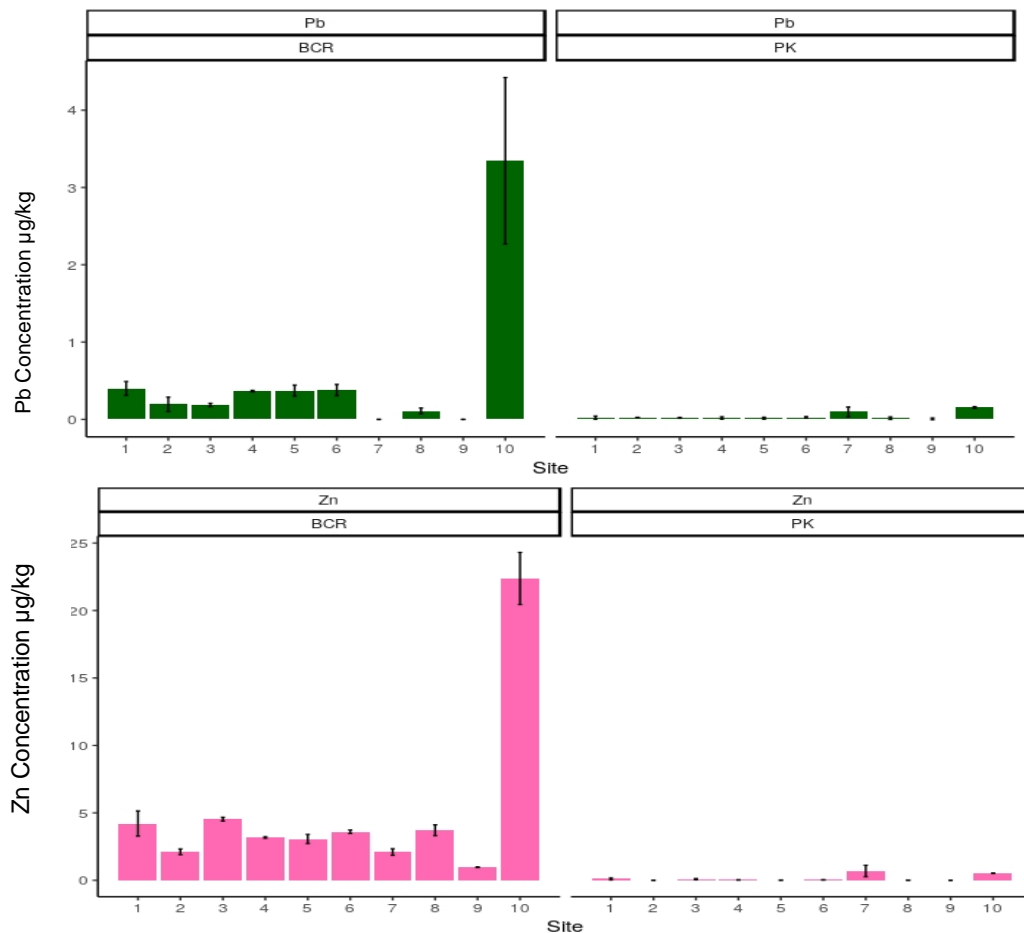


Figure 18. Comparison of metal concentrations (mg kg^{-1} d.w) obtained using BCR step 1 and proteinase K digestions. Error bars represent the $\pm 1\text{SE}$.

3.5.3.6 Relationships between sediment metal concentrations and worm tissue metal concentrations

Total metal sediment and total metal worm tissue concentrations were analysed using Spearman's correlation. Results show a positive relationship for As ($r_s = 0.460$, $p = 0.02$) and a negative relationship for Ni ($r_s = -0.52$, $p = < 0.01$). There were no significant relationships found for Cu, Pb or Zn.

3.5.3.7 Relationships between water metal concentrations and worm tissue metal concentrations

Spearman's correlations show a negative relationship for As ($r_s = -0.473$, $p = 0.02$) and Ni ($r_s = -0.414$, $p = 0.04$) with a very weak relationship for Cu ($r_s = 0.134$, $p = 0.53$).

3.5.3.8 Relationships between worm tissue and individual BCR Steps

Spearman's correlations were conducted to identify relationships between the concentration in worm tissues and both the BCR results for each step and the total BCR bioavailable concentration. For Step 1, there were no relationships between worm tissue and BCR step 1. A positive relationship was identified for Cu in Step 2 ($r_s = 0.809$, $p = 0.021$). A negative relationship was identified for Ni in Step 3 ($r_s = -0.62$, $p = < 0.01$). No relationships for any metal found for the Total BCR Concentrations.

3.5.3.9 Relationships between water metal and pore water concentrations

There were no significant relationships between water and that of pore water concentrations for any metal analysed.

3.5.4.0 Relationships between water and BCR sequential sediment extraction

Spearman's correlations between metal water results and individual BCR Steps revealed: Step 1; A negative relationship exists between Pb and water metal concentration ($r_s = -0.454$, $p = 0.03$): Step 2; A positive relationship was found for Cu ($r_s = 0.82$, $p = < 0.01$) and Pb ($r_s = 0.504$, $p = 0.01$): Step 3; A positive relationship was found for Ni ($r_s = 0.43$, $p = 0.03$) and Pb ($r_s = 0.429$, $p = 0.04$): Total BCR; A positive relationship was found for Ni ($r_s = 0.411$, $p = 0.04$) and Pb ($r_s = 0.507$, $p = 0.01$).

3.5.4.1 Relationships between sediment characteristics and metal concentrations

Pearson's correlation was performed on sediment characteristic results and total metal concentrations. There was no significant relationship between the sediment characteristics and the concentrations of the metal's As and Ni. Results for Cu show a significant negative correlation for medium silt (15.6 μm) ($r = -0.674$, $p = 0.03$), Coarse Silt (31 μm) ($r = -0.825$, $p = < 0.01$), and a significant

positive relationship for medium sand (250 μm) ($r = 0.659$, $p = 0.03$) and very coarse sand (1000 μm) ($r = 0.745$, $p = 0.01$). A negative significant relationship exists between Zn and coarse silt (31 μm) ($r = -0.861$, $p = 0.00$), Pb and coarse silt (31 μm) ($r = -0.751$, $p = 0.01$). A positive significant relationship exists between Pb and very coarse sand (1000 μm) ($r = 0.669$, $p = 0.03$).

3.5.4.2 Relationships between loss on ignition and total metal sediment concentrations

Loss on ignition and total metal concentrations for all samples site were analysed to assess for statistically significant relationships. A Pearson's correlation was performed which revealed a positive correlation between loss on ignition values and Cu ($r = 0.463$, $p = 0.010$), Pb ($r = 0.488$, $p = 0.006$) and Zn ($r = 0.448$, $p = 0.013$). There were no significant relationships for As and Ni.

3.5.4.3 Relationships between loss on ignition and sediment characteristics

Pearson's correlation was used to determine relationships between sediment characteristics and loss on ignition with results showing significant positive relationships for clay (0.06 μm) ($r = 0.711$, $p = 0.02$) and very fine silt (3.9 μm) ($r = 0.778$, $p = 0.00$). Negative significant relationships exist for very fine sand (63 μm) ($r = -0.817$, $p = 0.00$) and fine sand (125 μm) ($r = -0.791$, $p = 0.00$).

3.6 Discussion

3.6.1 Sediment characteristics

Granulometric composition of the sediment samples taken from all 10 sample sites showed differences in the composition of sand, clay and silt fractions. Generally, silt and clay fractions decreased from site 1 extending to site 10 whereas sand fractions increased. Silt may accumulate in the upper regions of the lagoon via deposition from

inlet streams, land run off and subsequent settlement of organic matter. Weber et al. (2006) detailed how strong tides originating from the entrance to the Fleet lagoon at Smallmouth influence the lagoon basin. Reduced tidal range then extends upwards towards Abbotsbury (Site 1) from the Narrows (Robinson 1983). A reduction of tidal exchange and water flushing may therefore decrease the potential for particles of silt to be drawn down towards the Ferrybridge end (Site 10) and may further explain the decrease of sand fractions from the Narrows extending to Abbotsbury.

LOI results for sampled locations show variability throughout the lagoon with the highest values found at sites 3, 4 and 10. Accumulation of organic matter may occur at sites 3 and 4 again, as a result of the reduced tidal flushing and water exchange in these regions of the lagoon. Moreover, the embayment features and shallow water depths may further reduce water flow and allow these areas to act as sinks for organic matter.

Total metal sediment concentrations show the highest Σ mean total for As, Cu, Ni, Pb and Zn at site 10. Pearson's correlation analysis revealed significant positive relationships: Cu with medium sand and very coarse sand fractions; Pb and very coarse sand with the highest values of these fractions found at site 10. Additionally, Mendiguchia et al. (2006), Perfetti-Bolano et al. (2018) and Abuchacra et al. (2015) identified positive correlations between LOI concentrations and the accretion of Cu, Pb and Zn in marine sediments. As statistically significant relationships between LOI, Cu, Pb and Zn were identified in the present study, this may suggest that the high LOI levels found at site 10, 4 and 3 influenced the accretion of Cu, Pb and Zn at these locations.

A statistically significant relationship exists between LOI and clay and very fine silt sediment fractions which may influence the LOI results found at sites 3 and 4. Importantly, the presence of the oyster aquaculture farm situated between sites 9 and 10 may influence LOI

levels. An increase of organic matter into surrounding environments related to oyster aquaculture has been evidenced (Erler et al., 2017; Forrest and Creese, 2006; Mitchell, 2006; Quintino et al., 2012). Furthermore, human activities associated with aquaculture re-disperse detritus settled beneath the growing racks which may then be transported by tides and currents (Mitchell, 2006). Therefore, high LOI results found at site 10 may be influenced by the presence of the aqua culture oyster fishery and release of organic detritus. However, the impact of transported detritus in the Fleet lagoon is unknown and warrants further investigation.

Relationships have been observed between small particle size sediment and organic matter (Froehner et al., 2009; He et al., 2016; Koiter et al., 2015; Ma et al., 2016). Results gained from this study are in agreement as correlations were identified between LOI, clay and very fine silt fractions from sediment samples. Organic particulate matter may enter the lagoon system via inlet streams, run off from land, breakdown of organic matter and detritus from fauna. Moreover, reduced tidal flushing and water exchange (Robinson, 1983) which occurs towards the Abbotsbury end of the lagoon may influence the concentrations of clay and silt fractions in these locations.

High Σ mean metal concentrations found at sites 10, 8, 3 and 1 were between 2 - 6 times higher than found at site 2, 5, 6, 4 and 9. Embayment features at sites 3 and 8 may influence the accumulation of metals in these regions, resultant from tidal flow, current exchange and reduced water depths (Ebrahimi, 2004; Robinson, 1983). High Σ mean metal concentrations found at site 1 may further be influenced by the reduced tidal flushing and potentially, the accumulation of metals in these locations.

3.6.1.1 Historic and current metal concentrations

Historic metal sediment analysis reported by Nunney and Smith (1995) show differing sample locations to those in this study.

However, similarities exist between sites 2C, 3C and the oyster aquaculture facility detailed in their study and those of sites 3, 7 and 10 in this study respectively.

Results show higher readings for Zn (205.5 mg kg^{-1}), Pb (38.5 mg kg^{-1}), Ni (68.2 mg kg^{-1}) and As (49.0 mg kg^{-1}) at site 3 than those found historically at site 2C (Zn 100 mg kg^{-1} , Pb 5 mg kg^{-1} , Ni 25 mg kg^{-1} and As 14 mg kg^{-1}). Comparisons for Cu (24.3 mg kg^{-1}) and (24 mg kg^{-1}) at site 3 and 2C respectively show similarities.

Similar concentrations for Zn (83.9 and 95 mg kg^{-1}), Ni (34.1 and 25 mg kg^{-1}) and Cu (23.3 and 20 mg kg^{-1}) were found between sites 7 in this study and location 3C. Significantly higher values for Pb were found at site 7 than 3C (21.1 and 5 mg kg^{-1}) respectively however, higher As values were reported at 3C (16 mg kg^{-1}) than this study (9.8 mg kg^{-1}).

Higher readings were found at site 10 for Zn, (242 mg kg^{-1}), Pb (94.0 mg kg^{-1}), Cu (51.3 mg kg^{-1}), and As (29.6 mg kg^{-1}) than at the oyster farm (72 mg kg^{-1}), (10 mg kg^{-1}), (24 mg kg^{-1}), (15 mg kg^{-1}) respectively. Concentrations of Ni (20.1 mg kg^{-1}) were of similar values to those found previously (18 mg kg^{-1}) and (24 mg kg^{-1}). The present study identified higher concentrations than those of the historic study of all metals at specific locations indicating both accretion and the continued environmental input of these metals.

Exact locations for the historic study are unknown due to lack of reported coordinates. Furthermore, the methods used to sample the sediment are also unreported and loss on ignition analysis was not conducted. General comparisons show significantly higher levels of Zn, Pb, Cu and As at site 10 in the present study than previously reported at the oyster farm location. It is supposed that elevated levels of LOI found at this location may contribute to the accumulation of these metals at this site.

Similar concentrations were found between site 7 and 3C for Zn, Ni, Cu and As. Pb at site 7 was significantly higher and may indicate

accumulation at this location in the period between the studies. Additionally, comparisons between site 5 for the present study and site 2C show that historic concentrations for Zn, Ni, Cu and As were significantly higher. However, results for Pb at this sample site again show elevated levels compared to the historic concentrations.

3.6.2 Metals bioavailability

The influence of environmental matrices, in particular pore water, on bioavailability of metals has been suggested as a primary exposure pathway for benthic organisms (Chapman et al., 2002; Li et al., 2014; Wang and Fisher, 1999b).

Within the present study, negative relationships were identified between pore water and worm tissue for Pb ($r = -0.631$, $p = 0.05$) and Zn ($r = -0.692$, $p = 0.027$). Furthermore, negative relationships were identified between water As ($r_s = -0.473$, $p = 0.02$) and Ni ($r_s = -0.414$, $p = 0.04$) concentrations. One very weak positive relationship was identified for water and worm tissue metal concentrations for Cu ($r_s = 0.134$, $p = 0.053$). However, partial correlations between worm tissue metal concentrations and proteinase K sediment digestion using worm tissue metal concentrations as the controlling factor revealed positive correlations for Cu ($p = 0.02$), Pb ($p = 0.05$) and Zn ($p = 0.01$). As *H diversicolor*, continually aerates its burrows with oxygenated water directed from the water column, contact with pore water will occur during movements through and ingestion of sediment as water bathing the worms will be from the overlying water column (Buffet et al., 2011; Rainbow et al., 2009a). However, there is no literature evident which determines whether bioaccumulation of metals from pore water occurs via epidermal uptake or ingestion during feeding and warrants further research.

Results gained in the present study identify that both pore water and sediment ingestion influence the assimilation of Cu, Pb and Zn in *H diversicolor*. The influence of pore water metal concentrations and assimilation have been reported where Pini et al. (2014),

demonstrated correlations between Zn concentrations in pore water and tissue concentrations in the polychaete *Nereis virens* although the authors did not identify positive relationships for Cu. Porewater cadmium uptake was also observed in the polychaete *Neanthes arenaceodentata* however, assimilation of Ni and Zn correlated to sediment digestion (Lee et al., 2000). It is assumed that the dominant pathway for metal assimilation in many benthic organisms is through ingestion (Baumann and Fisher, 2011a, b; Casado-Martinez et al., 2009; Lee et al., 2000). Yet, it is not clear whether the influence of pore water reported in the present study are assimilated during the ingestion process or through epidermal uptake.

There were no statistical relationships found between the concentrations of metals in sediment and tissue concentrations of worms the findings of which agree with Berthet et al. (2003), Mayer et al. 1997, Pueyo et al. 2008, Rainbow et al. (2009a), that total metal concentrations do not correlate with metal bioaccumulation.

Additionally, partial correlations between worm tissue and sediment concentrations and worm weight did not identify any significant correlations. Worms obtained from sample site 10 were significantly heavier than those from all other sample locations. Worm weight at this location may be influenced by the high levels of LOI, a result of possible detritus from the oyster farm present at this location as previously discussed. The influence of detritus from aquaculture facilities on benthic invertebrates has been evidenced where Huang et al. (2018) describe increased levels of polyunsaturated fatty acids in the bio-deposits from a scallop farm that increased the nutritional quality of *Canuellidae* that fed on the detritus. Additionally, Ferriss et al. (2016) demonstrate that aquaculture facilities can increase biomass densities in the surrounding environment partly related to the increase of detritus. However, to fully elucidate effects of oyster aquaculture detritus on the feeding behaviours, biomass and body mass of *H diversicolor*, further research is required.

There were no significant relationships found between worm tissue and sediment total metal concentrations using worm weight as a controlling factor. Poirier et al. (2006) describe how increased body weight was positively correlated to Pb and Ag whole body concentrations in *H diversicolor* used as a control group. However, they found an inverse relationships between Cd, Cu, Zn and worm tissue concentrations in *H diversicolor* from the Seine Estuary. Interestingly, Pini et al. (2015) demonstrated site specific correlations between Cu worm tissue and weight in *Nereis virens* although the mechanisms which account for this are not reported. Therefore, findings reported in the present study may indicate site specific tolerance, regulation and bioaccumulation of metals in resident Fleet lagoon populations. Site specific weight and assimilation of metal by *H diversicolor* have been reported in previous studies by Mouneyrac et al. (2003), McQuillan et al. (2014), Berthet et al. (2003), Rainbow et al. (2009). It is suggested that investigations of the influence of weight and bioaccumulation of metals in *H diversicolor* are conducted from various sites including individual's with differing weights, to further clarify the effects of worm weight on assimilation of metals.

Analysis of relationships between worm tissue metal concentrations and total metal in sediment identified a significant correlation for As ($r_s = 0.460$, $p = 0.02$). The predominate form of bioavailable As in the marine environment is arsenate (Ellwood and Maher, 2003), which is found co-precipitated or adsorbed to oxidizable fractions associated with Mg oxide, hydrous Fe or Fe arsenate (Neff, 1997). Bioaccumulated As within organisms is generally found in non-toxic species including arsenobetaine, arsenocholine, monomethylarsinate, dimethylarsinate and tetramethylarsonium (Ellwood and Maher 2003). Within the sediment samples of the present study, the predominant BCR As fraction was found to be oxidizable (64%) whereas the reducible (21%) and exchangeable (14%) fractions were lower across all sites. However, As bound to

the exchangeable fraction within sediment has been reported to be the most bioavailable to aquatic organisms (Liu et al., 2014a). It is suggested therefore, that the levels of As identified in the worms may directly relate to the exchangeable fraction however identification of this fraction in worm tissue was not conducted in the present study.

Furthermore, a negative relationship was found between water and worm tissue concentrations. Under reducing conditions, arsenate is reduced to As(III) which may then react with sulphides producing sulphide compounds (Gomez-Ariza et al., 2000). These compounds may then be released into pore water (Casado-Martinez et al., 2012). Results in this study from reducible fractions in BCR step 2 identified a correlation with pore water concentrations ($r_s = 0.582$, $p < 0.05$) and may indicate As (III) as the primary species in pore water.

However, there was no identifiable relationship for As between the individual BCR steps, pore water and worm tissue. Additionally, correlations between sediment As concentrations and proteinase K digestion were not identified. Assimilation of As from sediment ingestion has been identified in marine deposit feeding polychaetes (Baumann and Fisher, 2011b; Casado-Martinez et al., 2012; Rainbow et al., 2011). It is suggested that digested As species may be subject to metabolism allowing detoxification and excretion.

Transformation of bioaccumulated As in *Arenicola marina* where biomethylation of arsenate to dimethylarsinate has been observed (Geiszinger et al., 2002). Also, possible microbial conversion of arsenobetaine to dimethylarsinate within gut fluid of *Arenicola marina* have been suggested (Casado-Martinez et al., 2012). It is necessary therefore, that further investigations are conducted on As speciation within the environmental matrices of the Fleet lagoon to identify abiotic and biotic factors which may influence bioavailability to deposit feeding polychaetes. Also, identification of metabolic detoxification, transformation and excretion are essential in *H. diversicolor* to fully understand the mechanisms of bioaccumulation.

As previously discussed, the use of total metal sediment content has been found to be an unreliable indicator of metal bioaccumulation in marine species (Amiard et al., 2007; Baumann and Fisher, 2011b; Berthet et al., 2003; Luoma, 1983; Luoma and Rainbow, 2005; Pueyo et al., 2008; Rainbow P. S et al., 2009b; Rosado et al., 2016; Tessier et al., 1979; Wang and Fisher, 1999a). As the speciation of metals within sediment and water may primarily govern bioaccumulation results obtained from the individual steps of BCR sequential analysis show a correlation exists between the oxidizable fractions for Cu obtained in step 2 and in worm tissue. Cu concentrations were found to be highest across all sites in the oxidizable fraction (80%). This suggests the ingestion of sediment as the primary uptake pathway of Cu in *H diversicolor* in the present study. Additionally, as the oxidizable Cu fractions are assumed to be stable within sediment (Pini, 2014), it may be tentatively suggested that Cu levels found within the water samples may derive from the disturbance of sediment or potentially from new inputs.

Positive correlations were found between BCR Steps and water metal concentrations. For Step 2, correlations were found for Cu ($r_s = 0.82$, $p = < 0.01$) and Pb ($r_s = 0.504$, $p = 0.01$). In the case of Step 3, correlations were found for Ni ($r_s = 0.43$, $p = 0.03$) and Pb ($r_s = 0.429$, $p = 0.04$). In the case of the total BCR, Ni ($r_s = 0.411$, $p = 0.04$) and Pb ($r_s = 0.507$, $p = 0.01$) were correlated. Although this may suggest sediment as a possible source of water contamination, further research is required regards the species of metals found within the water in relation to fractions obtained in the BCR steps to elucidate this potential transference.

All steps of the BCR analysis were totalled to reveal the overall bioavailable fraction for each metal, which showed a clear difference to total metal concentrations obtained for all analysed metals at each sample site. Although results gained from the present study indicate that sequential extraction analysis proves to be a more accurate predictor of availability than total metal determination, it fails to

address the exposure pathway of contaminated sediment ingestion (Wang and Fisher, 1999b). Also, these extraction techniques do not address the influence of species mode of biological uptake and regulation of metals (Rainbow et al., 2011).

Marine benthic organisms may consume substantial quantities of sediment to extract food particulates and in doing so, gastrointestinal enzymes may release metal ions affecting their uptake (Rainbow et al., 2011). To evaluate this exposure pathway, biomimetic approaches which utilise digestive enzymes have been developed and employed (Bignasca et al., 2011; Ianni et al., 2010; Mayer et al., 1997; Rosado et al., 2016; Turner, 2006; Turner and Olsen, 2000). As previously determined by Turner (2006), Ianni et al. (2011) and Bignasca et al. (2011), comparisons between the first step of the BCR sequential method and proteinase K extraction may be conducted due to use of solution / solid ratio of 50:1. In the present study, comparisons showed how values for the metals Cu, Ni, Pb and Zn from the BCR extraction were higher than those of proteinase K. This agrees with Bignasca et al. (2011) author's work for metals excluding Cu where they found higher values for Cu obtained by proteinase K extraction. This may result from the complexation of Cu with the enzyme the concentration of which, acts as the limiting factor (Ianni et al., 2010).

Proteinase K extraction proved to be significantly correlated to concentrations found within the worm tissue for Cu ($r_s = 0.642$, $p = 0.050$) and Pb ($r_s = 0.686$, $p = < 0.01$) at all sites whereas a negative relationship for Ni ($r_s = -0.40$, $p = 0.049$) was identified. These results suggest that proteinase K extraction is a suitable method to quantitatively identify interactions for Cu and Pb contamination within the sediment and gastrointestinal environment of *H diversicolor*. Furthermore, results achieved in this present study are in agreement with the findings of Bignasca et al. (2011), Ianni et al. (2010), and Rosado et al. (2016), where comparisons between the proteinase K extraction and the first step of the BCR sequential analysis show that the chemical extraction overestimates the bioavailable fraction.

It is clear how bioavailability of metals remains a complicated issue. However, results from the present study support the use of a multifaceted approach. In particular, the use of both sequential extraction and digestive enzymes provide more accurate methods to determine bioaccumulation of environmental metals by *H diversicolor* than total metals. Additionally, identification and examination of the behaviour of metal ions within environmental matrices, the assimilation and excretion pathways of sediment dwelling organisms may increase the understanding of the bioavailability of environmental metals.

3.7 Conclusion

Sediment characteristics of the Fleet Lagoon, Dorset (UK) show variance. Higher concentrations of sand fractions towards the entrance at Ferrybridge extend towards site 5 whereas silt fractions are dominant at the Abbotsbury end extending towards site 5. Silt and sand composition at the sample locations may be influenced by land run off, freshwater inputs, and reduced tidal flushing towards the Abbotsbury embayment. Organic matter within sediment varies throughout the sampled locations with the highest values found at site 10. Organic matter at this sample location may derive from subsequent detritus from the oyster farm situated between sites 9 and 10. Sediment characteristics may further influence metal accumulation. A correlation between medium and coarse sand and Cu concentrations, and very coarse sand and Pb was identified. Furthermore, organic matter was shown to correlate between Cu, Pb and Zn.

Differences between historic metal concentrations and those found in this study show significantly higher levels of Zn, Pb, Cu and As at site 10 and may indicate continued inputs and accretion of these metals.

Additionally, metal accumulation at this location may be influenced by elevated LOI levels derived from detritus released from the oyster farm and industrial uses of Portland Harbour. Comparisons at other sample locations show either similar or lower levels for Zn, Ni, Cr, Cu and As than historically reported. Levels for Pb were significantly higher in both recent sample locations than previously reported. However, historic LOI analysis was not conducted, sample method and GPS locations were not reported therefore direct comparisons between results should be made with caution.

To assess metal bioavailability and bioaccumulation in the marine polychaete *H diversicolor*, a series of sediment analysis including total metal and BCR sequential extraction were conducted. Total metal results for As showed a correlation with concentrations found in worm tissue. However, the speciation of As in both sediment and worm tissue were not identified in this study and requires further research to determine bioavailability from environmental matrices. Total metal results showed higher concentrations than those extracted during BCR sequential sediment analysis. Moreover, analysis of worm tissue metal concentrations was not correlated with either the total metal or total BCR concentration. By contrast, a significant correlation existed between the oxidizable fraction of Cu in sediment and Cu concentrations found in worm tissue. Partial correlations between proteinase K and pore water metal concentrations using worm tissue metal concentrations as the controlling factor identified relationships for Cu, Pb and Zn. However, it is not clear whether the uptake of pore water during the ingestion process contributes to assimilation or if this occurs through epidermal contact.

Correlations of the first step of the BCR sequential analysis and that of proteinase K showed that for all metals analysed excluding Cu, the BCR stage overestimates the bioavailable fraction. Additionally, Cu results may have been confounded by sorption to the enzyme.

Worm tissue concentrations for Cu and Pb were significantly correlated to proteinase K digestion therefore, proteinase K digestion is suggested as a suitable method to quantify bioavailability and bioaccumulation for the metals Cu and Pb from sediment. However, it is acknowledged that further research is necessary to assess the suitability of using proteinase K for metal bioavailability investigations for metals other than Cu and Pb. Although BCR sediment digestion overestimated the bioavailable fraction, it proves a more accurate method to assess metal bioaccumulation than total metal concentrations.

4. Polycyclic aromatic hydrocarbons in Lagoon sediments and bioaccumulation by the marine polychaete *H diversicolor*

4.1 Introduction

Polycyclic aromatic hydrocarbons (PAH's) are naturally occurring compounds composed of two or more fused benzene rings which circulate through biogeochemical cycles from sources including natural oil seeps, volcanic eruptions and forest fires (Duran and Cravo-Laureau, 2016). However, anthropogenic activities and population expansion have increased both chronic and acute environmental inputs from pyrolytic and petrogenic sources including combustion of fossil fuels, accidental oil spills, terrestrial and fluvial run off or direct addition (Manuel Nicolaus et al., 2015).

Within the marine environment, PAH's are predominately found in complex mixtures within sediments the composition of which, results from the origin and rate of natural weathering by microbial and photo degradation (Sabaté et al., 2001). PAH's found within petrogenic sources including diesel and gasoline, are dependent on the refining process and distillation temperature range of the parent oil (Neff et al., 2005). Generally, these products are of low molecular weight comprising of two or three fused benzene rings although, middle distillate products including diesel and home heating fuel may contain species with four aromatic rings (Yunker et al., 2015).

Incomplete combustion of organic matter or the rapid cooling of combusted fuel releases PAH compounds either as unspent products or compounds re-formed during condensation processes (Lui et al., 2016). PAH's are found within combustion soot and vapour emitted from vehicle and industrial engine exhausts, wood and coke burning emissions and these sources are considered to be the major

contributors to environmental release of PAH's (Liu et al., 2016; Xue et al., 2016).

The individual physiochemical properties including vapour pressure, water solubility, Henry's law constant, octanol-water partition coefficient (K_{ow}), organic carbon partition coefficient (K_{oc}), and sediment composition influence behaviour of PAH's in the marine environment (Arias et al., 2016; Frapiccini and Marini, 2015).

Moreover, environmental persistence, toxicity, carcinogenicity and mutagenicity have led to the inclusion of 16 individual PAH's in the US Environmental Protection Agency (EPA) priority pollutant list (Duran and Cravo-Laureau, 2016; Frapiccini and Marini, 2015; Xue et al., 2016).

Due to the hydrophobic nature and low water solubility, PAHs have a high affinity for particulate matter found within the water column (Wang et al., 2015). Absorption to particulates is influenced by the particulate surface area, where smaller particles show increased absorbance capacity (Wang et al., 2015). Additionally, smaller particles may be subject to higher transportation rates which may result in accumulation of contaminated particles in coastal and tide driven areas (Duran and Cravo-Laureau, 2016). Indeed, higher concentrations of PAH's are recorded worldwide in sediments of coastal bays, lagoons and estuaries (Nikolaou et al., 2009).

Therefore, marine sediment remains the main receptacle for PAH's in the marine environment (Sun et al., 2016).

Determining potential sources of environmental PAH's is vital to understand the bioavailability to marine biota (Morales-Caselles et al., 2017; Yunker et al., 2002). For instance, pyrogenic PAH's show reduced environmental degradation, but are perceived to have limited bioavailability to marine organisms whereas petrogenic PAH's often dissolved in the water column, are rapidly bioavailable and subject to degradation and photooxidation (Yunker et al., 2015).

Identification of pyrolytic and petrogenic sources from marine sediment conducted through use of molecular indices formulated from environmental PAH's have been extensively proved (Cachada et al., 2012; Jiang et al., 2014; Tobiszewski and Namieśnik, 2012; Yunker et al., 2002). For example, high alkylated / parent PAH ratios signifies petrogenic sources (Rust et al., 2004; Yunker et al., 2002).

It is acknowledged that the bioavailability of PAH's to marine organism's may be influenced by individual physical properties and sorption to organic particulates (Dai et al., 2008; Tang et al., 2016). Low molecular weight and water - soluble PAH's dissolved within the water column may be taken up rapidly by organisms (Hylland, 2006) through dermal contact, irrigation and ingestion (Timmermann and Andersen, 2003). High molecular weight PAH's bound to organic matter present within marine sediment are hypothesised to be less bioavailable (Yunker et al., 2015; Yunker et al., 2002). However, ingestion of high molecular weight PAH's present in contaminated sediment by marine benthic species including the polychaete *H diversicolor* have been evidenced (Alessio et al., 2018; Christensen et al., 2002b; Lu et al., 2004; Rust et al., 2004). Yet, these species specific bioaccumulation traits are not commonly addressed during marine toxicology environmental risk assessments (Diepens et al., 2015).

Following biological uptake, activation of the transcription factor aryl hydrocarbon receptor by coplanar PAH's initiates induction of cytochrome P450 enzymes (Gauthier et al., 2014). These enzymes alter PAH's via hydroxylation, with further modifications producing soluble and excretable products (Hahn, 1998). However, rapid metabolism of PAH's by some species (Christensen et al., 2002b; Giessing et al., 2003; Malmquist et al., 2015) may produce confounding results as although the use of total tissue contents identifies exposure, it may suggest lower rates of bioaccumulation.

To fully understand the risk which environmental levels of PAH's pose to marine organisms it is vital that environmental monitoring including assessment of bioaccumulation is conducted. For the first time, this study will determine levels of 16 PAH's in the Fleet Lagoon, Dorset, UK and bioaccumulation in *H diversicolor* through the analysis of environmental matrices and worm tissue. The objectives of this study are:

- 1) Identification and quantification of the 16 PAH's listed as priority pollutants by the EPA within sediment, water and worm tissue
- 2) Determine origins of PAH's using isomer ratio analysis
- 3) Using sediment characteristics data, identify potential correlations between sediment types, concentrations of individual PAH's and whole worm tissue.

4.2 Materials and Methods

4.2.1 Site description

A full description of sample collection from the Fleet Lagoon, Dorset, UK is detailed in Chapter 2 (2.1.1.1).

4.2.1.1 Total PAH in Sediment and Water

Samples of sediment and water were sent to a commercial laboratory (I2 analytical Laboratory, Watford, UK) for determination of PAH concentrations by GCMS.

*4.2.1.2 Total PAH concentration in *H diversicolor* tissue*

Worm tissue was collected, prepared and analysed as previously described in Chapter 2 (2.1.1.4, 2.3.9, 2.4.1) respectively.

4.2.1.3 Isomer ratio source identification

Using the ratios of specific PAH compounds provides a method to distinguish sources of PAHs: Fluoranthene / (Fluoranthene +

Pyrene), Ant / (Anthracene + Phenanthrene), Fluoranthene / Pyrene, and HMW (4 - 6ring) / LMW (2 - 3 ring) (Morales-Caselles et al., 2017; Xue et al., 2016). PAHs of petrogenic origin contain higher concentrations of 2 - 3 ring alkylated PAHs for example, as anthracene is less thermodynamically stable than phenanthrene higher phenanthrene / anthracene ratios indicate petrogenic sources.

Pyrolytic PAH origins are identified by low phenanthrene / anthracene ratios. Ratios of Fluoranthene / Pyrene <1 indicate petrogenic origin whereas, Fluoranthene / Pyrene >1 suggests pyrolytic origin; HMW / LMW <1 indicates petrogenic origin whereas, HMW / LMW >1 indicates pyrolytic origin (Yunker et al., 2002).

Fluoranthene / (Fluoranthene (Fla) + Pyrene (Pyr)) values below 0.4 are related to petrogenic origins; values above 0.5 suggests biomass, wood and coal combustion; values between 0.4 and 0.5 are associated to petroleum combustion (Figure 20). Anthracene / (Anthracene (Ant) + Phenanthrene (Phe)) ratios less than 0.1 relate to petroleum pollution whereby, greater than 0.1 represents a pyrolytic source (Xue et al., 2016; Yunker et al., 2002)

4.2.1.4 Statistical analysis

All data were analysed using Ri386 statistics version 3.4.2. All analysis was tested to meet the assumptions for parametric tests. When assumptions were not met, data was transformed using square root, arcsine or \log^{10} transformation. Shapiro-Wilk tests were then performed to assess normality of transformed data. Pearson's correlation coefficient was conducted on raw or transformed data to identify linear correlations: sediment characteristics and PAH sediment concentrations; LOI and PAH sediment concentrations. Spearman's correlations were performed on worm tissue PAH concentrations and PAH sediment concentrations as data for worm tissue did not meet the assumptions for Pearson's correlations.

4.3 Results

4.3.1 PAH concentrations of environmental matrices

4.3.1.1 PAH Concentrations in Sediment

Concentrations of the 16 PAH's included by the EPA as priority pollutants were determined in sediment samples taken from the Eastern shoreline of the Fleet Lagoon as detailed in Table 24. Canadian sediment quality guidelines are included which detail concentrations applicable for both the threshold effect limit (TEL) (results above TEL highlighted in blue) and probable effects limit (PEL) (results above PEL highlighted in red) (CCME, 2001).

Table 24. PAH concentrations for sediment samples ($n = 3$) taken from 10 sample sites of the Fleet Lagoon. All concentrations are reported as mg kg^{-1} dry weight. Canadian sediment quality guidelines for Threshold effects limits (TEL) and Probable Effects Limits (PEL) are included (CCME, 2001). Results above the TEL are highlighted in blue and results above PEL highlighted in red.

PAH	TEL	PEL	Site1	Site2	Site3	Site4	Site5	Site6	Site7	Site8	Site9	Site10
Naphthalene	0.03	0.39	0.37	<0.05	<0.05	0.30	<0.05	<0.05	<0.05	<0.05	<0.05	<0.05
Acenaphthylene	0.005	0.13	<0.05	0.15	<0.05	0.39	<0.05	<0.05	<0.05	<0.05	<0.05	<0.05
Acenaphthene	0.006	0.089	<0.05	0.09	<0.05	0.39	<0.05	<0.05	<0.05	<0.05	<0.05	<0.05
Fluorene	0.021	0.14	<0.05	0.08	<0.05	0.56	<0.05	<0.05	<0.05	<0.05	<0.05	<0.05
Phenanthrene	0.042	0.52	0.51	1.0	0.10	6.4	<0.05	0.73	0.36	<0.05	0.16	0.75
Anthracene	0.047	0.24	0.13	0.42	<0.05	1.7	<0.05	0.24	0.13	<0.05	<0.05	0.22
Fluoranthene	0.11	2.4	0.78	7.9	0.21	16	<0.05	1.9	1.4	<0.05	0.46	2.3
Pyrene	0.053	0.88	0.57	8.5	0.18	14	<0.05	1.4	1.4	<0.05	0.40	2.1
Benzo (a)anthracene	0.032	0.39	0.33	4.4	0.11	7.1	<0.05	0.69	0.69	<0.05	0.16	0.97
Chrysene	0.057	0.86	0.34	2.7	0.08	5.1	<0.05	0.74	0.69	<0.05	0.23	0.89
Benzo (b) fluoranthene	-	-	0.30	4.70	0.08	7.3	<0.05	0.72	0.88	<0.05	0.23	1.2
Benzo (k) fluoranthene	-	-	0.29	2.4	0.07	4.2	<0.05	0.53	0.59	<0.05	0.19	0.79
Benzo (a) pyrene	0.032	0.78	0.36	4.1	0.13	7.2	<0.05	0.70	0.90	<0.05	0.28	1.3
Indeno (1,2,3-cd)pyrene	-	-	0.15	2.1	<0.05	3.4	<0.05	0.37	0.38	<0.05	<0.05	0.60
Dibenz (a,h) anthracene	0.006	0.14	<0.05	0.50	<0.05	0.90	<0.05	<0.05	0.11	<0.05	<0.05	0.15
Benzo (ghi) perylene	-	-	0.18	2.30	<0.05	3.7	<0.05	0.44	0.48	<0.05	<0.05	0.69
Total PAH			4.31	41.9	0.96	78.0	<0.80	8.38	7.92	<0.80	2.11	11.9

Results show that sites 2 and 4, 6, 7 and 10 had concentrations of specific individual PAH's which far exceed the PELs and TELs. The highest \sum PAH concentrations of 78.0 mg kg^{-1} were found at site 4. Furthermore, all reported individual PAH's excluding Naphthalene were highest at this location. Individual and total concentrations for PAH's then decrease in the order of site 2 > 10 > 6 > 7 > 1 > 9 > 3 < 8 ~ 5, with 41.9, 11.9, 8.38, 7.92, 4.31, 2.11, 0.96, < 0.80 and < 0.80 mg kg^{-1} respectively. Generally, Fluoranthene and Pyrene were the

most abundant compounds in the sediments with 31.05 and 28.65 mg kg⁻¹ respectively. Other total PAH concentrations: 14.55 mg kg⁻¹ for Benzo (a) anthracene; 10.87 mg kg⁻¹ for Chrysene; 10.11 mg kg⁻¹ for Phenanthrene; 9.16 mg kg⁻¹ for Benzo (k) fluoranthene; 7.99 mg kg⁻¹ for Benzo (g,h,i) perylene; 7.2 mg kg⁻¹ for Indeno (1, 2, 3 - cd) perylene; 1.96 mg kg⁻¹ for Dibenz (a, h) anthracene; 1.07 mg kg⁻¹ for Naphthalene; 1.04 mg kg⁻¹ for Fluorene; 0.94 mg kg⁻¹ for Acenaphthylene; 0.84 mg kg⁻¹ for Acenaphthene.

4.3.1.3 PAH concentrations in water

Concentrations of individual PAH's in all water samples taken from each location were below < 0.01 µg l⁻¹.

4.3.1.4 PAH concentrations in worm tissue

Worm tissue concentrations from site locations are detailed in Table 25. During sampling of these locations, *H diversicolor* was not found at locations 8 and 9 as described in Chapter 2 (2.1.1.4).

Table 25. PAH Concentrations of worm tissue $\mu\text{g ml}^{-1}$. Mean ($n=3$) values are \pm 1 SE.

PAH	Site1	Site2	Site3	Site4	Site5	Site6	Site7	Site10
Naphthalene	<1	<1	<1	<1	<1	<1	<1	<1
Acenaphthylene	<1	<1	<1	<1	<1	<1	<1	<1
Acenaphthene	<1	<1	<1	3.54	<1	<1	<1	<1
Fluorene	2.15 \pm 0.88	3.92 \pm 1.02	2.11 \pm 0.58	8.46 \pm 0.78	5.98 \pm 1.05	6.27 \pm 0.89	3.12 \pm 0.29	3.85 \pm 0.51
Phenanthrene	<1	<1	<1	<1	<1	<1	<1	<1
Anthracene	1.15 \pm 0.38	1.91 \pm 0.67	1.07 \pm 0.48	4.07 \pm 1.95	<1	2.81 \pm 0.21	1.56 \pm 0.43	2.96 \pm 1.77
Fluoranthene	<1	<1	<1	<1	<1	<1	<1	<1
Pyrene	<1	<1	1.09 \pm 0.65	1.01 \pm 0.51	<1	1.05 \pm 0.79	<1	<1
Benzo (a)anthracene	-	-	-	-	-	<1	-	-
Chrysene	-	-	-	-	-	<1	-	-
Benzo (b) fluoranthene	-	-	-	-	-	-	-	-
Benzo (k) fluoranthene	-	-	-	-	-	-	-	-
Benzo (a) pyrene	-	-	-	-	-	-	-	-
Indeno (1,2,3-cd)pyrene	-	-	<1	<1	<1	<1	<1	<1
Dibenz (a,h) anthracene	-	-	-	-	-	-	-	-
Benzo (ghi) perylene	-	-	-	-	-	-	-	-

Concentrations below $< 1\mu\text{g ml}^{-1}$ were found for Naphthalene, Acenaphthylene, Phenanthrene and Fluoranthene at all sample locations. The highest concentration of Acenaphthene was detected from site 4 whereas all other sites had values $< 1\mu\text{g ml}^{-1}$.

Concentrations of Fluorene were found at all site locations with the highest values of $8.46\mu\text{g ml}^{-1}$ detected in worm tissue from site 4. Anthracene was detected from worm tissue at all sample locations with the highest values of $4.07\mu\text{g ml}^{-1}$ again in worms from site 4. Pyrene was present in all worm tissue with slightly higher values found at sites 3 ($1.09\mu\text{g ml}^{-1}$), 4 ($1.01\mu\text{g ml}^{-1}$) and 6 ($1.05\mu\text{g ml}^{-1}$).

Indeno (1, 2, 3 - cd) pyrene was found at low concentrations ($< 1 \mu\text{g ml}^{-1}$) in worm tissue from all locations excluding sites 1 and 2.

4.3.2 Isomer source identification

4.3.2.1 PAH Origin and Source analysis

Using the method developed by Yunker et al. (2002), the 16 individual PAH's analysed were divided into 3 groups dependent upon the ring number: 2 and 3 ring PAH's (Acenaphthylene, Acenaphthene, Fluorene, Phenanthrene, Anthracene, Fluoranthene); 4 ring PAH's (Pyrene, Benz [a] anthracene, Chrysene, Benzo [b] Fluoranthene and Benzo [k] Fluoranthene); 5 and 6 ring PAH's (Benzo [a] Pyrene, Indeno [1, 2, 3 - cd] pyrene, Benzo [g h i] perylene and Dibenz [a, h] perylene). Group 2 and 3 ring represent low molecular weight; 4 ring represent medium molecular weight; 5 and 6 ring represent high molecular weight PAH's. Total concentration for 2 - 3 ring PAH's were $48.1 \mu\text{g kg}^{-1}$; 4 ring were $78.74 \mu\text{g kg}^{-1}$; 5 - 6 ring were $32.92 \mu\text{g kg}^{-1}$. 4 ring PAH's accounted for the highest percentage (49%) of all samples taken from the Fleet Lagoon, with 30% and 20% for 2 - 3 ring and 5 - 6 ring PAH's respectively.

Furthermore, 4 ring PAH's were the dominant species at sites 2, 4, 6, 7, 9 and 10 accounting for 54%, 48%, 47%, 52%, 48% and 49% respectively. 2 - 3 ring PAH's were dominant at sites: 1 (43%), 3 (41%), 5 (44%), 8 (44%), with 5 - 6 ring PAH's the lowest fraction at all sites: 1 (16%), 2 (23%), 3 (21%), 4 (19%), 5 (25%), 6 (18%), 7 (23%), 8 (25%), 9 (17%) and 10 (23%).

4.3.2.2 Isomer ratio source Identification

Isomer source identification for PAH's identified in the lagoon sediments (Figure 19) indicate both petrogenic and pyrogenic origins.

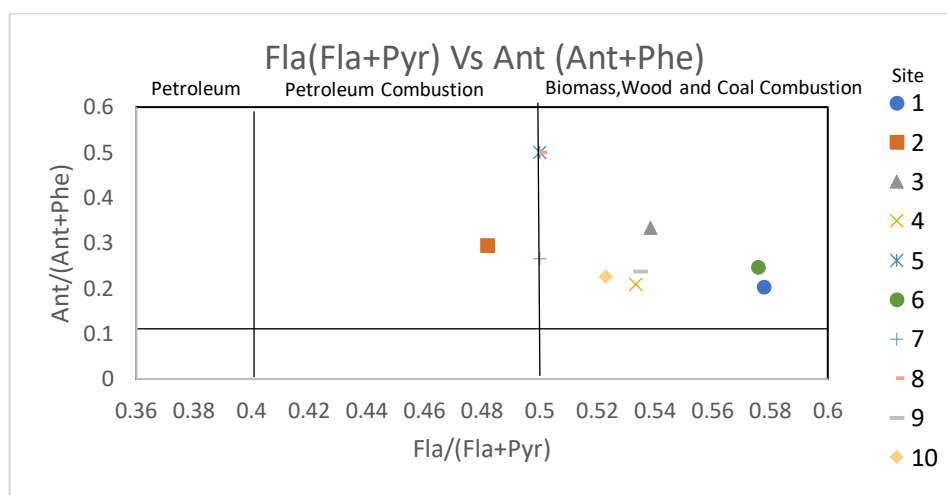


Figure 19. Fla / (Fla + Pyr) Vs Ant (Ant + Phe) graph. Results indicate the origins of PAH's concentrations found within the sediment samples of the Fleet Lagoon. Values between 0.4 and 0.5 indicate petroleum combustion, > 0.5 indicate biomass and fossil fuel combustion. Values below 0.1 are associated with petroleum pollution whereas values above 0.1, a pyrolytic origin.

Ratios of Fla (Fla + Pyr) Vs Ant (Ant + Phen) indicate that PAH sources found at sample locations 1, 3, 4, 5, 6, 7, 8, 9 and 10 originate from pyrolytic combustion of fossil fuels and biomass. Ratios for site 2 indicate petroleum combustion as the originator for PAH's found at this location.

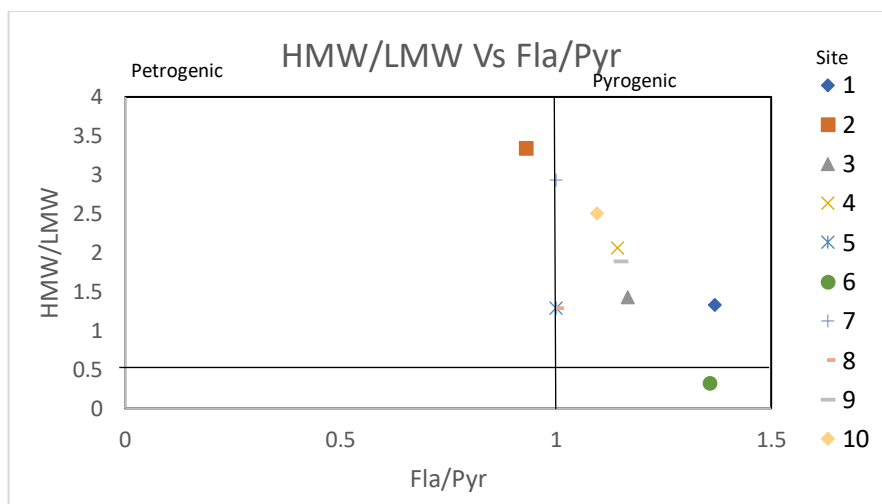


Figure 20. HMW / LMW Vs Fla / Pyr graph. Graph depicting ratios between HMW/LMW and Fla / Pyr. Values < 1 indicate PAH's originate from petrogenic sources whereas values > 1, pyrogenic sources.

Ratios of HMW / LMW vs Fla / Pyr indicate that PAH's for all sites excluding 2 and 6, originate from pyrogenic sources whereas PAH's for site 2 and 6 originate from petrogenic sources.

4.3.2.3 Relationships between sediment characteristics and PAH concentrations

Pearson's correlation was performed on sediment characteristics reported in Chapter 3, and PAH concentrations from sediment samples taken from each site. A significant positive relationship between naphthalene and clay ($r = 0.721$, $p = 0.02$), very fine silt, ($r = 0.699$, $p = 0.02$), and fine silt, ($r = 0.742$, $p = 0.01$). Furthermore, a negative correlation for naphthalene and very fine sand, ($r = -0.753$, $p = 0.01$), fine sand, ($r = -.0749$, $p = 0.01$) was found. There were no further significant relationships for any other individual PAH or sediment characteristic.

4.3.2.4 Relationships between loss on ignition and PAH sediment concentrations

Loss on ignition results and concentrations for each individual PAH covering all sample locations were assessed for relationships using Pearson's correlation. Results show a positive relationship with LOI for Acenaphthene ($r = 0.676$, $p = 0.032$), Phenanthrene ($r = 0.697$, p

= 0.025) and Anthracene ($r = 0.666$, $p = 0.035$). No further statistical correlations for remaining PAH's were found.

4.3.2.5 Relationships between worm tissue and sediment PAH concentration

A statistically significant relationship using Spearman's rank coefficient between PAH worm tissue and sediment concentration was found for Acenaphthene ($r_s = 0.763$, $p = 0.031$) and Anthracene ($r_s = 0.894$, $p = < 0.01$). There were no further statistically significant relationships found between any remaining PAH concentrations in worm tissue and associated sediment.

4.4 Discussion

4.4.1 Comparisons of historic and current PAH concentrations

Analysis of sediment from the Fleet lagoon conducted by Nunney and Smith (1995) determined concentrations of naphthalene, phenanthrene, fluoranthene and benzo [a] anthracene detailed in Table 26. Benzo - fluoranthene's were reported as a total concentration however, identification of the individual benzo-fluoranthene's were not reported. Additionally, sample locations used by Nunney and Smith (1995) to study PAH's (detailed in Chapter 3 3.2.2), were from locations towards the Western shoreline of the Fleet and are not therefore comparable to results determined in this study.

Table 26. PAH analysis of Fleet lagoon sediment conducted by Nunney and Smith (1995) ($\mu\text{g kg}^{-1}$ dry weight)

	Fleet 1C Sediment	Fleet 4C Sediment
Naphthalene	50	66
Phenanthrene	225	220
Fluoranthene	710	670
Benzo anthracene	450	320
Benzo fluoranthene's	1100	720
Total PAH	3200	2300

Their results for naphthalene range between 50 - 66 $\mu\text{g kg}^{-1}$, phenanthrene 220 - 225 $\mu\text{g kg}^{-1}$, fluoranthene 670 - 710 $\mu\text{g kg}^{-1}$, and benzo anthracene 320 - 45 $\mu\text{g kg}^{-1}$ for the two sample locations. Results from the present study range between < 50 - 370 $\mu\text{g kg}^{-1}$ for naphthalene, < 50 - 6400 $\mu\text{g kg}^{-1}$ for phenanthrene, < 50 - 16000 $\mu\text{g kg}^{-1}$ for fluoranthene and < 50 - 7100 $\mu\text{g kg}^{-1}$ for benzo(a) anthracene and therefore show a significant increase for these PAH's. However, it is acknowledged that the comparisons of study locations are not exact due to lack of coordinates reported in the Nunney and Smith (1995) study.

Although sample locations for the historic study conducted by Nunney and Smith (1995) and those chosen for this study cannot be directly compared, of the PAH's analysed in both studies (naphthalene, phenanthrene, fluoranthene and benzo [a] anthracene), results from the present study were appreciably higher. This may indicate accumulation of PAH's in the Lagoon from 1995 to present day. However, there is a lack of evident literature regarding PAH levels in marine sediment from the South West coastline. Therefore, it is not possible to use site comparison to establish whether PAH concentrations in this region have also increased. It is suggested to fully understand the spatial distribution of PAH's in lagoon sediments core sediment samples from site locations extending throughout the Lagoon should be taken. This may enable PAH identification and associated concentrations at specific time periods and provide clarification in terms of PAH accumulation and source identification.

4.4.2 PAH concentrations from present study

PAH concentrations in sediment varied throughout all sample locations for each of the 16 individual PAH's analysed. Notably, all sites excluding 5 and 8 had concentrations of specific PAH's which exceed the TEL's and PEL's of the Canadian sediment quality

guidelines. Importantly, results gained from this study show concentrations in sediment at specific locations exceed those of Poole Harbour (EA, 2016b), Milford Haven (Little et al., 2015), Mersey estuary (Vane et al., 2007), Brighton marina (King et al., 2004) and the Severn Estuary (Langston et al., 2010). As such, biota are exposed to high and potentially biologically harmful levels of PAH's which may result in severe consequences for the ecosystem and warrants urgent investigation.

Fluoranthene and pyrene were the most abundant compounds with Σ total values of 31.05 and 28.65 mg kg⁻¹ respectively, which far exceed the reported PEL of the Canadian sediment quality guidelines (CCME, 2001). For both fluoranthene and pyrene, concentrations at the levels found in this present study are subject of concern. Toxic responses at far lower concentrations have been observed: LC50 concentrations of 84.3 $\mu\text{g mg}^{-1}$ (dry weight) were reported following pyrene exposure for marine amphipod *Rhepoxinius abronius* (Clement et al., 2005) and LC50 concentrations of 23.8 $\mu\text{g l}^{-1}$ for *Rhepoxinius abronius* were reported following fluoranthene exposure (Swartz et al., 1990). Results gained in this study warrant further research due to these high concentrations and associated implications for biota within this ecosystem. Furthermore, due to the high concentrations of pyrene reported in this chapter, its ubiquitous presence in all environmental matrices (Beach et al., 2009) and its recognised metabolic pathway (Giessing et al., 2003), pyrene was selected as the PAH to use for exposure experiments reported in Chapters 5, 6 and 7 of the present study.

Interestingly, all water samples from each location had values < 0.01 mg kg⁻¹ which may be attributed to the bonding of PAH's to organic particles within the water column and subsequent settlement (Frapiccini and Marini, 2015; Stogiannidis and Laane, 2014). Distribution of PAH's in sediment may be influenced by partitioning behaviour, where smaller particulates including organic matter, clay and silt fractions have been evidenced to increased adsorption

(2000; Hassan et al., 2018; Ruiz-Fernández et al., 2012; Soliman et al., 2019; Wang et al., 2015; Wang et al., 2001). Statistically significant relationships found in the present study are in agreement, with this, as correlations were identified between naphthalene, clay, very fine silt and fine silt sediment fractions. The highest values for naphthalene (0.37 mg kg^{-1}) were found at site 1. High percentage values of clay, silt and very fine silt were fractions were found in sediment from site 1 (Chapter 3) and may therefore be an influencing factor. Furthermore, a statistically significant relationship exists between LOI and acenaphthene, phenanthrene and anthracene. The highest values for all 3 PAH's (0.39 mg kg^{-1}) (6.4 mg kg^{-1}) (1.7 mg kg^{-1}) were found at site 4. LOI values at site 4 (9.89%) were the second highest values from all sample locations and may therefore contribute to the accumulation of these PAH's in this location. However, there was no statistically significant relationship between the total concentrations of PAH's at each site and respective LOI value.

Based upon ring numbers of analysed PAH's in sediment samples, the 16 individual PAH's were grouped: 2 - 3 ring PAH's (Naphthalene, Acenaphthylene, Acenaphthene, Fluorene, Phenanthrene, Anthracene and Fluorene); 4 ring PAH's (Pyrene, Benz [a] anthracene, Chrysene, Benzo [b] fluoranthene, Benzo [k] fluoranthene); 5 - 6 ring PAH's (Benzo [a] pyrene, Indeno [1, 2,3 -cd] pyrene, Dibenz [a, h] anthracene, Benzo [g, h, i] perylene which represents low, medium and high molecular weight PAH's respectively (Jia et al., 2016). Of the sampled sites of the Fleet Lagoon, 4 ringed PAH's (49%) were the dominant species at sites 2, 4, 6, 7, 9 and 10 with values of 54%, 48%, 47%, 52%, 48% and 49% respectively. Medium molecular weight PAH's predominately originate from the atmospheric deposition of automobile exhaust products and urban runoff (Xue et al., 2016). However, environmental processes including microbial degradation and photooxidation increases concentrations of 4 - 6 ringed PAH's

(Stogiannidis and Laane, 2014). High concentrations of 4 - 6 ringed PAH's within the lagoonal sediment may suggest urban run - off and automobile combustion although these compounds may have originated from other sources. Low molecular weight 2 - 3 ring PAH's were dominant at sites: 1 (43%), 3 (41%), 5 (44%) and 8 (44%), which may originate from the lower temperature combustion of fossil fuels including wood, coal and biomass (Yunker et al., 2002).

PAH's with anthropogenic origin may be divided into petrogenic and pyrogenic sources (Zhang et al., 2017) where the ratios of similar weight individual PAH's may be used as indexes to determine the origin (Yunker et al., 2002). Ratios are formulated using the most thermodynamically stable isomer to the most unstable isomer (Stout 2007) as PAH distribution patterns are temperature dependant (Zimmermann et al., 2012). The use of the fluoranthene (Fla) to pyrene (Pyr) ratio (Fla / Pyr) correlates to formation temperature under fossil fuel combustion (Stogiannidis and Laane, 2014).

Thermodynamically, fluoranthene is less stable than pyrene therefore ratios of Fla / Pyr < 1 identify petrogenic products whereas values of Fla / Pyr > 1 are associated with biomass, wood and coal combustion. Ant / (Ant + Phe) < 0.1 corresponds to petroleum pollution whereas, a ratio > 0.1 represents a pyrolytic source (Yunker et al., 2002).

For ratio's which utilize molecular weights, a value of HMW / LMW < 1 indicates a petrogenic origin, whereas HMW / LMW > 1 represents a pyrolytic origin (Budzinski et al., 2000). Diagnostic ratios of PAH's to distinguish pyrolytic or petrogenic origin (Xue et al., 2016), show how those identified at site 2 originated from petrogenic combustion. All other sample locations were identified as originating from pyrogenic sources and indicate chronic anthropogenic pollution as the primary contributor. Within pyrogenic PAH arrangements, HMW PAH's are more abundant than LMW, related to increasing temperatures. Moreover, fluoranthene, pyrene and phenanthrene are the most abundant PAH's found in pyrogenic compounds which

associate with particulate soot rich particles (Yunker et al., 2002). HMW / LMW ratios further identify all sample locations with exception of site 2 to have PAH's of pyrogenic origin, whereas site 2 results show a petrogenic source.

Concentrations of pyrene, fluoranthene and phenanthrene were identified in worm tissue. As these PAH's are associated with pyrolytic emissions and predominately sorbed to soot particles (Yunker et al., 2002) this may suggest bioavailability of these fractions to *H diversicolor*. As such, this disagrees with the hypothesis of reduced bioavailability of PAH absorbed particles (Yunker et al., 2015; Yunker et al., 2002). Bioaccumulation of PAH's from sediment via ingestion by benthic invertebrates have been evidenced (Alessio et al., 2018; Liu et al., 2016; Rust et al., 2004). Although the fractions in the sediment and states of PAH's were not identified the present study, it is speculated that ingestion of pyrolytic PAH's is a bioaccumulation pathway for PAH's in *H diversicolor*.

The highest levels of pyrene in sediment found in this study were at site 4 (16 mg kg⁻¹) which are far in excess of the PEL indicating that biota found in this location may be exposed to biologically harmful levels. Low concentrations of pyrene in worm tissue from this site relative to high concentrations in sediment may indicate avoidance by this species. Even though rapid bioaccumulation and metabolism of pyrene have been reported by *H diversicolor* (Catalano et al., 2012; Christensen et al., 2002a; Giessing et al., 2003; Malmquist et al., 2013), exposure to the concentrations of pyrene found at this site would likely result in mortality based upon the PEL of the Canadian sediment quality guidelines.

PAH contamination avoidance has been observed by marine species: European seabass (*Dicentrarchus labrax*) to multi PAH contamination (Claireaux et al., 2018); Australian sea star (*Patiriella exigua*) to crude oil contaminated sediment (Ryder et al., 2004); red king crab (*Paralithodes camtschaticus*) to marine diesel oil in water

and contaminated food (Sagerup et al., 2016). Moreover, Schaum et al., (2013) report chemosensory detection in *H diversicolor* indicating that this species has the ability to sense and therefore actively avoid contamination. It is therefore plausible to suggest that the low concentrations of pyrene found in worm tissue from the Fleet lagoon were a result of the avoidance of highly contaminated areas.

The levels of some PAH's at these locations were found to be in excess of the PEL / TEL of the Canadian sediment quality guidelines and therefore presumed to elicit toxicity to resident populations of *H diversicolor*. However, the presence of *H diversicolor* at this apparently highly contaminated site may indicate genetic adaptation by this population of worms. Adaptations to contamination by this species have previously been observed, where adaptations to Cu stress proteins by individuals residing in Restronguet Creek, UK exposed to high levels of Cu have been identified (Berthet et al., 2003; McQuillan et al., 2014; Mouneyrac et al., 2003). It is suggested therefore, that further investigations are necessary focusing on sediment and worm tissue analysis of this shoreline habitat.

Conversely, < 3 ringed PAH's concentrations were the dominant species in all worm tissue and detected from each sample location. Significant relationships were identified between sediment concentrations for Acenaphthene ($r_s = 0.763$, $p = 0.031$) and Anthracene ($r_s = 0.894$, $p = < 0.01$). The apparent dominance of these PAH's in *H diversicolor* tissue may also indicate bioaccumulation and reduced metabolism and excretion by this species. Few studies in literature regarding bioaccumulation and metabolism of low ringed PAH's by benthic invertebrates are apparent. Interestingly, Landrum (1982), demonstrated that biotransformation of anthracene was not detected in the freshwater invertebrate *Pontoporeia hoyi* following exposure. Also, Badreddine et al. (2017) report continuous assimilation of anthracene and apparent lack of excretion by the mussel *Mytilus galloprovincialis* following 8 d exposure experiments. However, there is no evident

literature regarding the assimilation, biotransformation and excretion of these low molecular weight PAH's by marine polychaetes. One possible explanation for the presence of 3 ringed PAH's found within worm tissue is the potentially reduced affinity of the aryl - hydrocarbon receptor to low molecular weight compounds (Shailaja and D'Silva, 2003). Reduced potential for low molecular weight PAH's (≤ 3 rings) to activate the aryl hydrocarbon receptor have been suggested as detailed in the review conducted by Barron et al., (2004). As aryl hydrocarbon receptors are ligand activated transcription factors of cytochrome p450 gene regulation (Hahn, 1998), reduced affinity for low molecular weight PAH's may effect metabolization via reduced phase 1 oxidation rates. Importantly, this apparent reduced metabolism and excretion of low molecular weight PAH's may result in bio magnification via trophic transfer. As such, further research with regards to the bioaccumulation, metabolism, excretion and activation of aryl hydrocarbon receptors of low weight PAH's by this species may provide clarity regarding results found in this study.

4.5 Conclusion

PAH analysis of sediment samples from the Fleet lagoon show variance of both concentrations and spatial distribution. Results obtained for sites 2, 4, 6, 7 and 10 show concentrations for individual PAH's in excess of the TEL and PEL in accordance with the Canadian sediment quality guidelines. As such, this may have severe negative consequences for biota which reside in this environment and warrants urgent investigation.

Accumulation of PAH's in the sediment at specific sample sites may be influenced by the presence of fine particulate silt, clay and LOI fractions. PAH origin and isomer analysis identify the combustion of biomass and fossil fuel as the origin for PAH's found at most sites except 2 and 6, for which petroleum combustion as the indicated source. Bioaccumulation of the absorbed particles of medium weight

pyrolytic PAH's indicate that sediment ingestion is an important bioaccumulation pathway for *H diversicolor*.

Correlations between worm tissue and sediment concentrations were only identified for Anthracene and Acenaphthene. The dominance of low ringed PAH's in worm tissue may indicate recent acute inputs of these compounds into the lagoon or possibly, low affinity for aryl hydrocarbon receptors and subsequent reduced metabolism and excretion of these PAH's by *H diversicolor*. These findings may indicate altered metabolism and excretion of these PAH's by *H diversicolor*. There is no literature evident reporting subsequent toxicities and potential for trophic transfer, which may influence both the health status of *H diversicolor* and ecosystem functioning where these contaminants are present.

5. Behavioural and neurotoxicity assessment of *H diversicolor* following exposure to environmentally relevant concentrations of Cu, Pb and pyrene.

5.1 Introduction

Environmental investigations of toxicological contamination commonly use biological endpoints and biomarkers to identify toxicity (Viarengo et al., 2007). However, recognition of behavioural ecotoxicology is expanding, providing a non - invasive method identifying toxicity driven physiological change at the whole organism level (Canty et al., 2009). Importantly, cumulative adaptation of an organism to biological and environmental factors links physiology and ecology of an organism to its environment (Faimali et al., 2017). As such, monitoring of behaviour may provide information regarding an individual's fitness within an ecosystem (Dell'Omo, 2003), where altered responses may give rise to negative consequences at the population level (Bridges, 1997). Negative effects on populations following contaminant exposure have been observed. Significantly increased predation rates of mercury exposed mummichog (*Fundulus heteroclitus*) by the blue crab (*Callinectes sapidus*) were reported by Smith et al. (1997), a result of decreased escape response. Conversely, decreased predation rates of Cu exposed whelk *Urosalpinx cinerea* by the crab *Cancer productus* were observed by Kwan et al. (2015), a result of reduced whelk foraging activity. These reported behavioural changes following pollution exposure alters conspecific interactions of trophic levels the effects of which, may include a reduction of population density and biomass (Kwan et al., 2015).

Commonly, assessment of whole organism toxicity generally relates to mortality. In contrast, behavioural assessment provides a predictive method to determine whole organism physiological and neurological effects (Gauthier et al., 2016). For example,

chemosensory detection used by many species to locate food may permit contamination detection within their environment (Dell'Omo, 2003). Many organisms use chemosensory detection to avoid predation as alarm cues will elicit a behavioural retreat response (Schaum et al., 2013).

However, this chemical detection may also extend to contaminants and contaminated food sources, further provoking a behavioural avoidance response (Amiard-Triquet and Amiard, 2012). Avoidance responses to contamination have been evidenced: *H diversicolor* to mixed contaminated sediment (Durou et al., 2007) and Cu (Buffet et al., 2011); earthworm species exposed to Cu and Zn contaminated sediments (Lukkari and Haimi, 2005); common prawn, *Palaemon serratus* exposed to fenitrothion; freshwater shrimp, *Atyaephyra desmarestii* to Cu (Araújo et al., 2018).

Reduced feeding rates by *H diversicolor* following contaminant exposure (Berthet et al., 2003; Buffet et al., 2011; Christensen et al., 2002b; Cong et al., 2014; Mouneyrac et al., 2010), have also been recorded and may indicate attempts of contamination avoidance thereby reducing exposure (Amiard-Triquet and Amiard, 2012). Behavioural changes may also result from internal biochemical detoxification responses that in turn, require energy resources to shift from growth and reproduction to survival (Dell'Omo, 2003). Feeding and burrowing rate decline may therefore be an individual's attempt to conserve energy needed to metabolise or excrete noxious substances.

Moreover, behavioural changes may be invoked by neurotoxicity following the exposure and bioaccumulation of contamination (Basu, 2015). Both metals and PAH's have been observed to alter locomotive activities of marine species suggesting the impairment of physiological mechanisms (Amiard-Triquet and Amiard, 2012). Inhibition or hyperstimulation of the neurotransmitter acetylcholinesterase (AChE) (Amiard-Triquet, 2009) has been

evidenced following Pb exposure in the neotropical fish *Hoplias malabaricus* (Rabitto et al., 2005), freshwater oligochaete *Limnodrilus hoffmeisteri* (Martinez-Tabche et al., 2001) and juvenile rockfish *Sebastes schlegelii* (Kim and Kang, 2017a). Additionally, AChE inhibition has been recorded in *H diversicolor* following exposure to PAH's (Bouraoui et al., 2009; Christensen et al., 2002b; Kalman J et al., 2009) and Cu (Bonnard et al., 2009; Buffet et al., 2011; Burlinson and Lawrence, 2007; Mouneyrac et al., 2010).

Behavioural assessments following exposure to contaminants may therefore be suitable to assess sub - lethal effects, providing a sensitive biomarker of biological disturbance (Mouneyrac et al., 2010). Predominately research regarding behavioural alterations and neurotoxicity of contamination within the marine environment is mainly focused upon individual contaminants. Yet, contamination within the marine environment may be found with complex mixtures.

To determine potential co-toxic effects of Cu, Pb and pyrene the aim of this study is to determine behavioural alterations by *H diversicolor* following exposure to these contaminants, individually and in combination. The objectives are:

- 1) To assess burrowing behavioural alterations in *H diversicolor* exposed to environmentally relevant levels of Cu, Pb and pyrene individually and within mixtures.
- 2) Determine the levels of neurotoxicity in *H diversicolor* following exposure to both individual and mixtures of these contaminants.
- 3) Investigate the whole worm tissue bioaccumulation of these contaminants following exposure to both individual and mixtures of these contaminants.

5.2 Materials and methods

5.2.1 Chemicals

Lead chloride, copper chloride, pyrene (99%), sodium chloride, potassium phosphate and 5.5 – dithiobis – 2 - nitrobenzoic acid were purchased from Sigma Aldrich, UK.

Reduced glutathione was purchased from Thermo Fisher scientific, UK. All chemicals were of analytical reagent grade.

5.2.2 *H diversicolor*

700 individual *H diversicolor* were purchased from Sustainable Feeds Ltd, UK and acclimatised as detailed in Chapter 2 (2.5.2).

5.2.3 Sediment spiking and tank set up

Sediment spiking and tank set up used for this series of experiments was conducted as previously detailed in chapter 2 (2.6.1, 2.5.1 respectively). Initial analysis of sediment concentrations for all test tanks are shown in Table 27.

Table 27. Initial analysis of sediment following addition of manufactured sea water prior to the addition of worms. Sediment was taken 4 h after the addition of sea water. Reduction of pyrene from initial spiked concentration may result from adherence to tank walls and aeration pipe prior to sampling. Results are mean values +/- 1SE.

Test condition	Result Metal (mg kg ⁻¹)	Result Pyrene (µg kg ⁻¹)
Cu 31 µg kg ⁻¹	29.69 ± 0.03	
Cu 15 µg kg ⁻¹	12.9 ± 2.42	
Pb 9.2 µg kg ⁻¹	5.97 ± 0.04	
Pb 4.5 µg kg ⁻¹	3.58 ± 0.29	
Cu 31 mg kg ⁻¹ + Pyrene 970 µg kg ⁻¹	31.3 ± 0.07	633.28 ± 45.89
Cu 15.8 mg kg ⁻¹ + Pyrene 480 µg kg ⁻¹	12.03 ± 0.51	298.75 ± 28.38
Pb 9.2 mg kg ⁻¹ + Pyrene 970 µg kg ⁻¹	16.79 ± 0.54	616.74 ± 43.19
Pb 4.5 mg kg ⁻¹ + Pyrene 480 µg kg ⁻¹	8.70 ± 0.22	317.37 ± 11.06
Pyrene 970 µg kg ⁻¹		463.5 ± 87.5
Pyrene 480 µg kg ⁻¹		238.8 ± 33.8
Control Cu	1.27 ± 0.39	
Control Pb	0.59 ± 0.07	
Control Pyrene		0.0 ± 0.0

5.2.4 Burrowing Behaviour Assessment

1 worm per sediment spiked tank was removed and placed into a 1 l beaker which contained ~ 6 cm of clean sediment and artificial seawater (15 ppt salinity) (Moreira et al., 2006). The time for the individual worm to burrow in to the sediment was recorded (0, 1, ¾, ½, ¼, signifying depth) (Buffet et al., 2011). To account for bias, this experiment was repeated 10 times per test tank. Care was taken to ensure that different worms were selected for each behaviour recording.

5.2.5 Acetylcholinesterase Activity

Acetylcholinesterase activity was determined in accordance with the method described by Ellman et al., (1961). Worms were pooled ($n = 3$) (Bouroufi et al., 2009) and homogenised in 2 ml of NaCl, and 50 μ l of 0.1 M phosphate buffer. Homogenate was centrifuged at 9000 g for 30 min. 400 μ l of the supernatant was added to 1 ml of phosphate buffer (0.1 M pH 8) and to 100 μ l of Ellman's reagent (0.01 M 5,5-dithiobis - 2 - nitrobenzoic acid). Absorbance was read at 412 nm and set to zero. 20 μ l of 0.8 mM glutathione substrate was added to the cuvette and the absorbance read every 30 s for 3 min at 412 nm using a Varian Cary 50 probe UV - Vis spectrophotometer. Acetylcholinesterase activity is expressed in μ mol $\text{min}^{-1} \text{mg}^{-1}$ of proteins (Ellman et al., 1961). To determine protein concentration, a glutathione standard concentration curve (Appendix 1) was produced from a stock solution containing 25 mg of glutathione in 100 ml of distilled water. Aliquots of 0.1, 0.2, 0.3, 0.4 and 0.5 ml of stock solution were added to test tubes containing 4 ml of 5, 5 - dithiobis - 2 nitrobenzoic acid. All aliquots were diluted to a final volume of 5.5 ml using distilled water and mixed thoroughly using inversion. Aliquots were transferred to plastic cuvettes and read using a spectrophotometer at 412 nm. One cuvette which did not contain glutathione was used as a blank and subtracted from all readings.

5.2.6 Total Metal sediment and Worm Tissue Determination

Total concentrations of metals within the sediment samples and worm tissue were determined in accordance with method described in Chapter 2 (2.3.2 and 2.3.3 respectively).

5.2.7 Pyrene Sediment and Worm Tissue Determination

Worms were prepared for analysis as detailed in Chapter 2 (2.3.9). Pyrene sediment and worm tissue concentrations were determined following the method detailed in Chapter 2 (2.4.0, 2.4.2).

5.3 Statistical analysis

Data was analysed as described in Chapter 2 (2.8). A one - way ANOVA was performed on burrowing rates of the control and acetone exposure group. All other burrowing time results did not meet the assumptions of parametric tests and therefore, Welch 2 way t - tests were performed. Welch's robust ANOVA were performed on all AChE results for all exposed groups. Spearman's correlation coefficient analysis was performed on worm tissue, burrowing time and acetylcholinesterase concentrations to identify relationships.

5.4 Results

5.4.1 Acetone Control Burrowing Behaviour

Throughout the 7- day burrowing behaviour test, worms ($n = 10$) taken from the acetone control tank were assessed for burrowing rates against those of the control tank as shown in Figure 21.

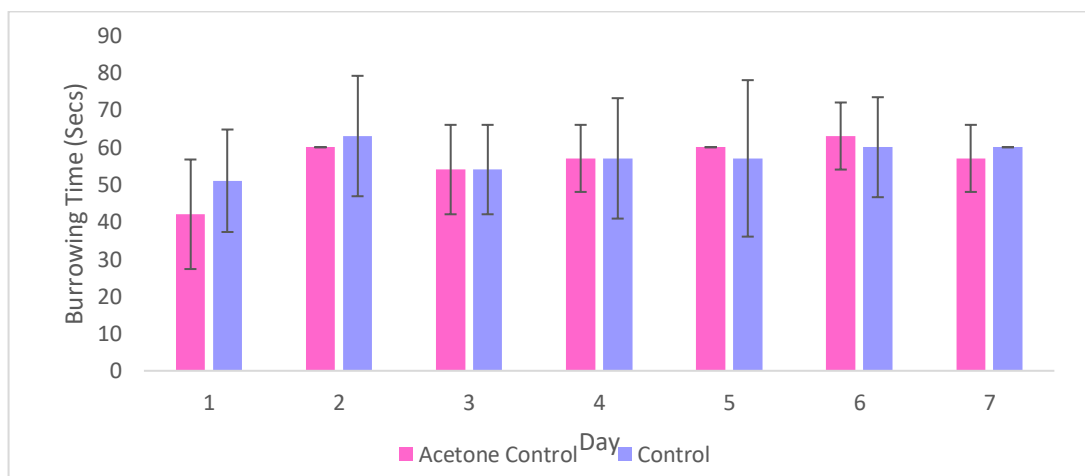


Figure 21. Acetone and control tanks Burrowing behaviour results ($n = 10$).

One - way ANOVA revealed that the control and acetone groups worm burrowing rates were not significantly different ($F_{(1, 20)} = 0.917$, $p = 0.515$). Therefore, only the control worm burrowing results have been included in the results.

5.4.2 Spiked sediment Cu 31.8 mg kg⁻¹

All worms from the test series which contained Cu spiked sediment at 31.8 mg kg⁻¹ died within the first 48 h of the start of the experiment.

5.4.3 Spiked sediment Cu 31.8 mg kg⁻¹ + Pyrene 970 µg kg⁻¹.

All worms from the test series which contained Cu spiked sediment at 31.8 mg kg⁻¹ and Pyrene 970 µg kg⁻¹ died within 48 h of the start of the experiment.

5.4.4 Spiked sediment Cu 15.8 mg kg⁻¹

Mortality rates for this test series were 30% during the first 48 h. There were no further mortalities for the remainder of the experiment. Burrowing behaviour assessment for this series of experiments, Cu sediment and whole worm tissue concentrations are illustrated in Figure 22.

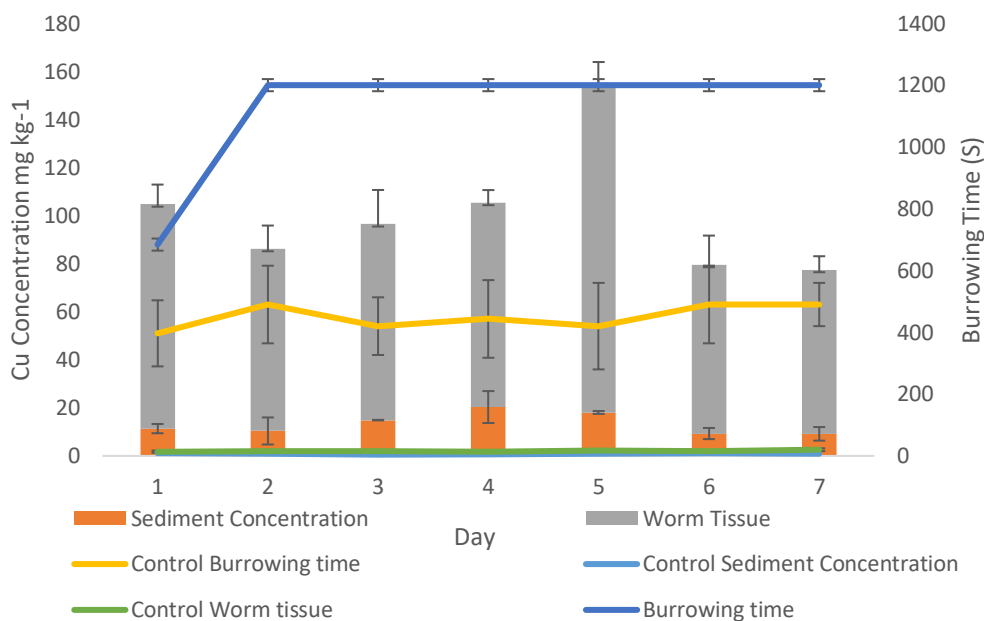


Figure 22. Cu 15 mg kg⁻¹ spiked sediment test series results showing burrowing behaviour time (s) and concentrations of Cu in whole worm tissue ($n = 10$ individual worms) and sediment.

A Welch 2 sample t – test performed for Cu exposed and control groups revealed significant differences in burrowing rates for each sample day: Day 1 ($t_{(9)} = 79.3, p = < 0.01$); Day 2 ($t_{(9)} = 211.1, p = < 0.01$); Day 3 ($t_{(9)} = 286.5, p = < 0.01$); Day 4 ($t_{(9)} = 212.3, p = < 0.01$); Day 5 ($t_{(9)} = 191, p = < 0.01$); Day 6 ($t_{(9)} = 211.1, p = < 0.01$); Day 7 ($t_{(9)} = 379, p = < 0.01$) indicating that Cu has a rapid and prolonged effect on burrowing rates. Worm burrowing behaviour increased from 660 s at day 1 to no burrowing recorded during the 1200 s duration of the experiment from day 2 to day 7. Worm tissue Cu concentration showed rapid uptake at day 1 of 98.35 mg kg⁻¹ increasing to 136.41 mg kg⁻¹ at day 5, followed by a decrease to 68.25 mg kg⁻¹ at day 7. Σ Mean whole worm tissue concentrations for this test series were 87.22 ± 9.23 mg kg⁻¹.

Cu sediment concentrations ranged between 9.17 - 20.30 mg kg⁻¹ during the test period.

5.4.5 Spiked sediment Cu 15.8 mg kg⁻¹ and Pyrene 480 µg kg⁻¹

Mortality rates were 10% during the first 72 h of this experiment. There were no further mortalities for the remainder of the experiment. Burrowing behaviour assessment, sediment and tissue concentrations and associated control group results are illustrated in Figure 23.

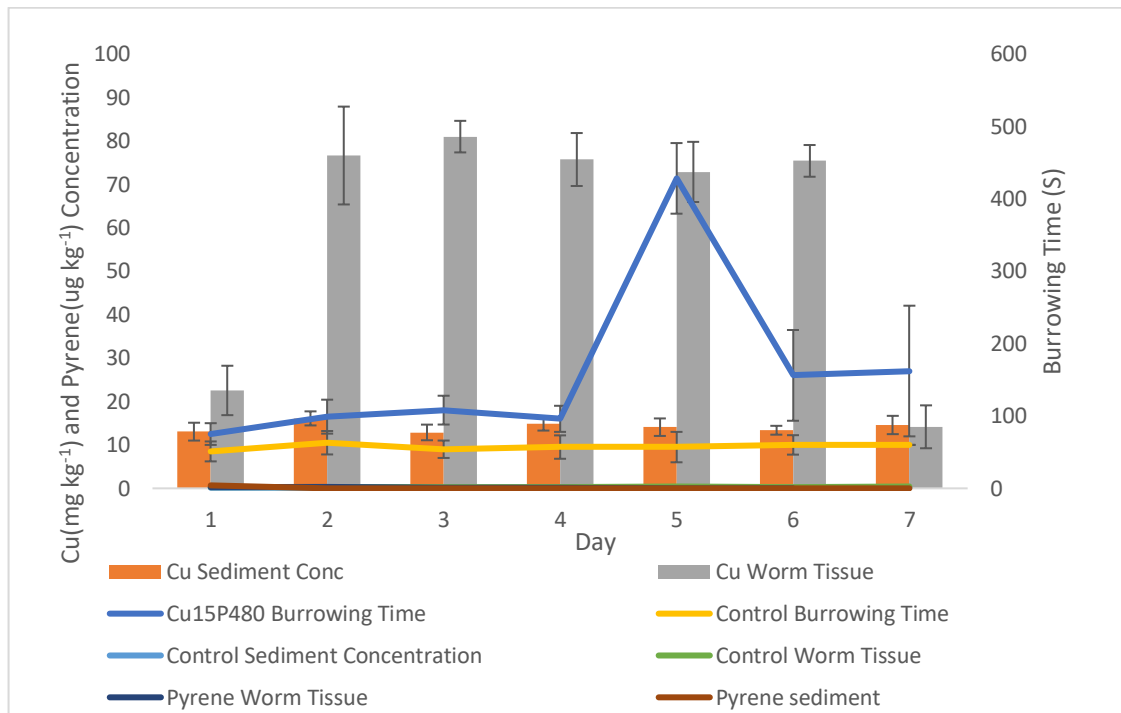


Figure 23. Burrowing time (s) for ($n = 10$ individual worms) Cu 15.8 mg kg⁻¹ +Pyrene 480 µg kg⁻¹ test condition over a period of 20 min. Sediment concentrations of pyrene and whole worm pyrene concentrations and associated control results are including to illustrate comparisons.

A Welch 2 sample t – test conducted on burrowing speed from the Cu + pyrene exposed and control group revealed significant differences in burrowing rates for each day: Day 1 ($t_{(17)} = 3.53$, $p = < 0.01$); Day 2 ($t_{(16)} = 3.79$, $p = < 0.01$); Day 3 ($t_{(15)} = 6.97$, $p = < 0.01$); Day 4 ($t_{(18)} = 4.83$, $p = < 0.01$); Day 5 ($t_{(11)} = 21.59$, $p = < 0.01$); Day 6 ($t_{(10)} = 4.31$, $p = < 0.01$) and Day 7 ($t_{(9)} = 3.28$, $p = < 0.01$) demonstrating that mixed Cu + pyrene exposure has a rapid and prolonged effect on burrowing rates. Worm burrowing behaviour for

Cu 15 mg kg⁻¹ and Pyrene 480 µg kg⁻¹ showed burrowing times between 75 - 108 s during days 1 - 4. Burrowing time increased rapidly for day 5 (428 s) followed by a decrease during days 6 (156 s) and day 7 (162 s).

Worm tissue Cu concentration at day 1 (22.53 mg kg⁻¹) was followed by a rapid accumulation at day 2 (76.59 mg kg⁻¹). Concentrations remained steady between day 3 (80.94 mg kg⁻¹), day 4 (75.67 mg kg⁻¹), day 5 (72.82 mg kg⁻¹) and day 6 (75.36 mg kg⁻¹), followed by rapid decrease at day 7 (14.16 mg kg⁻¹). Σ Mean whole worm tissue concentrations for this test series were 59.73 \pm 6.02 mg kg⁻¹.

Sediment Cu concentrations (12.86 mg kg⁻¹ - 16.10 mg kg⁻¹) remained constant throughout this test series. Sediment pyrene concentrations showed a reduction from 1.96 µg kg⁻¹ at day 1 to 0.67 µg kg⁻¹ at day 3. Results for days 4 - 7 were below the limits of detection < 500 ng kg⁻¹.

5.4.6 Cu 7 mg kg⁻¹ and Cu 4 mg kg⁻¹ spiked sediment condition

Due to the mortalities of worm exposed to previous Cu test conditions, experiments were repeated using Cu at levels 7 and 4 mg kg⁻¹. However, all worms for both test conditions died within 48 h of the start of the experiments.

5.4.7 Pb 9.2 mg kg⁻¹ spiked sediment condition

There were no mortalities during this experiment. Burrowing behaviour, whole worm tissue concentrations and sediment concentrations for Pb 9.2 mg kg⁻¹ are illustrated in Figure 24.

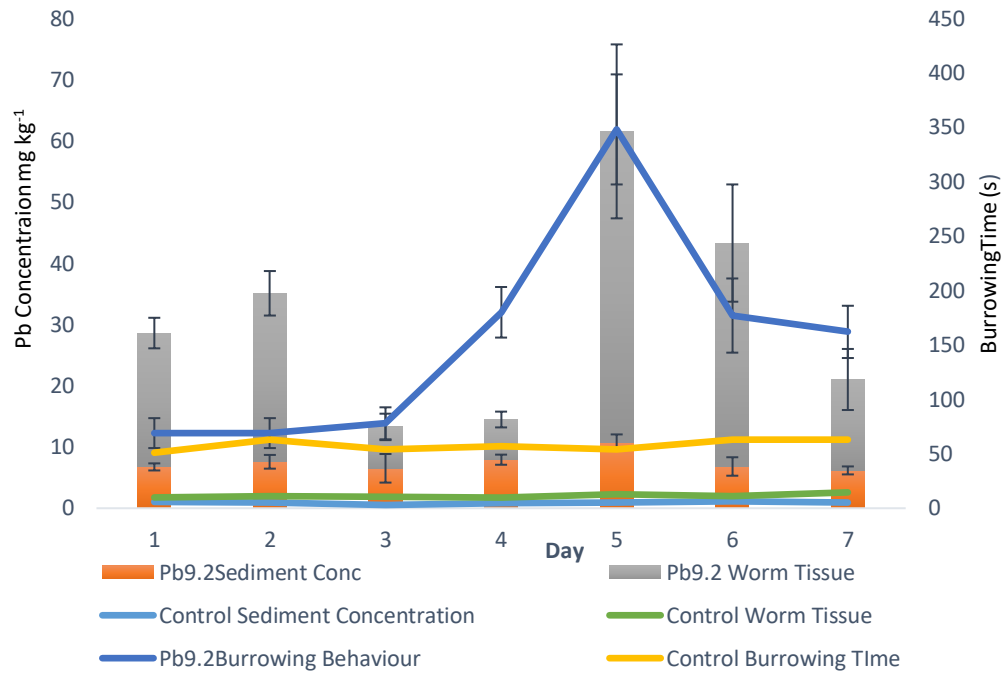


Figure 24. Burrowing time (s) for ($n = 10$ individual worms) Pb9.2 mg kg⁻¹ test condition over a period of 20 min. Sediment concentrations of Pb whole worm concentrations and associated control results are included to illustrate comparisons.

Significant differences were found between burrowing times of Pb exposed and control groups using Welch 2 sample t – tests for all sample days: Day 1 ($t_{(18)} = 2.78$, $p = 0.01$); Day 2 ($t_{(17)} = 3.99$, $p = 0.036$); (Day 3 ($t_{(17)} = 3.79$, $p < 0.01$); Day 4 ($t_{(16)} = 13$, $p < 0.01$); Day 5 ($t_{(16)} = 11$, $p < 0.01$); Day 6 ($t_{(13)} = 9.1$, $p < 0.01$) and Day 7 ($t_{(11)} = 11.6$, $p < 0.01$). These results demonstrate the immediate and continued effect that Pb exposure exerts on *H diversicolor* burrowing rates at this concentration. Burrowing behaviour ranged between 69-78 s (day 1 - 3) followed by an increase at day 4 (180 s). There was a further increase at day 5 (348 s) followed by a decrease for day 5 (177 s) and day 6 (162 s).

Whole worm tissue concentrations showed rapid accumulation at day 1 (21.86 mg kg⁻¹) and day 2 (27.52) followed by excretion to 6.76 mg kg⁻¹ and 6.56 mg kg⁻¹ at days 3 and 4 respectively. A sharp accumulation occurred at day 5 (50.81 mg kg⁻¹) followed by a further period of excretion to 36.49 mg kg⁻¹ at day 6 and 14.85 mg kg⁻¹ at

day 7. Σ mean whole worm tissue concentrations were 23.55 ± 5.48 mg kg^{-1} .

Sediment concentrations ranged between $6.17 - 10.73$ mg kg^{-1} throughout this test series.

5.4.8 Pb 9.2 mg kg^{-1} and Pyrene $970 \mu\text{g kg}^{-1}$ spiked sediment condition

There were no mortalities during this experiment. Burrowing time, whole worm tissue and sediment concentrations for this test condition are illustrated in Figure 25.

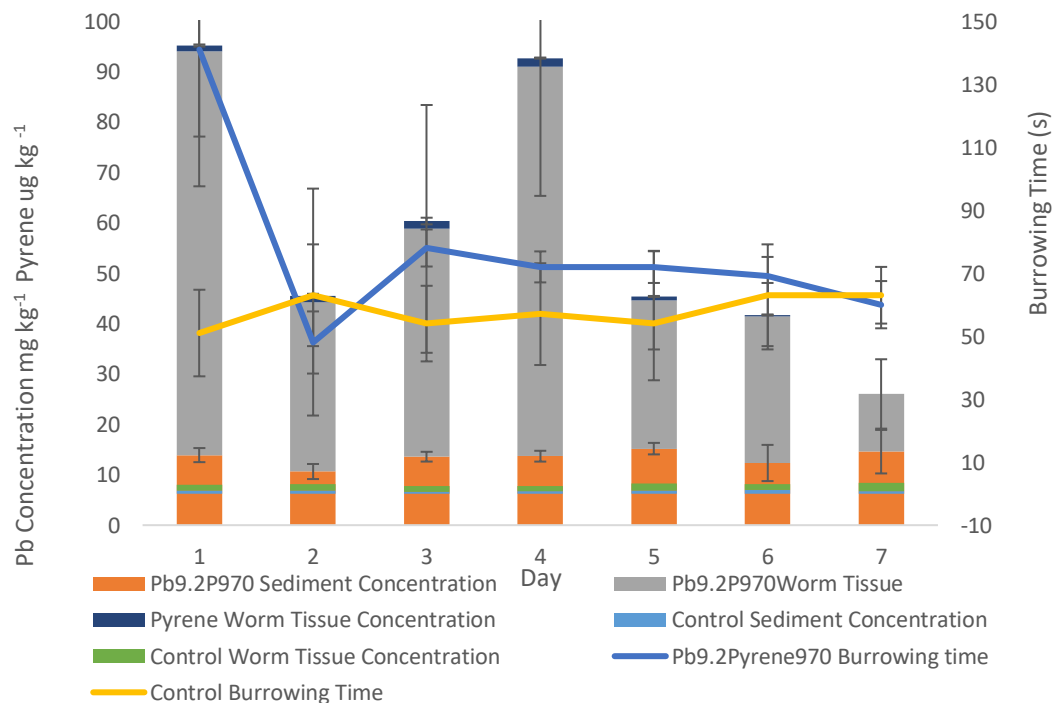


Figure 25. Burrowing time (s) for ($n = 10$ individual worms) $\text{Pb}9.2 \text{ mg kg}^{-1} + \text{Pyrene } 970 \mu\text{g kg}^{-1}$ test condition over a period of 20 min. Sediment concentrations of pyrene and whole worm pyrene concentrations and associated control results are included to illustrate comparisons.

Significant differences were found between burrowing times of Pb + pyrene exposed and control group using Welch 2 sample t – tests for sample days: Day 1 ($t_{(16)} = 11.4$, $p = <0.01$); Day 2 ($t_{(17)} = 2.99$, $p = 0.051$) and (Day 3 ($t_{(17)} = 3.78$, $p = < 0.01$). Interestingly, significant differences were not identified on Day 4 ($t_{(17)} = 1.76$, $p = 0.09$), Day 5

($t_{(17)} = 1.18$, $p = 0.06$), Day 6 ($t_{(17)} = 0.85$, $p = 0.41$) or Day 7 ($t_{(9)} = -1$, $p = 0.34$). Results indicate that although there was a rapid effect on burrowing rates from days 1 – 3, they did not differ significantly from the control group on days 4 – 7. Burrowing time ranged from 141 s at day 1 to a rapid decrease of 48 s at day 2. Burrowing rates between day 3 and day 7 (78 s, 72 s, 69 s, 66 s, 60 s respectively) showed a general reduction.

Whole worm tissue concentrations for Pb showed a rapid uptake at day 1 (80.07 mg kg⁻¹) followed by a decrease between day 2 (33.63 mg kg⁻¹) and day 3 (45.20 mg kg⁻¹). Tissue concentrations increased at day 4 (77.31 mg kg⁻¹) followed by a further decrease at day 5 (29.42 mg kg⁻¹), day 6 (29.13 mg kg⁻¹) and 11.46 mg kg⁻¹ at day 7. Σ Mean worm Pb tissue concentration (43.75 ± 9.48 mg kg⁻¹) was far higher than that of worms exposed to Pb9.2mg kg⁻¹ (23.55 mg kg⁻¹).

Sediment concentrations for Pb ranged between 10.64 mg kg⁻¹ and 15.18 mg kg⁻¹ during the test period.

Worm tissue pyrene concentrations were 0.98 μ g kg⁻¹ on day 1 increasing to 2.49 μ g kg⁻¹ on day 3. Pyrene levels then decreased to 0.38 μ g kg⁻¹ on day 7.

Sediment concentrations for pyrene ranged between 2.4 - 3.15 μ g kg⁻¹ for days 1 - 3. Concentrations were then below the limits of detection < 500 ng kg⁻¹.

5.4.9 Pb 4.5 mg kg⁻¹ spiked sediment condition

There were no mortalities during this test period. Burrowing behaviour, sediment and whole worm tissue concentrations are detailed in Figure 26.

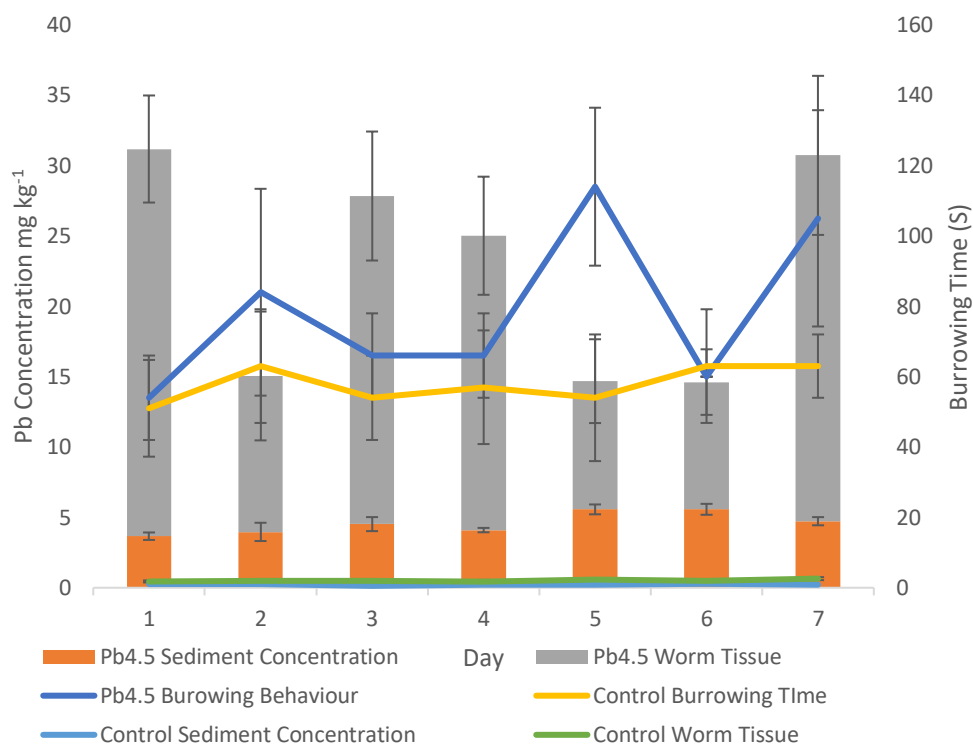


Figure 26. Burrowing time (s) for ($n = 10$ individual worms) Pb4.5 mg kg⁻¹ test condition over a period of 20 min. Sediment concentrations of pyrene and whole worm pyrene concentrations and associated control results are included illustrating comparisons.

Burrowing rates for this condition ranged between 54 and 114 s during the 7 - day test period. Significant differences were determined between the burrowing times of Pb exposed and the control group using a Welch 2 sample t – test: Day 1 ($t_{(11)} = 3.93$, $p = 0.01$); Day 3 ($t_{(18)} = 2.12$, $p = 0.048$); Day 5 ($t_{(17)} = 6.26$, $p < 0.01$) and Day 7 ($t_{(11)} = 3.93$, $p < 0.01$). However, significant differences were not identified on sample Day 2 ($t_{(14)} = 1.87$, $p = 0.08$), Day 4 ($t_{(17)} = 1.34$, $p = 0.20$) or Day 6 ($t_{(9)} = -0.56$, $p = 0.59$).

Worm tissue Pb concentrations showed a rapid accumulation at day 1, 3 and 7 (25.51, 23.31, 25.99 mg kg⁻¹ respectively) followed by periods of reduction at days 2, and 5 (11.07, 9.11 mg kg⁻¹ respectively). Σ Mean whole worm Pb tissue concentrations were 18.14 ± 4.02 mg kg⁻¹

Sediment concentrations remained stable throughout the duration of the experiment (3.66 - 5.57 mg kg⁻¹).

5.5.0 Pb 4.5 mg kg⁻¹ + Pyrene 480 µg kg⁻¹ spiked sediment condition

There were no mortalities for this test condition. Burrowing time, sediment and whole worm tissue concentrations are illustrated in Figure 27.

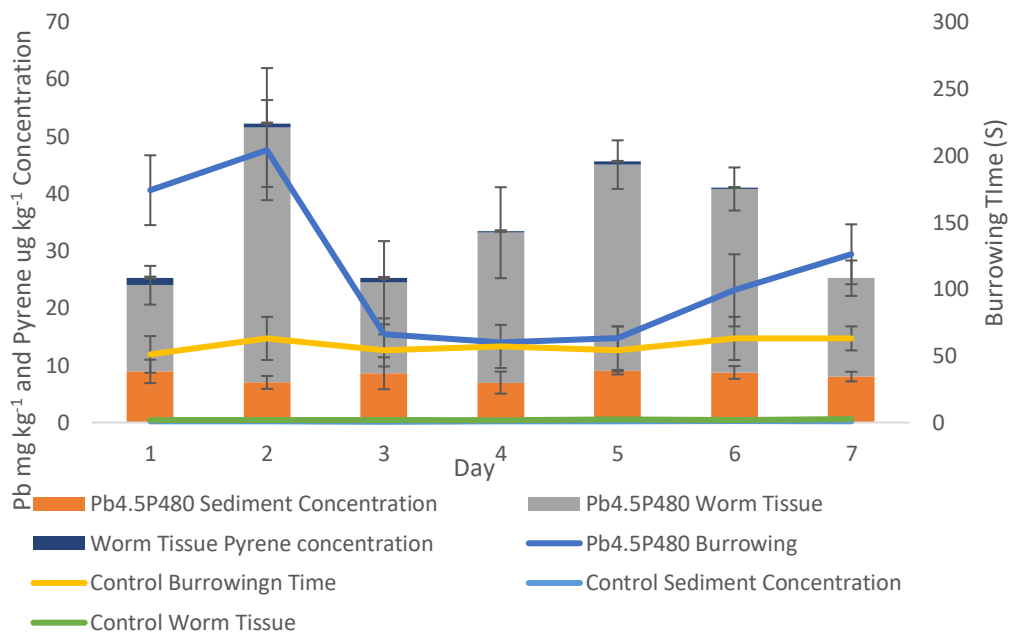


Figure 27. Burrowing time (s) for ($n = 10$ individual worms) Pb4.5 mg kg⁻¹ + Pyrene 480 µg kg⁻¹ test condition over a period of 20 min. Sediment concentrations of pyrene and whole worm pyrene concentrations and associated control results are included illustrating comparisons.

Worm burrowing rates ranged between 54 s (day 1) to 108 s (day 7). A Welch 2 sample t – test identified significant differences between burrowing times of Pb + pyrene exposed and control group for sample days: Day 1 ($t_{(14)} = 12.5$, $p = <0.01$); Day 2 ($t_{(12)} = 10.38$, $p = <0.01$); Day 3 ($t_{(18)} = 2.12$, $p = 0.048$); Day 6 ($t_{(15)} = 3.43$, $p = <0.01$) and Day 7 ($t_{(12)} = 7.81$, $p = <0.01$). However, significant differences were not identified on Day 4 ($t_{(9)} = 0.56$, $p = 0.59$), Day 5 ($t_{(13)} = 1.34$, $p = 0.20$) or Day 6 ($t_{(17)} = 0.85$, $p = 0.41$).

Whole worm tissue concentrations for Pb showed initial accumulation of 14.55 mg kg⁻¹ at day 1 to further rapid accumulation of 57.11 mg kg⁻¹ at day 2. A decrease at day 3 (7.79 mg kg⁻¹) was followed by fluctuations from 15.10 mg kg⁻¹, 35.61 mg kg⁻¹, 29.79 mg kg⁻¹ and 12.82 mg kg⁻¹ through day 4 to day 7 respectively. Σ Mean whole worm Pb tissue concentrations for this test condition were far higher (26.69 \pm 5.73 mg kg⁻¹) than those of test condition Pb4.5 mg kg⁻¹ (18.14 \pm 4.02 mg kg⁻¹).

Sediment Pb concentrations ranged between 3.3 mg kg⁻¹ to 5.03 mg kg⁻¹ throughout the duration of the test.

Whole worm tissue concentrations for pyrene decreased from 1.32 – 0.26 μ g kg⁻¹ between days 1 - 7.

Sediment concentrations for pyrene ranged from 16.99 μ g kg⁻¹ at day 1 to 1.658 μ g kg⁻¹ at day 4. Results for days 5 - 7 were below the limits of detection (< 500 ng kg⁻¹).

5.5.1 Pyrene 970 μ g kg⁻¹ spiked sediment condition

There were no mortalities for this test condition. Burrowing time, sediment and whole worm concentrations are detailed in Figure 28.

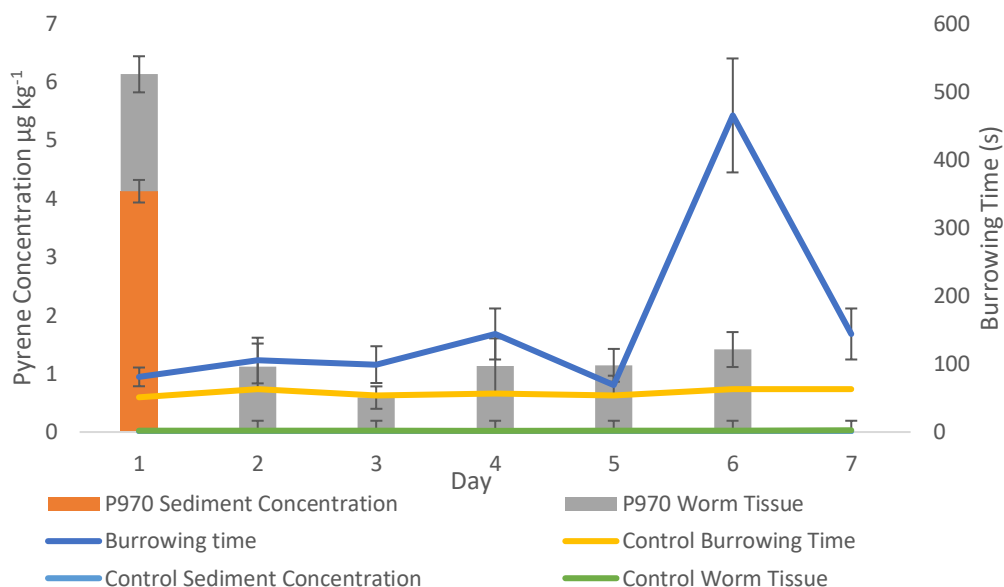


Figure 28. Burrowing time (s) for ($n = 10$ individual worms) Pyrene 970 $\mu\text{g kg}^{-1}$ test condition over a period of 20 min. Sediment concentrations of pyrene and whole worm pyrene concentrations and associated control results are included illustrating comparisons.

Significant differences between burrowing time for pyrene exposed worms and the control group were found using a Welch 2 sample t-test on sample Day 1 ($t_{(18)} = 4.63$, $p = < 0.01$), Day 2 ($t_{(13)} = 3.38$, $p = < 0.01$), Day 3 ($t_{(12)} = 4.57$, $p = < 0.01$), Day 4 ($t_{(12)} = 6.40$, $p = < 0.01$), Day 6 ($t_{(10)} = 14.15$, $p = < 0.01$) and Day 7 ($t_{(10)} = 6.31$, $p = < 0.01$) indicating a rapid effect initially. However, a significant relationship was not identified between the pyrene exposed and control group on sample Day 5 ($t_{(17)} = 1.20$, $p = 0.06$).

Initial burrowing time at day 1 (81 s) increased to 144 s at day 4. Reduced rates of 69 s occurred at day 5 followed by an increase to 465 s at day 6. Burrowing time then showed a decrease to 144 s at day 7. Initial uptake of pyrene in whole worm pyrene tissue concentrations was $2.00 \mu\text{g kg}^{-1}$ followed by a reduction at day 6 of $1.41 \mu\text{g kg}^{-1}$. Concentrations analysed at day 7 were below the limits of detection $< 500 \text{ ng kg}^{-1}$.

Pyrene sediment concentrations at day 1 were $4.12 \mu\text{g kg}^{-1}$. Sediment analysis of subsequent days were below the limits of detection $< 500 \text{ ng kg}^{-1}$.

5.5.2 Pyrene $480 \mu\text{g/Kg}$ spiked sediment condition

There were no mortalities for the duration of this test condition. Burrowing time, sediment and whole worm concentrations are found in Figure 29.

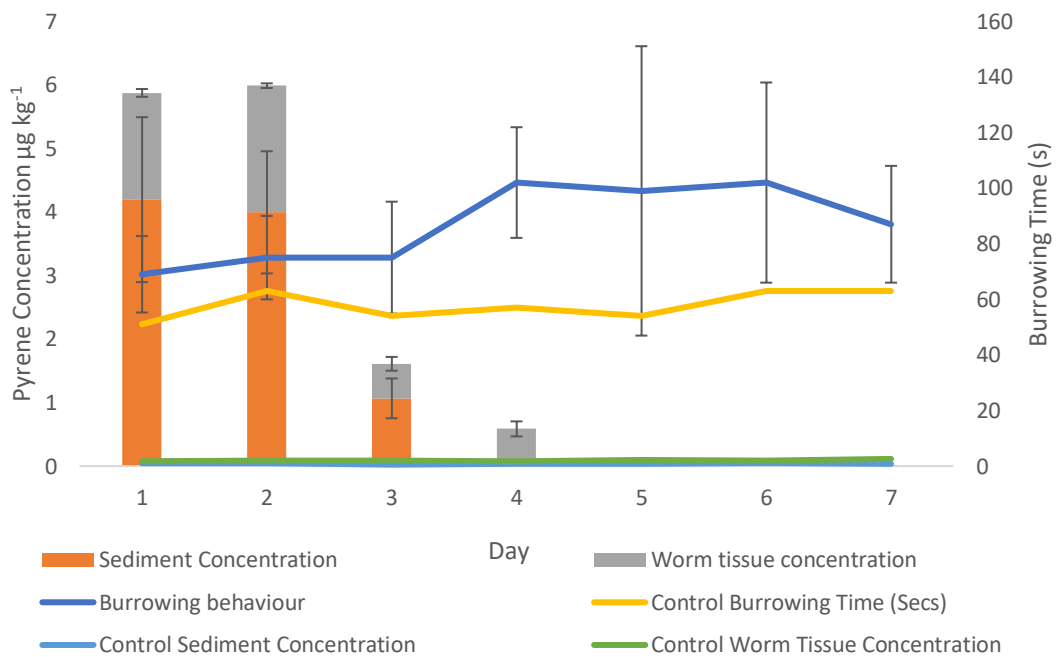


Figure 29. Burrowing time (s) for ($n = 10$ individual worms) Pyrene $480 \mu\text{g kg}^{-1}$ test condition over a period of 20 min. Sediment concentrations of pyrene and whole worm pyrene concentrations and associated control results are included illustrating comparisons.

Burrowing time at day 1 (69 s) increased to the maximum rate of 102 s at day 4. The rate then reduced to 87 s at day 7. A Welch 2 - sample t - test determined significant differences between burrowing time for pyrene exposed worms and the control group on sample Day 1 ($t_{(18)} = 2.28$, $p = 0.01$), Day 3 ($t_{(15)} = 2.69$, $p = 0.02$), Day 4 ($t_{(17)} = 5.27$, $p = <0.01$), Day 5 ($t_{(11)} = 2.45$, $p = 0.03$), Day 6 ($t_{(12)} = 2.97$, $p = 0.01$) and Day 7 ($t_{(12)} = 3.15$, $p = <0.01$). However, a significant

relationship was not identified on sample Day 2 ($t_{(17)} = 1.63$, $p = 0.12$).

Whole worm pyrene tissue concentration initially was $1.68 \mu\text{g kg}^{-1}$ followed by a decrease to $0.59 \mu\text{g kg}^{-1}$ at day 4. Results for days 5 to 7 were below the limits of detection $< 500 \text{ ng kg}^{-1}$.

Sediment pyrene concentrations decreased from $4.19 \mu\text{g kg}^{-1}$ at day 1 to 1.06 at day 3. Results for days 4 - 7 were below the limits of detection $< 500 \text{ ng kg}^{-1}$.

5.5.3 AChE Concentrations

The response for AChE activity for test conditions $\text{Pb}4.5 \text{ mg kg}^{-1}$, $\text{Pyrene } 480 \mu\text{g kg}^{-1}$, $\text{Pb}4.5 \text{ mg kg}^{-1} + \text{Pyrene } 480 \mu\text{g kg}^{-1}$ and control are detailed in Figure 30.

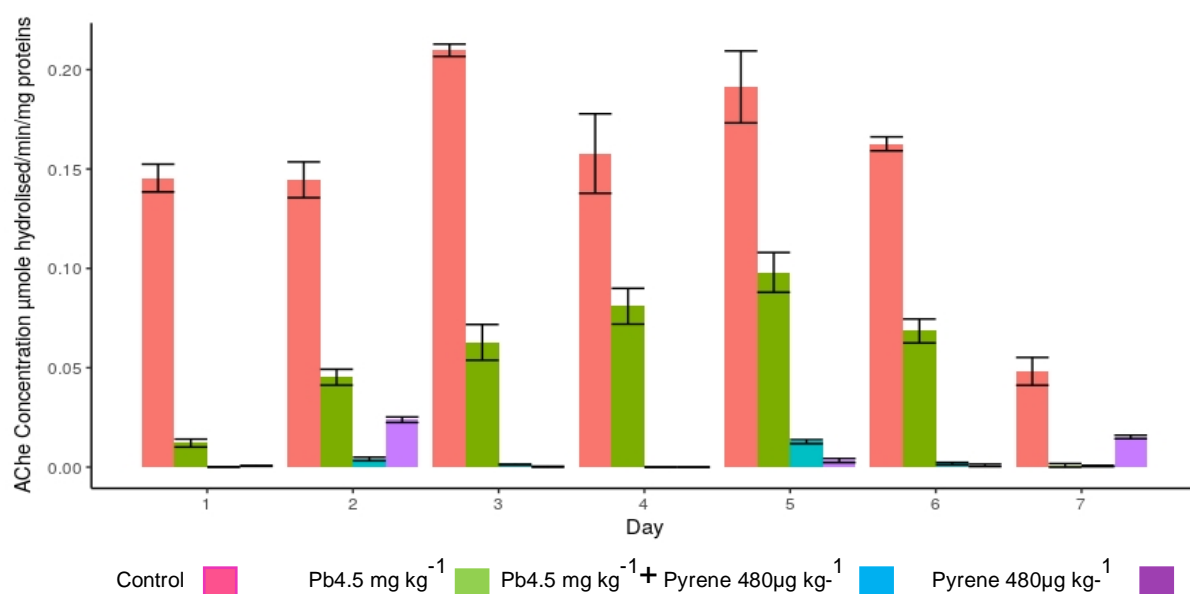


Figure 30. AChE activity for worms exposed to test conditions $\text{Pb}4.5 \text{ mg kg}^{-1}$, $\text{Pyrene } 480 \mu\text{g kg}^{-1}$, $\text{Pb}4.5 \text{ mg kg}^{-1} + \text{Pyrene } 480 \mu\text{g kg}^{-1}$ and control for a period of 7 days. Worms ($n = 3$) were extracted from the sediment daily, and frozen prior to analysis. Measurements represent the mean ± 1 SE of the $n = 3$ worms pooled for analysis. Data is expressed in $\mu\text{mol min}^{-1} \text{ mg}^{-1} \text{ proteins}$.

Results demonstrate reduced AChE activity for all test conditions when compared with control. Welch's robust ANOVA's revealed significant differences between test conditions and control group: Pb4.5 mg kg⁻¹ ($F_{(35)}= 7.49, p < 0.01$); Pyrene 480 µg kg⁻¹ ($F_{(21)} = 12, p = < 0.01$); Pb4.5 mg kg⁻¹ + Pyrene 480 µg kg⁻¹ ($F_{(20)} = 13, p = < 0.01$). Test condition Pb4.5 mg kg⁻¹ showed increasing levels from day 1 (0.012 µmol min⁻¹ mg⁻¹) to 0.09 µmol min⁻¹ mg⁻¹ on day 5 followed by further reductions (0.06, 0.0008 µmol min⁻¹ mg⁻¹) on days 6 and 7 respectively. Both test conditions Pb4.5mg kg⁻¹ + Pyrene 480 µg kg⁻¹ and Pyrene 480 µg kg⁻¹ showed concentrations between < 0.0001 and 0.08 µmol min⁻¹ mg⁻¹.

AChE response related to concentrations for test conditions Pb9.2 mg kg⁻¹, Pb9.2mg kg⁻¹ + Pyrene 970 µg kg⁻¹, Pyrene 970 µg kg⁻¹ and control are shown in Figure 31.

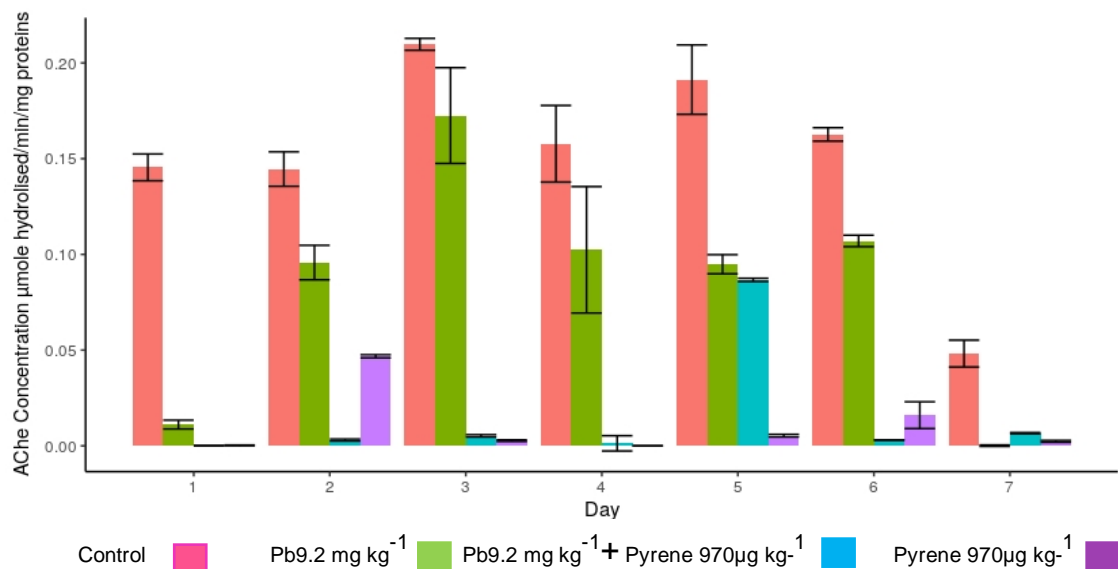


Figure 31. AChE activity for worms exposed to the test conditions Pb9.2 mg kg⁻¹, Pb9.2mg kg⁻¹ + Pyrene 970 µg kg⁻¹, Pyrene 970 µg kg⁻¹ and control (mg kg⁻¹/ µg kg⁻¹) for a period of 7 days. Worms ($n = 3$) were extracted daily and frozen prior to analysis. Measurements are expressed as mean activity \pm 1 SE of pooled worms. Data is expressed in µmol min⁻¹ mg⁻¹ proteins.

AChE response for all test conditions was lower than those of the control. Significant differences were found between all groups and the control using Welch's robust ANOVA's: Pb9.2 mg kg⁻¹ ($F_{(39)} = 4$, $p = < 0.01$); Pb9.2 mg kg⁻¹ + Pyrene970 µg kg⁻¹ ($F_{(33)} = 10$, $p = < 0.01$); Pyrene 970 µg kg⁻¹ ($F_{(24)} = 12$, $p = < 0.01$). AChE activity for test condition Pb9.2 mg kg⁻¹ showed levels of 0.011 µmol min⁻¹ mg⁻¹ on day 1 followed by an increase to 0.09 and 0.17 µmol min⁻¹ mg⁻¹ on days 2 and 3 respectively. Activity then reduced slightly to levels between 0.09 - 0.0.11 µmol min⁻¹ mg⁻¹ for days 4 - 6 followed by a further reduction to 0.0009 µmol min⁻¹ mg⁻¹ on day 7.

Activity for test conditions Pyrene 970 µg kg⁻¹ and Pb9.2 mg kg⁻¹ + Pyrene 970 µg kg⁻¹ were significantly lower than those of the control and condition Pb9.2 mg kg⁻¹, ranging between < 0.00 - 0.046 µmol min⁻¹ mg⁻¹ and 0.0006 - 0.01 µmol min⁻¹ mg⁻¹ respectively.

5.5.4 Relationships between whole worm tissue concentrations and burrowing time

Spearman rank coefficients were then performed to identify relationships between whole worm tissue concentrations (metal, pyrene, metal + pyrene) and sediment concentrations. There were no statistically significant relationships found between any test condition or factor.

Spearman's rank coefficients were then performed on results for burrowing time and whole tissue contamination levels. There were no statistically significant relationships found for whole worm tissue concentration and burrowing time for any test condition.

5.5.5 Relationships between AChE activity and burrowing time

Spearman's correlations were performed using AChE levels and burrowing time however, there were no statistically significant relationships.

5.6 Discussion

5.6.1 Cu test series

Median values of metal concentrations for Cu identified in Chapter 3, were chosen to reflect environmental concentrations for this test series. Unexpectedly, given the concentrations used, all Cu test series resulted in high or total mortalities for all conditions. Worms exposed to Cu 15.8 mg kg⁻¹ and Cu 15.8mg kg⁻¹ + Pyrene 480µg kg⁻¹ had the lowest mortalities although rates far exceeded test compliance of 20% mortality set by OECD guidelines for exposure experiments (OECD, 2005). Possible moribundity of individuals may have led to confounding results and therefore, AChE activities were not performed on individuals from these conditions and burrowing time results for the Cu 15.8 mg kg⁻¹ series have been included for information.

Burrowing rates for worms exposed to Cu 15.8 mg kg⁻¹ were far slower than those exposed to the Cu + pyrene mixture. Furthermore, worm Cu tissue concentrations for those exposed to Cu 15.5 mg kg⁻¹ + pyrene 480 µg kg⁻¹ were far lower (59.73 mg kg⁻¹), than those exposed to Cu 15.8 mg kg⁻¹ (87.22 mg kg⁻¹). As Cu is an essential metal and therefore highly regulated (Rainbow, 2002), the high mortality rates from the Cu conditions suggest that the mechanisms of Cu regulation in these worms may be compromised and may have resulted in the increased accumulation of Cu during these experiments. Upon accumulation, Cu has binding affinity for sulphur and nitrogen found in certain proteins (Rainbow, 2002). However, the binding of Cu to these proteins namely metallothionein's may occur after a lag of 24 h related to protein synthesis (Mouneyrac et al., 2003). Therefore, the increased accumulation of Cu in the exposure experiments to the delay in the increase metallothionein levels, leaving the worms unable to counter the toxic effects of Cu, may have contributed to the observed mortalities.

Worms used for this series of experiments were purchased from a commercial source. Individuals were the 5th - 6th generation from the founding stock obtained from an estuary in Northumberland, UK, which had been housed in a mixture of clean mud, sand and perlite (Craig, 2018 personal communication). As such, these worms are not exposed to environmental high levels of Cu and may contribute to the intolerance of these individuals.

It has been widely demonstrated that *H diversicolor* which inhabit Restronguet Creek, Cornwall, UK are exposed to exceptionally high Cu levels (5073 mg kg⁻¹) in sediment, as a result of historic mining industries (Bryan et al., 1987). Previous authors have described tolerance in resident populations attributed to increased numbers of Cu storage granules within tissue (Mouneyrac et al., 2003) which serve as storage / detoxification mechanism to mitigate the effects of high tissue concentrations. Moreover, Mcquillan et al. (2014) identified increased expression of Cu ion transporter, Cu ion chaperone, and metallothionein like protein genes in tolerant *H diversicolor* than individuals analysed from environments with lower Cu levels. Alterations of phenotype via upregulation of specific regulatory genes may therefore influence tolerance. It is reasonable to suggest that lack of exposure to the population where adaptation has led to the loss of these enhanced detoxification mechanisms and may explain the apparent intolerance displayed by the individuals used for the present study.

The presence of pyrene in the Cu test conditions reduced Cu concentrations in worm tissue, suggesting that the uptake of Cu was affected. Cu may pass through cellular membranes via the mimicking of Na⁺ ions, or via metal ion transporters such as the divalent metal transporter (DMT1) and Cu ATPase pump Cu transporter 1 (ctr1) (Gauthier et al., 2016). It is suggested that altered membrane fluidity related to membrane binding of PAH's and subsequent membrane electro - potential change may affect the rate of ion exchange (e.g.

Na⁺) across the membrane therefore reducing Cu uptake (Gauthier et al., 2016).

Burrowing rates of individuals from Cu 15.8 mg kg⁻¹ were higher than those exposed to the Cu + pyrene mixture and both test conditions showed higher burrowing rates than those of the control. The differences between burrowing rates and concentrations of Cu in worms exposed in combination with pyrene indicated an antagonistic toxicity. Although, burrowing rates were different from the control, they appeared to be less effected. Importantly, levels of Cu in worms exposed in combination with pyrene were greatly reduced again suggesting an antagonistic interaction and may relate to altered membrane fluidity and subsequent electro-membrane potential change. Therefore, the use of burrowing rates as an indicator of environmental Cu and pyrene contamination may be tentatively suggested. However, further research is required using a range of Cu concentrations to clarify results gained in this study.

5.6.2 Pb test series

Exposure to Pb and pyrene individually and in mixtures altered the burrowing behaviour of *H diversicolor*. Burrowing rates from all Pb and Pb + pyrene conditions showed that they were significantly different from those of the control from the first day of exposure indicating a rapid effect of both Pb and pyrene (alone and in combination) on burrowing behaviour. Worms exposed to the Pb9.2 mg kg⁻¹ + Pyrene 970 µg kg⁻¹ mixture showed significantly faster burrowing rates than those exposed separately to Pb9.2 mg kg⁻¹ and Pyrene 970 µg kg⁻¹. The Σ mean worm tissue Pb concentrations slightly higher for the Pb + pyrene exposure group: Pb9.2 mg kg⁻¹ (47.09 ± 6.26 mg kg⁻¹); Pb9.2 mg kg⁻¹ + Pyrene 970 µg kg⁻¹ (49.99 ± 10.84 mg kg⁻¹). Whereas pyrene tissue concentrations for Pb9.2 mg kg⁻¹ and Pyrene 970 µg kg⁻¹ were similar (0.95, 1.05 µg kg⁻¹

respectively). As such, the higher levels of Pb in the Pb + pyrene exposed condition may indicate an antagonistic toxicity where the presence of pyrene increases Pb accumulation at these concentrations.

Worms exposed to Pb4.5 mg kg⁻¹ + Pyrene 480 µg kg⁻¹ showed slower burrowing rates than those of the individual Pb4.5 mg kg⁻¹ and Pyrene 480 µg kg⁻¹ condition. The Σ mean worm Pb tissue concentrations for individuals exposed to the Pb condition were significantly lower (20.73 ± 4.59 mg kg⁻¹) than those exposed to the Pb + pyrene mixture (30.51 ± 6.55 mg kg⁻¹). This may suggest that the higher tissue concentration of Pb found in the Pb + pyrene test group may have negatively influenced burrowing rates. Σ mean pyrene tissue concentrations for Pb4.5 mg kg⁻¹ + Pyrene 480 µg kg⁻¹ and Pyrene 480 µg kg⁻¹ were similar (0.57 and 0.70 µg kg⁻¹ respectively). However, Spearman's rank coefficient analysis performed on worm tissue concentrations and burrowing rates did not show significant correlations. Increased assimilation of metals in conjunction with pyrene exposure have been reported where Wang et al., (2011a) described higher tissue contents of cadmium in the clam *Ruditapes philippinarum* following mixed exposures. Similarly, Diaz- Jarmillo et al., (2017) demonstrate increased uptake of mercury in the polychaete *Perineris gualpensis* in the presence of pyrene, suggesting additive toxicity. Again, results from the present study may indicate an antagonistic toxicity for Pb and pyrene in combination at these concentrations where exposure to the mixture has increased the accumulation of Pb in the worms.

It is suggested that the differences of Pb tissue concentrations between individuals exposed to individual Pb groups: Pb9.2 mg kg⁻¹, Pb4.5 mg kg⁻¹ and those to mixtures: Pb9.2 mg kg⁻¹ + Pyrene970 µg kg⁻¹, Pb4.5 mg kg⁻¹ + Pyrene 480 µg kg⁻¹, may result from the inhibition of both Pb⁺ and Ca²⁺ uptake by Pb exposure, where voltage independent Pb uptake via the Ca²⁺ channel has been proposed as the cellular uptake route (Rogers and Wood, 2004). Moreover,

cellular concentrations of Pb^{2+} have been evidenced to inhibit uptake of Ca^{2+} and subsequently further Pb^{2+} uptake via ATPase pump inhibition (Brix et al., 2017; Carfagna et al., 1996) and blockade of voltage dependant calcium channels in neurons (Busselberg et al., 1994; Büsselberg et al., 1998; Sanah et al., 2012).

As previously described, the lipophilic nature of pyrene may result in cellular membrane damage as the molecules bind directly to the membrane leading to expansion and increased fluidity (Sikkema et al., 1995). Consequently, alterations to cellular ion regulation related to membrane bound ion transporters including P - ATPases (Gauthier et al., 2014; Li et al., 2011) have been observed resulting in reduced cellular Ca^{2+} uptake in human (Krieger et al., 1995), rats (Yang et al., 2017), fish (Xu et al., 2017) and marine invertebrate cells (Guojun et al., 2017).

However, increased membrane fluidity prescribed to the lipophilicity of PAH and cellular membrane affinity may also influence the electrical potential across the cell membrane (Sikkema et al., 1995). Alterations of the electrical potential may affect the regulation of ions (Na^+ , Ca^+ , K^+) consequently altering metal ion uptake via these cellular ion pathways following exposure to Pb (Kim et al., 2016).

As all worms from each test condition were placed into beakers which contained clean water and sediment, it is reasonable to assume that avoidance of contamination did not influence burrowing rates. Therefore, differences in burrowing rates between the test conditions indicate that mechanisms of toxicity may be of influence. Furthermore, the biological energetic costs of maintaining detoxification mechanisms may further influence burrowing rates as energy budgets are re-allocated to ensure survival.

5.6.3 AChE

AChE activity from all test conditions were significantly reduced from the control suggesting that both Pb and pyrene elicit a neurotoxic effect on *H diversicolor*. Inhibition of AChE is commonly used as a biomarkers of neurotoxicity, where inhibition of AChE occurs when xenobiotic inhibitors bind to the active site of the cholinesterase enzyme (Pereira et al., 2019). AChE activity for individuals exposed to both Pb conditions (Pb4.5 mg kg⁻¹, Pb9.2 mg kg⁻¹) were far higher than those in the Pb + pyrene and pyrene mixtures, further indicating that pyrene is a stronger neurotoxin than Pb.

Interestingly, burrowing times for those exposed to the Pb9.2 mg kg⁻¹ + Pyrene970 µg kg⁻¹ were faster than those from the Pb9.2 mg kg⁻¹ condition. Although AChE activity for the Pb9.2 mg kg⁻¹ was significantly higher than that of the Pb + pyrene mixture, other mechanisms of toxicity may have influenced burrowing rates. As such, these results may indicate an additive effect for Pb and pyrene exposure at this concentration.

Individuals from the Pb4.5 mg kg⁻¹ + Pyrene 480 µg kg⁻¹ condition had slower burrowing rates than those from the Pb4.5 mg kg⁻¹ condition. It may be supposed that the higher AChE activities of condition Pb4.5 mg kg⁻¹ positively influenced the burrowing rates against the Pb4.5 mg kg⁻¹ + Pyrene 480 µg kg⁻¹ condition.

Altered burrowing rates recorded in this study may be influenced by one or more modes of toxicity. AChE levels clearly varied from those of the control group for all test tanks. Therefore, it is reasonable to suggest neurotoxicity via the depletion of AChE as a primary influence. However, cellular membrane change following exposure to pyrene (Gauthier et al., 2014) and Ca⁺ homeostasis disturbance following Pb exposure (Sanah et al., 2012; Shafer, 2004; Viarengo and Nicotera, 1991) may further impact burrowing behaviour in this species related to the alteration of muscle contraction (Holmes et al., 1999). Competitive inhibition of Ca⁺ ion flow in muscle tissue has

been evidenced where Holmes et al., (1999) demonstrate that exposure of the Norway lobster *Nephrops norvegicus* to Co^{2+} and Mn^{2+} altered muscle contraction. Disturbance of Ca^{+} homeostasis following Pb exposure has also been recorded (Gerald et al., 1989; Meng et al., 2018) although, studies regarding effects of Pb induced voltage sensitive Ca^{+} channel alteration are few, but Busselberg et al., (1991) found neuron disruption in the marine sea hare *Aplysia californica*. It is suggested that further investigations are warranted regards the influence of Pb on Ca^{+} related cellular, neuro toxicity, muscle contraction and behavioural alterations.

Results obtained for this test series show that the use of burrowing behaviour in *H diversicolor* to assess exposure to environmental concentrations of Cu, Pb and pyrene is a sensitive, non- invasive mechanism to determine exposure effects. Importantly, these results indicate an interactive effects on toxicity to *H diversicolor* following exposure to Pb and pyrene, observed as increased tissue accumulation of Pb and negative influence of AChE activity. As such, alterations of locative behaviour in individuals which inhabit Cu, Pb and pyrene contaminated environments may have negative impacts upon the survival of populations related to increased predation rates. Indeed, Metais et al., (2019) described how reduced AChE activity and burrowing activity correspond to lower population densities and biomass in populations of *H diversicolor* resident in the multi polluted sediments of the Loire estuary, France. Moreover, reduced population size for key species such as *H diversicolor* results in a diminished food source for higher trophic levels, reduced detritivore activity and bioturbation of the sediment further increasing negative impacts.

The assessment of AChE may demonstrate the neurotoxic status of a contaminant. However, there were no correlations found between AChE activity and burrowing rates in the present study. As previously discussed, it is possible that the lower burrowing rates were a result of Ca^{+} competition and adverse effects on the neuromuscular

system. However, to fully understand the uptake pathways of pyrene, Cu, and Pb, further research is required regarding alterations to cell membrane potential, its influence on ion uptake and influence on neuromuscular contraction. Additionally, energy alterations, assimilation and excretion efficiencies and mechanisms of toxicity of individual and mixtures of Pb, Cu and pyrene are necessary to fully understand the biological influence of these exposures.

5.7 Conclusion

The use of burrowing behaviour in toxicological assessment using the marine polychaete *H diversicolor*, is a sensitive biomarker of the exposure to Cu, Pb and pyrene individually and within mixtures. All burrowing rates for worms exposed to these contaminants were significantly different from those obtained from the control group. Exposure to Pb and pyrene in combination appeared to have a more than additive toxicity observed as increased accumulation of Pb and reduced AChE activity. Determination of AChE activity provides information regarding the neurotoxic status of a contaminant of which, both Pb and pyrene showed AChE activity levels which were significantly suppressed than the control for the 7- day test period. However, AChE activity may not directly correlate to the alteration of locomotive behaviours in *H diversicolor*.

6. Bioaccumulation and biochemical responses of *H diversicolor* following exposure to Pb and pyrene.

6.1 Introduction

As both pyrene and Pb are naturally occurring chemicals, organisms have developed biochemical detoxification mechanisms, to reduce potential toxic effects following exposure. The biochemical detoxification of pyrene involves the oxidative metabolization by the cytochrome P450 enzymes through the introduction of a functional group (- OH, - COOH etc.) producing the product: 1 - hydroxypyrene (1 - OHP) (Gauthier et al., 2014; Giessing et al., 2003). Identification of 1 - OHP in humans by Jongeneelen (2001) has led to its use as a biomarker to assess pyrene exposure. Moreover, Geissing et al. (2003) identified 1 - OHP in the marine invertebrate *H diversicolor*, allowing this species to be used as a model invertebrate for pyrene exposure research. Following phase I metabolization, products are conjugated to further antioxidant molecules by enzymes such as the abundant glutathione - s - transferases (GSTs), resulting in detoxification and allowing ease of excretion (Guo et al., 2017). However, during Phase I metabolism, formation of quinones and reactive oxygen species (ROS) may stimulate further cellular antioxidants including superoxide dismutase (SOD), an essential antioxidant enzyme, which catalyse ROS and reduce cellular oxidative damage (Dai et al., 2018; Gauthier et al., 2014).

SOD's are considered pivotal in cellular defence against metal induced ROS (Kim et al., 2018). Bioaccumulation of metals may culminate in metal induced ROS: redox active metals such as Cu and Zn form hydroxyl radicals via Haber-Weiss and Fenton reactions (Gutteridge, 1983; Morcillo et al., 2016; Regoli and Giuliani, 2014); non redox metals such as Pb and Cd, associate to the thiol group of the antioxidant glutathione, leading to inactivation (Kim et al., 2018; Patrick, 2006) and the build-up of ROS that glutathiones would otherwise reduce. ROS formed during these processes are highly

reactive, initiating lipid peroxidation which may lead to membrane function change and cellular damage (Aboul-Ela et al., 2011).

Regulation of accumulated metals may include attempts to detoxify, excrete and store excess metals via the association to cysteine rich proteins such as metallothionein's (MT) and metallothionein like proteins (MTLP) (Amiard et al., 2006). Although the induction of metallothionein's in response to the uptake of essential metals (Berthet et al., 2003; Cooper et al., 2013; Mouneyrac et al., 2003; Rainbow P. S et al., 2007; Serafim and Bebianno, 2007) and non-essential metals (Bebianno et al., 1993; Choi et al., 2008; Serafim and Bebianno, 2010; Viarengo et al., 1987) are established, inconsistencies regarding induction of MT's upon Pb uptake exist. As Pb shares similar chemical properties to essential metals including Cu and Zn (Gabriel et al., 2010), displacement of essential metals from MTs by Pb may occur due to the decrease of metal affinity of MTs, which is in the order $Hg^{2+} > Cu^+ Ag^+, Bi^{3+} \gg Cd^{2+} > Pb^{2+} > Zn^{2+} > Co^{2+}$ (Amiard et al., 2006).

Yet, bioaccumulation of both Pb and pyrene may overwhelm these defence mechanisms leading to oxidative damage (Meng et al., 2018; Wang et al., 2016) amongst other toxic effects. Although DNA damage due to environmental stressors is common place, genetic lesions formed by exposure of the nucleotide base guanosine to ROS may lead to the formation of a DNA lesion 8 – hydroxy - 2' - deoxyguanosine (8 - OHdG) (Nebert and Dalton, 2006; Oliveira et al., 2010a). Absence of base repair may then result in mutagenicity, altered gene expression, strand misreading, cytostasis, chromosomal alteration and loss of heterozygosity (Evans et al., 2004; Nebert and Dalton, 2006).

Presently, environmental toxicology research is mainly focused on effects of individual contaminants (Ashauer, 2010; Gauthier et al., 2014). However, as contamination within the marine environment has been observed to contain mixtures of contaminants it is necessary to

understand the bioaccumulation, potential co toxicities and the biochemical responses elicited by contamination mixtures. The aim of this study will investigate the bioaccumulation and biochemical responses in *H diversicolor* following exposure to Pb and pyrene individually and in mixtures. This research will specifically determine the objectives;

- (1) Determine the extent of bioaccumulation and excretion of the individual and mixtures of Pb and pyrene
- (2) Investigate the biotransformation of pyrene to its phase 1 metabolite
- (3) Determine the effects of Pb and pyrene individually and in combination on the biochemical response following production of ROS by *H diversicolor*.

6.2 Materials and Methods

H diversicolor was be exposed to spiked sediment containing individual concentrations and mixtures of Pb and pyrene as fully described in Chapter 2 (2.6), over a period of 28 d. Initial concentrations of Pb and pyrene within sediment prior to the addition of worms and start of the experiment are detailed in Table 28. Sediment spiking and tank set up are fully described in Chapter 2 (2.6.1, 2.5.1 respectively). After the 28 d assimilation phase, remaining worms were then removed from treatment tanks and placed into tanks containing clean sediment and water for an eliminate phase where the elimination of assimilated contamination could be determined. Individuals from each tank were removed at intervals (1, 7, 14, 21 and 28 d for both assimilation and elimination). Worms were depurated for a period of 48 h in clean water following removal and frozen at - 20°C prior to analysis. Biomarkers of cellular, molecular and genotoxic stress were determined.

Table 28. Initial analysis of sediment following addition of manufactured sea water prior to the addition of worms. Sediment samples were taken from the surface 4 hours after the addition of sea water. Results are reported as mean values +/- 1 SE. Reduction of pyrene from initial spiked concentration may result from adherence to tank walls and aeration pipe prior to sampling.

Test condition	Result Pb (mg kg ⁻¹)	Result pyrene (µg kg ⁻¹)
Pb 9.2 µg kg ⁻¹	7.37 ± 1.4	-
Pb 4.5 µg kg ⁻¹	3.77 ± 0.36	-
Pb 9.2mg kg ⁻¹ + Pyrene 970 µg kg ⁻¹	12.34 ± 1.9	848.74 ± 27.05
Pb 4.5mg kg ⁻¹ + Pyrene 480 µg kg ⁻¹	6.44 ± 0.45	441.67 ± 18.77
Pyrene 970 µg kg ⁻¹	-	782.0 ± 36.1
Pyrene 480 µg kg ⁻¹	-	430.8 ± 7.61
Control Pb concentration	0.60 ± 0.08	-
Control Pyrene concentration	-	0.0 ± 0.0

6.2.1 Chemicals

Pyrene (98%), 1 - hydroxypyrene, acetone, acetonitrile, methanol, Pb chloride, dibasic potassium phosphate, monobasic potassium phosphate, ethylenediaminetetraacetic acid (EDTA), Tris-HCl, sodium cholate, formic and sulfuric acid, 1 - chloro - 2, 4 - dinitrobenzene, ethanol, chloroform, super oxide dismutase and 5, 5' - dithiobis - nitrobenzoic acid were purchased from Sigma Aldrich Ltd, Gillingham, Dorset, UK. Reduced glutathione was purchased from Thermo fisher Scientific Ltd, UK. All reagents were of analytical grade.

Super oxide dismutase (SOD) ELISA kit was purchased from Sigma Aldrich Ltd, Gillingham, Dorset, UK.

8 - hydroxy - 2' - deoxyguanosine ELISA kit was purchased from Catlag medsystems Ltd, Buckingham, UK.

6.2.2 Super Oxide Dismutase Activity

The superoxide anion (O_2^-) is catalysed into hydrogen peroxide and molecular oxygen via the enzyme superoxide dismutase. Reduction of superoxide anions are quantified using Dojindos's water soluble tetrazolium salt (WST – 1 (2(4 - Iodophenyl) – 3 -(4-nitrophenyl) – 5 - (2, 4-disulfophenyl) - 2H - tetrazolium, monosodium salt) which produces formazan dye (Peskin and Winterbourn, 2000). The rate of reduction with O_2^- is linearly related to xanthine oxidase activity and is inhibited by SOD (Peskin and Winterbourn, 2000).

SOD activity was conducted as per the instructions of the commercial ELISA kit. 1 ml of working solution was diluted using 19 ml of buffer solution. The enzyme working solution was centrifuged for 5 s and mixed by pipetting. 15 μ l of enzyme solution was then diluted using 2.5 ml of Dilution buffer. Calibration standards were formulated using sequential dilution of 200 U ml^{-1} concentrate to obtain solutions at 100 U ml^{-1} , 50 U ml^{-1} , 20 U ml^{-1} , 10 U ml^{-1} , 5 U ml^{-1} , 1 U ml^{-1} , 0.1 U ml^{-1} , 0.05 U ml^{-1} , 0.01 U ml^{-1} and 0.001 U ml^{-1} . A calibration curve was produced with $r^2 = < 0.96$.

6.2.3 Cytochrome p450 Activity

Cytochrome P450 activity was determined in accordance with the method described by Guengerich et al. (2009). 200 μ l of worm tissue homogenate was centrifuged at 9000 g for 30 min. 100 μ l of supernatant was then added to 2.0 ml of phosphate buffer (7.4 mM) containing 1.0 mM EDTA, 20% glycerol (vol / vol), 0.5 g sodium cholate (wt / vol) and non- ionic detergent in a test tube. The contents were mixed by capping the test tube with parafilm and inverting. The sample was divided into two cuvettes using a glass Pasteur pipette. The cuvettes were placed into the spectrophotometer and the baseline between 400 and 500 nm are recorded. The cuvettes were

removed from the spectrophotometer and placed into fume cupboard. Carbon dioxide was added to one sample at a rate of one bubble per second for 60 s (Carbon dioxide produced using 2 ml concentrated sulphuric acid and 1 ml of formic acid in flask containing stopper with side arm). Carbon dioxide gas added to cuvette via tubing and glass Pasteur pipette). 1 mg of sodium dithionite was added to each cuvette. Parafilm was attached to the tops of the cuvettes and inverted. Cuvettes were returned to spectrophotometer and spectrum of 400 – 500 nm recorded several times. When the peak near 450 nm failed to increase, the analysis was terminated. Calculations were based on absorbance at 420, 450 and 490 nm using Eq (7):

$$(\Delta A_{450} - \Delta A_{490}) / 0.091 = \text{nmol of P450 ml}^{-1} \quad (7).$$

6.2.4 Glutathione-S-Transferases Activity

Glutathione – s - transferases activity was measured following Mannervik (1969); 900 μl of phosphate buffer (100 mM, pH 6.5), 10 μl of 100 mM reduced glutathione and 10 μl of 100 mM 1 – chloro -2, 4 - dinitrobenzene, were mixed in a test tube. 900 μl of the solution mix was added to a plastic cuvette and incubated for 5 min at 30°C. 100 μl of tissue homogenate was added to the plastic cuvette and mixed by covering with parafilm and inverting. 900 μl of the solution mix and 100 μl of phosphate buffer were added to plastic cuvette to act as the blank. Absorbance was measured at 340 nm using a linear setting for 5 min. The linear portion of the reading was used to determine GSTs activity:

The $\Delta_{340} / \text{min}$ blank reading was subtracted from the $\Delta_{340} / \text{min}$ sample reading

GSTs activity – (sample reading $\Delta_{340} / \text{min}$) / 0.0096 $\mu\text{M}^{-1} / \text{cm}$) * (1.0 ml / 0.1 ml) * sample dilution = U / ml

6.2.5 8 - hydroxy - 2' - deoxyguanosine

8 - hydroxy - 2' - deoxyguanosine activity was conducted using a commercial ELISA kit (Catlag industries Ltd, UK). Worm tissue homogenate was centrifuged at 1000 g for 20 min. The supplied standard was reconstituted with 1.0 ml of standard diluent, then shaken gently. A triple dilution series was then performed obtained 5 serial dilution of 6000 pg ml⁻¹, 2000 pg ml⁻¹, 666.67 pg ml⁻¹, 222.22 pg ml⁻¹, 74.07 pg ml⁻¹ then using the standard diluent as a blank. 50 µl of worm homogenate was added to the well plate. 50 µl of detection reagent was added, then the plate was shaken, covered with a plate sealer and incubated for 1 h at 37°C. The solution was aspirated 3 times using wash solution and liquid removed from wells. 100 µl of detection reagent B was added to each well and then incubated for 30 min at 37°C. The wells were aspirated 5 times, then 90 µl of substrate solution added, followed by a further incubation period of 20 min at 37°C. Finally, 50 µl of stop solution was added and read at 450 nm immediately afterwards. Results were calculated using data from standard readings to produce a log - log graph allowing direct readings of sample results to be established.

6.2.6 Metallothionein activity

Metallothionein (MT) activity was conducted using the method described by Viarengo et al. (1997). 200 µl of worm tissue homogenate was centrifuged at 6000 × g for 10 min. Pellets were then washed with ethanol: chloroform: homogenization buffer (87:1:12). The supernatant was then centrifuged again at 6000 × g for 10 min. Resulting supernatant was then dried under a nitrogen gas stream to complete evaporation. The pellet was then placed in a solution of 300 µl of 5 mM Tris - HCl, 1 mM EDTA, pH 7. The resuspended metallothionein fraction then added to 4.2 ml of 0.43 mM 5, 5' - dithiobis (nitrobenzoic acid) in 0.2 M phosphate buffer, pH

8, and left for 30 min at room temperature. The concentration of reduced sulfhydryl was determined by reading the absorbance at 412 nm using a Varian Cary Win 50 probe UV - Vis spectrophotometer. A standard curve with GSH is required as a standard reference for correct quantification of MT in the samples. GSH contains one cysteine residue per molecule; thus, it is a standard for quantifying cysteines residue in protein analyses. Solutions were prepared with different concentrations of GSH and absorbance measured at 412 nm.

The amount of metallothionein in the samples as determined using the GSH standard as detailed by Viarengo et al. (1997).

6.3 Statistical analysis

All data were analysed as detailed in Chapter 2 (2.8). Data which failed to meet assumptions of parametric analysis was transformed using \log^{10} , square root or arcsine transformations. One - way ANOVA's were conducted on raw or transformed worm tissue contaminant concentrations to determine differences between exposures. Two - way ANOVA's were performed to identify differences between biochemical determinants used as the dependant variable with time and exposure used as independent variables. Spearman's correlations were performed on worm tissue concentrations and biochemical responses to identify relationships between groups.

6.4 Results

There were no significant mortalities observed for any condition for the duration of this experiment in any test condition including that of the control which therefore suggest that experimental conditions were suitable and that observed biological responses are below lethal levels for *H diversicolor*.

6.4.1 Sediment Pb concentration

Sediment samples (~15 g) were taken on the sample days throughout the duration of the experiment. Sediment was extracted from the surface of the tank using a glass beaker, placed into a labelled plastic bag and frozen at - 20°C until analysis. Pb concentrations found in sediment throughout the duration of the experiment are illustrated in Table 29.

Table 29. Pb concentrations found in sediment from all Pb test conditions for the duration of the experiment. Samples ($n = 3$) were extracted from the surface of the tank and are reported as mean values ± 1 SE.

Concentration Pb	Pb9.2 mg kg ⁻¹	Pb9.2 mg kg ⁻¹ + Pyrene970 µg kg ⁻¹	Pb4.5 mg kg ⁻¹	Pb4.5 mg kg ⁻¹ Pyrene480 µg kg ⁻¹	Control mg kg ⁻¹
SS1	4.82±1.83	13.69±2.68	2.88±0.15	2.81±1.55	0.92±0.11
SS7	6.52±0.27	14.46±0.20	3.14±0.51	5.71±0.52	0.75±0.16
SS14	8.63±0.07	13.01±0.55	3.66±0.33	6.28±0.38	0.67±0.11
SS21	10.52±0.60	15.39±0.13	3.87±1.65	9.52±1.44	1.09±0.09
SS28	8.53±0.39	11.76±0.30	3.97±0.39	9.87±0.33	1.00±0.04
CS1	1.07±0.09	1.02±0.06	1.94±0.12	0.93±0.15	0.96±0.06
CS7	1.63±0.15	0.96±0.08	0.72±0.11	1.30±0.21	0.64±0.11
CS14	1.08±0.09	1.13±0.05	1.47±0.98	0.56±0.12	0.78±0.12
CS21	0.76±0.07	0.94±0.07	0.53±0.02	0.63±0.09	1.02±0.12
CS28	1.17±0.18	0.96±0.17	0.44±0.04	0.78±0.09	0.85±0.08

6.4.2 Pyrene sediment results

Sediment was extracted from each spiked tank on each sample day for the duration of the experiment. Sediment was sampled using a glass beaker (~15 g) which was then placed into a pre-formed bag made from commercially available aluminium tin foil. The foil bag was then placed into a labelled plastic sample bag and frozen at - 20°C until analysis. Results for pyrene concentrations for all spiked conditions are shown in Table 30.

Table 30. Pyrene concentrations in sediment from all test conditions throughout the duration of the experiment. Concentrations ($\mu\text{g kg}^{-1}$) are from samples ($n = 3$) extracted at a depth of ~ 3 cm using a glass beaker. Spiked sediment accumulation phase and clean sediment elimination phase are denoted by SS and CS respectively. Results are mean values ± 1 SE.

Sample Day	Pb9.2mg kg^{-1} + Pyrene970 $\mu\text{g kg}^{-1}$	Pyrene970 $\mu\text{g kg}^{-1}$	Pb4.5 mg kg^{-1} + Pyrene480 $\mu\text{g kg}^{-1}$	Pyrene480 $\mu\text{g kg}^{-1}$	Control $\mu\text{g kg}^{-1}$
SS1	11.4 \pm 3.9	3.8 \pm 1.2	14.0 \pm 4.2	45.0 \pm 3.8	0.0 \pm 0.0
SS7	2.7 \pm 1.1	1.4 \pm 0.05	4.4 \pm 0.9	2.0 \pm 0.03	0.0 \pm 0.0
SS14	0.5 \pm 0.05	0.0 \pm 0.0	1.0 \pm 0.02	1.0 \pm 0.0	0.0 \pm 0.0
SS21	0.1 \pm 0.03	0.0 \pm 0.0	0.0 \pm 0.0	0.0 \pm 0.0	0.0 \pm 0.0
SS28	0.0 \pm 0.0	0.0 \pm 0.0	0.0 \pm 0.0	0.0 \pm 0.0	0.0 \pm 0.0
CS1	0.0 \pm 0.0	0.0 \pm 0.0	0.0 \pm 0.0	0.0 \pm 0.0	0.0 \pm 0.0
CS7	0.0 \pm 0.0	0.0 \pm 0.0	0.0 \pm 0.0	0.0 \pm 0.0	0.0 \pm 0.0
CS14	0.0 \pm 0.0	0.0 \pm 0.0	0.0 \pm 0.0	0.0 \pm 0.0	0.0 \pm 0.0
CS21	0.0 \pm 0.0	0.0 \pm 0.0	0.0 \pm 0.0	0.0 \pm 0.0	0.0 \pm 0.0
CS28	0.0 \pm 0.0	0.0 \pm 0.0	0.0 \pm 0.0	0.0 \pm 0.0	0.0 \pm 0.0

6.4.3 Worm Tissue Pb concentration Results

Concentrations for the worm tissue from test condition Pb9.2 mg kg^{-1} and Pb9.2 mg kg^{-1} + Pyrene970 $\mu\text{g kg}^{-1}$ are illustrated in Figure 32.

Two - way ANOVA's showed that there were significant differences between Pb concentrations of worm tissue for each exposure group during the 28 d assimilation ($F_{(1,27)} = 46.8$, $p = <0.01$) and elimination phases ($F_{(1, 27)} = 46.8$, $p = <0.01$). Additionally, the interaction between time (days) and assimilation showed significant differences between the exposure groups during the assimilation ($F_{(1, 27)} = 5.42$, $p = 0.03$) and elimination phases ($F_{(1, 27)} = 5.52$, $p = 0.02$).

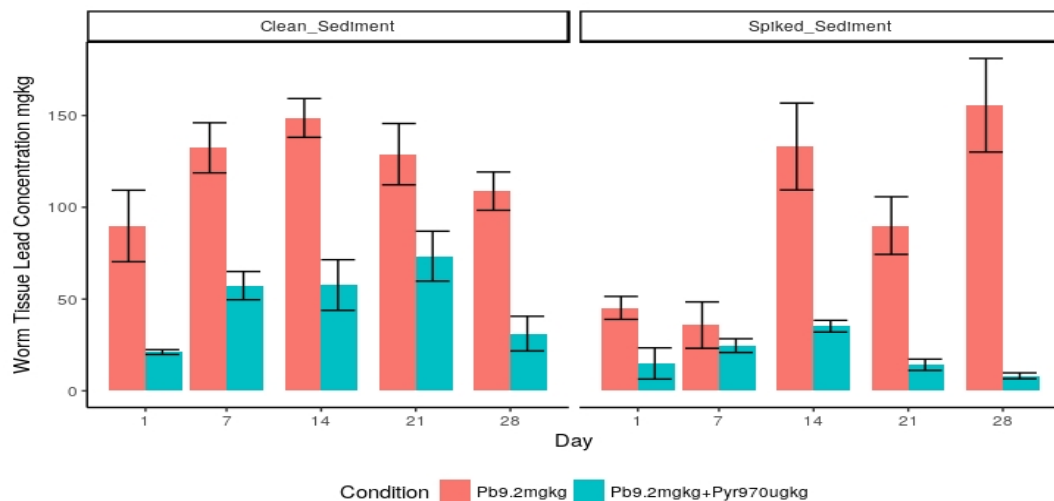


Figure 32. Mean worm tissue Pb concentrations; Pb9.2 mg kg⁻¹ and Pb9.2 mg kg⁻¹ + Pyrene 970 µg kg⁻¹. Error bars indicate the \pm 1SE of samples ($n = 3$).

Worm tissue Pb concentrations for test condition Pb9.2 mg kg⁻¹ showed initial uptake concentration of 45.13 and 35.7 mg kg⁻¹ for days 1 - 7 respectively. A rapid uptake at day 14 (133.1 mg kg⁻¹) was followed by a decrease at day 21 (90.02 mg kg⁻¹), then a further increase at day 28 (155.57 mg kg⁻¹). During the elimination phase, worm tissue concentrations decreased initially at day 1 (89.79 mg kg⁻¹) however, this was followed by a further increase to 132.38 mg kg⁻¹ at day 7. Concentrations increased further at day 14 (148.64 mg kg⁻¹), followed by further reductions to 128.92 and 108.78 mg kg⁻¹ at days 21 and 28 respectively. Σ worm tissue concentrations for Pb9.2 mg kg⁻¹ for the 28 d assimilation period was 459.6 mg kg⁻¹ whilst Σ worm tissue for the elimination period was 608.51 mg kg⁻¹.

Worm tissue Pb concentrations for condition Pb9.2 mg kg⁻¹ + Pyrene 970µg kg⁻¹ were far lower than those of Pb9.2 mg kg⁻¹ throughout the duration of the experiment.

The initial uptake at day 1 (15.38 mg kg⁻¹) was 34% lower than that of the Pb only condition. Concentrations remained between 8.19 - 35.02 mg kg⁻¹ during the following 7 - 28 d period. During the elimination period concentrations increased from those in the acclimation period where results ranged between 21.11 mg kg⁻¹ on day 1 to the highest concentration of 73.35 mg kg⁻¹ on day 21.

Results on day 28 showed a lower level of 31.17 mg kg⁻¹ at day 28. Σ worm tissue concentration for the assimilation period was 97.13 mg kg⁻¹ whereas Σ worm tissue content for the elimination period was 240.57 mg kg⁻¹

Pb worm tissue concentrations for test conditions Pb4.5 mg kg⁻¹ and Pb4.5 mg kg⁻¹ and Pyrene 480 μ g kg⁻¹ are illustrated in Figure 33. A two- way ANOVA revealed significant differences for each exposure group during the the 28 d assimilation phase ($F_{(1,27)} = 11.7, p = <0.01$) and the 28 d elimination phase ($F_{(1,27)} = 33.0, p = <0.01$). Additionally, significant results were identified for the interaction of time (days) on assimilation ($F_{(1, 27)} = 38.5, p = <0.01$) and elimination ($F_{(1, 27)} = 27.1, p = 0.01$) for all exposure groups.

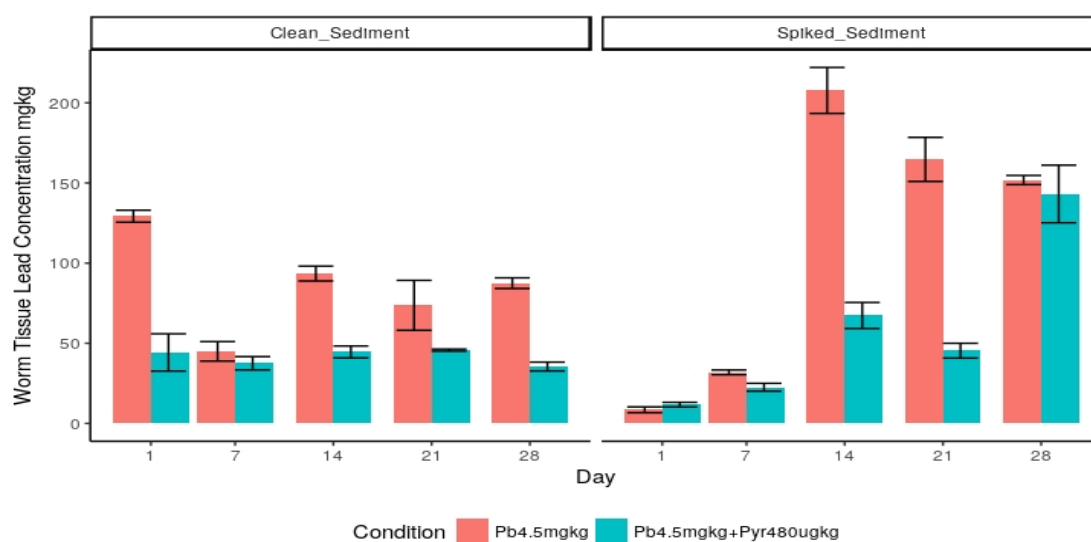


Figure 33. Mean worm tissue Pb concentrations; Pb4.5 mg kg⁻¹ and Pb4.5 mg kg⁻¹+Pyrene 480 μ g kg⁻¹. Error bars indicate the ± 1 SE of sample ($n = 3$)

Worm tissue Pb concentration of the test condition Pb4.5 mg kg⁻¹ showed initial levels of 8.52 mg kg⁻¹ on day 1 followed by a rapid accumulation to 207.72 mg kg⁻¹ on day 14. Concentrations then reduced (164.69, 151.81 mg kg⁻¹ on days 21 and 28 respectively). Concentration during the elimination phase showed a general decreasing trend from 129.28 mg kg⁻¹ on day 1 to 87.50 mg kg⁻¹ on day 28. The Σ worm tissue content during the assimilation period

was 564.59 mg kg⁻¹ with the elimination period showing a decrease at Σ 428.94 mg kg⁻¹.

Pb tissue concentrations for test condition Pb4.5 mg kg⁻¹ + pyrene 480 μ g kg⁻¹ showed overall lower levels than those of the Pb only condition. Initial uptake of 11.72 mg kg⁻¹ on day 1 was followed by a general increasing trend resulting in 143.12 mg kg⁻¹ on day 28. A rapid decrease to 44.29 mg kg⁻¹ during day 1 of the elimination phase was followed by relatively stable concentrations (37.53, 44.59, 45.74, 35.51 mg kg⁻¹) for the duration of the 28 d period. Σ Pb worm tissue concentrations for the assimilation period was 209.17 mg kg⁻¹ with lower Σ concentrations of 207.65 mg kg⁻¹ during the elimination period.

6.4.4 Worm Tissue Pyrene and 1-Hydroxypyrene metabolite concentrations

Pyrene and its phase 1 metabolite 1 - OHP concentrations found in worm tissue for the test conditions Pb9.2 mg kg⁻¹ + Pyrene 970 μ g kg⁻¹ and Pb4.5 mg kg⁻¹ + Pyrene 480 μ g kg⁻¹ are illustrated in Figures 34 and 35.

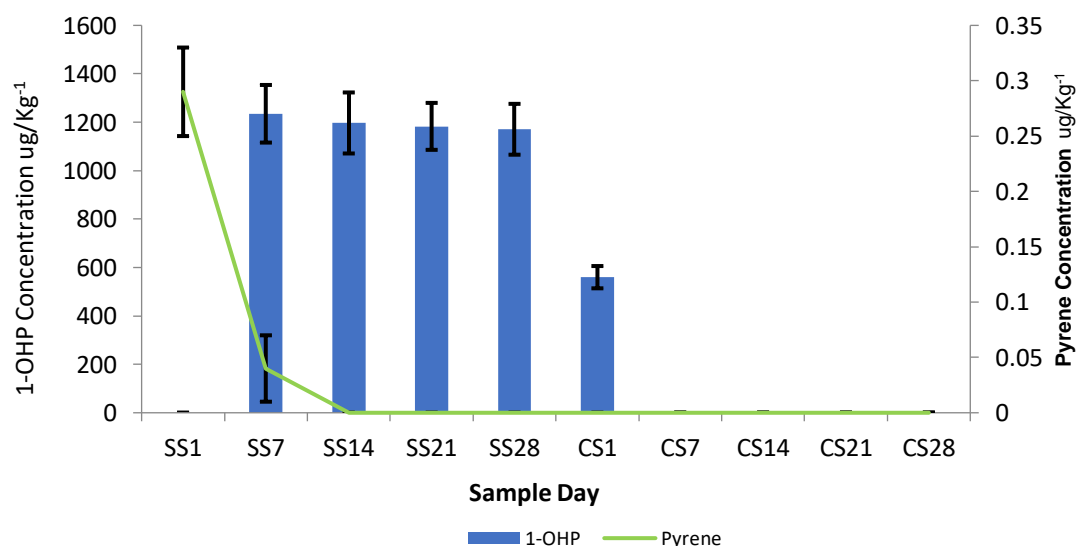


Figure 34. Pyrene and 1-OHP(μ g kg⁻¹) concentrations found in worm tissue ($n = 3$) from test conditions Pb4.5 mg kg⁻¹ + Pyrene 480 μ g kg⁻¹. Error bars show the ± 1 SE. SS denotes spiked sediment 28 d assimilation period whereas CS denotes clean sediment elimination period.

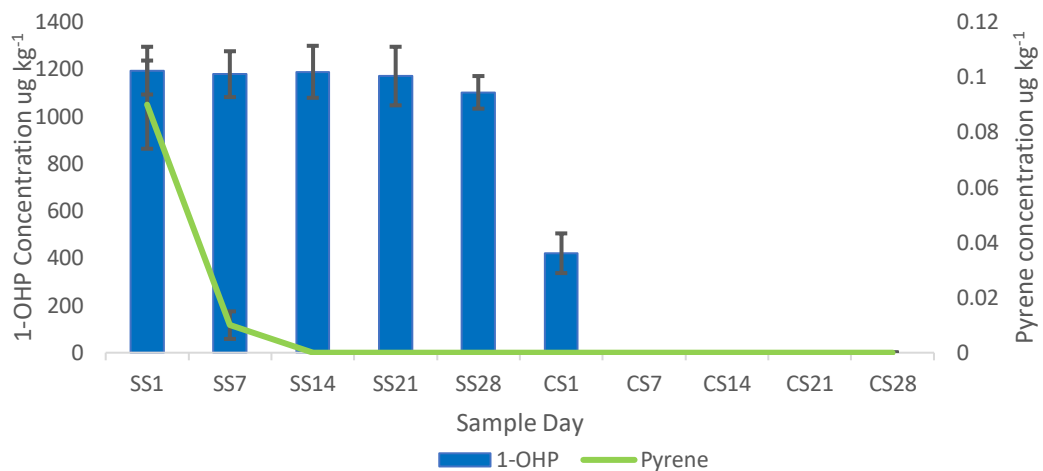


Figure 35. Pyrene and 1 - OHP concentrations found in worm tissue ($n = 3$) from test conditions $\text{Pb}9.2 \text{ mg kg}^{-1} + \text{Pyrene } 970 \text{ } \mu\text{g kg}^{-1}$. Error bars show the $\pm 1\text{SE}$. SS denotes spiked sediment 28 d assimilation period whereas CS denotes clean sediment elimination period

Pyrene concentrations in worm tissue for test condition $\text{Pb}9.2 \text{ mg kg}^{-1} + \text{Pyrene } 970 \text{ } \mu\text{g kg}^{-1}$ show an assimilation at day 1 of $0.29 \text{ } \mu\text{g kg}^{-1}$ which decreased to $0.04 \text{ } \mu\text{g kg}^{-1}$ at day 7. Tissue values for time period up to 28 d were below the limits of detection ($< 0.25 \text{ ng kg}^{-1}$). Concentrations of 1 - OHP of $1194 \text{ } \mu\text{g kg}^{-1}$ were recorded at day 1. Following concentrations show a general decreasing trend (1179 , 1189 , 1171 , $1102 \text{ } \mu\text{g kg}^{-1}$) found for days 7,14, 21 and 28 respectively. Tissues concentrations of $421 \text{ } \mu\text{g kg}^{-1}$ were found at day 1 of the elimination period however, concentrations were below detectable limits for the remaining test period ($< 0.25 \text{ ng kg}^{-1}$).

Pyrene tissue concentrations for test condition $\text{Pb}4.5 \text{ mg kg}^{-1} + \text{Pyrene } 480 \text{ } \mu\text{g kg}^{-1}$ showed initial values of $0.09 \text{ } \mu\text{g kg}^{-1}$ at day 1 reducing to $0.01 \text{ } \mu\text{g kg}^{-1}$ at day 7. Pyrene concentrations for the remainder of the experiment were below the limits of detection ($< 0.25 \text{ ng kg}^{-1}$). There were no concentrations recorded at day 1 for 1 - OHP tissue concentrations followed by $1235 \text{ } \mu\text{g kg}^{-1}$ at day 7. The levels showed a general decline (1197 , 1183 and $1171 \text{ } \mu\text{g kg}^{-1}$) for days 14, 21, and 28 respectively. 1 - OHP concentrations of $560 \text{ } \mu\text{g kg}^{-1}$ were found in worm tissue on day 1 of the elimination period

however, concentrations were below the limits of detection ($< 0.25 \text{ ng kg}^{-1}$) for the remainder of the elimination period.

Pyrene and 1 - OHP worm tissue concentrations from the test conditions Pyrene $480 \text{ } \mu\text{g kg}^{-1}$ and Pyrene $970 \text{ } \mu\text{g kg}^{-1}$ are illustrated in Figures 36 and 37.

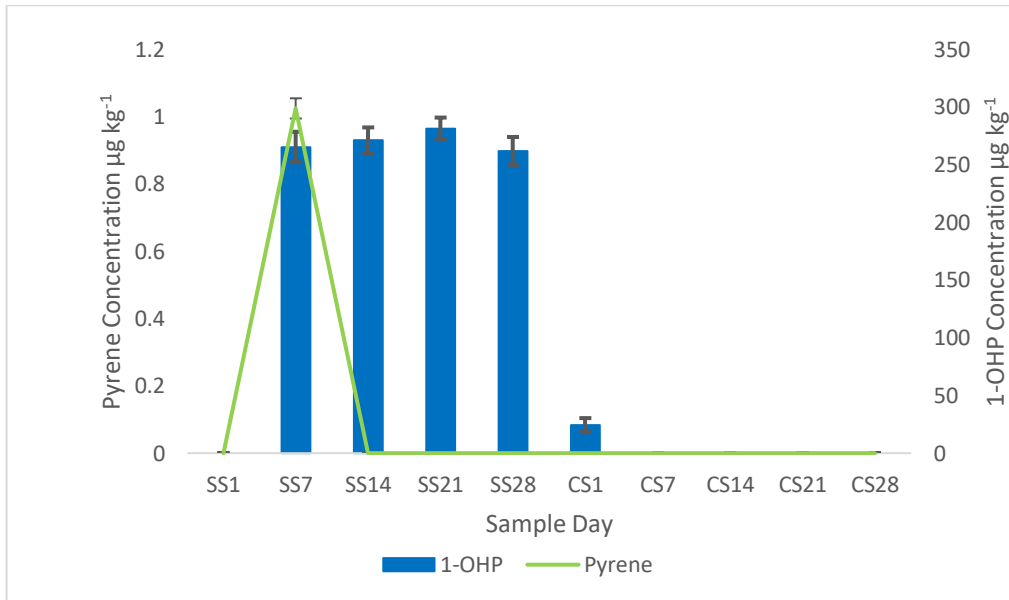


Figure 36. Pyrene and 1 - OHP concentrations found in worm tissue ($n = 3$) from test condition Pyrene $480 \text{ } \mu\text{g kg}^{-1}$. Error bars show the $\pm 1 \text{ SE}$. SS denotes spiked sediment 28 d assimilation period whereas CS denotes clean sediment elimination period

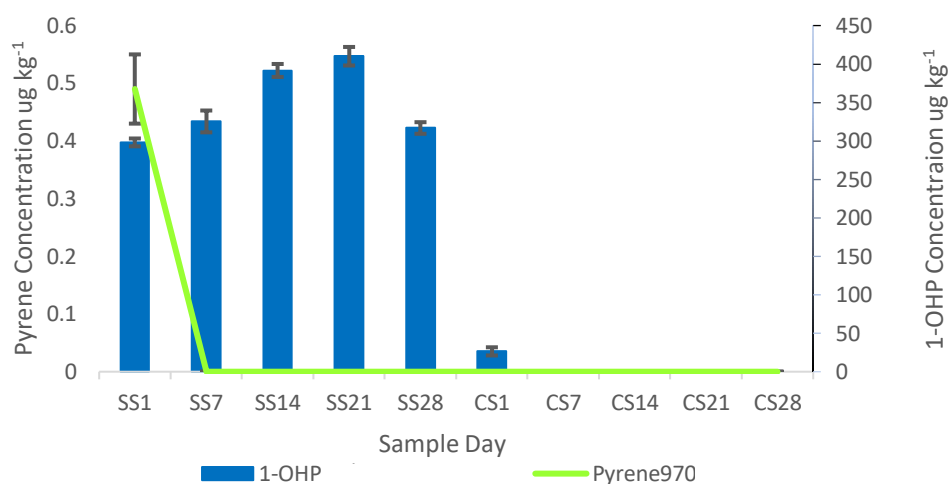


Figure 37. Pyrene and 1-OHP concentrations found in worm tissue ($n = 3$) from test condition Pyrene 970 $\mu\text{g kg}^{-1}$. Error bars show the ± 1 SE. SS denotes spiked sediment 28 d assimilation period whereas CS denotes clean sediment elimination period

Worm tissue pyrene concentrations for test condition Pyrene 480 $\mu\text{g kg}^{-1}$ showed no concentration at sample day SS1 and levels of 1.025 $\mu\text{g kg}^{-1}$ at day SS7. There were no further concentrations detected for the remainder of the test period. 1 - OHP concentrations were detected at sample day SS7 (265.5 $\mu\text{g kg}^{-1}$) and showed a slight increase during days SS14 (271.4 $\mu\text{g kg}^{-1}$) and day SS21 (281.6 $\mu\text{g kg}^{-1}$) followed by a decrease to 262.11 $\mu\text{g kg}^{-1}$ at day SS28. During the elimination phase, 1 - OHP was only detected at day 1 (CS29) of 24.31 $\mu\text{g kg}^{-1}$.

Test condition Pyrene 970 $\mu\text{g kg}^{-1}$ showed a lower worm tissue pyrene concentration of 0.49 $\mu\text{g kg}^{-1}$ for individuals sampled on day SS1. There were no further pyrene concentrations detected for the balance of the test series. 1 - OHP tissue concentrations showed an initial value of 298.1 $\mu\text{g kg}^{-1}$ at day SS1 increasing to 410.13 $\mu\text{g kg}^{-1}$ at day SS21. Concentrations then decreased from (316.84 $\mu\text{g kg}^{-1}$) at day SS28 to 26.43 $\mu\text{g kg}^{-1}$ at day CS1 (elimination day 1), with no further 1-OHP concentrations detected in worm tissue for the remainder of the test condition.

6.4.5 Biochemical responses

6.4.5.1 Metallothionein

MT's were not detected in worm tissue samples from all Pb exposed conditions.

6.4.5.2 SOD Activity

Total SOD activity in response to Pb9.2 mg kg⁻¹, Pyrene970 µg kg⁻¹ and the mixture Pb9.2 mg kg⁻¹ + Pyrene970 µg kg⁻¹ exposure for all test conditions show elevated SOD activity in comparison with the control group (Figure 38).

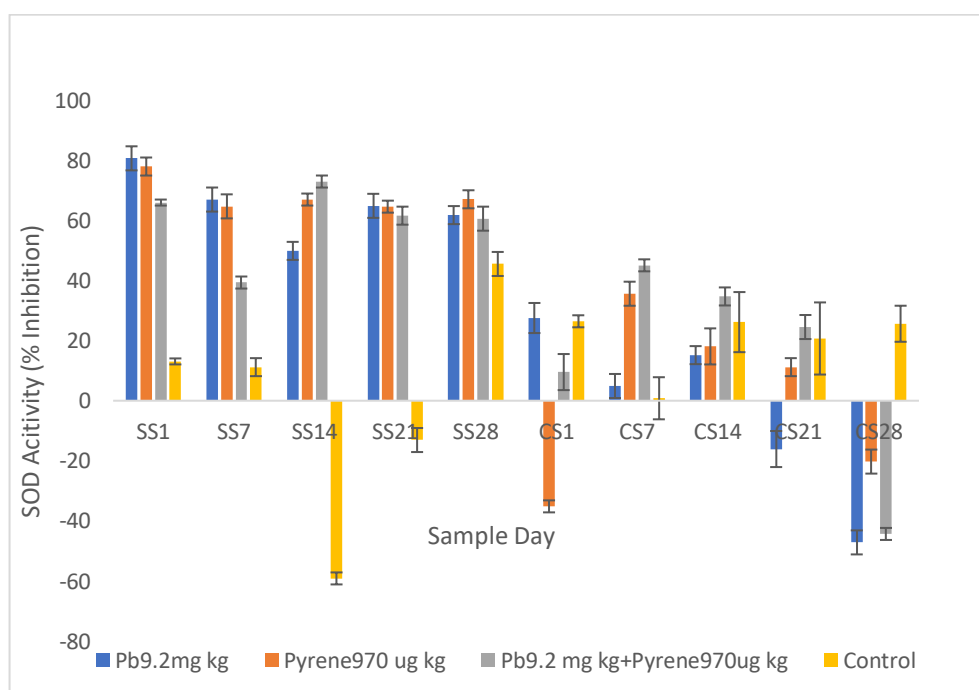


Figure 38. SOD activity expressed as 50% inhibition of SOD for the test conditions Pb9.2 mg kg⁻¹, Pyrene970 µg kg⁻¹, and Pb9.2 mg kg⁻¹ + Pyrene970 µg kg⁻¹. SS relates to Spiked Sediment phase, CS related to Clean Sediment phase. All values are means \pm 1 SE.

A two - way ANOVA revealed significant differences between all exposure groups during the assimilation phase ($F_{(3, 52)} = 40.9$, $p = 0.01$). However, significant differences were not identified for the interaction of time (days) and exposure group ($F_{(1, 52)} = 1.05$, $p = 0.38$).

A two – way ANOVA also revealed significant differences for all exposure groups during the elimination phase ($F_{(3, 52)} = 3.67$, $p = <0.01$). Furthermore, the interaction of time (days) on the elimination phase also identified significant results ($F_{(1, 52)} = 6.02$, $p = <0.01$).

Results demonstrate that although SOD activities were significantly different for all exposure groups during the assimilation and elimination phases, the interaction of time was significant only during the elimination phase.

Levels of SOD activity were far higher (Pb9.2 mg kg⁻¹: 38-67%, Pyrene970 µg kg⁻¹: 53-64%, Pb9.2 mg kg⁻¹ + Pyrene970 µg kg⁻¹ :28-61%) than those of the control for all conditions during the 28 d assimilation period (SS1-SS28). However, all activities for each test condition decreased during the 28 d excretion period (CS1 - CS28). Pb9.2 mg kg⁻¹ activity decreased during CS1 to 27% and further declined during sample day CS7 (5%). Followed by an increase to 15% during sample day CS14. Levels then dropped below zero for days CS21 and CS28 (-16, -47%) which were 27 - 58% lower than those of the control.

Levels for Pyrene970 µg kg⁻¹ decreased from 67% on sample day SS28 to below zero (-35%) for sample day CS1 followed by an increase to 35% on sample day CS7. Levels for the remainder of the test period were lower than those of the control (CS14:18%, CS21: 11%, CS28:-20%). SOD activity for Pb9.2 mg kg⁻¹ + Pyrene970 µg kg⁻¹ also decreased from 77% on sample day SS28 to 14% on sample day CS1 however, levels then increased (CS7:64%, CS14:71%, CS21:83%) until sample day CS28 where levels fell to 0.9%.

Mean values ranged during the assimilation: Pb9.2 mg kg⁻¹ (-3.1 + / - 26.2%); Pyrene970 µg kg⁻¹ (68.2 + / - 5.0%); Pb9.2 mg kg⁻¹ + Pyrene970 µg kg⁻¹ (60.1 + / - 11%); Control (-0.5 + / - 34.7%) and elimination phases: Pb9.2 mg kg⁻¹ (-3.1 + / - 26.2%); Pyrene970 µg

kg⁻¹ (1.88 + / - 25.8%); Pb9.2 mg kg⁻¹ + Pyrene970 µg kg⁻¹ (13.9 + / - 31.4%); Control (19.9 + / - 9.8%).

SOD activity levels for worms exposed to Pb4.5 mg kg⁻¹, Pyrene480 µg kg⁻¹ and the mixture Pb4.5 mg kg⁻¹ + Pyrene480 µg kg⁻¹ were all significantly higher (50 - 58, 43 - 65, 66 - 110% respectively) than those of the control during the 28 d assimilation period as shown in Figure 39.

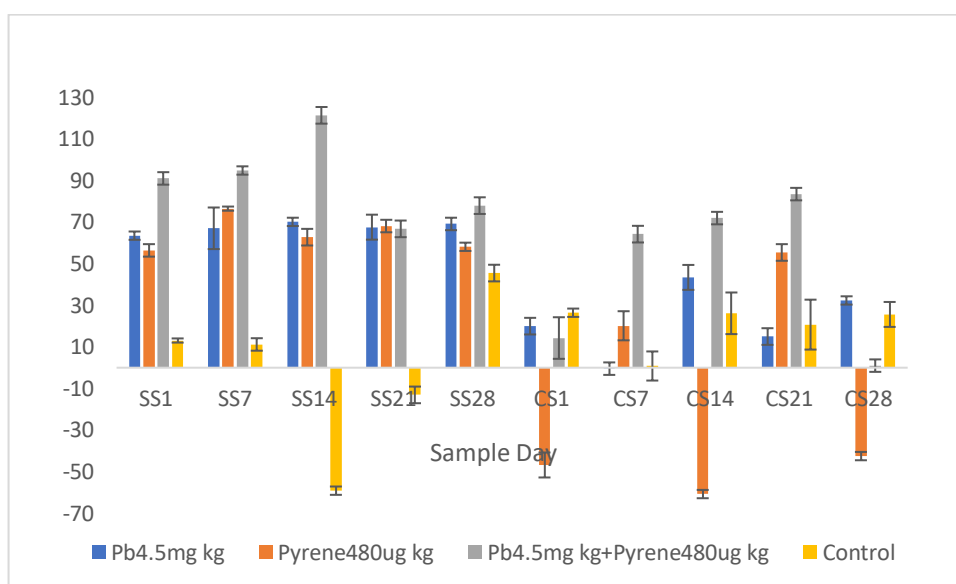


Figure 39. SOD activity expressed as 50% inhibition of SOD for the test conditions Pb4.5 mg kg⁻¹, Pyrene480 µg kg⁻¹, and Pb4.5 mg kg⁻¹ + Pyrene480 µg kg⁻¹. SS relates to Spiked Sediment phase, CS related to Clean Sediment phase. All values are means \pm 1 SE.

Statistical analysis using two - way ANOVA of all exposure groups showed that they were significantly different during the assimilation phase ($F_{(3,52)} = 48.5$, $p = < 0.01$). However, the interaction of time (days) and exposure group did not identify significant results for SOD activity ($F_{(1,52)} = 0.54$, $p = 0.66$).

A two - way ANOVA also revealed significant differences during the elimination phase for all exposure groups ($F_{(3,52)} = 18.0$, $p = < 0.01$). However, significant differences were not identified for the interaction of time (days) and exposure ($F_{(1,52)} = 0.26$, $p = 0.85$) during the

elimination phase. Results indicate that although SOD levels were significantly different between all exposure groups during the assimilation and elimination phases, there was no significant interaction between time and SOD levels.

Activities for test condition Pb4.5 mg kg⁻¹ showed a rapid decrease from 69% during sample day SS28 to 19% for sample day CS1. Levels decreased further to -0.4% during sample day CS7 followed by an increase to 43% on sample day CS14. Levels then dropped to below those of the control (Control: CS21:20%, Pb4.5 mg kg⁻¹: CS21:14%) followed by an increase to 32%.

SOD activity levels for Pyrene480 µg kg⁻¹ decreased from 58% on sample day SS28 to -46% on sample day CS1. Levels then increased to 20% (CS7) followed by a further decline to -60% on sample day CS14. Fluctuations then continued with an increase to 55% (CS21) followed by a decrease, lower than that of the control to -44% (CS28).

Levels of SOD activity for the mixture Pb4.5 mg kg⁻¹ + Pyrene480 µg kg⁻¹ decreased to 14% on sample day (CS1) from 77% on sample day SS28. Levels showed a general increase during sample days CS7 (64%), CS14 (71%) and CS21 (83%) followed by a rapid decrease to 0.9% on sample day CS28.

Mean concentration varied during the assimilation: Pb4.5 mg kg⁻¹ (67.5 + / - 2.3%); Pyrene480 µg kg⁻¹ (64.4 + / - 7.3); Pb4.5 mg kg⁻¹ + Pyrene480 µg kg⁻¹ (90.4 + / - 18.4%); Control (0.5 + / - 34.7%), and elimination phase: Pb4.5 mg kg⁻¹ (22.1 + / - 14.9%); Pyrene480 µg kg⁻¹ (-14.9 + / - 44.8%); Pb4.5 mg kg⁻¹ + Pyrene480 µg kg⁻¹ (46.9 + / - 32.9%); Control (19.9 + / - 9.9%).

6.4.5.3 GSTs Activity

Glutathione activity for test conditions Pb9.2 mg kg⁻¹, Pyrene970 µg kg⁻¹ and the mixture Pb9.2 mg kg⁻¹ + Pyrene 970 µg kg⁻¹ showed that

all exposure groups were significantly different during the 28 d assimilation phase when analysed using a two - way ANOVA, ($F_{(3, 52)} = 10.27, p = < 0.01$). Additionally, significant differences were identified for the interaction of time (days) and GSTs levels during the assimilation phase for all exposure groups ($F_{(1, 52)} = 5.50, p = < 0.01$).

A two – way ANOVA for exposure groups during the 28 d elimination phase also revealed significant differences ($F_{(3, 52)} = 7.26, p = < 0.01$). Additionally, the interaction of time (days) and exposure group on GST levels during the elimination phase identified significant results ($F_{(1, 52)} = 4.80, p = < 0.01$). Results show that GSTs levels for all exposure groups were significantly different, observed for the duration of the experiment. This may indicate that exposure to Pb and pyrene, individually and in combination, elicits an immediate and more ominously, continued elevation of GSTs levels post exposure.

Elevated GSTs levels were demonstrated for all test conditions against the control group up to sample day CS7 as shown in Figure 40.

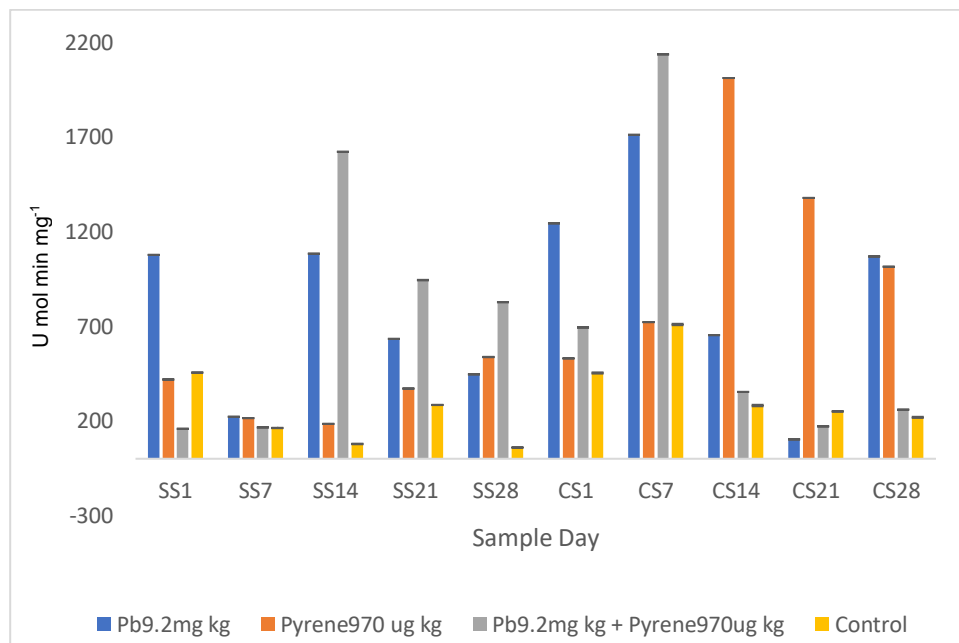


Figure 40. GSTs Activity (U mol min mg⁻¹) of worms ($n = 3$) from test conditions Pb9.2mg kg⁻¹, Pyrene 970µg kg⁻¹, Pb9.2mg kg⁻¹ + Pyrene 970 µg kg⁻¹ and control. SS relates to Spiked Sediment phase, CS related to Clean Sediment phase Concentrations are mean values \pm 1SE.

Levels for the mixture $\text{Pb}9.2 \text{ mg kg}^{-1} + \text{Pyrene}970 \text{ } \mu\text{g kg}^{-1}$ ($646 \text{ U mol min mg}^{-1}$) showed a slight decrease against the control ($709 \text{ U mol min mg}^{-1}$) on sample day CS7 whereas levels for $\text{Pb}9.2 \text{ mg kg}^{-1}$ ($1711 \text{ U mol min mg}^{-1}$) and $\text{Pyrene}970 \text{ } \mu\text{g kg}^{-1}$ ($1724 \text{ U mol min mg}^{-1}$) remained elevated. Levels for sample day CS14 for $\text{Pb}9.2 \text{ mg kg}^{-1}$: $653 \text{ U mol min mg}^{-1}$ and $\text{Pyrene}970 \text{ } \mu\text{g kg}^{-1}$: $108 \text{ U mol min mg}^{-1}$ showed a rapid decrease which continued on sample day CS21 ($\text{Pb}9.2 \text{ mg kg}^{-1}$: 102 , $\text{Pyrene}970 \text{ } \mu\text{g kg}^{-1}$: $108 \text{ U mol min mg}^{-1}$) whereas the mixture $\text{Pb}9.2 \text{ mg kg}^{-1} + \text{Pyrene}970 \text{ } \mu\text{g kg}^{-1}$ ($505 \text{ U mol min mg}^{-1}$) remained elevated against the control ($250 \text{ U mol min mg}^{-1}$). Levels for all conditions then showed a rapid increase during sample day CS28 ($\text{Pb}9.2 \text{ mg kg}^{-1}$: $1068 \text{ U mol min mg}^{-1}$, $\text{Pyrene}970 \text{ } \mu\text{g kg}^{-1}$: $1050 \text{ U mol min mg}^{-1}$, $\text{Pb}9.2 \text{ mg kg}^{-1} + \text{Pyrene}970 \text{ } \mu\text{g kg}^{-1}$: $1096 \text{ U mol min mg}^{-1}$) against the Control ($218 \text{ U mol min mg}^{-1}$).

Mean concentrations varied during the assimilation: $\text{Pb}9.22 \text{ mg kg}^{-1}$ ($694.13 + / - 373.93 \text{ U mol min mg}^{-1}$); $\text{Pyrene}970 \text{ } \mu\text{g kg}^{-1}$ ($375.75 + / - 138.17 \text{ U mol min mg}^{-1}$); $\text{Pb}9.2 \text{ mg kg}^{-1} + \text{Pyrene}970 \text{ } \mu\text{g kg}^{-1}$ ($734.76 + / - 500.96 \text{ U mol min mg}^{-1}$); Control ($249.59 + / - 152.99 \text{ U mol min mg}^{-1}$) and elimination phases : $\text{Pb}9.22 \text{ mg kg}^{-1}$ ($956.74 + / - 545.67 \text{ U mol min mg}^{-1}$); $\text{Pyrene}970 \text{ } \mu\text{g kg}^{-1}$ ($1131.31 + / - 525.85 \text{ U mol min mg}^{-1}$); $\text{Pb}9.2 \text{ mg kg}^{-1} + \text{Pyrene}970 \text{ } \mu\text{g kg}^{-1}$ ($722.54 + / - 728.16 \text{ U mol min mg}^{-1}$); Control ($348.75 + / - 175.59 \text{ U mol min mg}^{-1}$).

GSTs activity levels for the test conditions $\text{Pb}4.5 \text{ mg kg}^{-1}$, $\text{Pyrene}480 \text{ } \mu\text{g kg}^{-1}$, and the mixture $\text{Pb}4.5 \text{ mg kg}^{-1} + \text{Pyrene}970 \text{ } \mu\text{g kg}^{-1}$ illustrated in Figure 41 generally, elevated concentrations against the control.

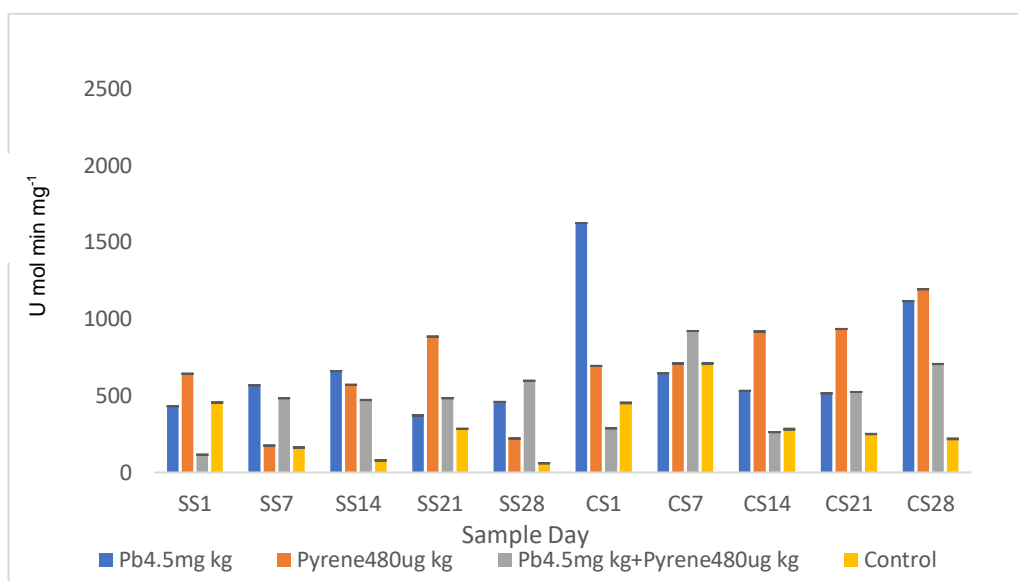


Figure 41. GSTs (U mol min mg⁻¹) activity for worms ($n = 3$) from test conditions Pb4.5 mg kg⁻¹, Pyrene480 μ g kg⁻¹ and the mixture Pb4.5 mg kg⁻¹+Pyrene480 μ g kg⁻¹. Results shown are mean values \pm 1SE.

Statistical analysis using a two - way ANOVA demonstrated that all exposure groups were significantly different during the 28 d assimilation phase: ($F_{(3, 55)} = 4.53, p = < 0.01$). The interaction of time (days) and exposure group on GSTs levels during the assimilation phase also identified significant differences ($F_{(1, 52)} = 5.21, p = < 0.01$).

Additionally, a two - way ANOVA determined significant differences during the 28 d elimination phase for all exposure groups ($F_{(3, 52)} = 15.8, p = < 0.01$). Furthermore, significant differences were identified for the interaction of time (days) and exposure group on GST levels ($F_{(1, 52)} = 5.21, p = < 0.01$). Results demonstrate that GST levels were significantly different for all exposure groups throughout the duration of the 28 d assimilation and elimination phases indicating both the rapid and prolonged effect of Pb and pyrene (alone and in combination) during and post exposure.

GSTs levels for the test conditions Pyrene480 μ g kg⁻¹ (645 U mol min mg⁻¹) and the mixture Pb4.5 mg kg⁻¹ + Pyrene480 μ g kg⁻¹ (646 μ g kg⁻¹) showed a reduction against the control (709 U mol min mg⁻¹) on

sample day CS7. Levels for all test conditions then remained elevated against the control for the remainder of the test period, with the exception of Pb4.5 mg kg⁻¹ which decreased from 646 U mol min mg⁻¹ on sample day CS14 to 105 U mol min mg⁻¹ on sample day CS21 (Control 250 U mol min mg⁻¹).

Mean concentrations during the assimilation phase ranged: Pb4.5 mg kg⁻¹ (684.10 + / - 427.64 U mol min mg⁻¹); Pyrene480 µg kg⁻¹ (533.04 + / - 256.311 U mol min mg⁻¹); Pb4.5 mg kg⁻¹ + Pyrene480 µg kg⁻¹ (405.59 + / - 158.39 U mol min mg⁻¹); Control (249.59 + / - 152.99 U mol min mg⁻¹). During the elimination phase, mean results ranged: Pb4.5 mg kg⁻¹ (882.15 + / - 426.32 U mol min mg⁻¹); Pyrene480 µg kg⁻¹ (889.21 + / - 181.78 U mol min mg⁻¹); Pb4.5 mg kg⁻¹+Pyrene480 µg kg⁻¹ (534.63 + / - 247.98 U mol min mg⁻¹); Control (348.75 + / - 175.59 U mol min mg⁻¹).

6.4.5.4 Cytochrome P450 activity

CYP450 concentrations for individuals exposed show elevated levels against those of the control group for these test conditions during both the assimilation and excretion periods, shown in Figure 42. Furthermore, results clearly indicate that levels of CYP450 are higher during the excretion phase (clean sediment) than during the assimilation phase (spiked sediment).

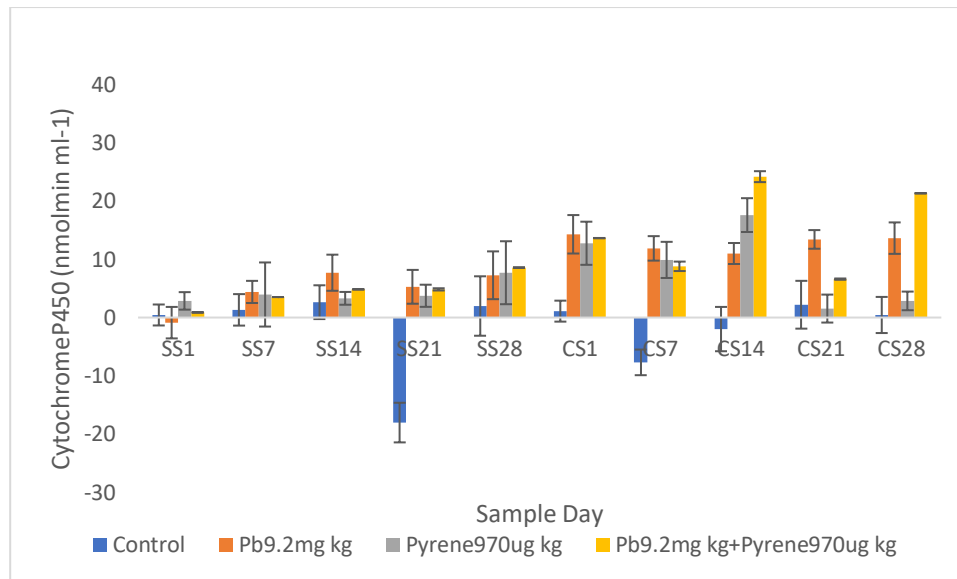


Figure 42. Cytochrome P450 concentrations (nmol min ml⁻¹) for individuals ($n=3$) exposed to the test conditions Pb9.2mg kg⁻¹, Pyrene970 μ g kg⁻¹ and the mixture Pb9.2mg kg⁻¹ + Pyrene 970 μ g kg⁻¹. SS relates to the Spiked Sediment phase, CS relates to the Clean Sediment phase. All results shown are mean values \pm 1 SE.

A two - way ANOVA determined significant differences between CYP450 concentrations in the exposure groups during the 28 d assimilation phase ($F_{(3, 55)} = 20.6, p = < 0.01$). Also, significant differences were identified for the interaction of time (days) and exposure group on CYP450 levels during the assimilation phase ($F_{(1, 52)} = 4.0, p = 0.01$).

Significant differences were also found between all exposure groups during the 28 d elimination phase ($F_{(3, 52)} = 28.9, p = <0.01$). The interaction of time (days) and exposure also revealed significant differences on GSTs levels ($F_{(3, 52)} = 4.01, p = 0.01$) demonstrating that during and post exposure to pyrene and Pb (individually and in mixtures) effects CYP450 levels.

Concentrations for those exposed to Pyrene970 μ g kg⁻¹ (2.85 nmol min ml⁻¹) were higher on sample day SS1 than those of Pb9.2mg kg⁻¹ (-0.87 nmol min ml⁻¹) and the control (0.43 nmol min ml⁻¹).

Concentrations then followed a generally increasing trend for all conditions for the remainder of the assimilation period (SS1 - SS28). Concentrations continued to increase for the first sample day (CS1)

of the excretion period for Pb9.2 mg kg⁻¹ (14.2 nmol min ml⁻¹), Pyrene970 µg kg⁻¹ (12.74 nmol min ml⁻¹), and the mixture Pb9.2 mg kg⁻¹ + Pyrene 970 µg kg⁻¹ (13.62 nmol min ml⁻¹). A rapid increase to 24.17 nmol min ml⁻¹ for mixture test condition Pb9.2 mg kg⁻¹ + Pyrene 970 µg kg⁻¹ and to 17.5 nmol min ml⁻¹ for Pyrene970 µg kg⁻¹ was found on sample day CS14 whereas concentrations for the Pb9.2 mg kg⁻¹ decreased slightly to 10.98 nmol min ml⁻¹. Concentrations for Pb9.2 mg kg⁻¹ remained constant during the sample days CS21 (13.40 nmol min ml⁻¹) and CS28 (13.62 nmol min ml⁻¹) whereas concentrations for Pyrene970 µg kg⁻¹ decreased to 1.53 nmol min ml⁻¹ for sample day CS21 and 2.85 nmol min ml⁻¹ on CS28. Results for the mixture Pb9.2mg kg⁻¹ + Pyrene970 µg kg⁻¹ showed a decrease on sample day CS21 (6.59 nmol min ml⁻¹) followed by an increase to 21.3 nmol min ml⁻¹ on sample day CS28.

Mean concentrations during the assimilation phase ranged: Pb9.2 mg kg⁻¹ (4.74 + / - 4.12 nmol min ml⁻¹); Pyrene970 µg kg⁻¹ (4.30 + / - 3.02 nmol min ml⁻¹); Pb9.2 mg kg⁻¹ + Pyrene970 µg kg⁻¹ (4.53 + / - 3.88 nmol min ml⁻¹); Control (-2.33 + / - 7.88 nmol/ml). During the elimination phase mean concentrations ranged: Pb9.2 mg kg⁻¹ (12.84 + / - 2.83 nmol min ml⁻¹); Pyrene970 µg kg⁻¹ (8.92 + / - 6.34 nmol min ml⁻¹); Pb9.2 mg kg⁻¹ + Pyrene970 µg kg⁻¹ (14.90 + / - 7.24 nmol min ml⁻¹); Control (-1.19 + / - 3.53 nmol min ml⁻¹).

Cytochrome P450 concentrations for the exposure groups Pb4.5 mg kg⁻¹, pyrene480 µg kg⁻¹, and Pb4.5 mg kg⁻¹ + pyrene480 µg kg⁻¹ during the 28 d assimilation phase were significantly different between the exposed groups using a two- way ANOVA ($F_{(3, 52)} = 11.2, p = <0.01$). However, results using the interaction of time (days) and exposure did not reveal significant differences ($F_{(3, 52)} = 1.03, p = 0.38$).

Similarly, a two - way ANOVA revealed significant differences between the exposure groups during the 28 d elimination phase ($F_{(3, 52)} = 13.04, p = <0.01$). Although there were no significant differences

identified using the interaction of time (days) and exposure on CYP450 levels ($F_{(3, 52)} = 1.55, p = 0.21$). Results indicate significant differences in CYP450 levels for all exposure groups.

Moreover, elevated concentrations were found for all test conditions against those of the control during both the assimilation and excretions periods as illustrated in Figure 43. Again, results show higher levels of CYP450 during the elimination than assimilation phase.

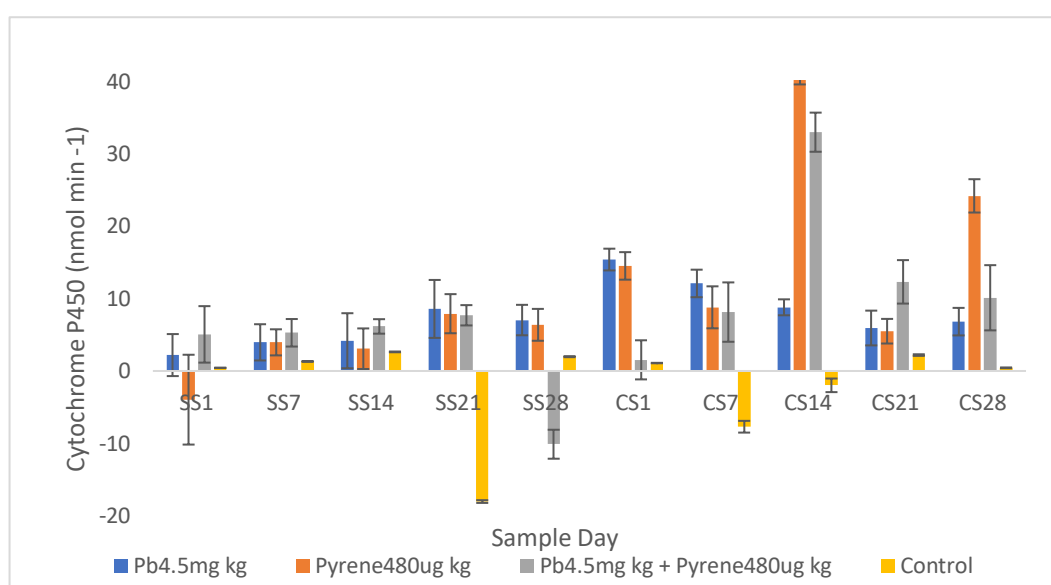


Figure 43. Cytochrome P450 concentrations (nmol min ml^{-1}) for individuals ($n = 3$) exposed to the test conditions $\text{Pb}4.5 \text{ mg kg}^{-1}$, $\text{Pyrene}480 \text{ } \mu\text{g kg}^{-1}$ and the mixture $\text{Pb}4.5 \text{ mg kg}^{-1} + \text{Pyrene} 480 \text{ } \mu\text{g kg}^{-1}$. SS relates to the Spiked Sediment phase and CS relates to the Clean Sediment phase. All results shown are mean values, error bars detail $\pm 1 \text{ SE}$.

Initial concentrations for $\text{Pb}4.5 \text{ mg kg}^{-1}$ ($2.19 \text{ nmol min ml}^{-1}$) and the mixture $\text{Pb}4.5 \text{ mg kg}^{-1} + \text{Pyrene} 480 \text{ } \mu\text{g kg}^{-1}$ ($5.05 \text{ nmol min ml}^{-1}$) were higher than those exposed to $\text{Pyrene}480 \text{ } \mu\text{g kg}^{-1}$ ($-3.95 \text{ nmol min ml}^{-1}$) and the control ($0.43 \text{ nmol min ml}^{-1}$). Concentrations for all conditions showed a general increase through assimilation sample days SS1-SS21 however, results for the mixture $\text{Pb}4.5 \text{ mg kg}^{-1} + \text{Pyrene} 480 \text{ } \mu\text{g kg}^{-1}$ decreased rapidly to $-10.1 \text{ nmol min ml}^{-1}$ on sample day SS28. During the excretion period, concentrations for all

test conditions remained elevated against the control with both Pyrene480 $\mu\text{g kg}^{-1}$ (40.65 nmol min ml^{-1}) and Pb4.5 mg kg^{-1} + Pyrene480 $\mu\text{g kg}^{-1}$ (32.96 nmol min ml^{-1}) showing a rapid increase for sample day CS14.

Mean concentrations during the assimilation phase ranged: Pb4.5 mg kg^{-1} (5.18 + / - 3.44 nmol min ml^{-1}); Pb4.5 mg kg^{-1} + Pyrene480 $\mu\text{g kg}^{-1}$ (2.89 + / - 6.85 nmol min ml^{-1}), Pyrene480 $\mu\text{g kg}^{-1}$ (3.47 + / - 5.00 nmol min ml^{-1}); Control (-2.33 + / - 7.88 nmol min ml^{-1}). During the elimination phase mean concentrations for all exposed groups increased: Pb4.5 mg kg^{-1} (9.80 + / - 3.80 nmol min ml^{-1}); Pb4.5 mg kg^{-1} + Pyrene480 $\mu\text{g kg}^{-1}$ (13.19 + / - 10.90 nmol min ml^{-1}); Pyrene480 $\mu\text{g kg}^{-1}$ (18.73 + / - 12.78 nmol min ml^{-1}); Control (-1.19 + / - 3.53 nmol min ml^{-1}).

6.4.5.5 8-OHdG Concentration

The levels of 8 - OHdG concentrations for test conditions Pb9.2 mg kg^{-1} , Pyrene970 $\mu\text{g kg}^{-1}$ and the mixture Pb9.2 mg kg^{-1} + Pyrene970 $\mu\text{g kg}^{-1}$ were between 119-124% higher than those of the control group in total. Furthermore, results for all test conditions were in excess of those from the control group for all sample days as shown in Figure 44.

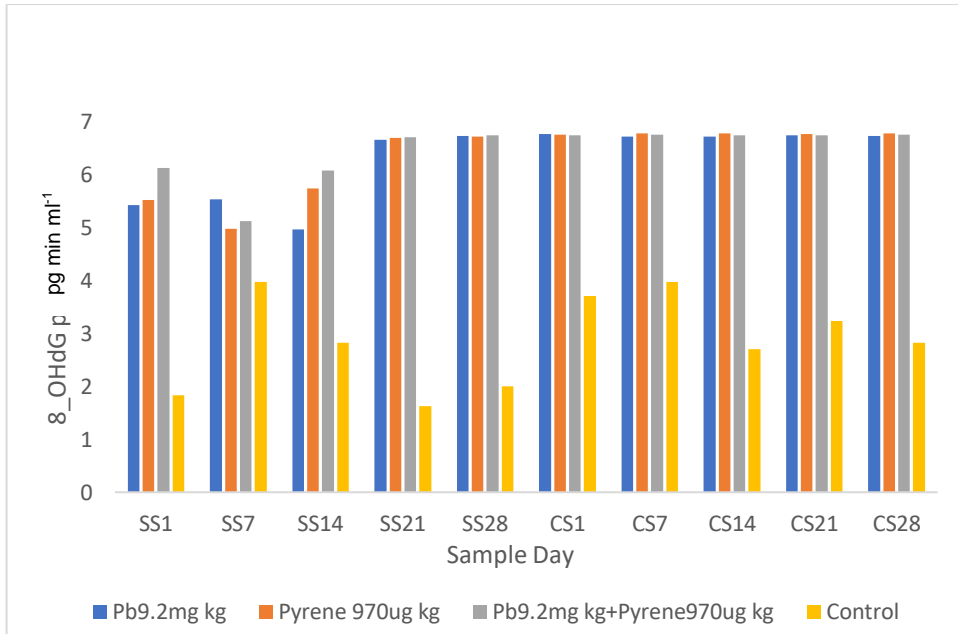


Figure 44. 8 - OHdG concentrations (pg min ml^{-1}) for individuals ($n = 3$) exposed to test conditions $\text{Pb}9.2 \text{ mg kg}^{-1}$, $\text{Pyrene}970 \text{ } \mu\text{g kg}^{-1}$, $\text{Pb}9.2 \text{ mg kg}^{-1} + \text{Pyrene}970 \text{ } \mu\text{g kg}^{-1}$ and the control group. SS relates to the Spiked Sediment phase, CS relates to the clean sediment phase.

Results for test conditions $\text{Pb}4.5 \text{ mg kg}^{-1}$, $\text{Pyrene}480 \text{ } \mu\text{g kg}^{-1}$, $\text{Pb}4.5 \text{ mg kg}^{-1} + \text{Pyrene}480 \text{ } \mu\text{g kg}^{-1}$ (Figure 45), show concentrations which were 116 - 122% higher than those of the control group in total for the duration of the experiment.

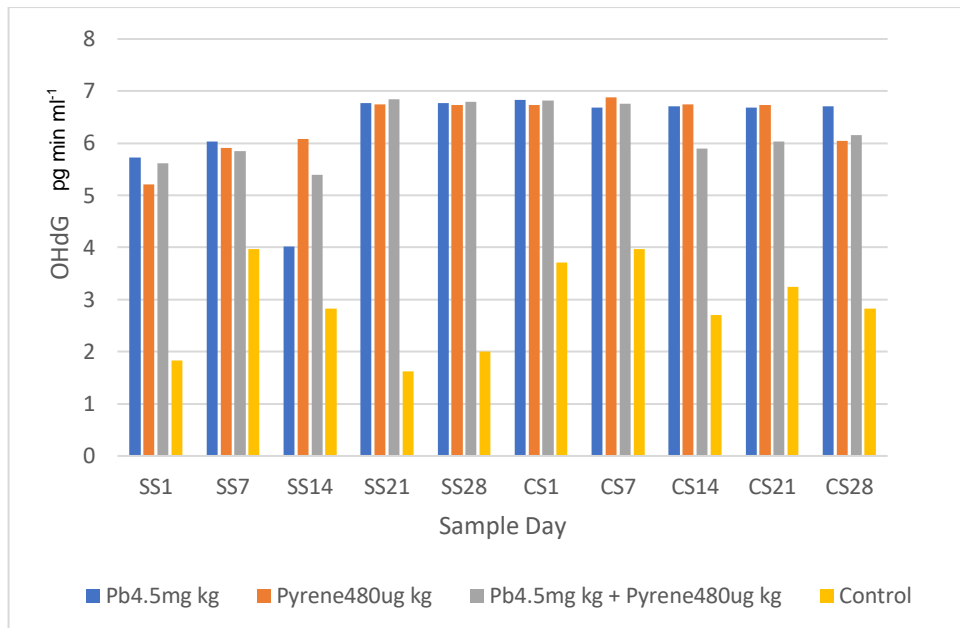


Figure 45. 8 - OHdG concentrations (pg min ml^{-1}) for individuals ($n = 3$) exposed to the test conditions $\text{Pb}4.5 \text{ mg kg}^{-1}$, $\text{Pyrene}480 \text{ } \mu\text{g kg}^{-1}$, $\text{Pb}4.5 \text{ mg kg}^{-1} + \text{Pyrene}480 \text{ } \mu\text{g kg}^{-1}$ and the control group. SS related to the Spiked Sediment phase, CS relates to the Clean Sediment phase.

6.4.6 Relationships of worm tissue concentrations and biochemical responses

Spearman's correlation coefficient revealed non- significant relationships between worm tissue Pb concentrations, single Pb exposure and Pb + pyrene exposure experiments: $\text{Pb}9.2 \text{ mg kg}^{-1}$ ($r_s = 0.127$, $p = 0.733$), $\text{Pb}9.2 \text{ mg kg}^{-1} + \text{Pyrene}970 \text{ } \mu\text{g kg}^{-1}$ ($r_s = -0.409$, $p = 0.241$); $\text{Pb}4.5 \text{ mg kg}^{-1}$ ($r_s = 0.067$, $p = 0.854$); $\text{Pb}4.5 \text{ mg kg}^{-1}$ and $\text{Pyrene}480 \text{ } \mu\text{g kg}^{-1}$ ($r_s = 0.267$, $p = 0.455$).

Furthermore, analysis of biochemical tests, worm tissue Pb and pyrene concentration did not reveal any significant relationships ($p = > 0.05$).

6.5 Discussion

6.5.1 Pb assimilation and excretion

Bioaccumulation of individual and mixtures of Pb and Pyrene within this study highlight that the presence of pyrene in mixtures with Pb,

reduced the bioaccumulation of Pb in *H diversicolor*. Levels of Pb within individuals exposed to the mixtures Pb9.2 mg kg⁻¹ + Pyrene970 µg kg⁻¹ and Pb4.5 mg kg⁻¹ + Pyrene480 µg kg⁻¹ had levels of Pb far lower than those exposed to identical Pb concentrations. These results agree with those observed in Chapter 6 for the test concentration Pb4.5 mg kg⁻¹ + Pyrene480 µg kg⁻¹ but are contrary to the exposure group Pb9.2 mg kg⁻¹ + Pyrene970 µg kg⁻¹ where higher Pb levels for this mixed group were recorded. One possible explanation for this is that this exposure experiment was conducted over 28 d as opposed to 7 d. Therefore, increased assimilation of Pb may have occurred over this longer test series. As previously discussed in Chapter 5, the hydrophobic and lipophilic nature of PAH's may result in the direct binding to biological membranes. Subsequent membrane structure and fluidity change may Pb to ion-regulatory dysfunction and the reduced transport of metal ions across the cell membrane via Ca²⁺ and Na⁺ / K⁺ ATPases (Gauthier et al., 2016; Kim et al., 2016; Shuona et al., 2017). Therefore, the lower Pb worm tissue concentrations found in Chapter 6 for test exposure group Pb9.2 mg kg⁻¹ + Pyrene970 µg kg⁻¹ may be related to an interaction of pyrene at the cellular membrane. Interestingly, worm tissue pyrene results for exposure group Pb9.2 mg kg⁻¹ + Pyrene970 µg kg⁻¹ in Chapter 6 ranged from 0.98, 2.49 and 0.38 µg kg⁻¹ on days 1, 3 and 7 respectively. Pyrene results for test group Pb9.2 mg kg⁻¹ + Pyrene970 µg kg⁻¹ in this chapter were lower with concentrations of 0.29 - 0.04 µg kg⁻¹ on days 1 and 7 respectively. Worm tissue pyrene concentrations for exposure group Pb4.5 mg kg⁻¹ + Pyrene480 µg kg⁻¹ were lower overall than exposure groups Pb9.2 mg kg⁻¹ + Pyrene970 µg kg⁻¹ in both chapters and may support the hypothesis that lower concentrations of pyrene may reduce Pb uptake whereas higher tissue pyrene concentrations increase Pb uptake correlated to pyrene concentration dependant membrane fluidity alterations. Although studies regarding co - exposures of PAH's and metals are few, Diaz-Jarmillo et al. (2017) and Wang et al. (2011a), reported

increased uptake of metals following pyrene co exposure, mercury in the polychaete *Perineries gualpensis* and cadmium in the clam *Ruditapes philipparum* respectively. However, Moreau et al., (1999) and Gust and Fleeger (2006), demonstrated a decrease in metal uptake following co exposure with phenanthrene: Zn in sheepshead minnows *Cyprinodon variegatus* and cadmium in the freshwater oligochaete *Llyodrilus temletoni* respectively. Clearly, further research regarding the effects of PAH exposure on cell membrane fluidity and damage are necessary including concentration related change, cell electric potential and influences of ion ATPases. Σ worm tissue concentrations for both Pb9.2 mg kg⁻¹ (assimilation: 459.67 mg kg⁻¹, elimination: 608.52 mg kg⁻¹) and Pb9.2 mg kg⁻¹+Pyrene970 µg kg⁻¹ (assimilation:97.13, elimination:240.57 mg kg⁻¹) showed higher Pb levels during the elimination phase than for the assimilation phase. A suggestion as to why an increase occurred during the elimination phase may be due to assimilation of Pb from sediment particles adhered to the mucous layer which surrounded the worms.

Mucous excretion by *H diversicolor* has been observed following exposure to metals (Buffet et al., 2011; Gomes et al., 2013; Mouneyrac et al., 2003), attributed as a regulatory protective barrier against metal uptake (Geffard et al., 2005; Mouneyrac et al., 2003). During this experiment the mucous layer was not removed intentionally when worms were moved from spiked sediment tanks and placed into clean sediment, as injury to the worms may have occurred. However, as sediment was adhered to the mucus layer it is possible that Pb contamination may have been present on the mucus layer, then transferred to the clean sediment tank and assimilated by worms.

The body size of the worms may have also influenced total metal results. Although worms were of similar age, dissimilar lengths (~ 40 – 60 mm) and body mass were observed. Although analysis using Spearman's correlation coefficient between worm weight and Pb

concentration did not highlight correlations reported in Chapter 6. Additionally, as worms were randomly allocated to tanks, there should be no effects of size or weight.

Results from this study clearly show interactions between Pb and pyrene regarding bioaccumulation. However, uptake of both contaminants via ingestion of contaminated particles have not been addressed. As previously discussed in Chapter 3, the bioavailability of Pb from sediment was shown to correlate with sediment digestion using proteinase K. This may indicate that ingestion of sediment is the primary uptake pathway for Pb assimilation in *H diversicolor*. However, there is limited research of how far digestive fluids from sediment dwelling invertebrates influence the assimilation of PAH's from sediment. Studies regarding the lug worm *Arenicola marina* gut fluids influence on the dissolution of PAH from sediment suggested that digestive surfactants play a pivotal role in bioaccumulation of PAH's from the environment (Voparil and Mayer, 2000). Additionally, high desorption and absorption efficiencies of the hydrophobic contaminants hexachlorobenzene and c -tetrachlorobiphenyl by gut fluid in the marine polychaete *Neries succinea* were attributed to increased surfactancy and higher micelle concentration. As such, digestion may prove to be a primary uptake pathway of sediment bound PAH's however, surfactants from *H diversicolor* gut fluids have not yet been identified limiting effectiveness of further research. Low pyrene concentrations were found in worm tissue from all test conditions during sample days SS1 - 7. The low levels of pyrene used in this series of experiments in conjunction with worm count in the tanks may have contributed to the rapid uptake of pyrene by worms. Rapid uptake and metabolism of PAH's by worms in the study are in agreement with previous observations (Carrasco-Navarro et al., 2015; de Gelder et al., 2016; Timmermann and Andersen, 2003; Wang and Wang, 2006). Following uptake, pyrene is metabolised to produce phase I metabolite by the enzyme Cytochrome P450 (CYP450) and phase II by enzymes including GSTs (Giessing et al., 2003). Although the

phase II metabolite of pyrene: 1 - hydroxy glucuronide has been suggested as the primary excretory product of pyrene by *H diversicolor*, the phase I product 1 - OHP was also found in gut tissue and excretion water (Giessing et al., 2003). Excretion of phase I and phase II metabolites of pyrene by this species into surrounding sediment following exposure have been previously reported (Christensen et al., 2002b; Giessing et al., 2003). It is reasonable to suggest that levels of 1 - OHP found in individuals for these experiment post pyrene exposure may be influenced by uptake of pre - excreted products into the sediment.

Further investigations regarding the bioaccumulation of pyrene and other PAH's may benefit from using 1 h sample periods from the immediate placement of the organism into the spiked matrix. This may allow a better understanding of the uptake rate and subsequent metabolization. It is clear that further investigations are warranted regards the assimilation, excretion and metabolization of pyrene and its metabolites by *H diversicolor*.

6.5.2 Metallothionein's

MT's were not detected from worm tissue in this test series following exposure to Pb. To determine the accuracy of MT induction, Cu exposed worms from Chapter 5 were analysed and MT's were identified. This observation agrees with previous studies reporting MT induction in *H diversicolor* by Rainbow et al. (2013) and Berthet et al. (2003) following Cu, cadmium and Zn exposure and Garcia-Alonso et al. (2011) following silver exposure. Although MT induction following exposure to Pb has been evidenced in crustaceans; Swimming crab (*Callinectes danae*)(Bordon et al., 2018); marine sponge (*Chondrilla nucula*) (Ferrante et al., 2018) marine polychaete (*Perinereis nuntia*) (Won et al., 2012) and the clam *Ruditapes philippinarum* (Aouini et al., 2018), there is no work evident in the literature regarding MT induction by Pb in *H diversicolor*. However, Poirier et al., (2006) detail investigations of *H diversicolor* from multi

- metal contaminated sediments which included Pb from the Seine Estuary where biochemical investigations revealed conjugation of Pb and S - H group suggestive of MT like proteins. Furthermore, MT's decreasing affinity for metals ($\text{Hg}^{2+} > \text{Cu}^+ \text{Ag}^+, \text{Bi}^{3+} \gg \text{Cd}^{2+} > \text{Pb}^{2+} > \text{Zn}^{2+} > \text{Co}^{2+}$) (Amiard et al., 2006) shows the lower rank of Pb ions, this non-essential metal has a higher affinity than the essential metal Zn, observed to induce MT synthesis (Buffet et al., 2011; Pini, 2014). Therefore, it may be assumed that exposure to Pb would result in the induction of MT's. However, it is plausible that the concentrations used in this series of experiments were too low to initiate a response or were below the levels of detection. Also, assimilation of Pb by worms in this test series may have been regulated by other biological processes including basic metal ATPase efflux or sequestration by lysosomes (Gauthier et al., 2014). Nonetheless, it is suggested that further investigations using Pb exposure and *H diversicolor* including genetic regulation, mRNA levels and tissue deposition may clarify mechanisms.

6.5.3 Regulation of reactive oxygen species

Levels of SOD in worm tissue were far higher than the control group from all test conditions during the assimilation phase (SS1 - SS28), indicating that both pyrene and Pb (alone and in combination) initiate the production of ROS in *H diversicolor*. Interestingly, the levels of SOD decreased for all test conditions during the excretion phase. Yet, levels of Pb in worm tissue for test condition Pb9.2 mg kg⁻¹ were found to be higher during the excretion phase and may indicate detoxification via subcellular partitioning (Berthet et al., 2003; Dang et al., 2012; García-Alonso et al., 2011; Rainbow P. S et al., 2007). Mean concentrations for test conditions were similar during the assimilation phase (60 - 68%) excluding Pb4.5 mg kg⁻¹ + Pyrene480 µg kg⁻¹ which showed increased levels (90.4%). During the elimination phase SOD concentrations ranged: Pb9.2 mg kg⁻¹ (-3%); Pyrene970 µg kg⁻¹ (1.9%); Pb9.2 mg kg⁻¹ + Pyrene970 µg kg⁻¹

(13.9%); Pb4.5 mg kg⁻¹ (22.1%); Pyrene480 µg kg⁻¹ (-14.9%), whereas values for Pb4.5 mg kg⁻¹ (46.9%) remained high suggesting continued presence of ROS at this Pb concentration.

GSTs levels remained high, with the exception of test conditions Pb9.2 mg kg⁻¹, Pyrene970 µg kg⁻¹ and Pb4.5 mg kg⁻¹ on sample day CS21 throughout the duration of the test period. Results for the combined test group Pb9.2 mg kg⁻¹ + Pyrene970 µg kg⁻¹ (734.76 U mol min ml⁻¹) were higher than Pyrene970 µg kg⁻¹ (375.75 U mol min ml⁻¹) and Pb9.2 mg kg⁻¹ (694.13 U mol min ml⁻¹). The higher values in the combined group may suggest that the combined exposure to Pb and pyrene at these concentrations increases overall ROS production.

Interestingly, during the assimilation phase results for the combined group Pb4.5 mg kg⁻¹ + Pyrene480 µg kg⁻¹ (405.59 U mol min ml⁻¹) results were lower than the Pb (Pb4.5 mg kg⁻¹ 684.10 U mol min ml⁻¹) and pyrene (Pyrene480 µg kg⁻¹ 533.04 U mol min ml⁻¹) exposed test groups. Reduction of GSTs has previously been reported following cadmium and benzo [a] pyrene exposure in sea bass *Centropritis striata* (Fair, 1986) and cadmium and mixed PAH's in the mussel *Mytilus trossulus* (Pempkowiak et al., 2006). Therefore, results from the present study may indicate an inhibitory effect of Pb and pyrene at these concentrations. Additionally, all GSTs results during the elimination phase exceeded those of the assimilation phase suggesting the continued metabolism of Pb, pyrene and ROS by this enzyme (Wang et al., 2011a) during the assimilation stage of the experiments. ROS generated by Pb assimilation may reduce glutathione concentrations due to its inhibiting mechanism with sulfhydryl groups (Dai et al., 2018; Dai et al., 2012; Kim et al., 2017). This reduction in GSTs following Pb exposure has been reported: Grey mullet *Mugli cephalus* and Tiger perch *Terapon jarbua* (Hariharan et al., 2012), Wistar rat liver cells (Liu et al., 2011),

common carp *Cyprinus carpio* (Özkan-Yılmaz et al., 2014) and are therefore in agreement with results from the present study.

Additionally, during the metabolism of PAH's, phase I products formed by hydroxylation are conjugated via phase II enzymes including GSTs (Shailaja and D'Silva, 2003). High levels of GSTs recorded for pyrene exposed test conditions may therefore have been influenced by this continued metabolism but also may highlight its role in ROS regulation following exposure to Pb and pyrene. These results are in agreement with Bourauoi et al., (2009) who describe similar increased levels of GST following exposure of *H diversicolor* to mixtures of Cu and benzo [a] pyrene.

CYP450 levels for all test conditions showed a general increasing trend throughout the assimilation phase (SS1 - SS28). However, higher levels of CYP450 were found for all conditions during the elimination phase of these experiments and may therefore suggest inhibition by both Pb and pyrene during the exposure phase.

Additionally, the continued expression during the elimination phase may relate to the presence of 1 - OHP in the pyrene exposed test groups and high Pb body burdens in Pb exposed groups.

Mean values of CYP450 were higher in both Pb exposed test groups than in respective mixed and pyrene only groups: Pb9.2 mg kg⁻¹ (4.75 nmol min ml⁻¹); Pb9.2 mg kg⁻¹ + Pyrene970 µg kg⁻¹ (4.52 nmol min ml⁻¹); Pyrene970 µg kg⁻¹ (4.30 nmol min ml⁻¹); Pb4.5 mg kg⁻¹ (5.18 nmol min ml⁻¹); Pb4.5 mg kg⁻¹+ Pyrene480 µg kg⁻¹ (2.89 nmol min ml⁻¹); Pyrene970 µg kg⁻¹ (4.31 nmol min ml⁻¹).

Production of ROS via both metal and PAH uptake may induce heme oxygenase 1 (HO - 1), which serves to transform the pro-oxidant heme into the anti-oxidant bilirubin (Benedetti et al., 2015). This may result in the either the degradation of existing CYP proteins or the reduction of heme groups required for synthesis of new CYP proteins (Gauthier et al., 2016). This down regulates the induction CYP450 at

both the transcriptional and post transcription levels (Bessette et al., 2005), which may explain higher levels of CYP450 during the elimination phase of these experiments. Therefore, reduced CYP450 levels in the mixed test groups may indicate that ROS generation by Pb decreased CYP activity and are in agreement with research conducted by Korashy and El-Kadi (2012). Furthermore, the lower levels of CYP450 in the pyrene only exposed test groups may relate directly to activation associated with pyrene at these concentrations.

Additionally, disruption of CYP450 following Pb and pyrene uptake may reduce the metabolism of the Phase I products of pyrene. Although, for this study pyrene levels in worm tissue in all exposed individuals decreased rapidly from days 1 - 14 indicating successful hydroxylation at recorded levels. It is suggested therefore, that the use of CYP450 activity following exposure to both metals and PAH's to determine exposure and ROS response may underestimate the biological stress to organisms.

Concentrations of Pb for all exposed conditions remained high during the excretion phase and may indicate the sub cellular partitioning of metals. Cellular partitioning of metals in *H. diversicolor* has been demonstrated (García-Alonso et al., 2011; Geffard et al., 2005; Li et al., 2012; Rainbow et al., 2004), ascribed as a detoxification strategy where accumulated metals are transferred and stored in cellular granules or bound to proteins (including MT) thereby eliminating toxic effects (Rainbow et al., 2004). As previously discussed, MT's were not detected in worm tissue from any Pb exposed condition. Moreover, Raimundo et al. (2010) (Common octopus, *Octopus vulgaris*), Gao et al. (2016) (Japanese scallop, *Mizuhopecten yessoensis*) evidenced that Pb extracted from exposed individuals were associated with high molecular weight proteins. This may suggest that low molecular weight MT's have no function in Pb regulation in *H. diversicolor* and may explain the continued expression of the high molecular weight Cytochrome P450 and GSTs. Further

research is required regarding the cellular partitioning of Pb by *H diversicolor* to elucidate the association between high and low molecular weight proteins.

6.5.4 Induction of oxidative damage in DNA by Pb and Pyrene

DNA adducts in marine invertebrates may be formed through a variety of processes where an organism is placed under biotic or abiotic stress such as variation in temperature, salinity, pH, oxygen and environmental pollution (de Almeida et al., 2003). However, the reaction of Pb and pyrene with nucleic acids may initiate modifications via direct binding to the phosphate backbone or indirectly through lesions produced by ROS production (Yu et al., 2016b). Lesions which result in the modification of guanosine to 8 - OHG or 8 - OHdG are widespread, leading to its use as a biomarker of oxidative damage (Simms and Zaher, 2016). Furthermore, it is acknowledged that Pb²⁺ ions may dissociate Zn²⁺ in Zn finger proteins leading to function impairment, adducts, improper protein folding (Huang et al., 2004a; Petering et al., 2000; Sivo et al., 2018) and subsequent alteration of gene expression (Kluska et al., 2018). 8 - OHdG concentrations for all test conditions were detected at higher levels than those of the control throughout the duration of the test period. As levels for all test conditions showed only a slight decline during the excretion phase, this may indicate continued ROS production brought by continued body burdens of Pb or more ominously, from exposure to pyrene post metabolism and excretion. Additionally, dissociation of Zn²⁺ by Pb²⁺ in Zn fingers may lead to the reduction of DNA binding capability therefore increasing the prevalence of adducts (Hartwig and Schwerdtle, 2002; Huang et al., 2004b; Petering, 2017). The high levels of 8 - OHdG found in this research may further highlight how mechanisms of detoxification in *H diversicolor* are insufficient to regulate ROS generated by individual and mixed concentrations of Pb and pyrene.

6.6 Conclusion

Both Pb and Pyrene are assimilated by the marine invertebrate *H diversicolor*. The presence of pyrene in both mixed test groups resulted in lower Pb assimilation and may indicate that combined exposure may elicit an antagonistic effect. Worm tissue concentrations for those exposed to Pb9.2 mg kg⁻¹ and Pb9.2 mg kg⁻¹ + Pyrene970 µg kg⁻¹ condition showed an increase in Pb tissue concentration during the excretion phase. This may be a result of bioaccumulation from Pb contaminated particles assimilated to the worm mucus layer however, to exclude the influence of worm weight on bioaccumulation, larger sample sizes are suggested. Pb may be partitioned into sub cellular granules to reduce toxicity. However, MT's were not detected in worms exposed to Pb which indicates that MT's are not involved in Pb detoxification. To understand this detoxification mechanism, further investigations regarding sub - cellular partitioning of Pb in *H diversicolor* are essential.

Pyrene metabolization to the phase 1 product 1 - OHP occurred in all test pyrene exposed test conditions from sample days SS1 - 7. 1 - OHP was detected in worm tissue for the duration of the assimilation phase. This may be a result of continued excretion and re - uptake of 1 - OHP.

Results indicate that both Pb and pyrene are ROS producers in *H diversicolor* alone and in combination. SOD, GSTs and Cytochrome P450 all showed elevated levels against the control group. Although, decreased levels of cytochrome P450 during the assimilation phase suggest inhibition.

GSTs levels were far higher in the Pb9.2 mg kg⁻¹ + Pyrene970 µg kg⁻¹ test group than respective individual Pb and pyrene exposures. This may indicate that this combined exposure, increases ROS production. However, reduced GSTs observed in the Pb4.5 mg kg⁻¹ +

Pyrene 480 $\mu\text{g kg}^{-1}$ test group than respective pyrene and Pb only groups suggest inhibition of GSTs at this concentration.

Elevated levels of the DNA adduct 8-OHdG in worm tissue from all test conditions indicated insufficient regulation of ROS following exposure to Pb and pyrene (alone and in combination). Additionally, dissociation of Zn^{2+} ions by Pb^{2+} in Zn fingers may lead to a reduction of DNA binding affinity, increased levels of DNA adducts and protein mis-folding. However, to elucidate the toxic action of Pb and pyrene in *H. diversicolor* further investigations including assessment of DNA binding domains, Zn finger proteins, cellular alterations and storage following exposure are warranted.

Results from the present study illustrate how pyrene and Pb assimilation initiate ROS in *H. diversicolor*. Ominously, ROS levels were not sufficiently regulated by *H. diversicolor* resulting in the formation of DNA adducts. Importantly, the concentrations of Pb and pyrene used in exposure tests in the present study were far lower than those reported in the Fleet lagoon (Chapters 3 and 4).

Therefore, the effects of exposure at these reported concentrations on resident Fleet lagoon populations may be severe. However, these findings highlight negative genotoxic effects following Pb and pyrene exposure relevant to all populations of *H. diversicolor* exposed to these contaminants within their environments.

7. Energy alterations of *H diversicolor* following exposure to pyrene and Pb.

7.1 Introduction

Contamination including Pb and pyrene within the marine environment may be observed to elicit toxicity, where the most severe cases results in the mass mortality of species (Blackstock and Pearson, 1985). Although such catastrophic events are easily recognised, contamination exposure may also alter biodiversity observed as overall species decline or an increase in less sensitive flora and fauna (Johnston and Roberts, 2009b). As organisms endeavour to detoxify contaminants, a reduction of fitness may occur as individuals attempt to re-establish their internal environment (Sokolova et al., 2012). As such, this reduced fitness may go unnoticed, detected as a reduction of biodiversity over long periods of time (Silva et al., 2018; Yeung et al., 2017).

Energy homeostasis may be considered as the requirement to obtain energy via food to maintain functions of survival and Darwinian fitness (Sokolova et al., 2012). Respiration and activities associated with basal metabolic rate may be considered as static survival whereas, for an organism to achieve fitness associated with somatic growth and reproduction, surplus energy from food uptake is necessary (Hummel and Patarnello, 1994; Sokolova et al., 2012). However, exposure to contamination necessitates the adaptation of this energy homeostasis as increased protein turnover, synthesis of specific proteins and excretion are energy demanding (Nilin et al., 2012).

Therefore, energetic costs associated with pollution exposure and subsequent biological responses are often witnessed as a depletion of the energy reserves in the form of proteins, lipids and carbohydrates (Pook et al., 2009). Repair of biological damage as a

consequence of exposure, modifies the organism's overall homeostasis to that of survival, shifting from growth and reproduction (Koojiman., 2001; Rombough, 1994). As growth is governed by an organism's surplus energy reserves (Koojiman., 2001), prolonged energy depletion may Pb to overall growth reduction. Observations of growth reduction have been observed following exposure to Pb including in the rock fish *Sebastes schlegelii* (Kim and Kang, 2017b), freshwater snail *Lymnaea stagnalis* (Brix et al., 2012) and rainbow trout *Oncorhynchus mykiss* (Alsop et al., 2016). Additionally, growth retardation following exposure to PAH has also been evidenced in the oyster *Crassostrea virginica* (Vignier et al., 2019), Japanese rice fish *Oryzia latipes* (Mu et al., 2017) and Chinook salmon *Oncorhynchus tshawytscha* (Meador et al., 2006).

Chronic energy depletion may be directly associated with reduced fecundity leading to overall decline in sexually mature individuals, reduction in viable gametes, larvae or juvenile's which impede population stability (Sokolova et al., 2012). Such effects have been evidenced for exposure to Pb where growth retardation in larvae of the marine bivalve *Meretrix meretrix* (Wang et al., 2009) and the earthworm *Eisenia fetida* (Ayanka Wijayawardena et al., 2018) have been reported. Additionally, pyrene has been evidenced to reduce ova production in the copepods *Calanus glacialis* (Toxværd et al., 2018) and *Calanus hyperboreus* (Nafa et al., 2014). Changes of energy homeostasis and reproduction to populations of *H diversicolor* resident in the infamously Cu contaminated Restronguet creek, Cornwall, have also reported depleted levels of lipids and carbohydrates and reduced fecundity (Pook et al., 2009). Decreased egg production and energy reserves were also observed in *H diversicolor* which inhabited the multi polluted site of the Seine estuary, France (Durou et al., 2007), and the Loire, France (Mouneyrac et al., 2010). Whereas mercury exposure was shown to depleted energy reserves in *H diversicolor* (Freitas et al., 2017). The consequences of reproduction impairment for species which inhabit

polluted environments are severe (Hollows Cam et al., 2007), and may lead to reductions of both population density and species diversity (Johnston and Roberts, 2009a).

In addition, individuals may attempt to avoid exposure to contamination through reduced consumption of contaminated food or by actively removing themselves from polluted matrices (Maryanski et al., 2002). This may also lead to altered predator - prey interactions where depleted energy levels in predators following contamination exposure led to the increased consumption of less mobile prey species (Weis et al., 2011). Active avoidance of contamination may also affect the energy homeostasis of an individual where subsequent increased activity levels reduce energy reserves (Nilin et al., 2012). In chronically polluted environments, this may result in a self - depleting cycle where avoidance of contamination leads to increased energy output and feeding rates. Increased energy expenditure and subsequent requirement to feed may again expose the individual to contamination or the organism may extend its feeding area to feed successfully.

Exposure to individual contaminants is commonplace for environmental toxicity testing however, contamination within the marine environment is comprised of complex mixtures. Although investigations of individual contaminants may illustrate specific biological effects, the bioaccumulation of multiple contaminants may elicit more than additive outcomes (Gauthier et al., 2014).

To determine potential alterations of energy reserves, this study will investigate the effects of both individual concentrations and mixtures of Pb and pyrene in the marine polychaete *H diversicolor* specifically to:

1. Investigate changes in proteins, lipids and carbohydrates following exposure.
2. Determine how energy reserves may alter on return to uncontaminated conditions.

7.2 Materials and methods

7.2.1 Reagents

Sodium, K -Tartrate, Cu Sulphate, Sodium Hydroxide, Bovine serum albumin, Phosphoric acid, sodium chloride, methanol, chloroform, Triglyceride tripalmitin, Sulphuric acid, Glucose, Pyrene, Pb chloride and 3, 5 - dinitrosalicylic acid were purchased from Sigma Aldrich Ltd, Gillingham, Dorset, UK. All reagents used were of analytical grade.

7.2.2 Tank Set up and sediment spiking

Sediment for each experiment was spiked and tanks set up as detailed in Chapter 2 (2.6.1, 2.5.1 respectively). Worms from each experiment tank were sampled as previously described

7.2.3 Worm tissue energy determination

Frozen worms ($n = 3$) from each test condition per sample day were defrosted, washed with distilled water and blotted. Worms were placed into a centrifuge tube which contained 2 ml of 0.1 mM Phosphate buffer then homogenised using an IKA T10 ULTRA-TURRAX homogenizer.

7.2.3.1 Protein analysis

Protein standard concentrations of 0, 2, 4, 6, 8 and 10 mg ml⁻¹ were prepared by dissolving 0.1 g of Bovine Serum Albumin (BSA) in 10 ml distilled water to obtain a final concentration of 10 mg ml⁻¹ of stock solution. Total protein content in worm tissue was conducted using the Biuret method (Gornall et al., 1949). 3 ml of Biuret solution (3 g of potassium sodium tartrate, 0.75 g of Cu sulphate and 150 ml of 10 % NaOH dissolved in 500 ml with distilled water) were added to

50 µl of worm homogenate or with associated 50 µl of protein standards in glass test tubes. All samples and standards were heated at 37 °C for 30 min before being transferred in disposable cuvettes and analysed at absorbance of 570 nm using a Varian Cary 50 probe UV-Visible spectrophotometer.

7.2.3.2 Lipid analysis

Total lipid content is determined based on the method developed by Bligh & Dyer (1959). 24 µl of worm homogenate was added to a centrifuged tube. 50 µl of acid salt solution (5 M NaCl and 1 M phosphoric acid) was then added to the homogenate. Methanol (600 µl) of and chloroform (1200 µl) were then added and the solution capped and vortexed for 10 min. 200 µl of methanol, 400 µl of chloroform, 240 µl of distilled water and 60 µl of acid salt solution was then added to the homogenate and mixed before a further vortex for 1 min. The solution was then centrifuged (3,500 g) for 10 min. Triglyceride tripalmitin standards were prepared using chloroform for 5, 2.5, 1.25, 0.625, 0.3125 and 0.150625 mg lipid ml⁻¹ standards. A chloroform blank was also prepared. One 100 µl of each sample and standard were transferred to glass test tubes and 500 µl of 95.0 - 98.0 % sulphuric acid added to each. All test tubes were then heated in an oven at 200 °C for 15 min. After cooling to room temperature, 1.5 ml of distilled water was added to each tube. All samples were mixed by inversion before being transferred to a quartz cuvette and read at 340 nm using a Varian Cary 50 Probe UV - Visible spectrophotometer.

7.2.3.3 Carbohydrate analysis

Total carbohydrate content (combined carbohydrate and glycogen) was determined using the method developed by Sumner and Graham (1921) by placing 500 µl of tissue homogenate into a glass

test tube. 2.5 ml of distilled water and 1.5 ml of 3, 5, dinitrosalicylic acid reagent were then added. The test tube was covered using parafilm to prevent evaporation and placed into a water bath with temperature of 90°C for 7 - 8 minutes. The test tubes were removed, samples poured into cuvettes and absorbance measured at 540 nm using a Varian Cary 50 Probe UV - Visible spectrophotometer.

7.2.4 Statistical analysis

Statistical analysis was conducted using Ri386 version 3.4.2 as fully detailed in Chapter 2 (2.8). All data was analysed to meet the assumptions for parametric tests, normality and equal variances. Two- way ANOVA's were performed on all raw, \log^{10} or square root transformed parametric data for all protein, lipid and carbohydrate results. The energy determinants were used as the dependant variable and both time and condition as the independent variables. Spearman's correlations were performed to identify relationships between all tested energy determinants and worm weight and Pb / pyrene worm tissue concentration. Partial Spearman's correlations were conducted using worm tissue weight as the controlling variable for Pb / pyrene tissue content and energy determinant.

7.3 Results

7.3.1 Worm tissue Pb concentrations

Tissue concentrations for Pb found in worm tissue for the duration of the experiment (28 d assimilation and 28 d excretion period) are presented in Table 31.

Table 31. Pb concentrations (mg kg⁻¹) in worm tissue (*n* = 3) from Pb exposed conditions taken on sample days over the duration of the test experiment. Results are mean values ± 1 SE. SS denotes spiked sediment and CS denotes clean sediment.

Day	Pb9.2 mg kg ⁻¹	Pb4.5 mg kg ⁻¹	Pb9.2 mg kg ⁻¹ + Pyrene970 µg kg ⁻¹	Pb4.5 mg kg ⁻¹ + Pyrene 480 µg kg ⁻¹	Control (mg kg ⁻¹)
SS1	45.18 ± 5.09	8.52 ± 1.47	14.90 ± 6.94	11.72 ± 1.19	0.85 ± 0.54
SS7	35.79 ± 10.31	31.84 ± 1.21	24.64 ± 3.04	22.60 ± 1.20	0.78 ± 0.09
SS14	133.1 ± 19.31	207.72 ± 11.70	35.21 ± 2.61	67.33 ± 6.64	0.86 ± 0.26
SS21	90.02 ± 12.82	164.69 ± 11.22	14.2 ± 2.51	45.38 ± 3.77	1.79 ± 0.29
SS28	155.57 ± 20.82	151.81 ± 2.33	8.19 ± 1.33	143.12 ± 14.66	1.17 ± 0.18
CS1	89.79 ± 15.91	129.28 ± 3.04	21.11 ± 1.08	44.29 ± 9.51	1.24 ± 1.06
CS7	132.38 ± 11.15	44.99 ± 4.96	57.31 ± 6.28	37.53 ± 3.38	1.09 ± 0.42
CS14	148.64 ± 8.61	93.50 ± 3.78	57.63 ± 11.25	44.59 ± 3.03	0.97 ± 0.47
CS21	128.92 ± 13.68	73.67 ± 3.79	73.35 ± 11.11	45.74 ± 0.56	1.07 ± 0.05
CS28	108.79 ± 8.50	87.50 ± 2.72	31.17 ± 7.71	35.51 ± 2.25	0.61 ± 0.23

Results from all test conditions on each sample day were found to be statistically different (*p* = > 0.05) using a one-way ANOVA from those of the control group. Concentrations of Pb in worm tissue for test condition Pb9.2 mg kg⁻¹ + Pyrene 970 µg kg⁻¹ show Σ values ~ 4 - fold lower than those exposed to Pb9.2 mg kg⁻¹. Similarly, concentrations for worms from test condition Pb4.5 mg kg⁻¹ + Pyrene 480 µg kg⁻¹ had Σ concentrations ~2 fold lower than those exposed to Pb4.5 mg kg⁻¹.

Worm tissue concentrations for worms exposed to pyrene individually, and in Pb mixtures are detailed in Table 32.

Table 32. Pyrene concentrations ($\mu\text{g kg}^{-1}$) in worm tissue ($n=3$) taken from individuals from all pyrene exposed conditions. Results are mean values ± 1 standard deviation. Results detailed as bdl (below detection limits) were $>0.25 \text{ ng kg}^{-1}$.

Sample Day	Pb4.5mg kg^{-1} + Pyrene 480 $\mu\text{g kg}^{-1}$	Pb9.2 mg kg^{-1} + Pyrene 970 $\mu\text{g kg}^{-1}$	Pyrene 970 $\mu\text{g kg}^{-1}$	Pyrene 480 $\mu\text{g kg}^{-1}$	Control ($\mu\text{g kg}^{-1}$)
SS1	0.09 \pm 0.03	0.29 \pm 0.07	0.49 \pm 0.06	1.03 \pm 0.00	0.00
SS7	0.01 \pm 0.02	0.04 \pm 0.04	bdl	bdl	0.00
SS14	bdl	bdl	bdl	bdl	0.00
SS21	bdl	bdl	bdl	bdl	0.00
SS28	0.00	0.00	0.00	0.00	0.00
CS1	0.00	0.00	0.00	0.00	0.00
CS7	0.00	0.00	0.00	0.00	0.00
CS14	0.00	0.00	0.00	0.00	0.00
CS21	0.00	0.00	0.00	0.00	0.00
CS28	0.00	0.00	0.00	0.00	0.00

Results from all pyrene exposed test conditions show low levels ($> 0.5 \mu\text{g kg}^{-1}$) of pyrene tissue concentrations between sample days SS1 - SS7.

7.3.2 Protein determination

Protein analysis for test conditions Pb9.2 mg kg^{-1} , Pyrene970 $\mu\text{g kg}^{-1}$ and Pb9.2 mg kg^{-1} + Pyrene970 $\mu\text{g kg}^{-1}$ are illustrated in Figure 46.

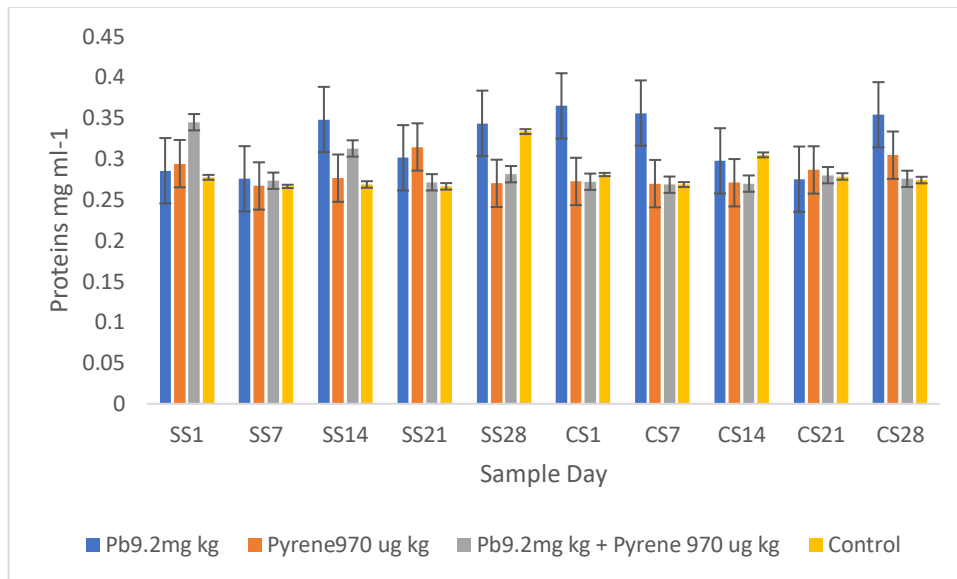


Figure 46. Protein concentrations (mg ml^{-1}) for worms ($n = 3$) from test conditions Pb9.2 mg kg^{-1} , $\text{Pyrene970 } \mu\text{g kg}^{-1}$ and $\text{Pb9.2 mg kg}^{-1} + \text{Pyrene970 } \mu\text{g kg}^{-1}$. Values are mean concentrations ± 1 SE.

During the assimilation period of the experiment (SS1 - SS28) test condition Pb9.2 mg kg^{-1} showed a lower Σ mean concentration of proteins (1.55 mg ml^{-1}) than during the excretion period (1.64 mg ml^{-1}). However, Σ mean concentration of proteins for the test conditions $\text{Pyrene970 } \mu\text{g kg}^{-1}$ (1.42 mg ml^{-1}), $\text{Pb9.2 mg kg}^{-1} + \text{Pyrene970 } \mu\text{g kg}^{-1}$ (1.48 mg ml^{-1}) and control (1.41 mg ml^{-1}) showed higher values during the assimilation period than the excretion period (1.39 , 1.36 , 1.40 mg ml^{-1}) respectively.

A two - way ANOVA of all exposure groups did not reveal significant differences during the 28 d assimilation phase using the interaction of time (days) and exposure ($F_{(3, 55)} = 2.17$, $p = 0.10$). Additionally, a significant difference was identified for both exposure groups ($F_{(3, 52)} = 2.75$, $p = 0.050$) and sample days ($F_{(1, 55)} = 9.46$, $p = <0.01$).

Results may indicate that protein levels for all exposure groups were affected during the assimilation phase.

However, a two - way ANOVA did not reveal significant differences for protein levels using the interaction of time (days) and exposure during the 28 d elimination phase ($F_{(3, 55)} = 2.14$, $p = 0.11$). Although, a significant difference was identified for exposure groups ($F_{(3, 55)} =$

11.02, $p = <0.01$) but not for sample days ($F_{(1, 55)} = 2.12$, $p = 0.12$) demonstrating the effects of the differing Pb and pyrene exposures on protein levels.

Protein determination for test conditions Pb4.5 mg kg⁻¹, Pyrene480 µg kg⁻¹ and Pb4.5 mg kg⁻¹ + Pyrene480 µg kg⁻¹ are presented in Figure 47.

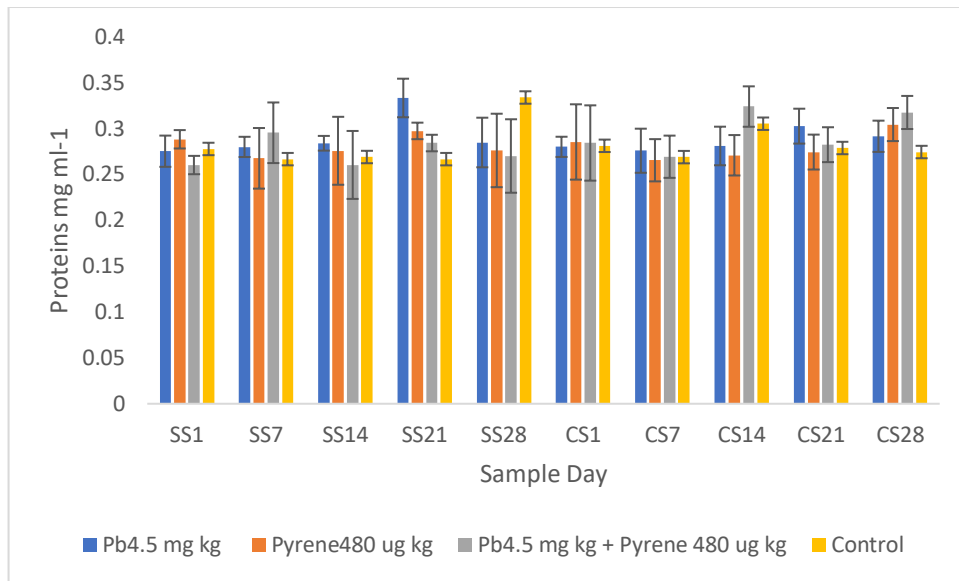


Figure 47. Protein concentrations (mg ml⁻¹) for worms ($n = 3$) from test conditions Pb4.5 mg kg⁻¹, Pyrene480 µg kg⁻¹ and Pb4.5 mg kg⁻¹ + Pyrene480 µg kg⁻¹. Results are shown as mean values \pm 1 SE.

Mean Σ Protein determinations for test condition Pb4.5 mg kg⁻¹ (3.00 mg ml⁻¹) showed higher value than those for Pyrene480 µg kg⁻¹ (2.80 mg ml⁻¹) and Pb4.5 mg kg⁻¹ + Pyrene480 µg kg⁻¹ (2.84 mg ml⁻¹) and control (2.81 mg ml⁻¹). Higher mean Σ values during the 28 d assimilation period than the elimination period were found for test condition Pb4.5 mg kg⁻¹ (1.46:1.43 mg ml⁻¹ respectively) and control (1.41:1.40 mg ml⁻¹ respectively). Mean Σ protein values for groups Pyrene480 µg kg⁻¹ (1.40:1.43 mg ml⁻¹ respectively) and Pb4.5 mg kg⁻¹ + Pyrene480 µg kg⁻¹ (1.36 :1.48 mg ml⁻¹ respectively) were lower during the assimilation than the elimination phase.

Statistical analysis using a two – way ANOVA showed significant differences for all exposure groups during the 28 d assimilation phase using the interaction of time (day) and exposure ($F_{(3, 55)} = 3.67$, $p = 0.02$). However, significant differences for all exposure groups and sample days did not reveal significant results ($p = 0.10$, $p = 0.57$ respectively).

Additionally, a two – way ANOVA did not reveal significant differences using the interaction of time (days) and exposure for protein levels during the elimination phase ($F_{(3, 55)} = 0.11$, $p = 0.95$). Also, there were no significant differences identified for exposure groups ($F_{(3, 55)} = 0.88$, $p = 0.45$) or for sample days ($F_{(1, 55)} = 1.92$, $p = 0.74$).

7.3.3 Lipid determination

Results of lipid determination for the test conditions Pb9.2 mg kg⁻¹, Pyrene970 µg kg⁻¹, Pb9.2 mg kg⁻¹ + Pyrene970 µg kg⁻¹ are illustrated in Figure 48.

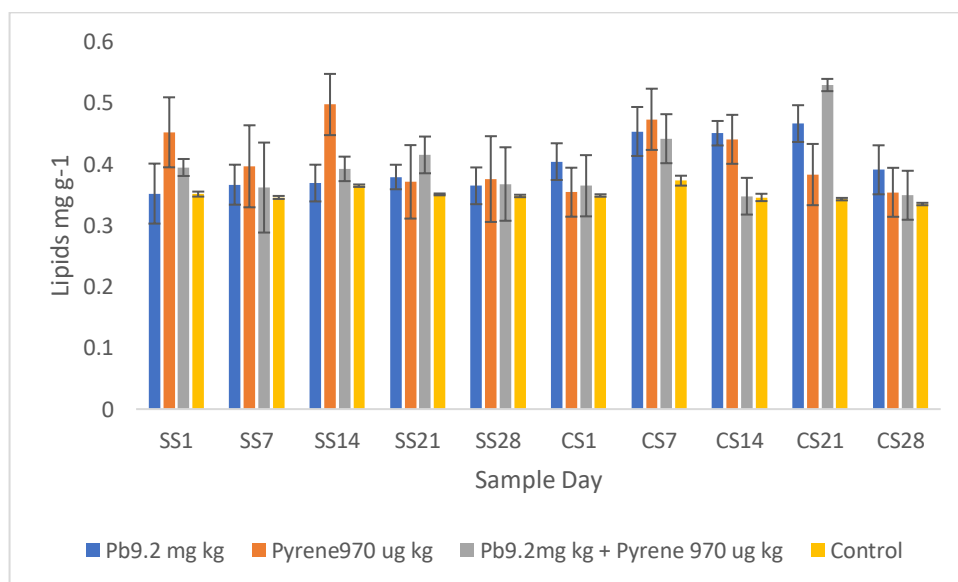


Figure 48. Lipid concentration (mg g⁻¹ wet weight) for test conditions Pb9.2mg kg⁻¹, Pyrene µg kg⁻¹, Pb9.2mg kg⁻¹ + Pyrene970 µg kg⁻¹ and control group (sample size $n=3$). SS relates to Spiked Sediment phase, CS relates to Clean Sediment phase. Results shown are mean values \pm 1 SE.

Mean Σ Lipid content for test conditions Pb9.2 mg kg⁻¹ (1.83 mg g⁻¹) and Pb9.2 mg kg⁻¹ + Pyrene970 μ g kg⁻¹ (19.3 mg g⁻¹) during the assimilation period were lower than during the excretion period (2.17, 2.03 mg g⁻¹ respectively). Results for test condition Pyrene970 μ g kg⁻¹ and control group showed mean Σ concentrations marginally higher for the assimilation period (2.09, 1.76 mg g⁻¹) opposed to excretion period (2.01, 1.75 mg g⁻¹ respectively).

A two - way ANOVA did not identify significant differences between lipid levels of the exposure groups during the 28 d assimilation phase ($F_{(3, 55)} = 0.92$, $p = 0.44$) using the interaction of time and exposure. However, a significant difference for exposure groups was identified ($F_{(3, 55)} = 4.05$, $p = 0.01$) although, no significant differences were observed for sample days ($F_{(1, 55)} = 0.92$, $p = 0.44$). Additionally, a two – way ANOVA did not reveal any significant differences using the interaction of time and exposure groups on lipid levels during the elimination phase ($F_{(3, 55)} = 0.32$, $p = 0.82$). Again, lipid levels for the exposure groups were significantly different ($F_{(3, 55)} = 4.55$, $p = < 0.01$) although, there were no significant differences for sample days ($F_{(1, 55)} = 0.29$, $p = 0.59$). Results suggest that exposure to Pb and pyrene individually and in combination effected lipids levels in all exposure groups.

Mean Σ Lipid concentrations for test conditions Pb4.5mg kg⁻¹ (1.85 mg g⁻¹), Pyrene480 μ g kg⁻¹ (1.87 mg g⁻¹), Pb4.5mg kg⁻¹ + Pyrene480 μ g kg⁻¹ (1.94 mg g⁻¹) during the assimilation phase (Figure 49) were all lower than during the elimination phase (2.17, 2.11, 2.16 mg g⁻¹ respectively). Results for all conditions were found to be higher than those of the control during the assimilation (1.76 mg g⁻¹) and elimination (1.75 mg g⁻¹) periods.

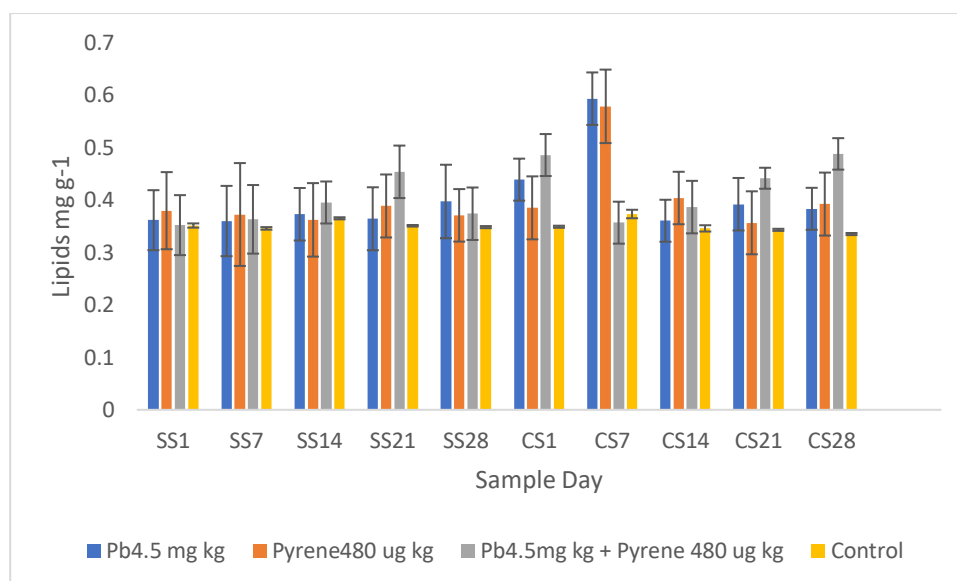


Figure 49. Lipid determination (mg g^{-1} wet weight) for test conditions Pb4.5mg kg^{-1} , $\text{Pyrene480 } \mu\text{g kg}^{-1}$, $\text{Pb4.5mg kg}^{-1} + \text{pyrene480 } \mu\text{g kg}^{-1}$ and the control group (sample size $n = 3$). SS relates to Spiked Sediment phase, CS relates to Clean Sediment phase Results are shown as mean values ± 1 SE.

A two – way ANOVA demonstrated that lipid contents were not significantly different for all exposure groups using the interaction of time (days) and exposure ($F_{(3, 52)} = 1.02, p = 0.39$) during the assimilation phase. Also, results were not significantly different for either exposure groups ($F_{(3, 52)} = 1.02, p = 0.39$) or on sample days ($F_{(1, 52)} = 0.46, p = 0.75$).

Additionally, a two- way ANOVA did not reveal significant lipid level differences during the elimination phase between all exposure groups using the interaction of time (days) and exposure ($F_{(3, 55)} = 1.04, p = 0.38$). Furthermore, there were no significant differences identified for both exposure groups ($F_{(3, 52)} = 2.47, p = 0.07$) or sample days ($F_{(1, 52)} = 1.04, p = 0.38$).

7.3.4 Total carbohydrate determination

Mean Σ carbohydrate analysis shown in Figure 50, revealed concentrations for test conditions Pb9.2 mg kg^{-1} (1.51 mg g^{-1}) and $\text{Pyrene970 } \mu\text{g kg}^{-1}$ (1.16 mg g^{-1}) were lower during the assimilation period than excretion ($1.99, 2.32 \text{ mg g}^{-1}$). Mean Σ carbohydrate

results for test condition Pb9.2 mg kg⁻¹ + Pyrene970 µg kg⁻¹ (1.50 mg g⁻¹ wet weight) and the control group (1.80 mg g⁻¹ wet weight) showed higher values during the assimilation than excretion (1.17, 1.25 mg g⁻¹ wet weight respectively) period.

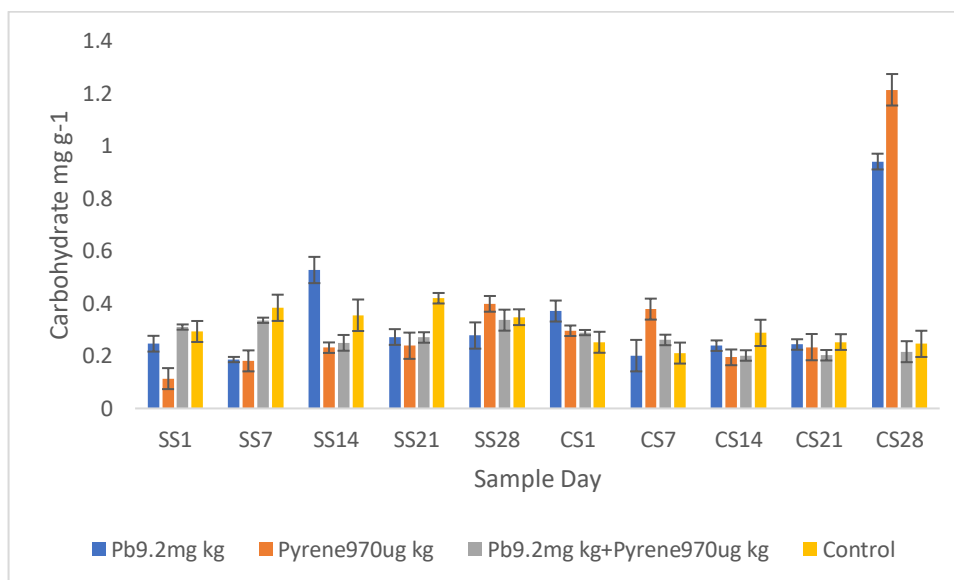


Figure 50. Total carbohydrate results (mg g⁻¹ wet weight) for worms ($n = 3$) exposed to test conditions Pb9.2 mg kg⁻¹, Pyrene970 µg kg⁻¹, Pb9.2mg kg⁻¹ + Pyrene970 µg kg⁻¹. SS relates to Spiked Sediment phase, CS relates to Clean Sediment phase. All results are mean values \pm 1 SE.

A two- way ANOVA revealed significant differences between the interaction of time and exposure group on carbohydrate levels during the 28 d assimilation phase ($F_{(3, 52)} = 2.89$, $p = 0.04$). Additionally, significant differences were identified for all exposure groups ($F_{(3,52)} = 8.56$, $p = <0.01$) and sample days ($F_{(1,52)} = 7.90$, $p = <0.01$).

Furthermore, a two – way ANOVA revealed significant differences between the interaction of time and exposure group on carbohydrate levels during the elimination phase ($F_{(3, 52)} = 6.42$, $p = <0.01$). Also, significant differences were identified for all exposure groups ($F_{(3, 52)} = 4.78$, $p = <0.01$) and all sample days ($F_{(1, 52)} = 14.34$, $p = <0.01$) Results demonstrate how exposure to Pb and pyrene (alone and in combination) altered the levels of carbohydrates during both the assimilation and elimination phases for all exposure groups.

Mean Σ carbohydrate concentrations for test condition Pb4.5 mg kg⁻¹ (Figure 51) were found to be lower during the assimilation (1.41 mg g⁻¹) than excretion period (1.45 mg g⁻¹). However, higher levels were identified in conditions Pyrene480 μ g kg⁻¹ (1.44 mg g⁻¹), and Pb4.5 mg kg⁻¹ + Pyrene480 μ g kg⁻¹ (1.42 mg g⁻¹) opposed to the elimination phase (1.24, 1.37 mg g⁻¹ respectively). The control group also showed higher levels during the assimilation (1.80 mg g⁻¹) than excretion (1.25 mg g⁻¹) phase.

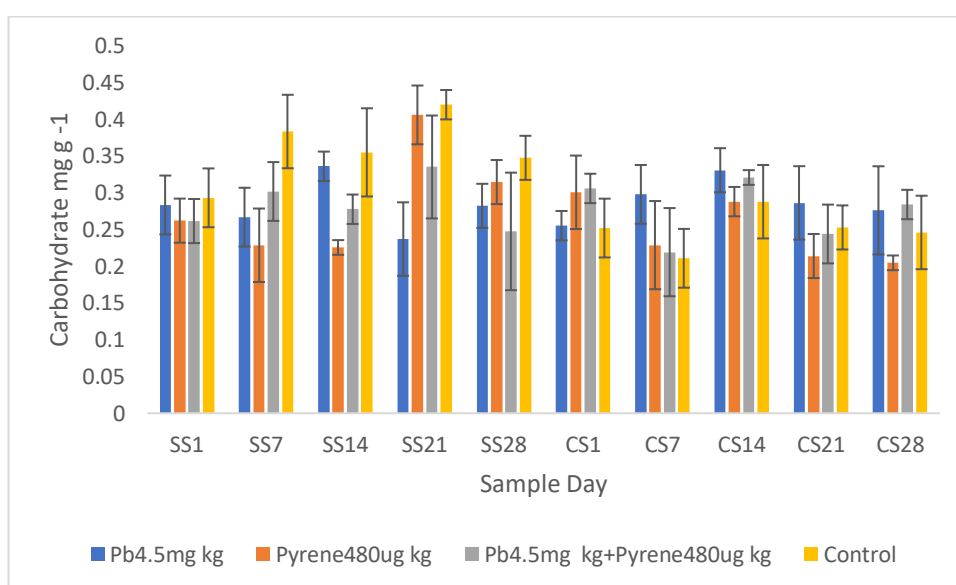


Figure 51. Total carbohydrate results (mg g⁻¹ wet weight) for worms ($n = 3$) exposed to test conditions Pb4.5mg kg⁻¹, Pyrene480 μ g kg⁻¹, Pb4.5mg kg⁻¹ + Pyrene480 μ g kg⁻¹. All results are mean values \pm 1 SE.

A two - way ANOVA revealed the interaction between exposure group and time (day) during the assimilation phase was significant ($F_{(3, 55)} = 7.23$, $p = < 0.01$). Furthermore, significant differences were identified for all exposure groups ($F_{(3,55)} = 7.22$, $p = < 0.01$) and for all sample days ($F_{(1,55)} = 6.74$, $p = < 0.01$). Therefore, carbohydrate levels for all exposure groups were affected throughout the duration of the assimilation phase.

A two- way ANOVA identified no significant interaction between the test exposure, time (day) and carbohydrate levels for all exposure

groups during the elimination phase ($F_{(3, 52)} = 1.70, p = 0.18$). A significant difference was identified for all exposure groups ($F_{(3, 52)} = 2.80, p = 0.049$) although, there was no significant difference for sample day ($F_{(1, 52)} = 0.91, p = 0.34$). Again, results indicate that carbohydrate levels were significantly different for all exposure groups.

7.3.5 Statistical relationships

7.3.5.1 Relationships between worm weight, lipid content and worm tissue Pb concentrations

Spearman's correlations between worm tissue lipid and worm weight showed a significant negative relationship for exposure condition Pb4.5 mg kg⁻¹ ($r_s = -.439, p = 0.015$) and a positive correlation for Pb9.2 mg kg⁻¹ ($r_s = .380, p = 0.038$). There were no further significant relationships identified for the remaining exposure groups ($p = > 0.05$).

Spearman's correlations performed on worm tissue Pb / pyrene content and lipid concentrations did not reveal any significant correlations for any exposure group ($p = > 0.05$).

Partial correlations using worm weight as the controlling variable for worm tissue Pb / pyrene content and lipid concentrations revealed a positive correlation for exposure group Pb9.2 mg kg⁻¹ ($r_s = 3.69, p = < 0.01$) although, no further significant correlations were identified for the remaining exposure groups ($p = > 0.05$).

7.3.5.2 Relationships between worm weight, protein content and worm tissue Pb concentrations

Spearman's correlations between worm weight and protein content revealed a negative relationship for exposure group Pb4.5 mg kg⁻¹ ($r_s = -0.375, p = 0.041$). There were no further significant correlations

between worm weight and protein content for the remaining groups ($p = > 0.05$). Additionally, there were no correlations identified between protein content and Pb / pyrene worm tissue concentrations for any exposure group ($p = > 0.05$).

Partial Spearman's correlations using worm weight as a controlling variable for Pb / pyrene tissue content and protein concentrations did not reveal any significant correlations ($p = > 0.05$).

7.3.5.3 Relationships between worm weight, carbohydrate content and worm tissue Pb/pyrene concentrations

Spearman's correlations revealed significant negative correlation between carbohydrate and worm tissue Pb concentrations for exposure group Pb9.2 mg kg⁻¹ and Pyrene970 µg kg ($r_s = - 6.34$, $p = < 0.01$). All other exposure groups were identified as non - significant ($p = > 0.05$).

Further Spearman's correlations between carbohydrate levels and worm weight revealed a positive correlation for exposure group Pb9.2 mg kg⁻¹ + Pyrene970 µg kg⁻¹ ($r_s = 0.387$, $p = 0.038$) and a negative relationship for Pb4.5 mg kg⁻¹ ($r_s = -0.439$, $p = 0.015$). All other test conditions were non-significant ($p > 0.05$).

Partial Spearman's correlations were performed using worm weight as the controlling variable for Pb / pyrene tissue content and carbohydrate concentrations. However, all results were found to be insignificant ($p = > 0.05$).

7.4 Discussion

Exposure to contaminants result in the up regulation of detoxification mechanisms (Fossi Tankoua et al., 2012). However, these processes are energetically costly to the organism, observed as depletion of energy stores (Drouou et al., 2005a; Holloway et al., 1990; Moolman et al., 2007; Mouneyrac et al., 2010; Pook et al.,

2009). As such, lower levels of lipids, carbohydrate or protein reserves observed for all test exposures in the present study demonstrates the energetic costs of Pb and pyrene exposure (individually or in combination) indicating higher energy expenditure than assimilation.

It is acknowledged that lipids and carbohydrates are primarily utilised as energy sources (Moolman et al., 2007; Smolders et al., 2004; Yeung et al., 2017). Lower levels of lipids recorded during the assimilation phases for all exposure groups excluding Pyrene970 $\mu\text{g kg}^{-1}$ and carbohydrates all exposure groups excluding Pb9.2 mg kg^{-1} + Pyrene970 $\mu\text{g kg}^{-1}$, Pb4.5 mg kg^{-1} + Pyrene480 $\mu\text{g kg}^{-1}$ and Pyrene480 $\mu\text{g kg}^{-1}$ suggest that lipids and carbohydrates are principally exploited during increased energy expenditure (Hori et al., 2006). These results are in agreement with previous research which observed the reduction of lipids and carbohydrates following contamination exposure in Zebra mussels *Dreissena polymorpha* following metal / PAH sludge exposure (Smolders et al., 2004); the terrestrial isopod *Porcellio dilatatus* following biocide exposure (Ribeiro et al., 2001); the marine mussel *Mytilus edulis* after exposure to the pharmaceutical compound atorvastatin (Falfushynska et al., 2019); and the green lipped mussel *Perna viridis* after cadmium and Cu exposure (Yeung et al., 2017).

Interestingly, mixed exposure groups Pb9.2 mg kg^{-1} + Pyrene970 $\mu\text{g kg}^{-1}$ and Pb4.5 mg kg^{-1} + Pyrene480 $\mu\text{g kg}^{-1}$ showed lower concentrations of lipids during the assimilation than elimination phase (1.93 : 2.03 : 1.94 : 2.11 respectively) whereas single exposure groups Pb9.2 mg kg^{-1} and Pb4.5 mg kg^{-1} showed lower levels of lipids (1.83 : 2.17 : 1.85 : 2.17 respectively) and carbohydrates (1.51:1.99: 1.41:1.45 respectively). Moreover, mean Σ worm tissue Pb concentrations for the mixed exposure groups were significantly lower than the individual Pb exposure groups: Pb9.2 mg kg^{-1} + Pyrene970 $\mu\text{g kg}^{-1}$ (337.71 mg kg^{-1}); Pb9.2 mg kg^{-1} (1068.18 mg kg^{-1}).

¹); Pb4.5 mg kg⁻¹ + Pyrene480 µg kg⁻¹ (497.81 mg kg⁻¹); Pb4.5 mg kg⁻¹(1033.88 mg kg⁻¹). This may indicate that the higher tissue concentrations of Pb deplete both lipid and carbohydrate reserves in *H diversicolor*. Also, statistical analysis from the present study revealed a partial correlation between worm weight, worm tissue Pb and lipid concentrations. In addition, a correlation exists between worm weight and lipid concentration for exposure group Pb9.2 mg kg⁻¹. These findings are in agreement with Durou et al. (2005a), who reported that lipid contents of *H diversicolor* from the contaminated Seine estuary, France, were positively correlated to weight further indicating the primary use of lipids in response to the increased demands of contamination exposure.

Lower concentrations of proteins were identified in the exposure groups Pb9.2 mg kg⁻¹, Pb4.5 mg kg⁻¹ + Pyrene480 µg kg⁻¹ and Pyrene480 µg kg⁻¹ during the assimilation phase suggesting that exposure to both Pb and pyrene (individually and in combination) resulted in the depletion of proteins to meet energetic demands. Utilisation of proteins to cope with increased energy requirements have been demonstrated following contamination exposure: phenol in the teleost fish *Brycon cephalus* (Hori et al., 2006); Cu in rainbow trout *Oncorhynchus mykiss* (Smith et al., 2001); atrazine in grass carp *Ctenopharyngodon Idilla* (Khan et al., 2016). Results gained in the present study agree with studies by Durou et al. (2005b), Pook et al. (2009) and Mouneyrac et al. (2010), where chronic exposure to toxicants depletes energy reserves in *H diversicolor*.

Lower energy determinants were observed during the elimination phase including reduced concentrations of proteins: Pb9. 2 mg kg⁻¹ + Pyrene 970 µg kg⁻¹ (1.48:1.36); Pyrene 970 µg kg⁻¹ (1.42:1.39); Pb 4.5 mg kg⁻¹(1.46:1.43), lipids :Pyrene 970 µg kg⁻¹ (2.09:1.76) and carbohydrates: Pb9. 2 mg kg⁻¹ + Pyrene 970 µg kg⁻¹ (1.50:1.17); Pb4.5 mg kg⁻¹ + Pyrene 480 µg kg⁻¹(1.42: 1.24); Pyrene 480 µg kg⁻¹ (1.44:1.37). Importantly, this may indicate the continued depletion of

energy reserves following exposure in response to increased transcription and production of detoxifying proteins and enzymes (Fossi Tankoua et al., 2012). As such, these results demonstrate long term toxic effects of Pb and pyrene on *H diversicolor* suggesting that detoxification has negative consequences for energy levels which continues post exposure.

As both pyrene and Pb are considered ubiquitous contaminants present globally in marine sediment (Beech et al., 2009), the effects of depleted energy determinants in populations of *H diversicolor* may be pervasive. As *H diversicolor* are considered a primary food source for fish and wading birds (Masero et al., 1999; Rosa et al., 2008), reduced energy determinants may cascade through trophic levels leading to increased predation rates to satiate calorific requirements in turn, reducing prey populations (Harborne et al., 2009; Smart and Gill, 2003). Reduced populations of invertebrate species have also resulted in high mortality rates of wading birds (Atkinson et al., 2000) and habitat switch, promoting competition of alternative resources (Smart and Gill, 2003). In addition, *H diversicolor* are key actors influencing sediment bioturbation (Gillet et al., 2012). Oxygenation of sediments, re-distribution of particulates and decomposition of organic matter (Bergström et al., 2019) are positively correlated to population density (Gillet et al., 2012). Therefore, reduced populations and health status of individuals may have adverse effects upon all ecosystems where *H diversicolor* are exposed to Pb and pyrene.

7.5 Conclusion

Lower levels of lipids, carbohydrates or proteins were found during the assimilation period for all individual and mixed exposure groups. This may indicate that exposure to both pyrene and Pb at both concentrations (individually and in combination) increase the energetic costs to *H diversicolor*.

Single Pb exposure groups: Pb9.2 mg kg⁻¹ and Pb4.5 mg kg⁻¹ had depleted lipids and carbohydrates levels whereas the mixed Pb / pyrene groups at respective concentrations showed only lower lipid levels. Higher concentrations of Pb were found in worm tissue for the Pb only exposure groups suggesting that the assimilation of higher concentrations of Pb were more energetically demanding.

Importantly, lower energy determinants were observed post exposure during the elimination phase for exposure groups: Pb9.2 mg kg⁻¹ + Pyrene 970 µg kg⁻¹; Pyrene 970 µg kg⁻¹; Pb 4.5 mg kg⁻¹; Pb4.5 mg kg⁻¹ + Pyrene 480 µg kg⁻¹; Pyrene 480µg kg⁻¹ and may suggest exposure and subsequent detoxification depletes energy reserves during and post exposure.

8 General Discussion

8.1 Thesis summary and contribution to original knowledge

The overall aim of the thesis was to identify bioaccumulation of metal (s) and PAH (s) by *H diversicolor* from environmental matrices of the Fleet Lagoon, Dorset UK and to assess potential co - toxicities of a selected metal (s) and PAH present in the lagoon. Using environmentally relevant concentrations from sediment analysis the biochemical responses, behavioural and energy budget change following exposure to individual and mixtures of metal (s) and PAH (s) was investigated. This aim was addressed through analysis of environmental matrices and worm tissue taken from a sample survey of the lagoon coupled with laboratory investigations where exposed worms were analysed for biochemical responses, behavioural change and energy budget alteration following exposure to selected individual and mixtures of metal (s) and PAH.

8.2 Metal bioavailability from environmental matrices of the Fleet lagoon, Dorset UK

Relationships between small sediment particle size and organic matter found in the present study are recognised (Froehner et al., 2009; Koiter et al., 2015; Ma et al., 2016). The transportation and accretion in the Fleet, may be influenced by reduced tidal flushing, water exchange, embayment features and shallow water depths (Robinson, 1983), evident towards the Abbotsbury end of the lagoon. As such, relationships between metal concentrations and granulometric sediment analysis revealed how these factors may influence accumulation of metals in the marine environment. Moreover, the apparent increase of metal concentrations at specific locations in comparison with historic studies (Nunney and Smith 1995) may relate to the sorption affinity of the sediment composition.

In particular, the high LOI results found at site 10 which may be attributed to the presence of the oyster farm and potential influence on the sorption of Cu, Pb and Zn at this site.

Metal bioavailability is defined as the fraction of metal which is biologically obtainable by an organism and is related to its speciation and ability for release from a bound particulate (Luoma, 1983; Meyer, 2002). Presently, there is no universally accepted approach to determine the bioavailability of metals to benthic invertebrates. Consequently, the use of several methods including fractionation analysis of sediment (Pueyo et al., 2008) are advised.

Additionally, it is known that some species of benthic marine polychaetes including *H diversicolor* obtain food particles from the ingestion of large quantities of sediment (Rainbow et al., 2009a). Consequently, digestive actions may act to release metals from sediments, providing a further route of metal uptake. Therefore, total metal and sediment fractionation analysis to determine metal bioavailability may not adequately address the uptake of metal fractions via ingestion, under-estimating the influence of sediment ingestion as an exposure pathway. To assess this apparent fundamental uptake pathway, digestive enzymes commonly Proteinase K (Ianni et al., 2010; Rosado et al., 2016; Turner and Olsen, 2000) have been used to investigate digestive influence on metal bioavailability from sediment. Specifically, the present study added to the understanding of exposure pathways and bioaccumulation estimation by finding that total metal concentrations of all studied metals were not correlated to worm tissue concentrations, whereas proteinase K analysis identified relationships between Cu, Pb and worm tissue concentrations. Sediment digestion as a primary uptake pathway for many benthic organisms is acknowledged (Baumann and Fisher, 2011a; Casado-Martinez et al., 2009; Lee et al., 2000; Wen-Xiong et al., 1999) therefore, results gained in the present study are comparable for Cu and Pb assimilation by *H diversicolor*. Moreover, results are in

agreement with Bignasca et al. (2011), Ianni et al. (2010) and Rosado et al. (2016) where the first step of sequential extraction overestimates the bioavailable fraction in comparison with proteinase K extraction. However, results from this study support the use of BCR as a more accurate indicator of metal bioavailability than total metals. Nonetheless, a relationship was identified between total metal As concentrations determined via BCR sequential extraction from sediment and worm tissue As concentrations. This may indicate that within the Fleet sediment, As is assimilated by *H diversicolor* from the bioavailable exchangeable fraction (Lui et al., 2014).

The influence of pore water as a primary route of metal exposure has been suggested for burrowing benthic invertebrates (Chapman et al., 2002, Li et al., 2014, Wang and Fisher., 1999b). Although, Rainbow et al., (2009) and Buffet et al., (2011) propose that *H diversicolor* exposure to pore water is minimal, due to burrow aeration using water drawn from the water column. Partial correlations between proteinase K and pore water using worm tissue metal concentrations as the controlling factor identified relationships for Cu, Pb and Zn. It is not clear whether pore water metals are ingested during the feeding process, or if assimilation occurs through epidermal uptake and requires further investigation to determine these specific exposure pathways.

It is evident that metal bioavailability remains a complex issue. Results from the present study support the acknowledged inaccuracies of the use of total metals in sediment (Berthet et al., 2003; Mayer et al., 1997; Pueyo et al., 2008; Rainbow P. S et al., 2009a) to determine metal bioavailability to benthic organisms. Results gained from this study identified that proteinase K is an appropriate method to determine metal assimilation in sediment ingesting species including *H diversicolor* as relationships for Cu, Pb and worm tissue concentrations were determined. There is no evident literature that this biomimetic approach has been conducted using *H diversicolor* and is therefore suggested that this method may

compliment future metal bioavailability studies using this species. Although, it is acknowledged that further investigations are required to determine the suitability of this method for other metals. Foremost, environmental research must address species specific ecology and biology to understand all the factors which may influence assimilation.

8.3 Polycyclic aromatic hydrocarbons within the environmental matrices of the Fleet lagoon and bioaccumulation by *H diversicolor*.

High concentrations of specific PAH's were found in the sediment samples of the Fleet lagoon. Comparisons with previous historic sediment analysis conducted by Nunney and Smith (1995) indicate significant accumulation. It is acknowledged that samples obtained for this investigation may have located hot spots of contamination also, it is possible that a recent input of PAH's into the Fleet may have occurred although there is no evidence of this from the landowners. Importantly, the concentrations identified in the Fleet lagoon by this study are alarming. Furthermore, there is no evident literature regarding studies of PAH identification and quantification along the South West coastline. Therefore, it is not possible to determine whether PAH concentrations are increasing in this region or if this chronic increase is specific to the Fleet Lagoon.

All locations excluding sites 5 and 8 had concentrations in sediments which exceeded the threshold and potential effects limits (TEL / PEL) of the Canadian sediment quality guidelines (CCME, 2001). It is recognised that distribution of PAH's in sediment maybe influenced by sediment characteristics including concentrations of organic matter (Hassan et al., 2018; Ruiz-Fernández et al., 2012; Soliman et al., 2019; Wang et al., 2015; Wang et al., 2001). Results from the present study are in agreement as significant relationships were found: clay, very fine silt, fine silt fractions and naphthalene; LOI and

acenaphthene, phenanthrene and anthracene. Importantly, reduced tidal flushing and water exchange (Robinson, 1983) towards the Abbotsbury end of the lagoon may be an influencing factor in PAH accumulation.

4 ringed PAH's were found to be the dominant species in sediment, which may originate from the atmospheric deposition of automobile exhaust products and urban run off (Xue et al., 2016). Isomer analysis indicated primary sources of PAH's in the Fleet were from pyrogenic origins excluding site 2 which originated from petrogenic combustion. However, isomer determination of PAH sources should be viewed with caution, as environmental factors including weathering and microbial degradation may alter the state of the PAH, giving a false indication of the original source (Turner 2002, Turner 2015, Stogiannidis and Lane., 2014).

Analysis of worm tissue identified concentrations of ≤ 4 ringed PAH's. Correlations were identified between both acenaphthene, anthracene in sediment and worm tissue concentrations. It is possible that the confounding influence of PAH metabolism on PAH bioavailability, where active metabolism of PAH's by organisms may indicate lower uptake (Rust et al., 2004) may influence the concentrations found. Furthermore, the dominance of low ringed PAH's in worm tissue may indicate reduced metabolism by this species, potentially a result of low affinity with the aryl hydrocarbon receptor (Shailaja and D'Silva, 2003). However, as there is no apparent research regarding the metabolism of low ringed PAH's by *H diversicolor* or marine polychaete species, therefore the assimilation and excretion by this species is uncertain.

Conversely, although pyrene levels found in the sediment were exceptionally high at some site locations, worm tissue concentrations were low. It is acknowledged that *H diversicolor* metabolise pyrene to excretable products (Geissing et al., 2003, Christensen et al., 2002). As such, the low levels recorded in these worms may not provide an

accurate picture of assimilation. Results from Chapter 6 in the present study showed pyrene worm tissue concentrations were < 1% after 7 days of exposure in relation to concentrations of the metabolic product 1 - OHP. Therefore, the use of total PAH concentrations may not be a reliable method to investigate uptake.

Worm tissue concentrations of pyrene, fluoranthene and phenanthrene were identified. These PAH's are acknowledged to sorb primarily to soot particulates originating from pyrolytic sources (Yunker, 2002). Yunker et al. (2015), hypothesise that these soot bound PAH's particulates are less bioavailable to organisms due to the reduced likelihood of dermal uptake. However, this does not account for uptake related to ingestion. As previously discussed, *H diversicolor* ingests large quantities of sediment to acquire sufficient energy from food particulates (Rainbow et al., 2009) therefore, ingestion and assimilation of soot bound PAH's by *H diversicolor* is possible. The presence of these PAH's in worm tissue from the present study therefore strongly suggests ingestion as the primary uptake pathway although it is acknowledged that other modes of assimilation may have occurred. Again, results from this study highlight how bioaccumulation of contamination by marine organisms must not be generalised, as differing physiologies and ecological niches among species are important factors governing accumulation.

8.4 Behavioural alterations of *H diversicolor* following exposure to Cu, Pb and pyrene individually and in combination.

The use of behaviour in environmental toxicology research provides a non - invasive method to detect toxicity at the whole organism level (Canty et al., 2009). Where behaviour following exposure has been negatively affected, this may have deleterious consequences for a whole population which may reside in polluted environments. Results from the present study clearly demonstrated that Cu, Pb and pyrene individually and in combination alter *H diversicolor* behaviour, confirming the usefulness of this parameter in ecotoxicological

investigation. However, high rates of mortality were observed in Cu exposure experiments. As median values of sediment concentrations obtained in Chapter 3 were used as environmentally relevant concentrations, these outcomes were surprising. Aqua cultured worms purchased for this series of experiments were selected as previous exposure to contamination may affect results due to genetic adaptation of detoxification mechanisms. As a result, normal regulation of specific enzymes and proteins associated with Cu regulation may have occurred. Additionally, higher bioavailability of metals in spiked sediment studies (Simpson et al., 2004) may also have contributed to the observed mortalities.

Importantly, burrowing rates for Cu exposed worms and the highest Pb exposure group were slower than those of the respective concentration metal + pyrene mixtures. Additionally, worm tissue concentrations of Pb and Cu were higher in these single metal exposed groups. This may indicate that body concentrations of metals influence burrowing behaviour in *H diversicolor*. Furthermore, lower metal body concentrations of Cu and Pb in the mixed Cu + pyrene and highest Pb + pyrene groups suggest an antagonistic interaction between these metals and pyrene.

Results from the present study indicate that both Pb and Cu tissue concentrations may influence the burrowing rates of *H diversicolor*. This may result from the inhibition of the ATPase Ca⁺ pump (Brix et al., 2017, Carfagna et al., 1996) or blockade of voltage dependant calcium channels in neurons (Busselberg et al., 1994; Büsselberg et al., 1998; Sanah et al., 2012). Additionally, cellular membrane alteration via pyrene uptake (Sikkema et al., 1995) may alter ion regulation and consequently, P - ATPase ion transporters (Gauthier et al., 2014, Li et al., 2011).

AChE activities for all Pb and pyrene exposed groups were significantly different from the control and support the neurotoxic status of both Pb and pyrene (Rabitto et al., 2005, Martinez-Tabche

et al., 2001, Kim and Kang., 2007, Christensen et al., 2002, Kalman et al., 2009). However, the combined pyrene + Pb, and individual pyrene groups had the lowest AChE levels indicating that pyrene is a stronger neurotoxin than Pb. Conversely, burrowing rates of the combined Pb9.2 mg kg⁻¹ + Pyrene970 µg kg were faster than the Pb9.2 mg kg⁻¹ exposure group suggesting that specific AChE activity levels may not relate directly to burrowing speed. The determination of AChE activity regarding a contaminants neurotoxic status are commonly used as biomarkers in toxicological research. However, results gained in the present study suggest that *H diversicolor* burrowing behaviour may be influenced by other modes of toxicity namely, Ca²⁺ regulation following exposure to Pb. Although, there is no evident literature regarding this interaction following Pb exposure in this species and warrants further investigation.

Importantly, results from this investigation clearly show that the burrowing rates of *H diversicolor* are negatively affected following exposure to Cu, Pb and pyrene. Also, Pb and pyrene elicit neurotoxicity in *H. diversicolor*. This may have adverse consequences for polychaete populations which reside in environments where these contaminants are present. Locomotory performance specifically burrowing speed relates directly to predator avoidance and survival. Therefore, higher predation rates may occur ultimately leading to reduced populations (Robinson and Peters, 2018). Additionally, altered AChE activity in *H diversicolor* reported in the present study has been directly linked to lower population density and biomass in contaminated environments (Métais et al., 2019).

8.5 Biochemical responses following exposure to Pb and pyrene by *H diversicolor*

Worm tissue results of both the higher (Pb9.2 mg kg⁻¹) and lower (Pb4.5 mg kg⁻¹) Pb series showed reduced assimilation of Pb when combined with pyrene at both concentrations (Pyrene970 µg kg⁻¹ +

Pyrene480 $\mu\text{g kg}^{-1}$). Interestingly, results from the 7- day behaviour exposure detailed in Chapter 6 showed that Pb concentrations from the lower combined group Pb4.5 mg kg^{-1} + Pyrene480 $\mu\text{g kg}^{-1}$ had higher worm tissue Pb concentrations. However, Pb concentrations in worm tissue from this test series showed concentrations between the Pb4.5 mg kg^{-1} and Pb4.5 mg kg^{-1} + Pyrene480 $\mu\text{g kg}^{-1}$ groups were similar for sample days 1, and 7. On sample day 14 and 21 there was a large increase in Pb concentration in the Pb only group. Thus, it is suggested that exposure to pyrene at 480 $\mu\text{g kg}^{-1}$ in combination with Pb over a time period >7 days may reduce assimilation related to the direct binding of pyrene to the cellular membrane. Subsequent alteration of membrane fluidity may then Pb to ion - regulatory dysfunction, reducing the transport of Pb^+ ions across the cell membrane via Ca^{2+} and Na^+ / K^+ ATPases (Gauthier et al., 2016, Kim et al., 2016, Shuona et al., 2017).

Pb concentrations in worms from exposure groups Pb9.2 mg kg^{-1} and Pb9.2 mg kg^{-1} + Pyrene970 $\mu\text{g kg}^{-1}$ increased during the elimination phase. It is possible that Pb particles were attached to the mucous membrane observed on all worms when they were removed from the spiked sediment tanks and placed into the clean sediment tanks.

Pyrene was assimilated by *H diversicolor* in all individual and combined exposure tanks where rapid uptake was observed between sample days 1 and 7 for all exposure groups. The phase I metabolic product of pyrene, 1 - OHP was then detected in tissue from all exposure groups between days 1 and 7. Interestingly, pyrene tissue concentrations for all exposure groups showed rapid decrease during sample days 1 - 14 for all exposure groups. However, 1 - OHP was detected until sample day 7 of the elimination phase. These results support research conducted by Christensen et al., (2002) who observed that this metabolite may be excreted and re – assimilated by *H diversicolor*. As both the phase I and phase II metabolic

products of pyrene have been identified in gut tissue of this species (Geissing et al., 2003, Christensen et al., 2002), it is reasonable to suggest that 1 - OHP may be excreted into the immediate environment. As such, these excretory products may be available to organisms, although there is no research evident regarding the distribution and fate of these products in the marine environment.

Metallothionein's (MT) were not detected in worm tissue following Pb exposure. There are no evident reports of MT induction following exposure to Pb alone by *H diversicolor* although, this has been witnessed in other species (Won et al., 2012, Aouini et al., 2018, Ferrante et al., 2018, Bordon et al., 2018). High molecular weight (HMW) proteins in association with assimilated Pb have been identified by Raimundo et al. (2010) in the Common octopus, *Octopus vulgaris* and the Japanese scallop, *Mizuhopecten yessoensis* (Gao et al., 2016). Therefore, HMW proteins may be responsible for Pb sequestration in *H diversicolor* rather than MT's. However, basic metal ATPase efflux or lysosome sequestration may be the primary mechanisms evoked following Pb exposure in this species although, there is no existing research to support these theories.

Both Pb and pyrene alone and in combination, initiate reactive oxygen species (ROS) production in *H diversicolor*. All biochemical responses of ROS showed higher values than those of the control group. Interestingly, GSTs levels in worms showed values lower during the assimilation than the elimination phase of the experiment. This may be attributed to inhibition of GSTs by these contaminants. Inhibition of GSTs following Pb exposure supports existing research (Hariharan et al., 2012, Lui et al., 2011, Ozkan-Yilmaz et al., 2014), which is attributed to an inhibiting mechanism related to interactions with sulfhydryl groups (Dai et al., 2018, Dai et al., 2012, Kim et al., 2017). Furthermore, GSTs levels in the exposure group Pb4.5 mg kg⁻¹ + Pyrene480 µg kg⁻¹ were lower than the Pb (Pb4.5 mg kg⁻¹) and pyrene (Pyrene480 µg kg⁻¹) groups. This may suggest that exposure

to these contaminants at these concentrations produces a co - toxic effect on GSTs in *H diversicolor*. Additionally, lower levels of GSTs during the assimilation phase may have affected the metabolism of pyrene through reduced conjugation reactions. Following transference of worms to clean sediment for the elimination phase, GSTs levels increased which may have resulted in the efficient metabolism of pyrene to 1 - OHP. This may explain the observed levels of I - OHP during both the assimilation and elimination phases of the experiment. Although metabolic products of pyrene in *H diversicolor* have been recorded (Geissing et al., 2003, Christensen et al., 2002) there is no existing research regarding how levels of GSTs may inhibit these processes.

Similarly, CYP450 levels were found to be lower during the assimilation than elimination phase of the experiment for all exposure groups. This may indicate an inhibitory response to these contaminants also, the continued expression of CYP450 during the elimination phase for pyrene exposed groups may be in response to the presence of the metabolite 1 - OHP. However, production of ROS following exposure to Pb and pyrene may increase the degradation of CYP proteins or inhibit synthesis (Gauthier et al., 2016). The lower CYP450 levels during the assimilation phase of the Pb exposure groups supports the research of Korashy and El-kadi (2012) although there is no existing research to support pyrene exposure CYP450 inhibition where these proteins are critical in metabolism (Geissing et al., 2003). Therefore, results gained in the present study suggest a novel finding regarding pyrene exposure in *H diversicolor* and warrants further investigation.

DNA adducts resulting from ROS in *H diversicolor* were detected in all exposure groups and were higher than those of the control. This suggests that Pb and pyrene individually and in combination at the concentrations used produce ROS to levels which result in lesions involving modified guanosine. Importantly, the pyrene only exposure groups showed that although both pyrene and the metabolite 1 -

OHP were undetected from day 7 of the elimination phase, 8 - OHdG levels remained high. This may indicate a slow rate of base repair or more ominously, that the adducts formed are unreparable. There is no evident literature regarding the formation or repair of DNA adducts following exposure to Pb and pyrene by marine polychaetes.

Therefore, results in the present study may indicate a novel finding. In addition, following Pb exposure, the dissociation of Zn²⁺ by Pb²⁺ in Zn fingers have been evidenced (Sivo et al., 2018) and may Pb to protein mis - folding and subsequent reduction of DNA binding affinity (Huang et al., 2004a; Petering et al., 2000). Again, there is no literature apparent regarding this dissociation for marine polychaetes and warrants further investigation. Importantly, consequences for *H diversicolor* which inhabit Pb and pyrene polluted environments, include altered gene expression, strand misreading, chromosomal alteration and loss of heterozygosity (Evans et al., 2004, Nerbert and Dalton., 2006).

8.6 Energetic costs of Pb and pyrene exposure.

Results from this investigation show lower levels of lipids, carbohydrates or proteins in all exposed groups during the assimilation phase of these experiments. These results clearly show the energetic costs of Pb and pyrene exposure individually, and in combination. Furthermore, these findings agree with the cost of tolerance theory proposed by Holloway et al. (2000) where exposure to chronic contaminants depletes energy reserves which in turn, may reduce feeding activities.

Mixed Pb + pyrene exposures revealed lower levels of lipids for all test exposures whereas, lower levels of carbohydrates and lipids were determined in the individual Pb test exposures. As worm tissue Pb concentrations were higher in the Pb only test exposures, increased Pb assimilation intensifies the energetic demands of *H diversicolor*. Lower concentrations of proteins were identified in mixed Pb + pyrene, individual Pb and individual pyrene exposure

groups. Although the exploitation of proteins following contaminant exposure have been reported (Khan et al., 2016, Hori et al., 2006, Smith et al., 2001), there is no literature evident reporting depletion of proteins following Pb or pyrene exposure, hence this is a novel finding.

Importantly, lower energy determinants were observed post exposure for both individual and mixed groups. Increased levels of detoxification proteins / enzymes reported in Chapter 6 during the elimination phase suggested that the toxic effects of Pb and pyrene endure post exposure. Continued depletion of energy stores Pb to increased food consumption following exposure to contaminants, in the earthworm *Eisenia andrei*, in response to the energetic demands of detoxification strategies (Svendsen and Weeks, 1997). As food availability *in situ* is variable, *H diversicolor* which inhabit Pb and pyrene contaminated environments may not meet increased energetic requirements leading to weight loss and reduced health status (Johnston et al., 2014). Moreover, slower burrowing rates for Pb and pyrene exposed worms ascribed to the alteration of AChE activity (reported in Chapter 5), may impair feeding mechanisms and food assimilation. The inability to satiate these increased energy requirements may ultimately Pb to slower growth and maturation rates, reduced health status and ultimately mortality (Johnston et al., 2014).

Svendsen and Weeks (1997) also reported that although food consumption of *Eisenia Andrei* increased following exposure, reproduction ceased. Cessation of reproduction following contamination exposure has been observed directly correlated to reduced energy budgets: zebrafish *Danio rerio* exposed to water effluent (Smolders et al., 2003); springtails *Proisotoma minuta* exposed to cadmium and Zn; fathead minnow *Pimephales promelas* exposed to bisphenol A (Sohoni et al., 2001). Furthermore, Durou et al. (2007), report the depletion of *H diversicolor* population densities from contaminated sediment of the Seine, France. They further

describe that low energy stores found in this population of worms correlated to decreased egg production and ultimately, reduced population structure. As a key species, these worms are considered a primary food source for higher organisms (Moreira, 1999) and as ecosystem engineers due to its role in sediment bioturbation (Gerino et al., 2003). Diminished health status of *H diversicolor* present a pervasive threat to the functioning not only of the Fleet lagoon, where concentrations of Pb (Chapter 3) and pyrene (Chapter 4) exceed those used in the present study, but all ecosystems where Pb and pyrene are present.

8.7 Limitations

The present study investigated water and sediment metal and PAH concentrations in the Fleet Lagoon to establish environmentally relevant concentrations of metals and PAH's. The bioavailability of these contaminants to the marine polychaete *H diversicolor* and metal (s) and PAH (s) would be identified for use in exposure investigations. The limitations of this investigation are explained below.

8.7.1 *Hediste diversicolor* from the Fleet Lagoon

Ideally, in - situ assessment of *H diversicolor* behaviour, biochemical responses and energetic determinants against a control group would provide information regarding the health status of these populations. Also, a full species survey of the selected sample locations may provide valuable information regarding the population density and biomass of this species. However, resident worms may be exposed to a variety of contaminants. Therefore, biochemical, behavioural and energetic comparisons between Pb, Cu and pyrene laboratory exposed worms and resident worms would not be relevant. Also, full contamination screening of the lagoon and labour - intensive site surveys would be beyond the time and financial budgets of the present study.

Worms were not identified in sample locations 8 and 9 detailed in Chapter 3. As *H diversicolor* builds burrows in soft sediments (Scaps 2002), the high concentration of larger stones found in the sediment at these locations may exclude this burrowing activity. Sampling further into the lagoon proved hazardous due to the presence of deep of mud away from the shoreline. To sample away from the shoreline would require access to a boat which was beyond the financial budget for this study.

8.7.2 Cu exposure to *H diversicolor*

Median values of Cu concentrations from lagoon sediments reported in Chapter 3 were used as environmentally relevant levels to conducted exposure experiments. However, high mortality rates of worms exposed to the initial (31 mg kg⁻¹ and 15 mg kg⁻¹) and subsequent reduced concentrations (7 mg kg⁻¹ and 4 mg kg⁻¹) occurred. This may relate to the increased bioavailability of Cu in spiked sediment experiments due to lower levels of available organic matter and subsequent fractionation (Simpson et al., 2004).

Individuals which inhabit contaminated environments may genetically increase the synthesis of proteins and enzymes responsible for regulation (Rainbow et al., 2009). However, worms used in the present study were purchased from a commercial aquaculture facility where they were housed in a mixture of clean sediment and vermiculite. These worms were not previously exposed to environmental concentrations of Cu. Therefore, mortality may have occurred as assimilation of Cu exceeded detoxification and excretion. Given this, pilot studies to determine sub-lethal concentrations of Cu for these worms may have provided clarity however, the costs were prohibitive to this study.

8.7.3 Pyrene assimilation

Pyrene exposure studies reported in Chapters 5 - 7 showed the rapid uptake of pyrene by *H diversicolor*. Sample days for behavioural

assessment were each day of a 7 - day period. Sample days for biochemical and energetic responses (Chapters 6 and 7 respectively) occurred each 7 days over a 56 - day period. This study may have benefitted from increased sample rates during the initial exposure to fully understand the assimilation rate of pyrene by these worms. However, this would have vastly increased the number of individuals required resulting in multiple tanks for each exposure. Therefore, the increased associated costs, equipment and facilities would have been beyond the financial budget of the present study.

8.8 Further research

Results gained from this study have highlighted areas where further research is necessary. To fully determine the spatial distribution of both metal (s) and PAH (s) in sediment of the Fleet Lagoon, Dorset, UK, it is suggested that further investigations are conducted. In particular, the use of sediment cores and radio isotope data analysis may provide clarification. As PAH levels were found to be extremely high in some sample locations it is advised that further sediment analysis is urgently required.

Research regarding alterations to cellular membranes following pyrene exposure should be conducted using cell membrane potential analysis and ATPase activity in relation to ion uptake. To determine the impact of GST and CYP450 levels on the metabolism of pyrene and its metabolic products by *H diversicolor*, further studies potentially using radiolabelled products may clarify any potential inhibition. Additionally, the detection of pyrene metabolites within marine sediment in environments where pyrene and *H diversicolor* are present may elucidate the fate and distribution of these products.

<4 ringed PAH exposure studies using *H diversicolor* are necessary to identify the assimilation, excretion and metabolic products. Reduced metabolism and excretion of these PAH's by *H diversicolor* may Pb to trophic transfer and warrants further investigation.

ROS, 8 - OHdG adducts and alterations of energy budgets were reported by *H diversicolor* in this study following exposure to pyrene and Pb. This may Pb to deleterious consequences for individuals and populations which reside in environments where these contaminants are present. However, to fully elucidate whether long term effects occur including fitness and reproduction it is suggested that epigenetic and genetic studies are conducted using this species.

8.9 Conclusion

The work presented in this thesis determined concentrations of metals and PAH's from water and sediment of the Fleet lagoon. The bioavailability of metals to *H diversicolor* was investigated using a variety of techniques. Although step 1 of the BCR sequential sediment digestion over - estimated the bioavailable fraction of metals to *H diversicolor*, this method proves to be a more reliable indicator of bioavailability than total metal concentrations . However, proteinase K sediment digestion correlated to Cu and Pb worm tissue concentration highlighting the role of sediment digestion and assimilation of metals by this species. Correlations between sediment characteristics were identified: Cu with medium and coarse sand; Pb with very coarse sand; LOI with Cu, Pb and Zn. The highest levels of LOI, Cu, Pb and Zn were found at site 10. Therefore, the high levels of LOI at this site location may influence accretion of these metals. Additionally, the presence of an oyster aquaculture facility near this location may affect the concentration of organic matter found at this location.

PAH concentrations were found to exceed the PEL of the Canadian sediment quality guidelines in sample locations 2, 4, 6, 7 and 10. Isomer source analysis indicated that PAH's found at sample locations 1, 3, 4, 5, 6 7, 8, 9 and 10 originate from pyrolytic combustion of fossil fuels and biomass whereas, petroleum combustion was identified as the original source at site 2. Correlations between naphthalene, clay, very fine silt and fine silt

sediment fractions were identified. High concentrations of these sediments were identified at site 1 and may influence the high naphthalene levels found at this site. Furthermore, a correlation was identified between LOI, acenaphthene, phenanthrene and anthracene. Σ concentrations of these PAH's were found at site 4 which had the second highest LOI levels and may therefore influence accretion.

≤ 4 ringed PAH's were identified in worm tissue and may indicate rapid assimilation and metabolism or reduced affinity of the aryl-hydrocarbon receptor and low molecular weight PAH's. Furthermore, the presence of the predominately soot bound PAH's pyrene, fluoranthene and phenanthrene in worm tissue suggest ingestion as an important uptake pathway.

Assimilation of Cu, Pb and pyrene adversely affected burrowing rates in *H diversicolor*. Moreover, interactions between Pb, Cu and pyrene were observed including change of metal assimilation rates in the presence of pyrene. Both Pb and pyrene were altered AChE activity however, mixed Pb + pyrene exposures demonstrated additive toxicity on AChE activity.

Both Pb and pyrene were assimilated by *H diversicolor*. Pyrene uptake was rapid resulting in the identification of the phase 1 metabolite 1 - OHP. Worm tissue Pb concentrations increased during the elimination phase of the 28 d exposure experiment. This may have occurred due to Pb contamination adhering to mucous layers present on worms when they were removed from spiked sediment tanks. As they were then placed into clean sediment tanks, adhered Pb particles may have then been assimilated by the worms. The apparent lack of Pb excretion by the worms suggests cellular and tissue sequestration.

MT's were not initiated by Pb assimilation during exposure tests indicating regulation by basic metal ATPase efflux or sequestration by lysosomes. Both Pb and pyrene exposure were found to initiate

ROS in *H diversicolor*, as increased levels of SOD, GST were identified for all exposure groups during the assimilation phase. However, SOD levels for exposure group Pb4.5 mg kg⁻¹ remained high during the elimination phase, indicating increased persistent levels of ROS. GST levels for the mixed group Pb9.2 mg kg⁻¹ + Pyrene970 µg kg⁻¹ exceed those of the individual exposures and may highlight additive effects of these contaminants. Interestingly, GST levels for all exposure groups during the elimination phase exceed levels of the assimilation phase. This reduction during the assimilation phase may relate to its exploitation, and therefore depletion, in ROS metabolism or more ominously, inhibition of synthesis. CYP450 levels were increased for all exposure groups during the assimilation phase. Again, higher levels of CYP450 were identified during the elimination phase for all exposure groups. This may indicate its role in ROS reduction or inhibition by Pb and pyrene. DNA adducts in the form of 8 - OHdG were identified for all exposure groups throughout the assimilation and elimination phases. The presence of these adducts during the elimination phase suggests ineffective regulation of ROS.

Exposure to Pb and pyrene reduced lipids, carbohydrates or proteins in *H diversicolor*. Individual Pb exposed groups showed lower lipid and carbohydrate levels than the mixed Pb + pyrene groups. Higher tissue concentrations of Pb in the individual Pb groups suggests that higher Pb assimilation is more energy depleting. Depleted energy stores were identified for both individual and mixed exposure groups during the elimination phase. This may relate to the continued expression of biochemical detoxification mechanisms during this phase reported in Chapter 6. This thesis set to determine bioaccumulation of metal (s) and PAH (s) by *H diversicolor* from environmental matrices of the Fleet lagoon, Dorset, UK, and to assess the behavioural, biochemical and energetic effects of exposure to both Pb and pyrene. All aims were addressed to improve

the understanding of assimilation and subsequent effects of exposure on the marine polychaete *H diversicolor*.

9. References

- Abebe, A.T., Devoid, S.J., Sugumaran, M., Etter, R. and Robinson, W.E., 2007. Identification and quantification of histidine-rich glycoprotein (HRG) in the blood plasma of six marine bivalves. *Comparative Biochemistry and Physiology Part B: Biochemistry and Molecular Biology*, 147(1), pp.74-81.
- Aberson, M. J. R., S. G. Bolam, and R. G. Hughes, 2011, The dispersal and colonisation behaviour of the marine polychaete *Nereis diversicolor* (O. F. Müller) in south-east England: *Hydrobiologia*, 672 (1), p. 3-14.
- Aberson, M. J. R., S. G. Bolam, and R. G. Hughes, 2016, The effect of sewage pollution on the feeding behaviour and diet of *Hediste* (*Nereis diversicolor* (O.F. Müller, 1776)) in three estuaries in south-east England, with implications for saltmarsh erosion: *Marine Pollution Bulletin*, 105 (1), p. 150-160.
- Aboul-Ela, H. M., A. A. Saad, A. M. A. El-Sikaily, and T. I. Zaghoul, 2011, Article: Oxidative stress and DNA damage in relation to transition metals overload in Abu-Qir Bay, Egypt: *Journal of Genetic Engineering and Biotechnology*, 9 (1), p. 51-58.
- Abuchacra, P.F.F., Aguiar, V.M.C., Abuchacra, R.C., Neto, J.B. and Oliveira, A.S., 2015. Assessment of bioavailability and potential toxicity of Cu, Zn and Pb, a case study in Jurujuba Sound, Rio de Janeiro, Brazil. *Marine pollution bulletin*, 100 (1), pp.414-425.
- Alsop, D., T. Y. T. Ng, M. J. Chowdhury, and C. M. Wood, 2016, Interactions of waterborne and dietborne Pb in rainbow trout, *Oncorhynchus mykiss*: Bioaccumulation, physiological responses, and chronic toxicity: *Aquatic Toxicology*, . 177, p. 343-354.
- Álvarez-Muñoz, D., Llorca, M., Blasco, J. and Barceló, D., 2016. Contaminants in the marine environment. In *Marine Ecotoxicology* (pp. 1-34). Academic Press.
- Alvarez, M. B., P. Y. Quintas, C. E. Domini, M. Garrido, and B. S. Fernández Band, 2014, Chemometric approach to visualize and easily interpret data from sequential extraction procedures applied to sediment samples: *Journal of Hazardous Materials*, 274, p. 455-464.
- Amiard, J. C., C. Amiard-Triquet, S. Barka, J. Pellerin, and P. S. Rainbow, 2006, Review: Metallothioneins in aquatic invertebrates: Their role in metal detoxification and their use as biomarkers: *Aquatic Toxicology*, 76 (2), p. 160-202.
- Amiard, J. C., A. Geffard, C. Amiard-Triquet, and C. Crouzet, 2007, Relationship between the lability of sediment-bound metals (Cd, Cu, Zn) and their bioaccumulation in benthic invertebrates: *Estuarine, Coastal and Shelf Science*, 72 (3) , p. 511-521.
- Amiard-Triquet, C., 2009, Behavioral Disturbances: The Missing Link between Sub-Organismal and Supra-Organismal Responses to Stress? Prospects Based on Aquatic Research: *Human and Ecological Risk Assessment: An International Journal*, 15 (1), p. 87-110.
- Amiard-Triquet, C. and Amiard, J.C., 2012. Behavioral ecotoxicology. *Ecological Biomarkers: Indicators of Ecotoxicological Effects*, 253.
- Aouini, F., C. Trombini, M. Volland, M. Elcafsi, and J. Blasco, 2018, Assessing Pb toxicity in the clam *Ruditapes philippinarum*: Bioaccumulation and biochemical responses: *Ecotoxicology and Environmental Safety*, 158, p. 193-203.

- Araújo, C. V. M., K. C. Pereira, and J. Blasco, 2018, Avoidance response by shrimps to a Cu gradient: Does high population density prevent avoidance of contamination?: *Environmental Toxicology & Chemistry*, 37(12), p. 3095-3101.
- Arfaeinia, H., I. Nabipour, A. Ostovar, Z. Asadgol, E. Abuee, M. Keshtkar, and S. Dobaradaran, 2016, Assessment of sediment quality based on acid-volatile sulfide and simultaneously extracted metals in heavily industrialized area of Asaluyeh, Persian Gulf: concentrations, spatial distributions, and sediment bioavailability/toxicity: *Environmental Science & Pollution Research*, 23 (10), p. 9871-9890.
- Arias, A. s., A. Souissi, M. Roussin, B. Ouddane, and S. Souissi, 2016, Bioaccumulation of PAHs in marine zooplankton: an experimental study in the copepod *Pseudodiaptomus marinus*: *Environmental Earth Sciences*, 75 (8), p. 1-9.
- Ashauer, R. and Escher, B.I., 2010. Advantages of toxicokinetic and toxicodynamic modelling in aquatic ecotoxicology and risk assessment. *Journal of Environmental Monitoring*, 12(11), pp.2056-2061.
- Atkinson, C. A., D. F. Jolley, and S. L. Simpson, 2007, Effect of overlying water pH, dissolved oxygen, salinity and sediment disturbances on metal release and sequestration from metal contaminated marine sediments: *Chemosphere*, 69 (6), p. 1428-1437.
- Atkinson, P.W., Clark, N.A., Clark, J.A., Bell, M.C., Dare, P.J. and Ireland, P.L., 2000. The effects of changes in shellfish stocks and winter weather on shorebird populations: results of a 30-year study on the Wash, England. *BTO research report*.
- Au, D. W., M. W. Chiang, and R. S. Wu, 2000, Effects of cadmium and phenol on motility and ultrastructure of sea urchin and mussel spermatozoa: *Archives Of Environmental Contamination And Toxicology*, 38 (4), p. 455-463.
- Ayanka Wijayawardena, M. A., M. Megharaj, R. Naidu, and E. Stojanovski, 2018, Chronic and reproductive toxicity of cadmium, Zn, and Pb in binary and tertiary mixtures to the earthworm (*Eisenia fetida*): *Journal of Soils & Sediments: Protection, Risk Assessment, & Remediation*, 18 (4), p. 1602-1609.
- Badreddine, S., K. Abdelhafidh, M. Dellali, E. Mahmoudi, D. Sheehan, and B. Hamouda, 2017, The effects of anthracene on biochemical responses of Mediterranean mussels *Mytilus galloprovincialis*: *Chemistry & Ecology*, 33 (4), p. 309-324.
- Baird, D., P. R. Evans, H. Milne, and M. W. Pienkowski, 1985, Utilization of shorebirds of benthic invertebrate production in intertidal areas, *Oceanic Marine Biology Annual Review* 23, p. 573-597.
- Bajger, G., P. Konieczka, and J. Namieśnik, 2011, Speciation of trace element compounds in samples of biota from marine ecosystems: *Chemical Speciation & Bioavailability*, 23 (3), p. 125-142.
- Bamber, R. N., S. D. Batten, M. Sheader, and N. D. Bridgwater, 1992, On the ecology of brackish water lagoons in Great Britain: *Aquatic Conservation*, 2 (1), p. 65.
- Banni, M., Bouraoui, Z., Clerandeanu, C., Narbonne, J.F. and Boussetta, H., 2009. Mixture toxicity assessment of cadmium and benzo [a] pyrene in the sea worm *Hediste diversicolor*. *Chemosphere*, 77(7), pp.902-906.

- Barhoumi, R., Y. Mouneimne, E. Ramos, C. Morisseau, B. D. Hammock, S. Safe, A. R. Parrish, and R. C. Burghardt, 2011, Multiphoton spectral analysis of benzo[a]pyrene uptake and metabolism in a rat liver cell line: *Toxicology and Applied Pharmacology*, 253 (1), p. 45-56.
- Barka, S., 2007. Insoluble detoxification of trace metals in a marine copepod *Tigriopus brevicornis* (Müller) exposed to copper, zinc, nickel, cadmium, silver and mercury. *Ecotoxicology*, 16 (7), pp.491-502.
- Barnes, N., Bamber, R.N., Moncrieff, C.B., Sheader, M. and Ferrero, T.J., 2008. Meiofauna in closed coastal saline lagoons in the United Kingdom: Structure and biodiversity of the nematode assemblage. *Estuarine, Coastal and Shelf Science*, 79(2), pp.328-340.
- Barnes, R. S. K., 1994, *The Brackish-Water Fauna of NorthWestern Europe*, v. 1: Cambridge, Cambridge University Press.
- Barron, M.G., Heintz, R. and Rice, S.D., 2004. Relative potency of PAHs and heterocycles as aryl hydrocarbon receptor agonists in fish. *Marine environmental research*, 58(2-5), pp.95-100.
- Basu, N., 2015, *Applications and implications of neurochemical biomarkers in environmental toxicology*. Great Britain :Blackwell Publishing.
- Baumann, Z., and N. S. Fisher, 2011a, Modeling metal bioaccumulation in a deposit-feeding polychaete from labile sediment fractions and from pore water: *Science of the Total Environment*, 409 (3), p. 2607-2615.
- Baumann, Z., and N. S. Fisher, 2011b, Relating the sediment phase speciation of As, cadmium, and chromium with their bioavailability for the deposit-feeding polychaete *Nereis succinea*: *Environmental Toxicology & Chemistry*, 30 (3), p. 747-756.
- Beach, D. G., M. A. Quilliam, and J. Hellou, 2009, Analysis of pyrene metabolites in marine snails by liquid chromatography using fluorescence and mass spectrometry detection: *Journal Of Chromatography*, 877(2), p. 2142-2152.
- Bebiano, M. J., J. A. Nott, and W. J. Langston, 1993, Cadmium metabolism in the clam *Ruditapes decussata*: the role of metallothioneins: *Aquatic Toxicology*, 27 (3-4), p. 315-333.
- Benedetti, M., M. E. Giuliani, and F. Regoli, 2015, Oxidative metabolism of chemical pollutants in marine organisms: molecular and biochemical biomarkers in environmental toxicology: *Annals Of The New York Academy Of Sciences*, 1340 (1), p. 8-19.
- Benitez-Trinidad, A. B., Y. Y. Bernal-Hernández, C. L. Moreno-Hernández, I. M. Medina-Díaz, M. L. Robledo-Marenco, B. S. Barrón-Vivanco, D. Domínguez-Ojeda, C. A. Romero-Bañuelos, M. I. Girón-Pérez, and A. E. Rojas-García, 2014, Acetylcholinesterase inhibition and micronucleus frequency in oysters (*Crassostrea corteziensis*) exposed to chlorpyrifos: *Invertebrate Survival Journal*, 11 (1), Pp 247-256 (2014), p. 247.
- Bergström, P., N. Hällmark, K.-J. Larsson, and M. Lindegarth, 2019, Biodeposits from *Mytilus edulis*: a potentially high-quality food source for the polychaete, *Hediste diversicolor*: *Aquaculture International*, 27 (1), p. 89.
- Berthet, B., C. Mouneyrac, J. C. Amiard, C. Amiard-Triquet, Y. Berthelot, A. Le Hen, O. Mastain, P. S. Rainbow, and B. D. Smith, 2003, Accumulation and soluble binding of cadmium, Cu, and Zn in the polychaete *Hediste diversicolor* from coastal sites with different trace metal bioavailabilities: *Archives Of Environmental Contamination And Toxicology*, 45 (4), p. 468-478.

- Bessette, E.E., Fasco, M.J., Pentecost, B.T. and Kaminsky, L.S., 2005. Mechanisms of arsenite-mediated decreases in benzo [k] fluoranthene-induced human cytochrome P4501A1 levels in HepG2 cells. *Drug metabolism and disposition*, 33(3), pp.312-320.
- Bignasca, A., C. Ianni, E. Magi, and P. Rivaro, 2011, Using proteolytic enzymes to assess metal bioaccessibility in marine sediments: *Talanta*, 86, p. 305-315.
- Birch, G. F., 2017, Determination of sediment metal background concentrations and enrichment in marine environments – A critical review: *Science of the Total Environment*, 580, p. 813-831.
- Bird, E.C., 1994. Physical setting and geomorphology of coastal lagoons. *Coastal lagoon processes*, 60, pp.9-37.
- Blackstock, J., and T. H. Pearson, 1985, Effects of solid waste disposal in coastal areas: Integration of biochemical, biological and environmental studies: *Marine Environmental Research*, 17 (2-4), p. 291-292.
- Bligh, E. G., and W. J. Dyer, 1959, A rapid method of total lipid extraction and purification: *Canadian Journal Of Biochemistry And Physiology*, 37 (8), p. 911-917.
- Blott, S.J. and Pye, K., 2001. GRADISTAT: a grain size distribution and statistics package for the analysis of unconsolidated sediments. *Earth surface processes and Landforms*, 26(11), pp.1237-1248.
- Bocchetti, R., C. V. Lamberti, B. Pisanelli, E. M. Razzetti, C. Maggi, B. Catalano, G. Sesta, G. Martuccio, M. Gabellini, and F. Regoli, 2008, Seasonal variations of exposure biomarkers, oxidative stress responses and cell damage in the clams, *Tapes philippinarum*, and mussels, *Mytilus galloprovincialis*, from Adriatic sea: *Marine Environmental Research*, 66 (1), p. 24-26.
- Boitsov, S., H. K. B. Jensen, and J. Klungsøyr, 2009, Natural background and anthropogenic inputs of polycyclic aromatic hydrocarbons (PAH) in sediments of South-Western Barents Sea: *Marine Environmental Research*, 68 (5), p. 236-245.
- Bonnard, M., M. Roméo, and C. Amiard-Triquet, 2009, Effects of Cu on the Burrowing Behavior of Estuarine and Coastal Invertebrates, the Polychaete *Nereis diversicolor* and the Bivalve *Scrobicularia plana*: *Human and Ecological Risk Assessment: An International Journal*, 15 (1), p. 11-26.
- Bordon, I. C., A. K. Emerenciano, J. R. C. Melo, J. R. M. C. d. Silva, D. I. T. Favaro, P. K. Gusso-Choueri, B. G. d. Campos, and D. M. d. S. Abessa, 2018, Implications on the Pb bioaccumulation and metallothionein levels due to dietary and waterborne exposures: The *Callinectes danae* case: *Ecotoxicology and Environmental Safety*, 162, p. 415-422.
- Bouraoui, Z., M. Banni, J. Ghedira, C. Clerandau, J. F. Narbonne, and H. Boussetta, 2009, Evaluation of enzymatic biomarkers and lipoperoxidation level in *Hediste diversicolor* exposed to Cu and benzo[a]pyrene: *Ecotoxicology and Environmental Safety*, 72 (7), p. 1893-1898.
- Breitbarth, E., R. J. Bellerby, C. C. Neill, M. V. Ardelan, M. Meyerhöfer, E. Zöllner, P. L. Croot, and U. Riebesell, 2010, Ocean acidification affects iron speciation during a coastal seawater mesocosm experiment: *Biogeosciences*, 7 (3) p. 1065-1073.
- Bridges, C.M., 1997. Tadpole swimming performance and activity affected by acute exposure to sublethal levels of carbaryl. *Environmental Toxicology and Chemistry: An International Journal*, 16(9), pp.1935-1939.

- Brix, K. V., A. J. Esbaugh, K. M. Munley, and M. Grosell, 2012, Investigations into the mechanism of Pb toxicity to the freshwater pulmonate snail, *Lymnaea stagnalis*: *Aquatic Toxicology*, 106, p. 147-156.
- Brix, K. V., M. S. Tellis, A. Crémazy, and C. M. Wood, 2017, Characterization of the effects of binary metal mixtures on short-term uptake of Cd, Pb, and Zn by rainbow trout (*Oncorhynchus mykiss*): *Aquatic Toxicology*, 193, p. 217-227.
- Brown, A.E., Burn, A.J., Hopkins, J.J. and Way, S.F., 1997. The Habitats Directive: selection of Special Areas of Conservation in the UK Joint Nature Conservation Committee.
- Brown, R. J., T. S. Galloway, D. Lowe, M. A. Browne, A. Dissanayake, M. B. Jones, and M. H. Depledge, 2004, Differential sensitivity of three marine invertebrates to Cu assessed using multiple biomarkers: *Aquatic Toxicology*, 66 (3), p. 267-278.
- Brown, T. M., and H. Takada, 2017, Indicators of Marine Pollution in the North Pacific Ocean: *Archives Of Environmental Contamination And Toxicology*, 73 (2), p. 171-175.
- Bryan, G., P. Gibbs, L. Hummerstone, and G. Burt, 1987, Cu, Zn, and organotin as long-term factors governing the distribution of organisms in the fal estuary in Southwest England: *Estuaries and Coasts*, 10, p. 208.
- Bryan, G. W., and W. J. Langston, 1992, Bioavailability, accumulation and effects of heavy metals in sediments with special reference to United Kingdom estuaries: a review: *Environmental Pollution*, 76, p. 89-131.
- Budzinski, H., M. Letellier, S. Thompson, K. LeMenach, and P. Garrigues, 2000, Combined protocol for the analysis of polycyclic aromatic hydrocarbons (PAHs) and polychlorobiphenyls (PCBx) from sediments using focussed microwave assisted (FMW) extraction at atmospheric pressure: *Fresenius' Journal Of Analytical Chemistry*, 367 (2), p. 165-171.
- Buffet, P.-E., O. F. Tankoua, J.-F. Pan, D. Berhanu, C. Herrenknecht, L. Poirier, C. Amiard-Triquet, J.-C. Amiard, J.-B. Bérard, C. Risso, M. Guibbolini, M. Roméo, P. Reip, E. Valsami-Jones, and C. Mouneyrac, 2011, Behavioural and biochemical responses of two marine invertebrates *Scrobicularia plana* and *Hediste diversicolor* to Cu oxide nanoparticles: *Chemosphere*, 84 (1), p. 166-174.
- Burlinson, F. C., and A. J. Lawrence, 2007, Development and validation of a behavioural assay to measure the tolerance of *Hediste diversicolor* to Cu: *Environmental Pollution*, 145 (1), p. 274-278.
- Busselberg, D., B. Platt, D. Michael, D. O. Carpenter, and H. L. Haas, 1994, Mammalian Voltage-Activated Calcium Channel Currents Are Blocked by Pb²⁺, Zn²⁺, and Al³⁺: *Journal of Neurophysiology*, 71 (4), p. 1491.
- Bustamante, P., J. Ross, S. Markich, J. L. Teyssié, F. Oberhänsli, T. Lacoue-Labarthe, and S. Martin, 2009, Effects of increased pCO₂ and temperature on trace element (Ag, Cd and Zn) bioaccumulation in the eggs of the common cuttlefish, *Sepia officinalis*
- Büsselberg, D., M. L. Evans, H. Rahmann, and D. O. Carpenter, 1991, Pb and Zn block a voltage-activated calcium channel of *Aplysia* neurons: *Journal Of Neurophysiology*, 65 (4), p. 786-795.
- Büsselberg, D., K. Schirrmacher, R. Domann, and M. Wiemann, 1998, Pb interferes with calcium entry through membrane pores: *Fresenius' Journal of Analytical Chemistry*, 361 (4), p. 372.

- Cabecinhas, A. S., S. C. Novais, S. C. Santos, A. C. M. Rodrigues, J. L. T. Pestana, A. M. V. M. Soares, and M. F. L. Lemos, 2015, Sensitivity of the sea snail *Gibbula umbilicalis* to mercury exposure – Linking endpoints from different biological organization levels: *Chemosphere*, 119, p. 490-497.
- Cachada, A., P. Pato, T. Rocha-Santos, E. F. da Silva, and A. C. Duarte, 2012, Levels, sources and potential human health risks of organic pollutants in urban soils: *Science of the Total Environment*, 430, p. 184-192.
- Caldwell, G. S., C. Lewis, G. Pickavance, R. L. Taylor, and M. G. Bentley, 2011, Exposure to Cu and a cytotoxic polyunsaturated aldehyde induces reproductive failure in the marine polychaete *Nereis virens* (Sars): *Aquatic Toxicology*, 104 (1-2), p. 126-134.
- Canesi, L., 2015, Pro-oxidant and antioxidant processes in aquatic invertebrates: *Annals of the New York Academy of Sciences*, 1340 (1), p. 1-7.
- Canesi, L., and I. Corsi, 2016, Effects of nanomaterials on marine invertebrates: *Science of The Total Environment*, 565, p. 933-940.
- Canty, M. N., J. A. Hagger, R. T. B. Moore, L. Cooper, and T. S. Galloway, 2007, Sublethal impact of short term exposure to the organophosphate pesticide azamethiphos in the marine mollusc *Mytilus edulis*: *Marine Pollution Bulletin*, 54 (4), p. 396-402.
- Canty, M. N., T. H. Hutchinson, R. J. Brown, M. B. Jones, and A. N. Jha, 2009, Linking genotoxic responses with cytotoxic and behavioural or physiological consequences: Differential sensitivity of echinoderms (*Asterias rubens*) and marine molluscs (*Mytilus edulis*): *Aquatic Toxicology*, 94 (1), p. 68-76.
- Cao, R., Y. Liu, Q. Wang, Z. Dong, D. Yang, H. Liu, W. Ran, Y. Qu, and J. Zhao, 2018, Seawater acidification aggravated cadmium toxicity in the oyster *Crassostrea gigas*: Metal bioaccumulation, subcellular distribution and multiple physiological responses: *Science of the Total Environment*, 642, p. 809-823.
- Carfagna, M. A., G. D. Ponsler, and B. B. Muhoberac, 1996, Inhibition of ATPase activity in rat synaptic plasma membranes by simultaneous exposure to metals: *Chemico-Biological Interactions*, 100 (1), p. 53-65.
- Carrasco Navarro, V., J.-M. Brozinski, M. T. Leppänen, J. O. Honkanen, L. Kronberg, and J. V. K. Kukkonen, 2011, Inhibition of pyrene biotransformation by piperonyl butoxide and identification of two pyrene derivatives in *Lumbriculus variegatus* (Oligochaeta): *Environmental Toxicology & Chemistry*, 30 (5), p. 1069-1078.
- Carrasco-Navarro, V., I. Jæger, J. O. Honkanen, J. V. K. Kukkonen, J. Carroll, and L. Camus, 2015, Bioconcentration, biotransformation and elimination of pyrene in the arctic crustacean *Gammarus setosus* (Amphipoda) at two temperatures: *Marine Environmental Research*, 110, p. 101-109.
- Casado-Martinez, M., E. Duncan, B. Smith, W. Maher, and P. Rainbow, 2012, As toxicity in a sediment-dwelling polychaete: detoxification and As metabolism: *Ecotoxicology*, 21 (2), p. 576-590.
- Casado-Martinez, M. C., B. D. Smith, T. A. DelValls, and P. S. Rainbow, 2009, Pathways of trace metal uptake in the lugworm *Arenicola marina*: *Aquatic Toxicology*, 92 (1), p. 9-17.
- Catalano, B., G. Moltedo, G. Martuccio, L. Gastaldi, C. Virno-Lamberti, A. Lauria, and A. Ausili, 2012, Can *Hediste diversicolor* (Nereidae, Polychaete) be considered a good candidate in evaluating PAH contamination? A multimarker approach: *Chemosphere*, 86 (9), p. 875-882.

- CCME, 2001, Canadian Sediment Quality Guidelines for the Protection of Aquatic Life, in G. a. S. Division, ed.: Canadian environmental quality guidelines, Winnipeg, Canadian Council Ministers of the Environment.
- Celia, Y. C., M. W. Darren, J. W. Jason, and S. F. Nicholas, 2016, Metal Bioaccumulation by Estuarine Food Webs in New England, USA: *Journal of Marine Science and Engineering*, 4, (2), p 41.
- Chan, C. Y. S., and J. M. Y. Chiu, 2015, Chronic Effects of Coated Silver Nanoparticles on Marine Invertebrate Larvae: A Proof of Concept Study: *PLoS ONE*, 10 (7), p. 1.
- Chapman, P.M., Wang, F., Germano, J.D. and Batley, G., 2002. Pore water testing and analysis: the good, the bad, and the ugly. *Marine Pollution Bulletin*, 44(5), pp.359-366.
- Chelomin, V. P., M. V. Zakhartsev, A. V. Kurilenko, and N. N. Belcheva, 2005, An in vitro study of the effect of reactive oxygen species on subcellular distribution of deposited cadmium in digestive gland of mussel *Crenomytilus grayanus*: *Aquatic Toxicology*, 73(2), p. 181-189.
- Chen, Z. and Mayer, L.M., 1999. Sedimentary metal bioavailability determined by the digestive constraints of marine deposit feeders: gut retention time and dissolved amino acids. *Marine Ecology Progress Series*, 176, pp.139-151.
- Chen, S., M. Qu, J. Ding, Y. Zhang, Y. Wang, and Y. Di, 2018, BaP-metals co-exposure induced tissue-specific antioxidant defense in marine mussels *Mytilus coruscus*: *Chemosphere*, 205, p. 286-296.
- Cherkasov, A. S., P. K. Biswas, D. M. Ridings, A. H. Ringwood, and I. M. Sokolova, 2006, Effects of acclimation temperature and cadmium exposure on cellular energy budgets in the marine mollusk *Crassostrea virginica*: linking cellular and mitochondrial responses: *The Journal Of Experimental Biology*, 209 (7), p. 1274-1284.
- Chiarelli, R., M. Agnello, L. Bosco, and M. C. Roccheri, 2014, Sea urchin embryos exposed to cadmium as an experimental model for studying the relationship between autophagy and apoptosis: *Marine Environmental Research*, 93, p. 47-55.
- Choi, Y.K., Jo, P.G. and Choi, C.Y., 2008. Cadmium affects the expression of heat shock protein 90 and metallothionein mRNA in the Pacific oyster, *Crassostrea gigas*. *Comparative Biochemistry and Physiology Part C: Toxicology & Pharmacology*, 147(3), pp.286-292.
- Christensen, M., O. Andersen, and G. T. Banta, 2002a, Metabolism of pyrene by the polychaetes *Nereis diversicolor* and *Arenicola marina*: *Aquatic Toxicology*, 58 (1-2), p. 15.
- Christensen, M., G. T. Banta, and O. Andersen, 2002b, Effects of the polychaetes *Nereis diversicolor* and *Arenicola marina* on the fate and distribution of pyrene in sediments: *Marine Ecology Progress Series*, 237, p. 159-172.
- Cristobal, S., 2008. Proteomics-based method for risk assessment of peroxisome proliferating pollutants in the marine environment. In *Environmental Genomics* (pp. 123-135). Humana Press.
- Chun-Mei, Z., P. G. C. Campbell, and K. J. Wilkinson, 2016, When are metal complexes bioavailable?: *Environmental Chemistry* (14482517), 13 (3), p. 425-433.
- Claireaux, G., P. Quéau, S. Marras, S. Le Floch, A. P. Farrell, A. Nicolas-Kopec, P. Lemaire, and P. Domenici, 2018, Avoidance threshold to oil water-soluble

- fraction by a juvenile marine teleost fish: *Environmental Toxicology & Chemistry*, 37(3), p. 854-859.
- Clément, B., Cauzzi, N., Godde, M., Crozet, K. and Chevron, N., 2005. Pyrene toxicity to aquatic pelagic and benthic organisms in single-species and microcosm tests. *Polycyclic Aromatic Compounds*, 25(3), pp.271-298.
- Cong, Y., G. T. Banta, H. Selck, D. Berhanu, E. Valsami-Jones, and V. E. Forbes, 2014, Toxicity and bioaccumulation of sediment-associated silver nanoparticles in the estuarine polychaete, *Nereis (Hediste) diversicolor*: *Aquatic Toxicology*, 156, p. 106-115.
- Connon, R. E., J. Geist, and I. Werner, 2012, Effect-Based Tools for Monitoring and Predicting the Ecotoxicological Effects of Chemicals in the Aquatic Environment: *Sensors*, 12 (9), p. 12741.
- Cooper, S., E. Bonneris, A. Michaud, B. Pinel-Alloul, and P. G. C. Campbell, 2013, Influence of a step-change in metal exposure (Cd, Cu, Zn) on metal accumulation and subcellular partitioning in a freshwater bivalve, *Pyganodon grandis*: a long-term transplantation experiment between lakes with contrasting ambient metal levels: *Aquatic Toxicology* (Amsterdam, Netherlands), 132, p. 73-83.
- Correia, A. D., and M. H. Costa, 2000, Effects of sediment geochemical properties on the toxicity of Cu-spiked sediments to the marine amphipod *Gammarus locusta*: *Science of The Total Environment*, 247 (2-3), p. 99-106.
- Costa, P. M., S. Caeiro, M. r. Diniz, J. Lobo, M. Martins, A. M. Ferreira, M. Caetano, C. Vale, T. n. DelValls, and M. H. Costa, 2009, Biochemical endpoints on juvenile *Solea senegalensis* exposed to estuarine sediments: the effect of contaminant mixtures on metallothionein and CYP1A induction, Great Britain, Springer Science + Business Media, p. 988.
- Costa, P. M., J. Lobo, S. Caeiro, M. Martins, A. M. Ferreira, M. Caetano, C. Vale, T. Á. DelValls, and M. H. Costa, 2008, Genotoxic damage in *Solea senegalensis* exposed to sediments from the Sado Estuary (Portugal): Effects of metallic and organic contaminants: *Mutation Research/Genetic Toxicology and Environmental Mutagenesis*, 654 (1), p. 29-37.
- Craig, S., 2018, Sustainable Feeds Ltd, in S. Bagwell, ed., Bournemouth University, Bournemouth University, p. 1.
- Dai, J., Li, S., Zhang, Y., Wang, R. and Yu, Y., 2008. Distributions, sources and risk assessment of polycyclic aromatic hydrocarbons (PAHs) in topsoil at Ji'nan city, China. *Environmental monitoring and assessment*, 147(1-3), pp.317-326.
- Dai, J., L. Zhang, X. Du, P. Zhang, W. Li, X. Guo, and Y. Li, 2018, Effect of Pb on Antioxidant Ability and Immune Responses of Crucian Carp: *Biological Trace Element Research*, 186 (2), p. 546-553.
- Dai, W., Liu, S., Fu, L., Du, H. and Xu, Z., 2012. Lead (Pb) accumulation, oxidative stress and DNA damage induced by dietary Pb in tilapia (*Oreochromis niloticus*). *Aquaculture Research*, 43(2), pp.208-214.
- Dailianis, S., G. P. Domouhtsidou, E. Raftopoulou, M. Kaloyianni, and V. K. Dimitriadis, 2003, Evaluation of neutral red retention assay, micronucleus test, acetylcholinesterase activity and a signal transduction molecule (cAMP) in tissues of *Mytilus galloprovincialis* (L.), in pollution monitoring: *Marine Environmental Research*, 56 (4), p. 443-470.

- Dang, F., P. S. Rainbow, and W.-X. Wang, 2012, Dietary toxicity of field-contaminated invertebrates to marine fish: Effects of metal doses and subcellular metal distribution: *Aquatic Toxicology*, 120, p. 1-10.
- Day, K. E., and I. M. Scott, 1990, Use of acetylcholinesterase activity to detect sublethal toxicity in stream invertebrates exposed to low concentrations of organophosphate insecticides: *Aquatic Toxicology*, 18 (2), p. 101-113.
- de Almeida, E.A., de Almeida Marques, S., Klitzke, C.F., Bainy, A.C.D., de Medeiros, M.H.G., Di Mascio, P. and de Melo Loureiro, A.P., 2003. DNA damage in digestive gland and mantle tissue of the mussel *Perna perna*. *Comparative Biochemistry and Physiology Part C: Toxicology & Pharmacology*, 135(3), pp.295-303.
- de Gelder, S., M. J. Bakke, J. Vos, J. D. Rasinger, K. Ingebrigtsen, M. Grung, A. Ruus, G. Flik, P. H. M. Klaren, and M. H. G. Berntssen, 2016, The effect of dietary lipid composition on the intestinal uptake and tissue distribution of benzo[a]pyrene and phenanthrene in Atlantic salmon (*Salmo salar*): *Comparative Biochemistry and Physiology*, 185, p. 65-76.
- De Jonge, M., F. Dreesen, J. De Paepe, R. Blust, and L. Bervoets, 2009, Do Acid Volatile Sulfides (AVS) Influence the Accumulation of Sediment-Bound Metals to Benthic Invertebrates under Natural Field Conditions?: *Environmental Science & Technology*, 43 (12), p. 4510-4516.
- De Wit, R., H. Rey-Valette, J. Balavoine, V. Ouisse, and R. Lifran, 2017, Restoration ecology of coastal lagoons: new methods for the prediction of ecological trajectories and economic valuation: *Aquatic Conservation*, 27 (1), p. 137-157.
- Dell'Omo, G. ed., 2002. *Behavioural ecotoxicology*. John Wiley & Sons.
- Depledge, M. H., and P. S. Rainbow, 1990, Mini-review: Models of regulation and accumulation of trace metals in marine invertebrates: *Comparative Biochemistry and Physiology. Part C, Comparative Pharmacology*, 97 (1), p. 1-7.
- Deutsch, C., A. Ferrel, B. Seibel, H.-O. Pörtner, and R. B. Huey, 2015, Climate change tightens a metabolic constraint on marine habitats: *Science*, v. 348 (6239)p. 1132-1135.
- Diepens, N.J., Van den Heuvel-Greve, M.J. and Koelmans, A.A., 2015. Modeling of bioaccumulation in marine benthic invertebrates using a multispecies experimental approach. *Environmental science & technology*, 49(22), pp.13575-13585.
- Dierschke, V., J. Kube, and H. Rippe, 1999, Feeding ecology of dunlins *Calidris alpina* staging in the southern Baltic Sea, 2. Spatial and temporal variations in the harvestable fraction of their favourite prey *Hediste diversicolor*: *Journal of Sea Research*, 42 (1), p. 65-82.
- DiToro, D. M., and L. D. DeRosa, 2001, Sediment Toxicity and Equilibrium Partitioning Development of Sediment Quality Criteria for Toxic Substances, (pp. 197-230).Springer, Berlin, Heidelberg
- Du Laing, G., J. Rinklebe, B. Vandecasteele, E. Meers, and F. M. G. Tack, 2009, Trace metal behaviour in estuarine and riverine floodplain soils and sediments: A review: *Science of The Total Environment*, 407 (13), p. 3972-3985.
- Duarte, I. A., P. Reis-Santos, S. França, H. Cabral, and V. F. Fonseca, 2017, Biomarker responses to environmental contamination in estuaries: A comparative multi-taxa approach: *Aquatic Toxicology*, 189, p. 31-41.

- Duffus, J.H., 2002. " Heavy metals" a meaningless term?(IUPAC Technical Report). *Pure and applied chemistry*, 74(5), pp.793-807.
- Duport, E., G. Stora, P. Tremblay, and F. Gilbert, 2006, Effects of population density on the sediment mixing induced by the gallery-diffusor Hediste (Nereis) diversicolor O.F. Müller, 1776: *Journal of Experimental Marine Biology and Ecology*, 336 (1), p. 33-41.
- Duran, R., and C. Cravo-Laureau, 2016, Role of environmental factors and microorganisms in determining the fate of polycyclic aromatic hydrocarbons in the marine environment: *FEMS Microbiology Reviews*, 40 (6), p. 814.
- Durou, C., C. Mouneyrac, and C. Amiard-Triquet, 2005a, Tolerance to Metals and Assessment of Energy Reserves in the Polychaete Nereis diversicolor in Clean and Contaminated Estuaries, United States, WILEY, p. 23.
- Durou, C., C. Mouneyrac, and C. Amiard-Triquet, 2005b, Tolerance to metals and assessment of energy reserves in the polychaete Nereis diversicolor in clean and contaminated estuaries: *Environmental Toxicology*, 20 (1), p. 23-31.
- Durou, C., L. Poirier, J.-C. Amiard, H. Budzinski, M. Gnassia-Barelli, K. Lemenach, L. Peluhet, C. Mouneyrac, M. Roméo, and C. Amiard-Triquet, 2007, Biomonitoring in a clean and a multi-contaminated estuary based on biomarkers and chemical analyses in the endobenthic worm Nereis diversicolor: *Environmental Pollution*, 148 (2), p. 445-458.
- Dutton, J., and N. S. Fisher, 2011, Salinity effects on the bioavailability of aqueous metals for the estuarine killifish Fundulus heteroclitus: *Environmental Toxicology & Chemistry*, 30 (9), p. 2107-2114.
- Dyrynda, P. E. J., and B. Cleator, 1995, Lyme Bay Environmental Study. The Fleet Lagoon, [s.l.] : Ambios Environmental Consultants, 1995.
- Díaz-Jaramillo, M., Miglioranza, K.B., Carriquiriborde, P., Marino, D., Pegoraro, C.N., Valenzuela, G. and Barra, R., 2017. Sublethal effects in Perinereis gualpensis (Polychaeta: Nereididae) exposed to mercury-pyrene sediment mixture observed in a multipolluted estuary. *Ecotoxicology*, 26(6), pp.792-801.
- EA, 2016a, Nitrate vulnerable zone (NVZ) designation 2017-Eutrophic Waters (Estuaries and Coastal Waters), UK, Environment Agency.
- EA, 2016b, Poole Harbour Sediment contamination levels, in E. Agency, ed., Blandford, Dorset.
- Ebrahimi, K., 2004, Development of an integrated free surface and groundwater flow model. *Cardiff University* (2004)
- Ebrahimi, K., R. A. Falconer, and B. Lin, 2007, Flow and solute fluxes in integrated wetland and coastal systems: *Environmental Modelling & Software*, 22 (9), p. 1337-1348.
- Echeveste, P., C. Galbán-Malagón, J. Dachs, N. Berrojalbiz, and S. Agustí, 2016, Toxicity of natural mixtures of organic pollutants in temperate and polar marine phytoplankton: *Science of The Total Environment*, 571, p. 34-41.
- Eggleton, J., and K. V. Thomas, 2004, Review article: A review of factors affecting the release and bioavailability of contaminants during sediment disturbance events: *Environment International*, 30 (7), p. 973-980.
- Ellman, G. L., K. D. Courtney, V. Andres, and R. M. Featherstone, 1961, A new and rapid colorimetric determination of acetylcholinesterase activity: *Biochemical Pharmacology*, 7 (2), p. 88-95.

- Ellwood, M. J., and W. A. Maher, 2003, Measurement of As species in marine sediments by high-performance liquid chromatography–inductively coupled plasma mass spectrometry: *Analytica Chimica Acta*, 477 (2), p. 279-291.
- EPA, 2018, Priority Pollution List, Washington, USA, United States Environment Protection Agency.
- Erler, D. V., D. T. Welsh, W. W. Bennet, T. Meziane, C. Hubas, D. Nizzoli, and A. J. P. Ferguson, 2017, The impact of suspended oyster farming on nitrogen cycling and nitrous oxide production in a sub-tropical Australian estuary: *Estuarine, Coastal and Shelf Science*, 192, p. 117-127.
- EU, 1992, Council Directive 92/43/EEC. The Habitats Directive.
- Evans, M.D., Dizdaroglu, M. and Cooke, M.S., 2004. Oxidative DNA damage and disease: induction, repair and significance. *Mutation Research/Reviews in Mutation Research*, 567(1), pp.1-61.
- Faimali, M., C. Gambardella, E. Costa, V. Piazza, S. Morgana, N. Estévez-Calvar, and F. Garaventa, 2017, Old model organisms and new behavioral endpoints: Swimming alteration as an ecotoxicological response: *Marine Environmental Research*, 128, p. 36-45.
- Fair, P., 1986, Interaction of benzo(a)pyrene and cadmium on GSH-S-transferase and benzo(a)pyrene hydroxylase in the black sea bass *Centropristis striata*: *Archives of Environmental Contamination & Toxicology*, 15 (3), p. 257.
- Falfushynska, H., E. P. Sokolov, F. Haider, C. Oppermann, U. Kragl, W. Ruth, M. Stock, S. Glufke, E. J. Winkel, and I. M. Sokolova, 2019, Effects of a common pharmaceutical, atorvastatin, on energy metabolism and detoxification mechanisms of a marine bivalve *Mytilus edulis*: *Aquatic Toxicology*, 208, p. 47-61.
- Fan, W., W.-X. Wang, J. Chen, X. Li, and Y.-F. Yen, 2002, Cu, Ni, and Pb speciation in surface sediments from a contaminated bay of northern China: *Marine Pollution Bulletin*, 44 (4), p. 820-826.
- Ferrante, M., M. Vassallo, A. Mazzola, M. V. Brundo, R. Pecoraro, A. Grasso, and C. Copat, 2018, In vivo exposure of the marine sponge *Chondrilla nucula* Schmidt, 1862 to cadmium (Cd), Cu (Cu) and Pb (Pb) and its potential use for bioremediation purposes: *Chemosphere*, 193, p. 1049-1057.
- Ferriss, B.E., Reum, J.C., McDonald, P.S., Farrell, D.M. and Harvey, C.J., 2016. Evaluating trophic and non-trophic effects of shellfish aquaculture in a coastal estuarine foodweb. *ICES Journal of Marine Science*, 73(2), pp.429-440.
- Fleeger, J.W., Gust, K.A., Marlborough, S.J. and Tita, G., 2007. Mixtures of metals and polynuclear aromatic hydrocarbons elicit complex, nonadditive toxicological interactions in meiobenthic copepods. *Environmental Toxicology and Chemistry: An International Journal*, 26(8), pp.1677-1685.
- Folk, R. L., and W. C. Ward, 1957, Brazos River Bar [Texas]; a study in the significance of grain size parameters, *Journal of Sedimentary Research*, 21 (2), p. 3-26.
- Forrest, B.M. and Creese, R.G., 2006. Benthic impacts of intertidal oyster culture, with consideration of taxonomic sufficiency. *Environmental Monitoring and Assessment*, 112(1-3), pp.159-176.
- Fossi Tankoua, O., P. E. Buffet, J. C. Amiard, C. Amiard-Triquet, V. Méléder, P. Gillet, C. Mouneyrac, and B. Berthet, 2012, Intersite variations of a battery of biomarkers at different levels of biological organisation in the estuarine

- endobenthic worm *Nereis diversicolor* (Polychaeta, Nereididae): *Aquatic Toxicology*, 114-115, p. 96-103.
- Franzellitti, S., A. Viarengo, E. Dinelli, and E. Fabbri, 2012, Molecular and cellular effects induced by hexavalent chromium in Mediterranean mussels: *Aquatic Toxicology*, 124-125, p. 125-132.
- Frapiccini, E., and M. Marini, 2015, Polycyclic Aromatic Hydrocarbon Degradation and Sorption Parameters in Coastal and Open-Sea Sediment: *Water, Air & Soil Pollution*, 226 (8), p. 1-8.
- Freitas, R., L. de Marchi, A. Moreira, J. L. T. Pestana, F. J. Wrona, E. Figueira, and A. M. V. M. Soares, 2017, Physiological and biochemical impacts induced by mercury pollution and seawater acidification in *Hediste diversicolor*: *Science of The Total Environment*, 595, p. 691-701.
- Freitas, R., A. Pires, C. Velez, Â. Almeida, A. Moreira, F. J. Wrona, A. M. V. M. Soares, and E. Figueira, 2016, Effects of seawater acidification on *Diopatra neapolitana* (Polychaete, Onuphidae): *Biochemical and regenerative capacity responses: Ecological Indicators*, 60, p. 152-161.
- Frignani, M. and Bellucci, L.G., 2004. Heavy metals in marine coastal sediments: Assessing sources, fluxes, history and trends. *Annali di Chimica: Journal of Analytical, Environmental and Cultural Heritage Chemistry*, 94(7-8), pp.479-486.
- Froehner, S., J. Zeni, E. C. da Luz, and M. Maceno, 2009, Characterization of Granulometric and Chemical Composition of Sediments of Barigui River Samples and their Capacity to Retain Polycyclic Aromatic Hydrocarbons: *Water, Air & Soil Pollution*, 203 (1-4), p. 381-389.
- Frémion, F., F. Bordas, B. Mourier, J.-F. Lenain, T. Kestens, and A. Courtin-Nomade, 2016, Influence of dams on sediment continuity: A study case of a natural metallic contamination: *The Science Of The Total Environment*, 547, p. 282-294.
- Gaillard, J. F., C. Jeandel, G. Michard, E. Nicolas, and D. Renard, 1986, Interstitial water chemistry of villefranche bay sediments: Trace metal diagenesis: *Marine Chemistry*, 18 (2-4), p. 233-247.
- Gallo, A., R. Boni, I. Buttino, and E. Tosti, 2016, Spermiotoxicity of Ni nanoparticles in the marine invertebrate *Ciona intestinalis* (ascidians): *Nanotoxicology*, 10 (8), p. 1096-1104.
- Gao, J., Ishizaki, S. and Nagashima, Y., 2016. Purification and characterization of metal-binding proteins from the digestive gland of the Japanese scallop *Mizuhopecten yessoensis*. *Fisheries science*, 82(2), pp.337-345.
- García-Alonso, J., F. R. Khan, S. K. Misra, M. Turmaine, B. D. Smith, P. S. Rainbow, S. N. Luoma, and E. Valsami-Jones, 2011, Cellular Internalization of Silver Nanoparticles in Gut Epithelia of the Estuarine Polychaete *Nereis diversicolor*: *Environmental Science & Technology*, 45 (10), p. 4630-4636.
- Garrett, R. G., 2000, Natural Sources of Metals to the Environment: *Human & Ecological Risk Assessment*, 6 (6), p. 945.
- Gauthier, P. T., W. P. Norwood, E. E. Prepas, and G. G. Pyle, 2014, Metal-PAH mixtures in the aquatic environment: A review of co-toxic mechanisms leading to more-than-additive outcomes: *Aquatic Toxicology*, 154, p. 253-269.
- Gauthier, P. T., W. P. Norwood, E. E. Prepas, and G. G. Pyle, 2016, Behavioural alterations from exposure to Cu, phenanthrene, and Cu-phenanthrene mixtures: linking behaviour to acute toxic mechanisms in the aquatic amphipod, *Hyalella azteca*: *Aquatic Toxicology*, 170, p. 377-383.

- Gedan, K. B., M. L. Kirwan, E. Wolanski, E. B. Barbier, and B. R. Silliman, 2011, The present and future role of coastal wetland vegetation in protecting shorelines: answering recent challenges to the paradigm: *Climatic Change*, 106 (1), p. 7-29.
- Geffard, A., B. D. Smith, C. Amiard-Triquet, A. Y. Jeantet, and P. S. Rainbow, 2005, Kinetics of trace metal accumulation and excretion in the polychaete *Nereis diversicolor*: *Marine Biology*, 147 (6), p. 1291-1304.
- Geiszinger, A.E., Goessler, W. and Francesconi, K.A., 2002. The marine polychaete *Arenicola marina*: its unusual arsenic compound pattern and its uptake of arsenate from seawater. *Marine environmental research*, 53(1), pp.37-50.
- Gerald, A., S. David, N. Gina, and P. Julie, 1989, Organic and Inorganic Pb Inhibit Neurite Growth in Vertebrate and Invertebrate Neurons in Culture: *In Vitro Cellular & Developmental Biology*, 25 (12), p. 1121.
- Gérino, M., Stora, G., Francois, F., Gilbert, F., Poggiale, J.C., Mermillod-Blondin, F., Desrosiers, G. and Vervier, P., 2003. Macro-invertebrate functional groups in freshwater and marine sediments: a common mechanistic classification. *Vie et milieu*, 53(4), pp.221-232.
- Giacomin, M., M. B. Jorge, and A. Bianchini, 2014, Effects of Cu exposure on the energy metabolism in juveniles of the marine clam *Mesodesma mactroides*: *Aquatic Toxicology*, 152, p. 30-37.
- Giessing, A.M., Mayer, L.M. and Forbes, T.L., 2003. 1-hydroxypyrene glucuronide as the major aqueous pyrene metabolite in tissue and gut fluid from the marine deposit-feeding polychaete *Nereis diversicolor*. *Environmental Toxicology and Chemistry: An International Journal*, 22(5), pp.1107-1114.
- Gillet, P., Mouloud, M., Mouneyrac, C., Simo, P. and Gilbert, F., 2012. Preliminary data on the bioturbation activity of *Hediste Diversicolor* (Polychaeta, Nereididae) from the Loire Estuary, France.
- Gomes, T., O. Araújo, R. Pereira, A. C. Almeida, A. Cravo, and M. J. Bebianno, 2013, Genotoxicity of Cu oxide and silver nanoparticles in the mussel *Mytilus galloprovincialis*: *Marine Environmental Research*, 84, p. 51-59.
- Gomiero, A., Strafella, P., Pellini, G., Salvalaggio, V. and Fabi, G., 2018. Comparative effects of ingested PVC micro particles with and without adsorbed benzo (a) pyrene vs. spiked sediments on the cellular and sub cellular processes of the benthic organism *hediste diversicolor*. *Frontiers in Marine Science*, 5, p.99.
- Gómez-Ariza, J.L., Sánchez-Rodas, D., Giráldez, I. and Morales, E., 2000. A comparison between ICP-MS and AFS detection for arsenic speciation in environmental samples. *Talanta*, 51(2), pp.257-268.
- González-Fernández, D., M. C. Garrido-Pérez, E. Nebot-Sanz, and D. Sales-Márquez, 2011, Source and Fate of Heavy Metals in Marine Sediments from a Semi-Enclosed Deep Embayment Subjected to Severe Anthropogenic Activities: *Water, Air & Soil Pollution*, 221 (1-4), p. 191-202.
- Gopalakrishnan, S., W.-B. Huang, Q.-W. Wang, M.-L. Wu, J. Liu, and K.-J. Wang, 2011, Effects of tributyltin and benzo[a]pyrene on the immune-associated activities of hemocytes and recovery responses in the gastropod abalone, *Haliotis diversicolor*: *Comparative Biochemistry and Physiology*, 154 (2), p. 120-128.
- Gornall, A. G., C. J. Bardawill, and M. M. David, 1949, Determination of serum proteins by means of the biuret reaction: *The Journal Of Biological Chemistry*, 177 (2), p. 751-766.

- Granberg, M.E. and Forbes, T.L., 2006. Role of sediment organic matter quality and feeding history in dietary absorption and accumulation of pyrene in the mud snail (*Hydrobia ulvae*). *Environmental Toxicology and Chemistry: An International Journal*, 25(4), pp.995-1006.
- Guengerich, F. P., M. V. Martin, C. D. Sohl, and Q. Cheng, 2009, Measurement of cytochrome P450 and NADPH-cytochrome P450 reductase: *Nature Protocols*, 4 (9), p. 1245-1251.
- Guo, R., L. Pan, P. Lin, and L. Zheng, 2017, The detoxification responses, damage effects and bioaccumulation in the scallop *Chlamys farreri* exposed to single and mixtures of benzo[a]pyrene and chrysene: *Comparative Biochemistry and Physiology Part C: Toxicology & Pharmacology*, 191, p. 36-51.
- Guojun, Y., S. Lun, L. Xiaoqian, W. Nianbin, and L. Yang, 2017, Effect of the exposure to suspended solids on the enzymatic activity in the bivalve *Sinonovacula constricta*: *Aquaculture and Fisheries*, 2, (1), p 10-17 (2017), p. 10.
- Gust, K.A. and Fleeger, J.W., 2006. Exposure to cadmium-phenanthrene mixtures elicits complex toxic responses in the freshwater tubificid oligochaete, *Ilyodrilus templetoni*. *Archives of environmental contamination and toxicology*, 51(1), pp.54-60.
- Gutteridge, J. M. C., 1983, Antioxidant properties of caeruloplasmin towards iron- and Cu-dependent oxygen radical formation: *FEBS Letters*, 157(1), p. 37-40.
- Hahn, M. E., 1998, Review: The aryl hydrocarbon receptor: A comparative perspective. This article was invited by Guest Editors Dr John J. Stegeman and Dr David R. Livingstone to be part of a special issue of CBP on cytochrome P450. *Comp. Biochem. Physiol.* 121 (1), p. 23-53.
- Hannam, M. L., S. D. Bamber, T. S. Galloway, A. John Moody, and M. B. Jones, 2010, Effects of the model PAH phenanthrene on immune function and oxidative stress in the haemolymph of the temperate scallop *Pecten maximus*: *Chemosphere*, 78 (7), p. 779-784.
- Harborne, A.R., Renaud, P.G., Tyler, E.H.M. and Mumby, P.J., 2009. Reduced density of the herbivorous urchin *Diadema antillarum* inside a Caribbean marine reserve linked to increased predation pressure by fishes. *Coral Reefs*, 28(3), pp.783-791.
- Hariharan, G., C. Suresh Kumar, S. Laxmi Priya, A. Paneer Selvam, D. Mohan, R. Purvaja, and R. Ramesh, 2012, Acute and chronic toxic effect of Pb (Pb) and Zn (Zn) on biomarker response in post larvae of *Penaeus monodon* (Fabricus, 1798): *Toxicological & Environmental Chemistry*, 94 (8), p. 1571.
- Hartwig, A., and T. Schwerdtle, 2002, Interactions by carcinogenic metal compounds with DNA repair processes: toxicological implications: *Toxicology Letters*, 127 (1-3), p. 47-54.
- Hassan, H. M., A. B. Castillo, O. Yigiterhan, E. A. Elobaid, A. Al-Obaidly, E. Al-Ansari, and J. P. Obbard, 2018, Baseline concentrations and distributions of Polycyclic Aromatic Hydrocarbons in surface sediments from the Qatar marine environment: *Marine Pollution Bulletin*, 126, p. 58-62.
- He, W., C. Yang, W. Liu, Q. He, Q. Wang, Y. Li, X. Kong, X. Lan, and F. Xu, 2016, The partitioning behavior of persistent toxicant organic contaminants in eutrophic sediments: Coefficients and effects of fluorescent organic matter and particle size: *Environmental Pollution*, 219, p. 724-734.

- Hechun, P., Y. Zhiyun, and H. Yetang, 1988, The rule of release of carbon and heavy metals during weathering of rocks-A preliminary study: Chinese *Journal of Geochemistry*, 7(3), p. 259.
- Hiddink, J. G., R. ter Hofstede, and W. J. Wolff, 2002, Predation of intertidal infauna on juveniles of the bivalve *Macomabalthica*: *Journal of Sea Research*, 47 (2), p. 141-159.
- Holloway, G. J., R. M. Sibly, and S. R. Povey, 1990, Evolution in Toxin-Stressed Environments: *Functional Ecology*, 4 (3)p. 289.
- Hollows Cam, F., L. Johnston Emma, and J. Marshall Dustin, 2007, Cu reduces fertilisation success and exacerbates Allee effects in the field: *Marine Ecology Progress Series*, 333, p. 51.
- Hopkin, S. P., 1990, Critical Concentrations, Pathways of Detoxification and Cellular Ecotoxicology of Metals in Terrestrial Arthropods: *Functional Ecology*, p. 321-327.
- Hori, T.S.F., Avilez, I.M., Inoue, L.K. and Moraes, G., 2006. Metabolical changes induced by chronic phenol exposure in matrixã Brycon cephalus (teleostei: characidae) juveniles. *Comparative Biochemistry and Physiology Part C: Toxicology & Pharmacology*, 143(1), pp.67-72.
- Huang, M., Krepkiy, D., Hu, W. and Petering, D.H., 2004. Zn-, Cd-, and Pb-transcription factor IIIA: properties, DNA binding, and comparison with TFIIIA-finger 3 metal complexes. *Journal of inorganic biochemistry*, 98(5), pp.775-785.
- Huang, Q., S. Olenin, S. Sun, and M. De Troch, 2018, Impact of farming non-indigenous scallop *Argopecten irradians* on benthic ecosystem functioning: a case-study in Laizhou Bay, China: *Aquatic Environment Interactions*, 10, p. 227-241.
- Hummel, H. and Patarnello, T., 1994. Genetics and pollution. *Genetics and Evolution of Aquatic Organisms*. London: Chapman and Hall, pp.425-434.
- Hylland, K., 2006, Polycyclic Aromatic Hydrocarbon (PAH) Ecotoxicology in Marine Ecosystems: *Journal of Toxicology & Environmental Health: Part A*, 69 (1-2), p. 109-123.
- Hübner, R., K. B. Astin, and R. J. H. Herbert, 2010, 'Heavy metal'--time to move on from semantics to pragmatics?: *Journal Of Environmental Monitoring: JEM*, 12 (8), p. 1511-1514.
- Ianni, C., A. Bignasca, E. Magi, and P. Rivaro, 2010, Metal bioavailability in marine sediments measured by chemical extraction and enzymatic mobilization: *Microchemical Journal*, 96 (2), p. 308-316.
- Ibrahim, W. M., A. F. Hassan, and Y. A. Azab, 2016, Full Length Article: Biosorption of toxic heavy metals from aqueous solution by *Ulva lactuca* activated carbon: *Egyptian Journal of Basic and Applied Sciences*, 3 (3), p. 241-249.
- Ibrahim, W. M., and H. H. Mutawie, 2013, Bioremoval of heavy metals from industrial effluent by fixed-bed column of red macroalgae: *Toxicology & Industrial Health*, 29 (1), p. 38-42.
- Jambeck, J. R., R. Geyer, C. Wilcox, T. R. Siegler, M. Perryman, A. Andrady, R. Narayan, and K. L. Law, 2015, Marine pollution. Plastic waste inputs from land into the ocean: *Science*, 347(6223), p. 768-771.
- Jia, F., C. Liao, J. Xue, A. Taylor, and J. Gan, 2016, Comparing different methods for assessing contaminant bioavailability during sediment remediation: *Science of The Total Environment*, 573, p. 270-277.
- Jiang, Y., X. Hu, U. J. Yves, H. Zhan, and Y. Wu, 2014, Status, source and health risk assessment of polycyclic aromatic hydrocarbons in street dust of an industrial city, NW China: *Ecotoxicology and Environmental Safety*, 106, p. 11-18.

- Jiao, L., G. J. Zheng, T. B. Minh, B. Richardson, L. Chen, Y. Zhang, L. W. Yeung, J. C. W. Lam, X. Yang, P. K. S. Lam, and M. H. Wong, 2009, Persistent toxic substances in remote lake and coastal sediments from Svalbard, Norwegian Arctic: Levels, sources and fluxes: *Environmental Pollution*, 157 (4), p. 1342-1351.
- Jing, G., Y. Li, L. Xie, and R. Zhang, 2006, Metal accumulation and enzyme activities in gills and digestive gland of pearl oyster (*Pinctada fucata*) exposed to Cu: *Comparative Biochemistry and Physiology Part C: Toxicology & Pharmacology*, 144 (2), p. 184-190.
- Johnston, A. S. A., M. E. Hodson, P. Thorbek, T. Alvarez, and R. M. Sibly, 2014, An energy budget agent-based model of earthworm populations and its application to study the effects of pesticides: *Ecological Modelling*, 280, p. 5-17.
- Johnston, C. M., and P. M. Gilliland, 2000, Investigating and managing water quality in saline lagoons.
- Johnston, E. L., and D. A. Roberts, 2009a, Contaminants reduce the richness and evenness of marine communities: a review and meta-analysis: *Environmental Pollution* (Barking, Essex: 1987), 157 (6), p. 1745-1752.
- Jongeneelen, F. J., 2001, Benchmark guideline for urinary 1-hydroxypyrene as biomarker of occupational exposure to polycyclic aromatic hydrocarbons: *Annals of Occupational Hygiene*, 45(1), p. 3-13.
- Jorge, M. B., M. M. Lauer, C. D. M. G. Martins, and A. Bianchini, 2016, Impaired regulation of divalent cations with acute Cu exposure in the marine clam *Mesodesma mactroides*: *Comparative Biochemistry and Physiology*, 179, p. 79-86.
- Kalman J, a., a. Palais F, a. Amiard J. C, a. Mouneyrac C, a. Muntz A, a. Blasco J, a. Riba I, and a. Amiard-Triquet C, 2009, Assessment of the health status of populations of the ragworm *Nereis diversicolor* using biomarkers at different levels of biological organisation: *Marine Ecology Progress Series*, 393, p. 55.
- Kelly, C. A., R. J. Law, and H. s. Emerson, 2000, *Methods for analysis for Hydrocarbons and polycyclic aromatic hydrocarbons (PAH) in marine samples*. CEFAS
- Kershaw, S. and Acornley, R., 2008. Classification of Bivalve mollusc production areas in England and Wales. *Sanitary survey report, Medina Estuary-Isle of Wight: CEFAS*.
- Ketkar, S.N. and Bzik, T.J., 1998. Method Detection Limits for Trace Metals Analysis by ICP-MS. In *ANNUAL TECHNICAL MEETING-INSTITUTE OF ENVIRONMENTAL SCIENCES AND TECHNOLOGY* (Vol. 14, pp. 377-384). INSTITUTE OF ENVIRONMENTAL SCIENCES AND TECHNOLOGY.
- Khan, A., N. Shah, Muhammad, M. S. Khan, M. S. Ahmad, M. Farooq, M. Adnan, S. M. Jawad, H. Ullah, and A. M. Yousafzai, 2016, Quantitative Determination of Lethal Concentration Lc50 of Atrazine on Biochemical Parameters; Total Protein and Serum Albumin of Freshwater Fish Grass Carp (*Ctenopharyngodon idella*): *Polish Journal of Environmental Studies* 25, no.4, (2016): 1555-1561.
- Kim, B.-M., J.-S. Rhee, G. S. Park, J. Lee, Y.-M. Lee, and J.-S. Lee, 2011, Cu/Zn- and Mn-superoxide dismutase (SOD) from the copepod *Tigriopus japonicus*: Molecular cloning and expression in response to environmental pollutants: *Chemosphere*, 84 (10), p. 1467-1475.
- Kim, J.S., Kim, H., Yim, B., Rhee, J.S., Won, E.J. and Lee, Y.M., 2018. Identification and molecular characterization of two Cu/Zn-SODs and Mn-SOD in the

- marine ciliate *Euplotes crassus*: modulation of enzyme activity and transcripts in response to copper and cadmium. *Aquatic toxicology*, 199, pp.296-304.
- Kim, H., B. Lim, B.-D. Kim, and Y.-M. Lee, 2016, Effects of heavy metals on transcription and enzyme activity of Na/K-ATPase in the monogonont rotifer, *Brachionus koreanus*: *Toxicology & Environmental Health Sciences*, 8 (2), p. 128.
- Kim, J.-H., and J.-C. Kang, 2017a, Effects of sub-chronic exposure to Pb (Pb) and ascorbic acid in juvenile rockfish: Antioxidant responses, MT gene expression, and neurotransmitters. *Chemosphere* 171, pp. 520-527
- Kim, J.-H., and J.-C. Kang, 2017b, Toxic effects on bioaccumulation and hematological parameters of juvenile rockfish *Sebastes schlegelii* exposed to dietary Pb (Pb) and ascorbic acid: *Chemosphere*, 176, pp. 131-140.
- Kim, J.-H., C. W. Oh, and J.-C. Kang, 2017, Antioxidant Responses, Neurotoxicity, and Metallothionein Gene Expression in Juvenile Korean Rockfish *Sebastes schlegelii* under Dietary Pb Exposure: *Journal Of Aquatic Animal Health*, 29 (2), p. 112-119.
- Kim, J.-S., H. Kim, B. Yim, J.-S. Rhee, E.-J. Won, and Y.-M. Lee, 2018, Identification and molecular characterization of two Cu/Zn-SODs and Mn-SOD in the marine ciliate *Euplotes crassus*: Modulation of enzyme activity and transcripts in response to Cu and cadmium: *Aquatic Toxicology*, 199, p. 296-304.
- King, A.J., Readman, J.W. and Zhou, J.L., 2004. Dynamic behaviour of polycyclic aromatic hydrocarbons in Brighton marina, UK. *Marine Pollution Bulletin*, 48(3-4), pp.229-239.
- Kjerfve, B. ed., 1994. *Coastal lagoon processes*. Elsevier.
- Kluska, K., J. Adamczyk, and A. Krężel, 2018, Review: Metal binding properties, stability and reactivity of Zn fingers: *Coordination Chemistry Reviews*, 367, p. 18-64.
- Koiter, A., P. Owens, E. Petticrew, and D. Lobb, 2015, The role of gravel channel beds on the particle size and organic matter selectivity of transported fine-grained sediment: implications for sediment fingerprinting and biogeochemical flux research: *Journal of Soils & Sediments: Protection, Risk Assessment, & Remediation*, 15 (10), p. 2174-2188.
- Kooijman, S.A.L.M. and Kooijman, S.A.L.M., 2000. *Dynamic energy and mass budgets in biological systems*. Cambridge university press.
- Korashy, H. M., and A. O. S. El-Kadi, 2012, Transcriptional and posttranslational mechanisms modulating the expression of the cytochrome P450 1A1 gene by Pb in HepG2 cells: A role of heme oxygenase: *Toxicology*, 291 (1-3), p. 113-121.
- Krieger, J. A., D. R. Davila, J. Lytton, J. L. Born, and S. W. Burchiel, 1995, Inhibition of Sarcoplasmic/Endoplasmic Reticulum Calcium ATPases (SERCA) by Polycyclic Aromatic Hydrocarbons in HPB-All Human T Cells and Other Tissues: *Toxicology and Applied Pharmacology*, 133 (1), p. 102.
- Kristensen, E., 1984, Life Cycle, Growth and Production in Estuarine Populations of the Polychaetes *Nereis virens* and *N. diversicolor*: *Holarctic Ecology*, 7 (3), p. 249.
- Kuppusamy, S., P. Thavamani, M. Megharaj, and R. Naidu, 2016, Biodegradation of polycyclic aromatic hydrocarbons (PAHs) by novel bacterial consortia tolerant to diverse physical settings – Assessments in liquid- and slurry-phase systems: *International Biodeterioration & Biodegradation*, 108, p. 149-157.

- Kwan, C. K., E. Sanford, and J. Long, 2015, Cu Pollution Increases the Relative Importance of Predation Risk in an Aquatic Food Web: *Plos One*, 10 (7).
- Laitano, M., and A. Fernández-Gimenez, 2016, Are Mussels Always the Best Bioindicators? Comparative Study on Biochemical Responses of Three Marine Invertebrate Species to Chronic Port Pollution: *Bulletin of Environmental Contamination & Toxicology*, 97 (1), p. 50-55.
- Langston, W. J., M. J. Bebianno, and Z. Mingjiang, 1989, A comparison of metal-binding proteins and cadmium metabolism in the marine molluscs *Littorina littorea* (gastropoda), *Mytilus edulis* and *Macoma balthica* (bivalvia): *Marine Environmental Research*, 28 (1-4), p. 195-200.
- Langston, W. J., B. S. Chesman, G. R. Burt, M. Taylor, R. Covey, N. Cunningham, P. Jonas, and S. J. Hawkins, 2006, Characterisation of the European Marine Sites in South West England: The Fal and Helford Candidate Special Area of Conservation (cSAC): *Hydrobiologia*, 555 (1), p. 321-333.
- Langston, W. J., N. D. Pope, P. J. C. Jonas, C. Nikitic, M. D. R. Field, B. Dowell, N. Shillabeer, R. H. Swarbrick, and A. R. Brown, 2010, Contaminants in fine sediments and their consequences for biota of the Severn Estuary: *Marine Pollution Bulletin*, 61 (1-3), p. 68-82.
- Le, T. T. Y., S. Zimmermann, and B. Sures, 2016, How does the metallothionein induction in bivalves meet the criteria for biomarkers of metal exposure?: *Environmental Pollution*, 212, p. 257-268.
- Lee, B.G., Lee, J.S., Luoma, S.N., Choi, H.J. and Koh, C.H., 2000. Influence of acid volatile sulfide and metal concentrations on metal bioavailability to marine invertebrates in contaminated sediments. *Environmental science & technology*, 34(21), pp.4517-4523.
- Lee, K.-M., and E. L. Johnston, 2007, Low levels of Cu reduce the reproductive success of a mobile invertebrate predator: *Marine Environmental Research*, 64 (3), p. 336-346.
- Lee, S. H., S. Mukherjee, B. Brewer, R. Ryan, H. Yu, and M. Gangoda, 2013, A Laboratory Experiment To Measure Henry's Law Constants of Volatile Organic Compounds with a Bubble Column and a Gas Chromatography Flame Ionization Detector (GC-FID), United States, *Journal of Chemical Education* p90, no.4 (2013): 495-499.
- Lee, S. Y., and Y. K. Nam, 2016, Transcriptional responses of metallothionein gene to different stress factors in Pacific abalone (*Haliotis discus hannai*): *Fish & Shellfish Immunology*, 58, p. 530-541.
- Lewis, C., R. P. Ellis, E. Vernon, K. Elliot, S. Newbatt, and R. W. Wilson, 2016, Ocean acidification increases Cu toxicity differentially in two key marine invertebrates with distinct acid-base responses: *Scientific Reports*, 6, (2016) p. 21554
- Li, E., Z. Xiong, L. Chen, C. Zeng, and K. Li, 2008, Acute toxicity of boron to juvenile white shrimp, *Litopenaeus vannamei*, at two salinities: *Aquaculture*, 278 (1-4), p. 175-178.
- Li, L., X. Liu, L. You, L. Zhang, J. Zhao, and H. Wu, 2012, Uptake pathways and subcellular fractionation of Cd in the polychaete *Nereis diversicolor*: *Ecotoxicology*, 21 (1), p. 104-110.
- Li, L., X. Wang, J. Liu, X. Shi, and D. Ma, 2014, Assessing metal toxicity in sediments using the equilibrium partitioning model and empirical sediment quality guidelines: A case study in the nearshore zone of the Bohai Sea, China: *Marine Pollution Bulletin*, 85 (1), p. 114-122.
- Li, R., Z. Zuo, D. Chen, C. He, R. Chen, Y. Chen, and C. Wang, 2011, Inhibition by polycyclic aromatic hydrocarbons of ATPase activities in *Sebastiscus*

- marmoratus larvae : Relationship with the development of early life stages: *Marine Environmental Research*, 71 (1), p. 86-90.
- Liebeke, M., I. Garcia-Perez, C. J. Anderson, A. J. Lawlor, M. H. Bennett, C. A. Morris, P. Kille, C. Svendsen, D. J. Spurgeon, and J. G. Bundy, 2013, Earthworms produce phytochelatins in response to As: *Plos One*, 8 (11).
- Lister, K. N., M. D. Lamare, and D. J. Burritt, 2015, Pollutant resilience in embryos of the Antarctic sea urchin *Sterechinus neumayeri* reflects maternal antioxidant status: *Aquatic Toxicology*, 161, p. 61-72.
- Little, D.I., Galperin, Y., Bullimore, B. and Camplin, M., 2015. Environmental forensics evaluation of sources of sediment hydrocarbon contamination in Milford Haven Waterway. *Environmental Science: Processes & Impacts*, 17(2), pp.398-420.
- Liu, C.-M., J.-Q. Ma, and Y.-Z. Sun, 2011, Protective role of puerarin on Pb-induced alterations of the hepatic glutathione antioxidant system and hyperlipidemia in rats: *Food and Chemical Toxicology*, 49 (12), p. 3119-3127.
- Liu, J., H. Wu, J. Feng, Z. Li, and G. Lin, 2014a, Heavy metal contamination and ecological risk assessments in the sediments and zoobenthos of selected mangrove ecosystems, South China: *Catena*, 119, p. 136-142.
- Liu, L., R. Liu, W. Yu, F. Xu, C. Men, Q. Wang, and Z. Shen, 2016, Risk assessment and uncertainty analysis of PAHs in the sediments of the Yangtze River Estuary, China: *Marine Pollution Bulletin*, 112 (1-2), p. 380-388.
- Liu, Y.-W., D.-H. Shi, A.-J. Chen, Q. Zhu, J.-T. Xu, and X.-X. Zhang, 2014b, Acetylcholinesterase inhibition effects of marine fungi: *Pharmaceutical Biology*, 52 (5), p. 539-543.
- Lu, X., Reible, D.D. and Fleeger, J.W., 2004. Relative importance of ingested sediment versus pore water as uptake routes for PAHs to the deposit-feeding oligochaete *Ilyodrilus templetoni*. *Archives of Environmental Contamination and Toxicology*, 47(2), pp.207-214.
- Lukkari, T. and Haimi, J., 2005. Avoidance of Cu-and Zn-contaminated soil by three ecologically different earthworm species. *Ecotoxicology and Environmental Safety*, 62(1), pp.35-41.
- Luna-Acosta, A., P. Bustamante, H. Budzinski, V. Huet, and H. Thomas-Guyon, 2015, Persistent organic pollutants in a marine bivalve on the Marennes–Oléron Bay and the Gironde Estuary (French Atlantic Coast)—Part 2: Potential biological effects: *Science of The Total Environment*, 514, p. 511-522.
- Luo, X.J., Chen, S.J., Mai, B.X., Sheng, G.Y., Fu, J.M. and Zeng, E.Y., 2008. Distribution, source apportionment, and transport of PAHs in sediments from the Pearl River Delta and the northern South China Sea. *Archives of Environmental Contamination and Toxicology*, 55(1), pp.11-20.
- Luoma, S. N., 1983, Bioavailability of trace metals to aquatic organisms — A review: *Science of The Total Environment*, 28 (1-3), p. 1-22.
- Luoma, S. N., and P. S. Rainbow, 2005, Why is metal bioaccumulation so variable? Biodynamics as a unifying concept: *Environmental Science & Technology*, 39 (7), p. 1921-1931.
- Ma, W.-C., and L. T. C. Bonten, 2011, Bioavailability pathways underlying Zn-induced avoidance behavior and reproduction toxicity in *Lumbricus rubellus* earthworms: *Ecotoxicology and Environmental Safety*, 74 (6), p. 1721-1726.
- Ma, X., H. Zuo, M. Tian, L. Zhang, J. Meng, X. Zhou, N. Min, X. Chang, and Y. Liu, 2016, Assessment of heavy metals contamination in sediments from three adjacent regions of the Yellow River using metal chemical fractions and multivariate analysis techniques: *Chemosphere*, 144, p. 264-272.

- Macedo-Sousa, J. A., A. Gerhardt, C. M. A. Brett, A. J. A. Nogueira, and A. M. V. M. Soares, 2008, Behavioural responses of indigenous benthic invertebrates (*Echinogammarus meridionalis*, *Hydropsyche pellucidula* and *Choroterpes picteti*) to a pulse of Acid Mine Drainage: A laboratorial study: *Environmental Pollution*, 156 (3), p. 966-973.
- Malmquist, L. M. V., J. H. Christensen, and H. Selck, 2013, Effects of *Nereis diversicolor* on the Transformation of 1-Methylpyrene and Pyrene: Transformation Efficiency and Identification of Phase I and II Products: *Environmental Science & Technology*, 47 (10), p. 5383-5392.
- Malmquist, L. M. V., H. Selck, K. B. Jørgensen, and J. H. Christensen, 2015, Polycyclic Aromatic Acids Are Primary Metabolites of Alkyl-PAHs--A Case Study with *Nereis diversicolor*: *Environmental Science & Technology*, 49 (9), p. 5713-5721.
- Manduzio, H., T. Monsinjon, B. Rocher, F. Leboulenger, and C. Galap, 2003, Characterization of an inducible isoform of the Cu/Zn superoxide dismutase in the blue mussel *Mytilus edulis*: *Aquatic Toxicology*, 64 (1), p. 73-83.
- Mannervik, B., and G. Nise, 1969, Synthesis and some reactions of the pantetheine-glutathione mixed disulfide: *Archives Of Biochemistry And Biophysics*, 134 (1), p. 90-94.
- Manuel Nicolaus, E. E., R. J. Law, S. R. Wright, and B. P. Lyons, 2015, Spatial and temporal analysis of the risks posed by polycyclic aromatic hydrocarbon, polychlorinated biphenyl and metal contaminants in sediments in UK estuaries and coastal waters: *Marine Pollution Bulletin*, 95 (1), p. 469.
- Mao, H., D.-H. Wang, and W.-X. Yang, 2012, Review: The involvement of metallothionein in the development of aquatic invertebrate: *Aquatic Toxicology*, 110, p. 208-213.
- Marangoni, L. F. B., M. M. d. A. N. Pinto, J. A. Marques, and A. Bianchini, 2019, Cu exposure and seawater acidification interaction: Antagonistic effects on biomarkers in the zooxanthellate scleractinian coral *Mussismilia harttii*: *Aquatic Toxicology*, 206, p. 123-133.
- Maranho, L. A., C. André, T. A. DelValls, F. Gagné, and M. L. Martín-Díaz, 2015, Toxicological evaluation of sediment samples spiked with human pharmaceutical products: Energy status and neuroendocrine effects in marine polychaetes *Hediste diversicolor*: *Ecotoxicology and Environmental Safety*, 118, p. 27-36.
- Martinez-Tabche, L., Ortega, M.D.L.A.G., Mora, B.R., Faz, C.G., Lopez, E.L. and Martinez, M.G., 2001. Hemoglobin concentration and acetylcholinesterase activity of oligochaetes in relation to lead concentration in spiked sediments from Ignacio Ramirez reservoir. *Ecotoxicology and environmental safety*, 49(1), pp.76-83.
- Martins, M., P. M. Costa, A. M. Ferreira, and M. H. Costa, 2013, Comparative DNA damage and oxidative effects of carcinogenic and non-carcinogenic sediment-bound PAHs in the gills of a bivalve: *Aquatic Toxicology*, 142, p. 85-95.
- Martín-Díaz, M. L., J. Blasco, D. Sales, and T. A. DelValls, 2008, Field validation of a battery of biomarkers to assess sediment quality in Spanish ports: *Environmental Pollution*, 151 (3), p. 631-640.
- Maruya, K. A., P. F. Landrum, R. M. Burgess, and J. P. Shine, 2012, Incorporating contaminant bioavailability into sediment quality assessment frameworks: *Integrated Environmental Assessment And Management*, 8 (4), p. 659-673.

- Maryanski, M., Kramarz, P., Laskowski, R. and Niklinska, M., 2002. Decreased energetic reserves, morphological changes and accumulation of metals in carabid beetles (*Poecilus cupreus* L.) exposed to zinc-or cadmium-contaminated food. *Ecotoxicology*, 11(2), pp.127-139.
- Masero, J. A., M. Pérez-González, M. Basadre, and M. Otero-Saavedra, 1999, Food supply for waders (Aves: Charadrii) in an estuarine area in the Bay of Cádiz (SW Iberian Peninsula): *Acta Oecologica*, 20 (4), p. 429-434.
- Mayer, L. M., L. L. Schick, R. F. L. Self, P. A. Jumars, R. H. Findlay, Z. Chen, and S. Sampson, 1997, Digestive environments of benthic macroinvertebrate guts: Enzymes, surfactants and dissolved organic matter: *Journal of Marine Research*, 55 (4), p. 785-812.
- McCauley, D. J., G. M. DeGraeve, and T. K. Linton, 2000, Sediment quality guidelines and assessment: overview and research needs: *Environmental Science and Policy*, 3, p. 133-144.
- McGrath, S. P., and C. H. Cunliffe, 1985, A simplified method for the extraction of the metals Fe, Zn, Cu, Ni, Cd, Pb, Cr, Co and Mn from soils and sewage sludges: *Journal of the Science of Food and Agriculture*, 36 (9), p. 794-798.
- McQuillan, J. S., P. Kille, K. Powell, and T. S. Galloway, 2014, The Regulation of Cu Stress Response Genes in the Polychaete *Nereis diversicolor* during prolonged Extreme Cu Contamination: *Environmental Science & Technology*, 48 (22), p. 13085-13092.
- Meade, R.H. ed., 1995. *Contaminants in the Mississippi River, 1987-92* (Vol. 1133). US Government Printing Office.
- Meador, J. P., F. C. Sommers, G. M. Ylitalo, and C. A. Sloan, 2006, Altered growth and related physiological responses in juvenile Chinook salmon (*Oncorhynchus tshawytscha*) from dietary exposure to polycyclic aromatic hydrocarbons (PAHs): *Canadian Journal of Fisheries & Aquatic Sciences*, 63 (10), p. 2364.
- Mendiguchía, C., C. Moreno, M. P. Manuel-Vez, and M. García-Vargas, 2006, Preliminary investigation on the enrichment of heavy metals in marine sediments originated from intensive aquaculture effluents: *Aquaculture*, 254 (1-4), p. 317-325.
- Meng, J., W.-X. Wang, L. Li, and G. Zhang, 2018, Tissue-specific molecular and cellular toxicity of Pb in the oyster (*Crassostrea gigas*): mRNA expression and physiological studies: *Aquatic Toxicology*, 198, p. 257-268.
- Meyer, J. S., 2002, The utility of the terms “bioavailability” and “bioavailable fraction” for metals: *Marine Environmental Research*, 53 (4), p. 417-423.
- Mitchell, I. M., 2006, In situ biodeposition rates of Pacific oysters (*Crassostrea gigas*) on a marine farm in Southern Tasmania (Australia): *Aquaculture*, 257 (1-4), p. 194-203.
- Moolman, L., J. H. J. Van Vuren, and V. Wepener, 2007, Comparative studies on the uptake and effects of cadmium and Zn on the cellular energy allocation of two freshwater gastropods: *Ecotoxicology and Environmental Safety*, 68 (3), p. 443-450.
- Moore, M. N., 2004, Diet restriction induced autophagy: A lysosomal protective system against oxidative- and pollutant-stress and cell injury: *Marine Environmental Research*, 58 (2-5), p. 603-607.
- Morales-Caselles, C., M. B. Yunker, and P. S. Ross, 2017, Identification of Spilled Oil from the MV Marathassa (Vancouver, Canada 2015) Using Alkyl PAH Isomer Ratios: *Archives Of Environmental Contamination And Toxicology*, 73 (1), p. 118-130.

- Morcillo, P., M. Á. Esteban, and A. Cuesta, 2016, Heavy metals produce toxicity, oxidative stress and apoptosis in the marine teleost fish SAF-1 cell line: *Chemosphere*, 144, p. 225-233.
- Moreau, C.J., Klerks, P.L. and Haas, C.N., 1999. Interaction between phenanthrene and zinc in their toxicity to the sheepshead minnow (*Cyprinodon variegatus*). *Archives of environmental contamination and toxicology*, 37(2), pp.251-257.
- Moreira, F., 1999. On the use by birds of intertidal areas of the Tagus estuary: implications for management. *Aquatic Ecology*, 33(3), pp.301-309.
- Moreira, S. M., I. Lima, R. Ribeiro, and L. Guilhermino, 2006, Effects of estuarine sediment contamination on feeding and on key physiological functions of the polychaete *Hediste diversicolor*: Laboratory and in situ assays: *Aquatic Toxicology*, 78 (2), p. 186-201.
- Mouneyrac, C., P.-E. Buffet, L. Poirier, A. Zalouk-Vergnoux, M. Guibbolini, C. Faverney, D. Gilliland, D. Berhanu, A. Dybowska, A. Châtel, H. Perrein-Ettajni, J.-F. Pan, H. Thomas-Guyon, P. Reip, and E. Valsami-Jones, 2014, Fate and effects of metal-based nanoparticles in two marine invertebrates, the bivalve mollusc *Scrobicularia plana* and the annelid polychaete *Hediste diversicolor*: *Environmental Science & Pollution Research*, 21, no. 13 (2014): 7899-7912.
- Mouneyrac, C., O. Mastain, J. C. Amiard, C. Amiard-Triquet, P. Beaunier, A. Y. Jeantet, B. D. Smith, and P. S. Rainbow, 2003, Trace-metal detoxification and tolerance of the estuarine worm *Hediste diversicolor* chronically exposed in their environment: *Marine Biology*, 143 (4), p. 731-744.
- Mouneyrac, C., H. Perrein-Ettajani, and C. Amiard-Triquet, 2010, Influence of anthropogenic stress on fitness and behaviour of a key-species of estuarine ecosystems, the ragworm *Nereis diversicolor*: *Environmental Pollution*, 158 (1), p. 121-128.
- Mu, J., M. Chernick, W. Dong, R. T. Di Giulio, and D. E. Hinton, 2017, Early life co-exposures to a real-world PAH mixture and hypoxia result in later life and next generation consequences in medaka (*Oryzias latipes*): *Aquatic Toxicology*, 190, p. 162-173.
- Métais, I., A. Châtel, M. Mouloud, H. Perrein-Ettajani, M. Bruneau, P. Gillet, N. Jrad, and C. Mouneyrac, 2019, Is there a link between acetylcholinesterase, behaviour and density populations of the ragworm *Hediste diversicolor*?: *Marine Pollution Bulletin*, 142, p. 178-182.
- Nørregaard, R.D., Nielsen, T.G., Møller, E.F., Strand, J., Espersen, L. and Møhl, M., 2014. Evaluating pyrene toxicity on Arctic key copepod species *Calanus hyperboreus*. *Ecotoxicology*, 23(2), pp.163-174.
- Nardi, A., M. Benedetti, D. Fattorini, and F. Regoli, 2018, Oxidative and interactive challenge of cadmium and ocean acidification on the smooth scallop *Flexopecten glaber*: *Aquatic Toxicology*, 196, p. 53-60.
- Nebert, D. W., and T. P. Dalton, 2006, The role of cytochrome P450 enzymes in endogenous signalling pathways and environmental carcinogenesis: *Nature Reviews. Cancer*, 6 (12), p. 947-960.
- Nechev, J., K. Stefanov, D. Nedelcheva, and S. Popov, 2007, Effect of cobalt ions on the metabolism of some volatile and polar compounds in the marine invertebrates *Mytilus galloprovincialis* and *Actinia equina*: *Comparative Biochemistry and Physiology Part B: Biochemistry and Molecular Biology*, 146 (4), p. 568-575.
- Neff, J.M., 1997. Ecotoxicology of arsenic in the marine environment. *Environmental Toxicology and Chemistry: An International Journal*, 16(5), pp.917-927.

- Neff, J. M., S. A. Stout, and D. G. Gunster, 2005, Ecological risk assessment of polycyclic aromatic hydrocarbons in sediments: identifying sources and ecological hazard: *Integrated Environmental Assessment And Management*, 1 (1), p. 22-33.
- Nesto, N., D. Cassin, and L. Da Ros, 2010, Is the polychaete, *Perinereis rullieri* (Pilato 1974), a reliable indicator of PCB and PAH contaminants in coastal sediments?: *Ecotoxicology and Environmental Safety*, 73 (2), p. 143-151.
- Newton, A., J. Icely, S. Cristina, A. Brito, A. C. Cardoso, F. Colijn, S. D. Riva, F. Gertz, J. W. Hansen, M. Holmer, K. Ivanova, E. Leppäkoski, D. M. Canu, C. Mocenni, S. Mudge, N. Murray, M. Pejrup, A. Razinkovas, S. Reizopoulou, A. Pérez-Ruzafa, G. Schernewski, H. Schubert, L. Carr, C. Solidoro, Pierluigi Viaroli, and J.-M. Zaldívar, 2014, An overview of ecological status, vulnerability and future perspectives of European large shallow, semi-enclosed coastal systems, lagoons and transitional waters: *Estuarine, Coastal and Shelf Science*, 140, p. 95-122.
- Nikolaou, A., M. Kostopoulou, A. Petsas, M. Vagi, G. Lofrano, and S. Meric, 2009, Levels and toxicity of polycyclic aromatic hydrocarbons in marine sediments: *Trends in Analytical Chemistry*, 28 (6), p. 653-664.
- Nilin, J., J. L. T. Pestana, N. G. Ferreira, S. Loureiro, L. V. Costa-Lotufo, and A. M. V. M. Soares, 2012, Physiological responses of the European cockle *Cerastoderma edule* (Bivalvia: Cardidae) as indicators of coastal lagoon pollution: *Science of the Total Environment*, 435, p. 44-52.
- Nixon, S., B. Buckley, S. Granger, and J. Bintz, 2001, Responses of Very Shallow Marine Ecosystems to Nutrient Enrichment: *Human & Ecological Risk Assessment*, 7(5), p. 1457-1481.
- Nunney, R. S., and P. R. J. Smith, 1995, Lyme Bay Environmental Study; Environmental Quality: existing contaminant levels, v. 15: UK.
- Oaten, J. F. P., M. D. Hudson, A. C. Jensen, and I. D. Williams, 2017, Seasonal effects to metallothionein responses to metal exposure in a naturalised population of *Ruditapes philippinarum* in a semi-enclosed estuarine environment: *Science of The Total Environment*, 575, p. 1279-1290.
- Chemicals, D.O.F.O., 2005. OECD Guideline for testing of chemicals. *The Organisation for Economic Co-operation and Development: Paris, France*, pp.1-13.
- Olafson, R.W., Kearns, A. and Sim, R.G., 1979. Heavy metal induction of metallothionein synthesis in the hepatopancreas of the crab *Scylla wra/ u*. *Camp. Biwhem Physiol.* 62B, 4, p.17424.
- Oliveira, M., I. Ahmad, V. L. Maria, C. S. S. Ferreira, A. Serafim, M. J. Bebianno, M. Pacheco, and M. A. Santos, 2010a, Evaluation of oxidative DNA lesions in plasma and nuclear abnormalities in erythrocytes of wild fish (*Liza aurata*) as an integrated approach to genotoxicity assessment: *Mut.Res.Genetic Toxicology and Environmental Mutagenesis*, 703 (2), p. 83-89.
- Oliveira, M., V. L. Maria, I. Ahmad, M. Teles, A. Serafim, M. J. Bebianno, M. Pacheco, and M. A. Santos, 2010b, Golden grey mullet and sea bass oxidative DNA damage and clastogenic/aneugenic responses in a contaminated coastal lagoon: *Ecotoxicology and Environmental Safety*, 73 (8), p. 1907-1913.
- Özkan-Yılmaz, F., Özlüer-Hunt, A., Gündüz, S.G., Berköz, M. and Yalın, S., 2014. Effects of dietary selenium of organic form against lead toxicity on the antioxidant system in *Cyprinus carpio*. *Fish physiology and biochemistry*, 40(2), pp.355-363.

- Page, D. S., P. D. Boehm, G. S. Douglas, A. E. Bence, W. A. Burns, and P. J. Mankiewicz, 1999, Pyrogenic Polycyclic Aromatic Hydrocarbons in Sediments Record Past Human Activity: A Case Study in Prince William Sound, Alaska: *Marine Pollution Bulletin*, 38 (4), p. 247-260.
- Parente, T. E. M., P. Urban, D. Pompon, and M. F. Rebelo, 2014, Altered substrate specificity of the *Pterygoplichthys* sp. (Loricariidae) CYP1A enzyme: *Aquatic Toxicology*, 154, p. 193-199.
- Park, J., S. Kim, J. Yoo, J.-S. Lee, J.-W. Park, and J. Jung, 2014, Effect of salinity on acute Cu and Zn toxicity to *Tigriopus japonicus*: The difference between metal ions and nanoparticles: *Marine Pollution Bulletin*, 85 (2), p. 526-531.
- Patrick, L., 2006, Pb Toxicity Part II: The Role of Free Radical Damage and the Use of Antioxidants in the Pathology and Treatment of Pb Toxicity: *Alternative Medicine Review*, Part A, 4111 (2).
- Pempkowiak, J., Pazdro, K., Kopecka, J., Perez, E. and Sole, M., 2006. Toxicants accumulation rates and effects in *Mytilus trossulus* and *Nereis diversicolor* exposed separately or together to cadmium and PAHs. *Journal of Environmental Science and Health, Part A*, 41(11), pp.2571-2586.
- Peng, J.-f., Y.-h. Song, P. Yuan, X.-y. Cui, and G.-l. Qiu, 2009, Review: The remediation of heavy metals contaminated sediment: *Journal of Hazardous Materials*, 161 (2-3), p. 633-640.
- Pereira, B. V. R., E. C. M. Silva-Zacarin, M. J. Costa, A. C. A. Dos Santos, J. B. do Carmo, and B. Nunes, 2019, Cholinesterases characterization of three tropical fish species, and their sensitivity towards specific contaminants: *Ecotoxicology & Environmental Safety*, 173, p. 482-493.
- Perfetti-Bolaño, A., L. Moreno, R. Urrutia, A. Araneda, and R. Barra, 2018, Influence of *Pygoscelis* Penguin Colonies on Cu and Pb Concentrations in Soils on the Ardley Peninsula, Maritime Antarctica: *Water, Air & Soil Pollution*, 229 (12), p. 1-1.
- Peskin, A.V. and Winterbourn, C.C., 2000. A microtiter plate assay for superoxide dismutase using a water-soluble tetrazolium salt (WST-1). *Clinica chimica acta*, 293(1-2), pp.157-166.
- Petering, D. H., 2017, Reactions of the Zn Proteome with Cd²⁺ and Other Xenobiotics: Trafficking and Toxicity: *Chemical Research in Toxicology*, v. 30(1), p. 189-202.
- Petering, D. H., M. Huang, S. Moteki, and C. F. Shaw, 3rd, 2000, Cadmium and Pb interactions with transcription factor IIIA from *Xenopus laevis*: a model for Zn finger protein reactions with toxic metal ions and metallothionein: *Marine Environmental Research*, 50 (1-5), p. 89-92.
- Peña-Icart, M., C. Mendiguchía, M. E. Villanueva-Tagle, M. S. Pomares-Alfonso, and C. Moreno, 2014, Revisiting methods for the determination of bioavailable metals in coastal sediments: *Marine Pollution Bulletin*, 89 (1-2), p. 67-74.
- Peña-Icart, M., E. R. Pereira-Filho, L. Lopes Fialho, J. A. Nóbrega, C. Alonso-Hernández, Y. Bolaños-Alvarez, and M. S. Pomares-Alfonso, 2017, Combining contamination indexes, sediment quality guidelines and multivariate data analysis for metal pollution assessment in marine sediments of Cienfuegos Bay, Cuba: *Chemosphere*, 168, p. 1267-1276.
- Pie, H. V., A. Heyes, and C. L. Mitchelmore, 2015, Investigating the use of oil platform marine fouling invertebrates as monitors of oil exposure in the Northern Gulf of Mexico: *Science of The Total Environment*, 508, p. 553-565.

- Pini, J., 2014. *An assessment of the impacts of chronic exposure of copper and zinc on the polychaete Nereis (Alitta) virens using an integrated ecotoxicological approach* (Doctoral dissertation, University of Portsmouth).
- Pires, A., Â. Almeida, V. Calisto, R. J. Schneider, V. I. Esteves, F. J. Wrona, A. M. V. M. Soares, E. Figueira, and R. Freitas, 2016, Hediste diversicolor as bioindicator of pharmaceutical pollution: Results from single and combined exposure to carbamazepine and caffeine: Comparative Biochemistry and Physiology Part C: *Toxicology & Pharmacology*, 188, p. 30-38.
- Piña, B., and C. Barata, 2011, A genomic and ecotoxicological perspective of DNA array studies in aquatic environmental risk assessment: *Aquatic Toxicology*, 105 (3-4), p. 40-49.
- Poirier, L., B. Berthet, J.-C. Amiard, A.-Y. Jeantet, and C. Amiard-Triquet, 2006, A suitable model for the biomonitoring of trace metal bioavailabilities in estuarine sediments: the annelid polychaete Nereis diversicolor: *Journal of the Marine Biological Association of the United Kingdom*, 86 (1) p. 71.
- Polidoro, B.A., Comeros-Raynal, M.T., Cahill, T. and Clement, C., 2017. Land-based sources of marine pollution: Pesticides, PAHs and phthalates in coastal stream water, and heavy metals in coastal stream sediments in American Samoa. *Marine pollution bulletin*, 116(1-2), pp.501-507.
- Pook, C., C. Lewis, and T. Galloway, 2009, The metabolic and fitness costs associated with metal resistance in Nereis diversicolor: *Marine Pollution Bulletin*, 58 (7), p. 1063-1071.
- Pueyo, M., J. Mateu, A. Rigol, M. Vidal, J. F. López-Sánchez, and G. Rauret, 2008, Use of the modified BCR three-step sequential extraction procedure for the study of trace element dynamics in contaminated soils: *Environmental Pollution*, 152 (2), p. 330-341.
- Qu, X., Wang, X. and Zhu, D., 2007. The partitioning of PAHs to egg phospholipids facilitated by copper and proton binding via cation- π interactions. *Environmental science & technology*, 41(24), pp.8321-8327.
- Quintino, V., A. Azevedo, L. Magalhães, L. Sampaio, R. Freitas, A. M. Rodrigues, and M. Elliott, 2012, Indices, multispecies and synthesis descriptors in benthic assessments: Intertidal organic enrichment from oyster farming: *Estuarine, Coastal and Shelf Science*, 110, p. 190-201.
- Rabbitto, I. S., J. R. M. Alves Costa, H. C. Silva de Assis, É. Pelletier, F. M. Akaishi, A. Anjos, M. A. F. Randi, and C. A. Oliveira Ribeiro, 2005, Effects of dietary Pb(II) and tributyltin on neotropical fish, Hoplias malabaricus: histopathological and biochemical findings: *Ecotoxicology and Environmental Safety*, 60 (2), p. 147-156.
- Raimundo, J., C. Vale, R. Duarte, and I. Moura, 2010, Association of Zn, Cu, Cd and Pb with protein fractions and sub-cellular partitioning in the digestive gland of Octopus vulgaris living in habitats with different metal levels: *Chemosphere*, 81(10), p. 1314.
- Rainbow P. S, a., a. Amiard J.-C, a. Amiard-Triquet C, a. Cheung M.-S, a. Zhang L, a. Zhong H, and a. Wang W.-X, 2007, Trophic transfer of trace metals : subcellular compartmentalization in bivalve prey, assimilation by a gastropod predator and in vitro digestion simulations: *Marine Ecology Progress Series*, 348, p. 125.
- Rainbow P. S, a., a. Smith B. D, and a. Luoma S. N, 2009a, Biodynamic modelling and the prediction of Ag, Cd and Zn accumulation from solution and

- sediment by the polychaete *Nereis diversicolor*: *Marine Ecology Progress Series*, 390, p. 145-155.
- Rainbow P. S., a., a. Smith B. D, and a. Luoma S. N, 2009b, Differences in trace metal bioaccumulation kinetics among populations of the polychaete *Nereis diversicolor* from metal-contaminated estuaries: *Marine Ecology Progress Series*, 376, p. 173-184.
- Rainbow, P. S., 1995, Biomonitoring of heavy metal availability in the marine environment: *Marine Pollution Bulletin*, 31 (4-12), p. 183-192.
- Rainbow, P.S., 2002. Trace metal concentrations in aquatic invertebrates: why and so what?. *Environmental pollution*, 120(3), pp.497-507.
- Rainbow, P.S., Geffard, A., Jeantet, A.Y., Smith, B.D., Amiard, J.C. and Amiard-Triquet, C., 2004. Enhanced food-chain transfer of copper from a diet of copper-tolerant estuarine worms. *Marine Ecology Progress Series*, 271, pp.183-191.
- Rainbow, P. S., S. Kriefman, B. D. Smith, and S. N. Luoma, 2011, Have the bioavailabilities of trace metals to a suite of biomonitors changed over three decades in SW England estuaries historically affected by mining?: *Science of the Total Environment*, 409(8), p. 1589-1602.
- Rainbow, P. S., D. J. H. Phillips, and M. H. Depledge, 1990, The significance of trace metal concentrations in marine invertebrates: A need for laboratory investigation of accumulation strategies: *Marine Pollution Bulletin*, 21(7), p. 321-324.
- Rajkumar, J. S. I., and T. Samuel, 2013, Mercury Induced Biochemical Alterations As Oxidative Stress In Mugil Cephalus In Short Term Toxicity Test: *Current World Environment*, 8(1), p. 55.
- Razinkovas, A., Gasiūnaitė, Z., Viaroli, P. and Zaldivar, J.M., 2008. Preface: European lagoons—need for further comparison across spatial and temporal scales. *Hydrobiologia*, 611(1), pp.1-4.
- Regoli, F., and M. E. Giuliani, 2014, Oxidative pathways of chemical toxicity and oxidative stress biomarkers in marine organisms: *Marine Environmental Research*, 93, p. 106-117.
- Regoli, F., M. E. Giuliani, M. Benedetti, and A. Arukwe, 2011, Molecular and biochemical biomarkers in environmental monitoring: A comparison of biotransformation and antioxidant defense systems in multiple tissues: *Aquatic Toxicology*, 105(3-4), p. 56-66.
- Remali, T. M., S. L. Simpson, E. D. Amato, D. A. Spadaro, C. V. Jarolimek, and D. F. Jolley, 2016a, The impact of sediment bioturbation by secondary organisms on metal bioavailability, bioaccumulation and toxicity to target organisms in benthic bioassays: Implications for sediment quality assessment: *Environmental Pollution*, 208, p. 590-599.
- Remali, T. M., S. L. Simpson, E. D. Amato, D. A. Spadaro, C. V. Jarolimek, and D. F. Jolley, 2016b, The impact of sediment bioturbation by secondary organisms on metal bioavailability, bioaccumulation and toxicity to target organisms in benthic bioassays: Implications for sediment quality assessment: *Environmental Pollution*, 208, p. 590-599.
- Remali, T. M., N. Yin, W. W. Bennett, S. L. Simpson, D. F. Jolley, and D. T. Welsh, 2018, Contrasting effects of bioturbation on metal toxicity of contaminated sediments results in misleading interpretation of the AVS-SEM metal-sulfide paradigm: *Environmental Science. Processes & Impacts*, 20(9), p. 1285-1296.

- Resing, J. A., P. N. Sedwick, C. R. German, W. J. Jenkins, J. W. Moffett, B. M. Sohst, and A. Tagliabue, 2015, Basin-scale transport of hydrothermal dissolved metals across the South Pacific Ocean: *Nature*, 523 (7559), p. 200-203.
- Ribeiro, A. P., A. M. G. Figueiredo, J. O. d. Santos, E. Dantas, M. E. B. Cotrim, R. Cesar Lopes Figueira, E. V. Silva Filho, and J. Cesar Wasserman, 2013, Combined SEM/AVS and attenuation of concentration models for the assessment of bioavailability and mobility of metals in sediments of Sepetiba Bay (SE Brazil): *Marine Pollution Bulletin*, 68(1-2), p. 55-63.
- Ribeiro, S., Sousa, J.P., Nogueira, A.J.A. and Soares, A.M.V.M., 2001. Effect of endosulfan and parathion on energy reserves and physiological parameters of the terrestrial isopod *Porcellio dilatatus*. *Ecotoxicology and Environmental Safety*, 49(2), pp.131-138.
- Riisgård, H.U., Poulsen, L. and Larsen, P.S., 1996. Phytoplankton reduction in near-bottom water caused by filter-feeding *Nereis diversicolor*-implications for worm growth and population grazing impact. *Marine Ecology Progress Series*, 141, pp.47-54.
- Robinson, I. S., 1983, A tidal flushing model of the Fleet--an English tidal lagoon: *Estuarine Coastal & Shelf Science*, 16(6), p. 669-688.
- Robinson, N. J., and W. S. Peters, 2018, Complexity of the prey spectrum of *Agaronia propatula* (Caenogastropoda: Olividae), a dominant predator in sandy beach ecosystems of Pacific Central America: *PeerJ*, 6, p. e4714-e4714.
- Rodríguez-Romero, A., M. D. Basallote, M. R. De Orte, T. Á. DelValls, I. Riba, and J. Blasco, 2014a, Simulation of CO₂ leakages during injection and storage in sub-seabed geological formations: Metal mobilization and biota effects: *Environment International*, 68, p. 105-117.
- Rodríguez-Romero, A., N. Jiménez-Tenorio, M. D. Basallote, M. R. De Orte, J. Blasco, and I. Riba, 2014b, Predicting the Impacts of CO₂ Leakage from Subseabed Storage: Effects of Metal Accumulation and Toxicity on the Model Benthic Organism *Ruditapes philippinarum*: *Environmental Science & Technology*, 48(20), p. 12292-12301.
- Rogers, J. T., and C. M. Wood, 2004, Characterization of branchial Pb-calcium interaction in the freshwater rainbow trout *Oncorhynchus mykiss*: *Journal of Experimental Biology*, 207(5), p. 813-825.
- Rombough, P. J., 1994, Energy Partitioning During Fish Development: Additive or Compensatory Allocation of Energy to Support Growth?: *Functional Ecology*, p. 178-186.
- Rosa, S., J. P. Granadeiro, C. Vinagre, S. França, H. N. Cabral, and J. M. Palmeirim, 2008, Impact of predation on the polychaete *Hediste diversicolor* in estuarine intertidal flats: *Estuarine, Coastal and Shelf Science*, 78(4), p. 655-664.
- Rosado, D., J. Usero, and J. Morillo, 2016, Ability of 3 extraction methods (BCR, Tessier and protease K) to estimate bioavailable metals in sediments from Huelva estuary (Southwestern Spain): *Marine Pollution Bulletin*, 102(1), p. 65-71.
- Rossi, F., S. Palombella, C. Pirrone, G. Mancini, G. Bernardini, and R. Gornati, 2016, Evaluation of tissue morphology and gene expression as biomarkers of pollution in mussel *Mytilus galloprovincialis* caging experiment: *Aquatic Toxicology*, 181, p. 57-66.

- Rougée, L.R.A., Richmond, R.H. and Collier, A.C., 2014. Natural variations in xenobiotic-metabolizing enzymes: developing tools for coral monitoring. *Coral Reefs*, 33(2), pp.523-535.
- Ruiz-Fernández, A. C., M. Sprovieri, R. Piazza, M. Frignani, J.-A. Sanchez-Cabeza, M. L. Feo, L. G. Bellucci, M. Vecchiato, L. H. Pérez-Bernal, and F. Páez-Osuna, 2012, 210Pb-derived history of PAH and PCB accumulation in sediments of a tropical inner lagoon (Las Matas, Gulf of Mexico) near a major oil refinery: *Geochimica et Cosmochimica Acta*, 82, p. 136-153.
- Rust, A.J., Burgess, R.M., Brownawell, B.J. and McElroy, A.E., 2004. Relationship between metabolism and bioaccumulation of benzo [α] pyrene in benthic invertebrates. *Environmental Toxicology and Chemistry: An International Journal*, 23(11), pp.2587-2593.
- Ryder, K., Temara, A. and Holdway, D.A., 2004. Avoidance of crude-oil contaminated sediment by the Australian seastar, *Patiriella exigua* (Echinodermata: Asteroidea). *Marine pollution bulletin*, 49(11-12), pp.900-909.
- Ryvolova, M., V. Adam, and R. Kizek, 2012, Analysis of metallothionein by capillary electrophoresis: *Journal of Chromatography A*, 1226, p. 31-42.
- Sabaté, J., J. M. Bayona, and A. M. Solanas, 2001, Photolysis of PAHs in aqueous phase by UV irradiation: *Chemosphere*, 44(2), p. 119-124.
- Sagerup, K., J. Nahrgang, M. Frantzen, L.-H. Larsen, and P. Geraudie, 2016, Biological effects of marine diesel oil exposure in red king crab (*Paralithodes camtschaticus*) assessed through a water and foodborne exposure experiment: *Marine Environmental Research*, 119, p. 126-135.
- Sanah, S., G. Zena, C. Arnab, and B. Dietrich, 2012, Metal Toxicity at the Synapse: Presynaptic, Postsynaptic, and Long-Term Effects: *Journal of Toxicology*, 2012.
- Santos, C. D., S. Saraiva, J. M. Palmeirim, and J. P. Granadeiro, 2009, How do waders perceive buried prey with patchy distributions? The role of prey density and size of patch: *Journal of Experimental Marine Biology and Ecology*, 372(1-2), p. 43-48.
- Scaps, P., 2002. A review of the biology, ecology and potential use of the common ragworm *Hediste diversicolor* (OF Müller)(Annelida: Polychaeta). *Hydrobiologia*, 470(1-3), pp.203-218.
- Schaum, C. E., R. Batty, and K. S. Last, 2013, Smelling danger - alarm cue responses in the polychaete *Nereis* (*Hediste*) *diversicolor* (Müller, 1776) to potential fish predation: *Plos One*, 8(10).
- Schiedek, D., B. Sundelin, J. W. Readman, and R. W. Macdonald, 2007, Interactions between climate change and contaminants: *Marine Pollution Bulletin*, 54(12), p. 1845-1856.
- Schöne, B. R., and R. A. Krause Jr, 2016, Retrospective environmental biomonitoring – Mussel Watch expanded: *Global and Planetary Change*, 144, p. 228-251.
- Seo, Y.N. and Lee, M.Y., 2011. Inhibitory effect of antioxidants on the benz [a] anthracene-induced oxidative DNA damage in lymphocyte. *Journal of environmental biology*, 32(1), pp.7-10.
- Serafim, A., and M. J. Bebianno, 2007, Involvement of Metallothionein in Zn Accumulation and Elimination Strategies in *Ruditapes decussatus*: *Archives of Environmental Contamination & Toxicology*, 52(2), p. 189-199.

- Serafim, A., and M. J. Bebianno, 2010, Effect of a polymetallic mixture on metal accumulation and metallothionein response in the clam *Ruditapes decussatus*: *Aquatic Toxicology*, 99(3), p. 370-378.
- Serafim, M.A. and Bebianno, M.J., 2001. Variation of metallothionein and metal concentrations in the digestive gland of the clam *Ruditapes decussatus*: sex and seasonal effects. *Environmental Toxicology and Chemistry: An International Journal*, 20(3), pp.544-552.
- Serpe, F. P., M. Esposito, P. Gallo, and L. Serpe, 2010, Analytical Methods: Optimisation and validation of an HPLC method for determination of polycyclic aromatic hydrocarbons (PAHs) in mussels: *Food Chemistry*, 122(3), p. 920-925.
- Shafer, T. J., and Meyer, D.A, 2004, Effects of pyrethroids on voltage-sensitive calcium channels: a critical evaluation of strengths, weaknesses, data needs and relationship to assessment of cumulative neurotoxicity: *Toxicology and Applied Pharmacology*, 196(2), p. 303-319.
- Shailaja, M. S., and C. D'Silva, 2003, Evaluation of impact of PAH on a tropical fish, *Oreochromis mossambicus* using multiple biomarkers: *Chemosphere*, 53(8), p. 835-841.
- Shuona, C., Y. Hua, C. Jingjing, P. Hui, and D. Zhi, 2017, Physiology and bioprocess of single cell of *Stenotrophomonas maltophilia* in bioremediation of co-existed benzo[a]pyrene and Cu: *Journal of Hazardous Materials*, 321, p. 9-17.
- Sikkema, J., J. A. de Bont, and B. Poolman, 1995, Mechanisms of membrane toxicity of hydrocarbons: *Microbiological Reviews*, 59(2), p. 201-222.
- Silva, C. S. E., S. C. Novais, T. Simões, M. Caramalho, C. Gravato, M. J. Rodrigues, P. Maranhão, and M. F. L. Lemos, 2018, Original Articles: Using biomarkers to address the impacts of pollution on limpets (*Patella depressa*) and their mechanisms to cope with stress: *Ecological Indicators*, 95, p. 1077-1086.
- Silva, S.J., Carman, K.R., Fleeger, J.W., Marshall, T. and Marlborough, S.J., 2009. Effects of phenanthrene-and metal-contaminated sediment on the feeding activity of the harpacticoid copepod, *Schizopera knabeni*. *Archives of environmental contamination and toxicology*, 56(3), pp.434-441.
- Simms, C.L. and Zaher, H.S., 2016. Quality control of chemically damaged RNA. *Cellular and Molecular Life Sciences*, 73(19), pp.3639-3653.
- Simpson, S.L., Angel, B.M. and Jolley, D.F., 2004. Metal equilibration in laboratory-contaminated (spiked) sediments used for the development of whole-sediment toxicity tests. *Chemosphere*, 54(5), pp.597-609.
- Sivo, V., D'Abrosca, G., Baglivo, I., Iacovino, R., Pedone, P.V., Fattorusso, R., Russo, L., Malgieri, G. and Isernia, C., 2018. Ni (II), Hg (II), and Pb (II) coordination in the prokaryotic zinc-finger Ros87. *Inorganic chemistry*, 58(2), pp.1067-1080.
- Sizmur, T., Canário, J., Edmonds, S., Godfrey, A. and O'Driscoll, N.J., 2013. The polychaete worm *Nereis diversicolor* increases mercury lability and methylation in intertidal mudflats. *Environmental toxicology and chemistry*, 32(8), pp.1888-1895.
- Slobodskova, V.V., Solodova, E.E. and Chelomin, V.P., 2012. ACCUMULATION OF CADMIUM IN THE MARINE SCALLOP *MIZUHOPECTEN YESSOENSIS* AND ITS POTENTIAL CONSEQUENCES ON DNA DAMAGE. *Environmental Research Journal*, 6(2).

- Smart, J. and Gill, J.A., 2003. Non-intertidal habitat use by shorebirds: a reflection of inadequate intertidal resources?. *Biological Conservation*, 111(3), pp.359-369.
- Smith, G.M. and Weis, J.S., 1997. Predator-prey relationships in mummichogs (*Fundulus heteroclitus* (L.)): Effects of living in a polluted environment. *Journal of Experimental Marine Biology and Ecology*, 209(1-2), pp.75-87.
- Smith, R.W., Blaney, S.C., Dowling, K., Sturm, A., Jönsson, M. and Houlihan, D.F., 2001. Protein synthesis costs could account for the tissue-specific effects of sub-lethal copper on protein synthesis in rainbow trout (*Oncorhynchus mykiss*). *Aquatic Toxicology*, 53(3-4), pp.265-277.
- Smolders, R., Bervoets, L., De Coen, W. and Blust, R., 2004. Cellular energy allocation in zebra mussels exposed along a pollution gradient: linking cellular effects to higher levels of biological organization. *Environmental Pollution*, 129(1), pp.99-112.
- Smolders, R., De Boeck, G. and Blust, R., 2003. Changes in cellular energy budget as a measure of whole effluent toxicity in zebrafish (*Danio rerio*). *Environmental Toxicology and Chemistry: An International Journal*, 22(4), pp.890-899.
- Sohoni, P.C.R.T., Tyler, C.R., Hurd, K., Caunter, J., Hetheridge, M., Williams, T., Woods, C., Evans, M., Toy, R., Gargas, M. and Sumpter, J.P., 2001. Reproductive effects of long-term exposure to bisphenol A in the fathead minnow (*Pimephales promelas*). *Environmental science & technology*, 35(14), pp.2917-2925.
- Sokolova, I.M., Frederich, M., Bagwe, R., Lannig, G. and Sukhotin, A.A., 2012. Energy homeostasis as an integrative tool for assessing limits of environmental stress tolerance in aquatic invertebrates. *Marine environmental research*, 79, pp.1-15.
- Soliman, Y.S., Alansari, E.M., Sericano, J.L. and Wade, T.L., 2019. Spatio-temporal distribution and sources identifications of polycyclic aromatic hydrocarbons and their alkyl homolog in surface sediments in the central Arabian Gulf. *Science of the Total Environment*, 658, pp.787-797.
- Solé, M., Kopecka-Pilarczyk, J. and Blasco, J., 2009. Pollution biomarkers in two estuarine invertebrates, *Nereis diversicolor* and *Scrobicularia plana*, from a Marsh ecosystem in SW Spain. *Environment International*, 35(3), pp.523-531.
- Stogiannidis, E. and Laane, R., 2015. Source characterization of polycyclic aromatic hydrocarbons by using their molecular indices: an overview of possibilities. In *Reviews of environmental contamination and toxicology* (pp. 49-133). Springer, Cham.
- Sumner, J.B. and Graham, V.A., 1921. Dinitrosalicylic acid: a reagent for the estimation of sugar in normal and diabetic urine. *J Biol Chem*, 47(1), pp.5-9.
- Sun, R.X., Lin, Q., Ke, C.L., Du, F.Y., Gu, Y.G., Cao, K., Luo, X.J. and Mai, B.X., 2016. Polycyclic aromatic hydrocarbons in surface sediments and marine organisms from the Daya Bay, South China. *Marine pollution bulletin*, 103(1-2), pp.325-332.
- Svendsen, C. and Weeks, J.M., 1997. Relevance and Applicability of a Simple Earthworm Biomarker of Copper Exposure. I. Links to Ecological Effects in a Laboratory Study with *Eisenia andrei*. *Ecotoxicology and Environmental Safety*, 36(1), pp.72-79.

- Swartz, R.C., Schults, D.W., Ditsworth, G.R., Lamberson, J.O. and Dewitt, T.H., 1990. Toxicity of fluoranthene in sediment to marine amphipods: A test of the equilibrium partitioning approach to sediment quality criteria. *Environmental Toxicology and Chemistry: An International Journal*, 9(8), pp.1071-1080.
- Tang, W., Duan, S., Shan, B., Zhang, H., Zhang, W., Zhao, Y. and Zhang, C., 2016. Concentrations, diffusive fluxes and toxicity of heavy metals in pore water of the Fuyang River, Haihe Basin. *Ecotoxicology and environmental safety*, 127, pp.80-86.
- Tessier, A., Campbell, P.G. and Bisson, M., 1979. Sequential extraction procedure for the speciation of particulate trace metals. *Analytical chemistry*, 51(7), pp.844-851.
- Timmermann, K. and Andersen, O., 2003. Bioavailability of pyrene to the deposit-feeding polychaete *Arenicola marina*: importance of sediment versus water uptake routes. *Marine Ecology Progress Series*, 246, pp.163-172.
- Tobiszewski, M. and Namieśnik, J., 2012. PAH diagnostic ratios for the identification of pollution emission sources. *Environmental Pollution*, 162, pp.110-119.
- Topal, A., Alak, G., Altun, S., Erol, H.S. and Atamanalp, M., 2017. Evaluation of 8-hydroxy-2-deoxyguanosine and NFkB activation, oxidative stress response, acetylcholinesterase activity, and histopathological changes in rainbow trout brain exposed to linuron. *Environmental toxicology and pharmacology*, 49, pp.14-20.
- Toxværd, K., Van Dinh, K., Henriksen, O., Hjorth, M. and Nielsen, T.G., 2018. Impact of pyrene exposure during overwintering of the Arctic copepod *Calanus glacialis*. *Environmental science & technology*, 52(18), pp.10328-10336.
- Turner, A., 2006. Enzymatic mobilisation of trace metals from estuarine sediment. *Marine chemistry*, 98(2-4), pp.140-147.
- Turner, A. and Olsen, Y.S., 2000. Chemical versus enzymatic digestion of contaminated estuarine sediment: relative importance of iron and manganese oxides in controlling trace metal bioavailability. *Estuarine, Coastal and Shelf Science*, 51(6), pp.717-728.
- Vane, C.H., Harrison, I. and Kim, A.W., 2007. Polycyclic aromatic hydrocarbons (PAHs) and polychlorinated biphenyls (PCBs) in sediments from the Mersey Estuary, UK. *Science of the Total Environment*, 374(1), pp.112-126.
- Viarengo, A., Dondero, F., Pampanin, D.M., Fabbri, R., Poggi, E., Malizia, M., Bolognesi, C., Perrone, E., Gollo, E. and Cossa, G.P., 2007. A biomonitoring study assessing the residual biological effects of pollution caused by the HAVEN wreck on marine organisms in the Ligurian sea (Italy). *Archives of environmental contamination and toxicology*, 53(4), pp.607-616.
- Viarengo, A., Moore, M.N., Mancinelli, G., Mazzucotelli, A., Pipe, R.K. and Farrar, S.V., 1987. Metallothioneins and lysosomes in metal toxicity and accumulation in marine mussels: the effect of cadmium in the presence and absence of phenanthrene. *Marine Biology*, 94(2), pp.251-257.
- Viarengo, A. and Nicotera, P., 1991. Possible role of Ca²⁺ in heavy metal cytotoxicity. *Comparative Biochemistry and Physiology Part C: Comparative Pharmacology*, 100(1-2), pp.81-84.
- Viarengo, A. and Nott, J.A., 1993. Mechanisms of heavy metal cation homeostasis in marine invertebrates. *Comparative Biochemistry and Physiology Part C: Comparative Pharmacology*, 104(3), pp.355-372.

- Viarengo, A., Pertica, M., Canesi, L., Accomando, R., Mancinelli, G. and Orunesu, M., 1989. Lipid peroxidation and level of antioxidant compounds (GSH, vitamin E) in the digestive glands of mussels of three different age groups exposed to anaerobic and aerobic conditions. *Marine environmental research*, 28(1-4), pp.291-295.
- Viarengo, A., Ponzano, E., Dondero, F. and Fabbri, R., 1997. A simple spectrophotometric method for metallothionein evaluation in marine organisms: an application to Mediterranean and Antarctic molluscs. *Marine Environmental Research*, 44(1), pp.69-84.
- Vignier, J., Rolton, A., Soudant, P., Chu, F.L.E., Robert, R. and Volety, A.K., 2019. Interactions between *Crassostrea virginica* larvae and Deepwater Horizon oil: Toxic effects via dietary exposure. *Environmental pollution*, 246, pp.544-551.
- Virgilio, M., Fauvelot, C., Costantini, F., Abbiati, M. and Backeljau, T., 2009. Phylogeography of the common ragworm *Hediste diversicolor* (Polychaeta: Nereididae) reveals cryptic diversity and multiple colonization events across its distribution. *Molecular Ecology*, 18(9), pp.1980-1994.
- Voparil, I.M. and Mayer, L.M., 2000. Dissolution of sedimentary polycyclic aromatic hydrocarbons into the lugworm's (*Arenicola marina*) digestive fluids. *Environmental science & technology*, 34(7), pp.1221-1228.
- Vriens, B., Peterson, H., Laurenzi, L., Smith, L., Aranda, C., Mayer, K.U. and Beckie, R.D., 2019. Long-term monitoring of waste-rock weathering at the Antamina mine, Peru. *Chemosphere*, 215, pp.858-869.
- Wan, R., Meng, F., Fu, W., Wang, Q. and Su, E., 2015. Biochemical responses in the gills of *Meretrix meretrix* after exposure to treated municipal effluent. *Ecotoxicology and environmental safety*, 111, pp.78-85.
- Wang, H., Yang, H., Liu, J., Li, Y. and Liu, Z., 2016. Combined effects of temperature and copper ion concentration on the superoxide dismutase activity in *Crassostrea ariakensis*. *Acta Oceanologica Sinica*, 35(4), pp.51-57.
- Wang, J., Wang, C., Huang, Q., Ding, F. and He, X., 2015. Adsorption of PAHs on the sediments from the yellow river delta as a function of particle size and salinity. *Soil and Sediment Contamination: An International Journal*, 24(2), pp.103-115.
- Wang, L., Pan, L., Liu, N., Liu, D., Xu, C. and Miao, J., 2011. Biomarkers and bioaccumulation of clam *Ruditapes philippinarum* in response to combined cadmium and benzo [a] pyrene exposure. *Food and chemical toxicology*, 49(12), pp.3407-3417.
- Wang, Q., Li, Y. and Wang, Y., 2011. Optimizing the weight loss-on-ignition methodology to quantify organic and carbonate carbon of sediments from diverse sources. *Environmental Monitoring and Assessment*, 174(1-4), pp.241-257.
- Wang, Q., Liu, B., Yang, H., Wang, X. and Lin, Z., 2009. Toxicity of lead, cadmium and mercury on embryogenesis, survival, growth and metamorphosis of *Meretrix meretrix* larvae. *Ecotoxicology*, 18(7), pp.829-837.
- Wang, W.X. and Fisher, N.S., 1999. Delineating metal accumulation pathways for marine invertebrates. *Science of the Total Environment*, 237, pp.459-472.
- Wang, X. and Wang, W.X., 2006. Bioaccumulation and transfer of benzo (a) pyrene in a simplified marine food chain. *Marine Ecology Progress Series*, 312, pp.101-111.

- Wang, W.X., Stupakoff, I. and Fisher, N.S., 1999. Bioavailability of dissolved and sediment-bound metals to a marine deposit-feeding polychaete. *Marine Ecology Progress Series*, 178, pp.281-293.
- Wang, X.C., Zhang, Y.X. and Chen, R.F., 2001. Distribution and partitioning of polycyclic aromatic hydrocarbons (PAHs) in different size fractions in sediments from Boston Harbor, United States. *Marine Pollution Bulletin*, 42(11), pp.1139-1149.
- Watson, G.J., Leach, A. and Fones, G., 2008. Effects of copper and other metals on fertilization, embryo development, larval survival and settlement of the polychaete *Nereis (Neanthes) virens*. *Invertebrate Reproduction & Development*, 52(1-2), pp.101-112.
- Weber, G.J., O'Sullivan, P.E. and Brassley, P., 2006. Hindcasting of nutrient loadings from its catchment on a highly valuable coastal lagoon: the example of the Fleet, Dorset, UK, 1866–2004. *Saline Systems*, 2(1), p.15.
- Weis, J.S., Bergey, L., Reichmuth, J. and Candelmo, A., 2011. Living in a contaminated estuary: behavioral changes and ecological consequences for five species. *BioScience*, 61(5), pp.375-385.
- WEST, I., WEST, C., WEST, T. and BENTLEY, J., 2010. Barton and Highcliffe, Eocene Strata: Geology of the Wessex Coast of southern England. *Internet site: www.soton.ac.uk/~imw/barton.htm. Version: 30th June.*
- Williams, J.J., Dutton, J., Chen, C.Y. and Fisher, N.S., 2010. Metal (As, Cd, Hg, and CH₃Hg) bioaccumulation from water and food by the benthic amphipod *Leptocheirus plumulosus*. *Environmental toxicology and chemistry*, 29(8), pp.1755-1761.
- Won, E.J., Rhee, J.S., Ra, K., Kim, K.T., Au, D.W., Shin, K.H. and Lee, J.S., 2012. Molecular cloning and expression of novel metallothionein (MT) gene in the polychaete *Perinereis nuntia* exposed to metals. *Environmental science and pollution research*, 19(7), pp.2606-2618.
- Xiu, M., Pan, L. and Jin, Q., 2016. Toxic effects upon exposure to polycyclic aromatic hydrocarbon (chrysene) in scallop *Chlamys farreri* during the reproduction period. *Environmental toxicology and pharmacology*, 44, pp.75-83.
- Xu, E.G., Mager, E.M., Grosell, M., Hazard, E.S., Hardiman, G. and Schlenk, D., 2017. Novel transcriptome assembly and comparative toxicity pathway analysis in mahi-mahi (*Coryphaena hippurus*) embryos and larvae exposed to Deepwater Horizon oil. *Scientific reports*, 7, p.44546.
- Xue, R., Chen, L., Lu, Z., Wang, J., Yang, H., Zhang, J. and Cai, M., 2016. Spatial distribution and source apportionment of PAHs in marine surface sediments of Prydz Bay, East Antarctica. *Environmental Pollution*, 219, pp.528-536.
- Yang, K., Chen, C., Cheng, S., Cao, X. and Tu, B., 2017. Effects of benzo (a) pyrene exposure on the ATPase activity and calcium concentration in the hippocampus of neonatal rats. *International journal of occupational medicine and environmental health*, 30(2), p.203.
- Yeung, J.W., Zhou, G.J. and Leung, K.M., 2017. Spatiotemporal variations in metal accumulation, RNA/DNA ratio and energy reserve in *Perna viridis* transplanted along a marine pollution gradient in Hong Kong. *Marine pollution bulletin*, 124(2), pp.736-742.
- Yin, H., Cai, Y., Duan, H., Gao, J. and Fan, C., 2014. Use of DGT and conventional methods to predict sediment metal bioavailability to a field inhabitant

- freshwater snail (*Bellamya aeruginosa*) from Chinese eutrophic lakes. *Journal of hazardous materials*, 264, pp.184-194.
- Yoo, J.C., Lee, C.D., Yang, J.S. and Baek, K., 2013. Extraction characteristics of heavy metals from marine sediments. *Chemical engineering journal*, 228, pp.688-699.
- Young, S.M. and Ishiga, H., 2014. Environmental change of the fluvial-estuary system in relation to Arase Dam removal of the Yatsushiro tidal flat, SW Kyushu, Japan. *Environmental earth sciences*, 72(7), pp.2301-2314.
- Yu, D., Ji, C., Zhao, J. and Wu, H., 2016. Proteomic and metabolomic analysis on the toxicological effects of As (III) and As (V) in juvenile mussel *Mytilus galloprovincialis*. *Chemosphere*, 150, pp.194-201.
- Yu, H., Xia, Q., Yan, J., Herreno-Saenz, D., Wu, Y.S., Tang, I.W. and Fu, P.P., 2006. Photoirradiation of polycyclic aromatic hydrocarbons with UVA light—a pathway leading to the generation of reactive oxygen species, lipid peroxidation, and DNA damage. *International journal of environmental research and public health*, 3(4), pp.348-354.
- Yu, Y., Cui, Y., Niedernhofer, L.J. and Wang, Y., 2016. Occurrence, biological consequences, and human health relevance of oxidative stress-induced DNA damage. *Chemical research in toxicology*, 29(12), pp.2008-2039.
- Yunker, M.B., Macdonald, R.W., Ross, P.S., Johannessen, S.C. and Dangerfield, N., 2015. Alkane and PAH provenance and potential bioavailability in coastal marine sediments subject to a gradient of anthropogenic sources in British Columbia, Canada. *Organic Geochemistry*, 89, pp.80-116.
- Yunker, M.B., Macdonald, R.W., Vingarzan, R., Mitchell, R.H., Goyette, D. and Sylvestre, S., 2002. PAHs in the Fraser River basin: a critical appraisal of PAH ratios as indicators of PAH source and composition. *Organic geochemistry*, 33(4), pp.489-515.
- Zacchi, F.L., Flores-Nunes, F., Mattos, J.J., Lima, D., Lüchmann, K.H., Sasaki, S.T., Bicego, M.C., Taniguchi, S., Montone, R.C., de Almeida, E.A. and Bainy, A.C.D., 2018. Biochemical and molecular responses in oysters *Crassostrea brasiliana* collected from estuarine aquaculture areas in Southern Brazil. *Marine pollution bulletin*, 135, pp.110-118.
- Zhang, C., Yu, Z.G., Zeng, G.M., Jiang, M., Yang, Z.Z., Cui, F., Zhu, M.Y., Shen, L.Q. and Hu, L., 2014. Effects of sediment geochemical properties on heavy metal bioavailability. *Environment international*, 73, pp.270-281.
- Zhang, R., Zhang, F., Guan, M., Shu, Y. and Li, T., 2017. Sources and chronology of combustion-derived pollution to Shilianghe Reservoir, eastern China: Evidences from PAHs profiles, As, Hg, Pb and Pb isotopes. *Catena*, 149, pp.232-240.
- Zheng, Jisi, Bo Liu, Jing Ping, Bing Chen, Hongjing Wu, and Baiyu Zhang. "Vortex- and shaker-assisted liquid–liquid microextraction (VSA-LLME) coupled with gas chromatography and mass spectrometry (GC-MS) for analysis of 16 polycyclic aromatic hydrocarbons (PAHs) in offshore produced water." *Water, Air, & Soil Pollution* 226, no. 9 (2015): 318.
- Zhou, Q., Rainbow, P.S. and Smith, B.D., 2003. Tolerance and accumulation of the trace metals zinc, copper and cadmium in three populations of the polychaete *Nereis diversicolor*. *Journal of the Marine Biological Association of the United Kingdom*, 83(1), pp.65-72.
- Zhuang, W. and Gao, X., 2014. Assessment of heavy metal impact on sediment quality of the Xiaoqinghe estuary in the coastal Laizhou Bay, Bohai Sea:

Inconsistency between two commonly used criteria. *Marine pollution bulletin*, 83(1), pp.352-357.

Zimmermann, K., Atkinson, R., Arey, J., Kojima, Y. and Inazu, K., 2012. Isomer distributions of molecular weight 247 and 273 nitro-PAHs in ambient samples, NIST diesel SRM, and from radical-initiated chamber reactions. *Atmospheric environment*, 55, pp.431-439.

Appendix 1
I2 Analytical PAH Test results

Appendix 2

Glutathione Calibration Curve

